OBSERVATIONAL STUDIES OF THE GALAXY PECULIAR VELOCITY FIELD

by

Philip Andrew James

Astrophysics Group
Blackett Laboratory
Imperial College of Science, Technology and Medicine
London SW7 2BZ

A thesis submitted for the degree of
Doctor of Philosophy of the University of London
and for the
Diploma of Imperial College

November 1988

ABSTRACT

This thesis describes two observational studies of the peculiar velocity field of galaxies over scales of 50-100 h^{-1} Mpc, and the consequences of these measurements for cosmological theories.

An introduction is given to observational cosmology, emphasising the crucial questions of the nature of the dark matter and the formation of structure. The principal cosmological models are discussed, and the rôle of observations in developing these models is stressed. Consideration is given to those observations that are likely to prove good discriminators between the competing models, particular emphasis being given to studies of the coherent velocities of samples of galaxies.

The first new study presented here uses optical photometry and redshifts, from the literature, for First Ranked Cluster Galaxies (FRCG's). These galaxies are excellent standard candles, and thus ideal for peculiar velocity studies. A simple one-dimensional analysis detects no relative motion between the Local Group of galaxies and 60 FRCG's with redshifts of up to 15000 kms^{-1}. This is shown to imply a streaming motion of the cluster galaxies of at least 600 kms^{-1} relative to the CBR.

The second observational study is a reanalysis of the Rubin et al. (1976a,b) sample of Sc galaxies. Near-IR photometry is used in our reanalysis to minimise the effects of extinction and to facilitate the use of luminosity indicators in reducing the effects of selection biases. The velocity anisotropy found by Rubin et al. is confirmed with the new data, which excludes the possibility that extinction causes this effect.

The near-IR Tully-Fisher relation and the B-H colour-magnitude relation are used, to investigate whether the effect is caused by true bulk motions. Both relations are shown to be subject to strong biases and uncertainties resulting from the galaxy selection, and thus do not add significant information on the basis of the measured effect.

Monte Carlo simulations of the galaxy selection procedure undertaken by Rubin et al. are then described. These show conclusively that Malmquist bias, combined with an anisotropic sampling depth, can explain the whole effect, which therefore does not provide evidence for large scale galaxy streaming.

The consequences of these and other recent results are considered, with particular reference to the Hot Dark Matter vs. Cold Dark Matter controversy. A new study of the galaxy peculiar velocity field, using a new spiral galaxy sample, is then introduced.

ACKNOWLEDGEMENTS

There are many people who have helped to make the three years of my Ph.D research very enjoyable and fulfilling, but there are three I would particularly like to thank here. The first is of course my supervisor, Bob Joseph, who was a constant source of encouragement and ideas, and who has tried to give me, as with all of his students, a sense of the breadth and richness of astrophysics and cosmology. His enthusiasm and dedication will long remain a source of inspiration for me.

The other collaborator in the project described here, Chris Collins, must also receive my warmest thanks. He has spent many hours giving me the benefit of his deep understanding of cosmology, both on observing trips and during my many enjoyable visits to the Royal Observatory, Edinburgh. His friendship and hospitality, and that of his colleagues at ROE, are greatly appreciated.

During August and September of 1987, I was lucky enough to be given the opportunity to work at the Joint Astronomy Centre in Hawaii. This was a most enjoyable stay, made possible through the kindness of Gillian Wright, who both provided a roof over my head and her considerable experience of observing at UKIRT. I also benefited greatly from her knowledge of the wider aspects of extragalactic astronomy and image processing, during this and other observing trips in Hawaii. I also thank the rest of the JAC staff for a most enjoyable stay, at a very exciting time.

I would also like to acknowledge the day-to-day help and encouragement of my colleagues in the Imperial College Astrophysics group. Special mention should go to Martyn Wells, Simon Chase, René Doyon, Arvind Pattni and Jason Spyromilio for practical help and many interesting and informative discussions about physics. There are many others, too numerous to list, whose friendship and help is much appreciated, and from whom I beg forgiveness for not mentioning them individually.

Finally, I must thank my family, and particularly my mother and sister Katy, for their continuing support and encouragement throughout this period.

CONTENTS

ABSTRACT 2

ACKNOWLEDGEMENTS 3

LIST OF TABLES 7

LIST OF FIGURES 8

CHAPTER ONE INTRODUCTION

I Cosmological models

I.1 Description of structures of cosmological interest 12

I.2 The gravitational collapse of primordial density fluctuations 15

I.3 Non-gravitational collapse processes 19

I.4 Modifications to the standard (baryon dominated model) 21

I.5 The dark matter 24

II Observational tests of cosmological models

II.1 Galaxy catalogues and redshift surveys 28

II.2 CBR anisotropies 31

II.3 Structure at high redshift--quasars and primeval galaxies 32

II.4 Density enhancements and streaming motions 32

II.5 Observational searches for deviations from isotropic Hubble flow

II.5a The local velocity field 36

II.5b The large scale velocity field

i Studies which support significant streaming motions 38

ii Studies which find no significant streaming motions 41

iii Conclusions from previous streaming motion studies 44

CHAPTER TWO MEASUREMENT OF GALAXY STREAMING USING FIRST RANKED CLUSTER ELLIPTICALS

I The cluster galaxy sample and data

I.1 Suitability of first ranked cluster galaxies for streaming studies 45

I.2 The data 46

II Data analysis 50

III Solutions for the Local Group motion 53

IV Interpretation of the Local Group velocity relative to First Ranked Cluster Galaxies

IV.1 Comparison with the Local Group motion relative to the CBR 56

IV.2 Comparison with previous studies 58

IV.3 The effect of choice of frame on streaming solutions 60

CHAPTER THREE GALAXY STREAMING FROM AN ALL-SKY SAMPLE OF SCI SPIRALS

I The Rubin et al. (1976a,b) study

I.1 Galaxy sample selection 62

I.2 Rubin et al. data and analysis 63

II Criticisms of the Rubin et al. result

II.1 The Fall and Jones interpretation 63

II.2 Weaknesses in the Rubin et al. data and analysis 64

III A reanalysis of the Rubin et al. sample using near-IR photometry 65

III.1 Advantages of near-IR photometry 66

III.2 New data--near-IR galaxy photometry 68

III.3 Photometric corrections 72

III.4 Galactic and internal extinction corrections 75

III.5 Luminosity indicators

III.5a The B-H colour-magnitude relation 78

III.5b The Infrared Tully-Fisher relation 80

III.6 Solutions for galaxy streaming velocities 83

III.7 The importance of choice of <HM> 86

IV Estimating the likely impact of selection effects

IV.1 A 'Monte Carlo' simulation of selection effects 88

IV.2 Directionality in the Malmquist bias 97

IV.3 Conclusions from simulations of selection bias 101

CHAPTER FOUR COMPARISON OF RESULTS WITH PREVIOUS STUDIES, AND CONSEQUENCES FOR COSMOLOGICAL MODELS

I Related observational results

I.1 A comparison of recent studies of galaxy peculiar velocities 103

I.2 Other recent results of importance to cosmology 107

II Consequences for cosmological models 108

II.1 Neutrino-dominated cosmologies 109

II.2 The cold dark matter model 110

II.3 Other models--strings and isocurvature fluctuations 111

III Conclusions 112

CHAPTER FIVE FURTHER STUDIES OF GALAXY STREAMING MOTIONS

I A new study of the peculiar velocities of field spirals

I.1 Scientific justification 113

I.2 Use of modern instrumentation 114

I.3 Selection criteria 114

I.4 Observational methods: Photometry and luminosity indicators 119

I.5 Observations 123

I.6 Analysis of the new galaxy sample 123

II Further analysis of galaxy streaming using First Ranked Cluster Ellipticals 128

III Future work 130

REFERENCES 132

APPENDIX 139

PUBLICATIONS 150

LIST OF TABLES

TableNumber	Title	Page
2.1	Photometric and redshift data for 60 First Ranked Cluster Galaxies.	48
2.2	Solutions for Local Group motion, relative to the sample of 60 cluster galaxies.	54
2.3	Local Group motions derived from previous streaming studies.	59
3.1	Photometric and redshift data for 86 Sc galaxies from the Rubin et al. Minimum Bias Subset.	70
3.2	CBR-frame streaming velocities for the 86 MBS galaxies, using the Rubin et al. 'Hubble Modulus' technique.	85
3.3	CBR-frame streaming velocities for the 86 MBS galaxies, with <HM> varied to minimise streaming amplitude or errors.	87
5.1	Names, coordinates, approximate diameters and inclinations for the sample of 218 Sc galaxies.	115

LIST OF FIGURES

Figure Number	Title	Page
2.1	Sky distribution of 60 cluster galaxies from Sandage and Hardy (galactic coordinates).	51
2.2	CBR-frame velocity residuals for the 60 cluster galaxies, projected onto the galactic plane. The position of the 'Great Attractor' is also shown.	57
3.1	Sky distribution of 86 Sc galaxies from Rubin et al. (1976) (galactic coordinates).	69
3.2	Malmquist bias shown as a trend in absolute B & H magnitude with redshift for 86 Sc galaxies.	76
3.3	B-H colour-magnitude relation for 86 Sc galaxies.	79
3.4	H-band Tully-Fisher relation for 68 Sc galaxies.	82
3.5	Distribution of apparent B magnitudes for the 86 Rubin et al. galaxies.	90
3.6	The Schechter luminosity function for field galaxies, used for weighting the selection in the Monte Carlo simulations.	91
3.7	Distribution of streaming amplitudes for simulated data sets, using the Rubin et al. 'mean HM' type of solution and a Schechter luminosity function.	93
3.8	Directional distribution of streaming solutions for simulated data sets, using the Rubin et al. 'mean HM' type of solution and a Schechter luminosity function.	94

LIST OF FIGURES (contd.)

Figure Number	Title	Page
3.9	Distribution of streaming amplitudes for simulated data sets, using the Rubin et al. 'mean HM' type of solution and a flat luminosity function.	95
3.10	Directional distribution of streaming solutions for simulated data sets, using the Rubin et al. 'mean HM' type of solution and a flat luminosity function.	96
3.11	Distribution of minimised streaming amplitudes for simulated data sets, using a flat luminosity function.	98
3.12	Directional distribution of streaming solutions for simulated data sets, with a superimposed streaming of 600 kms^{-1} toward l=180°, b=0°.	99
3.13	Directional distribution of streaming solutions for simulated data sets, with a superimposed streaming of 600 kms^{-1} toward b=-90°.	100
5.1	Distribution of inclinations for the ScI galaxies in our new sample (black) compared with that for the Rubin et al. sample (shaded).	120
5.2	Sky coverage of 218 Sc spirals (galactic coordinates).	124
5.3	Linear diameter-redshift relation for galaxies in new sample with catalogued redshifts.	126
5.4	Calibration of the apparent diameter-redshift relation for the new sample of Sc galaxies.	127

LIST OF FIGURES (contd.)

Figure Number	Title	Page
5.5	Completeness of the new streaming sample as a function of redshift.	129

OBSERVATIONAL STUDIES OF THE GALAXY PECULIAR VELOCITY FIELD

CHAPTER ONE INTRODUCTION

In this thesis I will discuss an observational approach aimed at tackling two of the most fundamental problems in modern cosmology. These are the nature of the dark matter, which is indicated by a growing body of evidence to dominate the mass density of the Universe, and the processes by which the galaxies, clusters and superclusters we now observe came into existence. The method I have been using to attack these problems is to map the galaxy peculiar velocity field on scales of tens of Mpc. If this can be done to sufficient accuracy, it should enable us to place very stringent constraints on the cosmological models presently under discussion. The method is powerful since it probes the mass distribution more directly than measurements of the luminosity distribution can, given the uncertainties of differing mass to light ratios on different scales and in different environments. In addition, it is possible to make measurements on scales far larger than are available to other dynamical studies, and indeed on scales at which correlation function methods applied to redshift surveys become noisy and almost impossible to interpret. As with all techniques in observational cosmology, however, the results obtained from streaming motion studies are very sensitive to systematic effects resulting from, for example, poor sample selection or inappropriate data analysis techniques, and such problems will thus be examined very closely.

In this introductory chapter I will first give an overview of the most important features of the standard cosmological models in vogue at present, and the problems they pose. I will then discuss the various observational methods which have been used to try to answer these questions, concluding with those attempting to map the galaxy peculiar velocity field.

Chapters Two and Three will be devoted to an explanation of the methods, analysis and results of the two projects in which I have been involved, to measure large-scale streaming motions. The first of these involved the use of data taken from the literature on First Ranked Cluster Galaxies, which were used to test whether such galaxies define a rest frame identical to that of the Cosmic Background Radiation (CBR). The second was the reanalysis of a sample of Sc spiral galaxies, for which a previous analysis using optical photometry had derived a Local Group (LG) motion now seen to be discrepant with measurements of the CBR anisotropy. By using infrared photometry we addressed many of the inherent problems of these previous studies, and were able to test this claim more stringently.

Chapter Four will contain a comparison of the results from the above two studies with other similar studies in the literature, and will attempt to reach a consensus view with regard to the status of galaxy streaming. The consequences of these results for cosmological models, and in particular the nature of the dark matter, will then be considered.

Work carried out to date on a new long-term project aimed at measuring streaming for a new, independently selected sample of ScI spirals will be considered in Chapter Five. This will be concerned particularly with the selection of suitable galaxy samples for such work, in order that the biases which have thrown doubt on previous studies are minimised. This should enable peculiar velocities to be determined with the greatest possible accuracy over the largest possible volume. Chapter Five will conclude with a summary of the earlier chapters, and will point out some ways in which the observational and analytical techniques described in this thesis could be improved and extended in the future.

I COSMOLOGICAL MODELS

In order to define the aims of the observational projects to be described in chapters two and three, it is first necessary to describe the theoretical framework of modern cosmology, and the outstanding questions which these observations are likely to address.

I.1 DESCRIPTION OF STRUCTURES OF COSMOLOGICAL SIGNIFICANCE.

The motivation for the majority of cosmological scenarios currently being researched is the need to explain the existence of structures such as galaxies, clusters and superclusters. In the conventional Hot Big Bang cosmology, which will be assumed as the basis for all the models discussed here, the timescale for the formation of such structures is constrained by the age of the Universe and, more stringently, by the expansion factor since the matter decoupled from the radiation field now seen as the CBR. These time constraints, taken together with the isotropy of the CBR which strongly limits the amplitude of the fluctuations in the cosmic fluid at decoupling, make it difficult to explain the formation of structure by the present day. In order to explain the nature of these constraints, I shall first discuss the important classes of structure we observe.

Galaxies form the most obvious single class of objects of cosmological interest. They have masses typically in the range 10^{10} - 10^{12} M_o and, with the exception of a minority of disturbed or irregular examples, they have attained relaxed distributions. This is to be expected for objects of this size, particularly if violent relaxation processes can be invoked, assuming their ages are within an order of magnitude of the Hubble Time. The existence of two distinct populations of galaxies, spirals and ellipticals, may be of cosmological significance, reflecting some basic characteristic of the Universe at the time of galaxy formation. This could lead to varying degrees of dissipation as a function of the density and radius of collapsing regions (Jones 1988); however it may be explicable in terms of evolutionary processes such as proto-galaxy mergers (Larson 1987), which are of no direct relevance to the cosmological questions we are addressing here. The epoch of galaxy formation is a parameter that has been widely discussed, but no real consensus has been reached. One possible constraint is the existence of quasars with redshifts as high as 4.4, although with the nature of quasars remaining a controversial issue, this does not necessarily imply galaxy formation by a similar epoch. Indeed, as will be discussed later, many models indicate that galaxy formation probably occurred later than this.

The only objects smaller than galaxies which seem of sufficient importance to consider in cosmological models are globular clusters. These are tight, spherically symmetric, relaxed clusters of stars, with masses ranging from 10^4 to 10^6 M_o. Age estimates made from the turn-off point of the main sequence reveal highly evolved stellar populations, i.e. the stars making up globulars appear to have ages on the order of the age of the Universe. The strong inference is that the clusters now containing these stars are of similarly extreme ages. The accuracy of these estimates is the subject of a great deal of discussion, however, since it is by no means certain that the globular cluster ages do not contradict current estimates of the age of the Universe. They certainly impose a strong lower bound. The other characteristic of globulars which makes them of interest here is their ubiquity; they seem to represent a strongly preferred scale in the hierarchy of mass structures, strengthening the supposition that they may be amongst the earliest objects to form.

Moving to scales larger than those of galaxies, the pattern becomes less well defined, possibly as a result of the characteristic relaxation times of these structures being on the order of, or greater than, the time since decoupling. We are thus looking at objects presently undergoing collapse and relaxation, as is further suggested by the finding of bulk mass motions on these scales.

Looking first at galaxy clusters, there again seems to be a natural division between two distinct types of object, the regular and irregular clusters. Regular clusters have spherically symmetric density profiles with a degree of central condensation which suggests that they are dynamically relaxed. They are very rich, containing 10^3 - 10^4 galaxies within a diameter of only a few Mpc, and thus represent extreme density fluctuations. In spite of this, they are predicted to have relaxation times, via two body interactions, of 10^{16} - 10^{18} years. Clearly, some other process must have brought about the relaxed state implied by these mass distributions, and it seems likely that violent relaxation is involved. The Coma cluster, a particularly large and rich cluster, could relax in a time on the order of $2x10^9$ years if this were the case, but it should be noted that the resulting equilibrium state is somewhat indeterminate (Lynden-Bell and Wood 1968). This is important, since the velocity dispersions of galaxies within rich clusters are used in arguments for missing mass, which will be considered later.

Density enhancements associated with rich clusters can be traced out to some tens of Mpc (Chincarini and Rood 1975), although the crossing times for galaxies in these outer halos are far too long for them to have reached dynamical equilibrium. It is therefore to be expected that the dominant motion of these galaxies will be infall towards the centre of the density enhancement, at least in the outer reaches of the halo. There will be a region of complex motions at intermediate radii, where two-body gravitational interactions will have affected the velocity field, without having yet brought about an equilibrium state.

Irregular clusters are amorphous groupings of galaxies, with numbers of members ranging from a few to about a thousand, although the borderline between these clusters and the larger superclusters is anything but clear. They contain galaxies of all types, unlike the regular clusters which are composed predominantly of gas-poor elliptical and lenticular galaxies. There is no evidence for irregular clusters having undergone any substantial evolution towards equilibrium states- they represent only moderate density enhancements, giving evolution timescales, even for violent relaxation processes, that are longer than a Hubble Time.

The largest structures which have been identified with any degree of certainty are the superclusters (e.g. Shapley 1930, Shane & Wirtanen 1967, Bahcall & Soneira 1984; reviewed by Oort 1983). These have typical sizes up to an order of magnitude greater than those of the largest clusters, being around 50 Mpc rather than 10 Mpc, but they have much lower densities than the regular clusters. It is not yet clear whether they truly represent a separate class of objects, or whether clustering occurs on a continuum of

scales from the smallest clusters to the superclusters, or even beyond. Superclusters often have filamentary shapes (e.g. Bahcall et al. 1986), giving rise to the possibility that collapse and dynamical equilibration may have already occurred about the shorter axis or axes, whilst the crossing time in their longest dimension will certainly exceed the age of the Universe. We might then expect to see anisotropic collapse occurring, aligned with the longer dimension, a process of considerable relevance to the mass flow studies with which we are concerned here. The reality of such structures also requires a knowledge of the peculiar velocities of galaxies, which could be at least partially responsible for the structures found by Bahcall et al. (1986).

The structure of the Universe on the scale of superclusters is also remarkable for the presence of voids, supercluster-sized holes in which the number density of galaxies is possibly an order of magnitude lower than the average (Kirshner et al. 1981). There has been some doubt as to the reality of these voids, and in particular that they might be filled by Markarian galaxies (Balzano & Weedman 1982). However the consensus now seems to be that all types of galaxies, including dwarf, low surface brightness and Markarian galaxies, are significantly underdense in these regions, Markarians less markedly than other types (Thompson 1982, Bothun et al. 1986, Haynes 1986 & Oemler 1987).

It has been suggested that voids are distributed throughout the Universe like the holes in a sponge, with the superclusters lining the boundaries of the holes (de Lapparent et al. 1986). Whilst this model is only tentative, it does give some idea of the sort of velocity field we might expect to observe if such structures are still in the process of forming, or if the matter "walls" are further collapsing into large scale filaments. However, Peebles (1982) has shown that the voids themselves could have been made without large galaxy peculiar velocities, so we should not expect to find significant galaxy streaming out of voids. This is because small voids in the early universe would grow with the expansion, whilst peculiar velocities would diminish. Thus only small velocities would be required if the voids formed at an early epoch, and these would have 'redshifted away' to an undetectable level by the present.

I.2 THE GRAVITATIONAL COLLAPSE OF PRIMORDIAL DENSITY FLUCTUATIONS

I will now consider how the structures outlined above could have formed via a process of gravitational collapse from primordial density fluctuations. We will not be concerned

here with the details of how objects with the specific characteristics of, say, spiral galaxies can form; for the purposes of arriving at a valid cosmological model we will be content with showing that density enhancements on the appropriate scales could become non-linear by the present day. Indeed, given the constraints imposed by the CBR isotropy, which severely limit the size of fluctuations present at decoupling, even this restricted condition proves hard enough to satisfy.

Over the largest scales, gravitational collapse processes are always likely to dominate. The long range nature of the gravitational force, the lack of repulsive effects and the interaction of gravity with all types of matter make collapse inevitable given enough time. It thus becomes important to try to determine scales on which gravitational collapse is prevented, either because the timescale is long compared with the time since decoupling, or because gas pressure or some other effect stabilises matter against collapse. The spectrum of the primordial density fluctuations is obviously important in determining the size of the objects likely to be the first to separate out from the general expansion, and collapse.

A central concern when postulating galaxy formation mechanisms is to find a way to produce a fluctuation spectrum with power on scales fitting the presently observed clustering hierarchy. Knowledge of the large scale velocity field enables us to extend this to a study of the scales on which structure is presently forming. As an example, there is as yet no firm evidence for the clustering of superclusters into yet larger structures, but the measurement of coherent large scale streaming motions might indicate that such super-superclusters are in the early stages of formation.

Since the nature of the initial fluctuations largely determines the subsequent evolution of structure, it is worth trying to understand what forms these are likely to have taken. Two modes have been identified (see, e.g. Peebles 1980), which are conventionally termed adiabatic and isothermal. Isothermal fluctuations are fluctuations of the matter density only, the radiation field remaining unperturbed; adiabatic fluctuations affect both the matter and radiation fields according to the relation:

$$\frac{\delta\rho_r}{\rho_r} = \frac{4}{3}\frac{\delta\rho_m}{\rho_m} \qquad 1.1$$

Isothermal and adiabatic fluctuations evolve independently of one another as long as the wavelength of the perturbation is very much less than (ct), where t is the characteristic

time for contraction or expansion. Any fluctuation can be represented as the sum of isothermal and adiabatic components.

Models in which isothermal fluctuations dominate predict that the earliest structures to form after decoupling should be small, of the same order as the Jeans mass after decoupling, i.e. about 10^6 M_o (Peebles, 1965). Fluctuations smaller than this tend to oscillate, and are damped out by photon diffusion during the decoupling era. The nature of these first structures is not defined by the theory, but it is suggestive that the masses are roughly those of globular clusters. It has also been postulated that they might be massive individual stars, the rapid and catastrophic evolution of which can then be used to explain some aspects of the later development of structure.

If adiabatic fluctuations dominated prior to decoupling, the preferred mass scales for the earliest structures, post-decoupling, are very much larger. The characteristic mass is fixed by the smallest adiabatic perturbations that can escape being dissipated by photon diffusion. Detailed calculations put this limit at 10^{12} - 10^{14} M_o (Silk 1967), corresponding to large galaxies or to moderately rich clusters respectively. There are reasons for preferring adiabatic over isothermal fluctuations, since they are a consequence of the inflationary models, to be discussed in section I.4.

Whether isothermal or adiabatic fluctuations were in fact dominant determines the order in which structures form. The isothermal-dominated picture has small, sub-galaxy sized objects forming first, which then cluster successively to form the galaxies, galaxy clusters and superclusters we now see. This process is known as hierarchical clustering. Adiabatic fluctuations will tend initially to produce large scale structures, possibly as large as superclusters, which must then break up into objects with smaller masses, a process known as fragmentation. Since the overdensity is unlikely to to be spherically symmetric, the initial evolution of these large scale structures is likely to be infall predominantly along one axis, leading to 2-dimensional "pancake" structures (Zeldovich 1970). These in turn might be expected to evolve further into 1-dimensional filamentary structures. Neither the adiabatic nor the isothermal model has yet been shown to be in obvious disagreement with the observed properties of the mass spectrum, and one of the attractions of measuring streaming velocities is that they may be able to discriminate between the two.

More recently, attention has focussed on isocurvature fluctuations, an alternative to the isothermal scenario, in which the space curvature is unperturbed but the baryon number is clustered (e.g. Peebles 1987a). Thus fluctuations in relativistic matter (radiation and

possibly neutrinos) must be such as to cancel the fluctuations in the baryon density. This model is essentially ad hoc (as is the isothermal model) in that such fluctuations do not arise naturally prior to decoupling, except possibly in axion dominated models (Bardeen et al. 1987). However, it does have attractive features in that the first generation of objects to form have masses roughly equal to those of galaxies, and there is a relatively greater amount of power in the fluctuation spectrum on large scales (to 200 Mpc) compared to other models. This latter feature is important in explaining the evolution of clustering and superclustering, and gives larger predictions for the size of galaxy peculiar velocities smoothed over these scales.

In all these models, a significant quantity in determining which of the initial fluctuations will be able to develop is the Jeans mass (Jeans 1902), a mass limit above which it becomes impossible for internal pressure to support a gas cloud against gravitational collapse. This mass is given for the non-relativistic case by the following expression:

$$M_J = (4\pi m_H n/3)(\pi v_s^2/G\rho)^{3/2} \qquad 1.2$$

where m_H is the mass of the hydrogen atom, n is the total baryon number density, v_s is the adiabatic sound speed and ρ is the mass density. Any fluctuations having a mass greater than this limit under the conditions prevailing will then undergo essentially free-fall collapse. Knowledge of the value of the Jeans mass throughout the evolution of the Universe has long been regarded as an important way of defining preferred mass scales, since pure gravitational processes do not themselves yield any. The Jeans mass between the matter domination epoch and recombination is $\sim 10^{17}$ M_o, falling to $\sim 10^6$ M_o at recombination (Primack 1984). If 10^6 M_o objects are the first to form, a process of hierarchical clustering is the expected to form galaxies, clusters and superclusters successively.

There are several problems with the simple picture in which primordial fluctuations develop via gravitational instability into the structures observed today. The principal one is the timescale apparently required for the growth of the slight perturbations implied by the CBR isotropy into dynamically-relaxed objects such as galaxies and regular clusters. Gravitational instability can bring about rapid collapse and relaxation of extreme density perturbations, but the initial stages of collapse from near homogeneity seem to demand excessive lengths of time. Such constraints are particularly severe for the adiabatic case, since all density enhancements will be reflected in corresponding temperature changes in the CBR, with $\frac{\delta T}{T} \approx \frac{1}{3}\frac{\delta\rho}{\rho}$. Observations constrain $\frac{\delta T}{T}$ to be less than 1 part in 10^4 over a wide range of angular scales (Fomalont et al. 1984, Uson & Wilkinson 1984,

Mandolesi et al. 1986, Kaiser & Silk 1986). This is surprising since the density fluctuations $\frac{\delta\rho}{\rho}$ grow as $(1+z)^{-1}$ and hence can only have grown by a factor of $\sim 10^3$ since decoupling. Thus we would expect that non-linearity by the present epoch would only occur for fluctuations causing temperature fluctuations $\frac{dT}{T} \sim 3\ 10^4$. This might be seen as an indication favouring isothermal models, since it is possible to "hide" mass fluctuations which are not reflected in the radiation field, but there are other reservations in this case. It is not clear how such fluctuations might arise in the first place, whereas adiabatic fluctuations are specifically predicted to arise on the assumption of an inflationary phase in the early Universe. Fragmentation processes are also generally considered to give rise to the observed structures more naturally than would hierarchical clustering. The isocurvature model shows possibly the greatest promise in explaining the formation of structure over the required range of scales without violating the CBR isotropy. However, all models appear to have sufficiently serious shortcomings that there is a need to look for some additional factor. The consensus appears to be that this is probably a background of some type of dark matter, for which there are several independent indications. This and the related biasing processes will be considered below, but we will first look briefly at some other alternatives.

I.3 NON-GRAVITATIONAL COLLAPSE PROCESSES

Non-gravitational processes have frequently been applied to the problem of structure formation, but none have seemed likely to challenge gravitational collapse as the dominant effect. This does not prevent their playing a vital role in some aspects of the structure-forming process, and it is primarily in this light that they will be discussed.

Primeval turbulence has been considered as a process potentially able to bring about the rapid formation of structures on all scales, even down to planetary systems (von Weizsäcker 1951). The cosmic fluid in the early Universe is postulated to be subject to turbulent motions, with vortex-type irregularities developing on all scales corresponding to present day structures, arranged in a hierarchical fashion. The turbulent motions can then be assumed to dissipate their kinetic energy via collisions and shocks, collapsing rapidly. The resulting objects would be expected to have net angular momentum, which is in accordance with observations.

Problems with this model include the need for the initial turbulence, since there seems no way of generating it from an initially kinematically quiet expansion. Gravitational torques on asymmetric overdense regions will have some effect, possibly enough to explain the

presently observed angular momentum of structures, but not enough to bring about rapid dissipation and collapse (Peebles 1969). This model has the additional problem of not leading to naturally preferred scales, which thus require additional mechanisms. Most troublesome is the finding that turbulence tends to dissipate too rapidly, forming high density objects well before galaxies could have formed (Peebles 1971). It appears that this disagreement can be avoided only by a fine-tuning of parameters, which diminishes the appeal of the model.

Even though turbulence appears untenable as the dominant structure-forming process, it is likely to play some part in determining the nature of structures formed by other mechanisms. This is because any turbulence, even if initially weak, is likely to give rise to a net angular momentum for any finite volume of collapsing matter, which, if conserved during collapse, will stabilise the object at a given radius in the plane of rotation. The most obvious examples of rotation-supported flattened structures are spiral galaxies. It remains to be seen whether this is the case for clusters, superclusters and beyond. This is an interesting possibility which might be investigated via velocity field studies.

Gas dynamic effects may play an important part in the rapid formation of highly condensed masses. Cooling flows provide a well studied example of how hot interstellar gas can have cooling times via radiative energy loss which are shorter than free-fall times (Fabian et al. 1984), and it seems likely that such processes should be included when considering the post-decoupling evolution of overdensities.

Some consideration has also been given to the effects of a primordial magnetic field, which could interact with the ionised component of matter in the early Universe to produce a spectrum of density enhancements. Magnetic fields could also affect the collapse of overdensities (Wasserman 1978), since matter will tend to move along field lines rather than perpendicular to them, and magnetic coupling may be important in transferring angular momentum from rotationally supported structures to the surrounding medium.

Finally, it may be useful to consider the possibility of explosive events resulting from the earliest objects. The proposal that 10^6 M_o stars may result from the development of isothermal fluctuations gives rise to an extreme form of this scenario, but any primeval stars with masses greater than about 10 M_o would be likely to evolve to a supernova stage in time to affect the formation of neighbouring structures. This could provide a form of negative feedback, inhibiting the growth of structures in the near vicinity of

these first generation objects, in a variant of the biasing mechanisms (see e.g. Rees 1985) to be discussed later.

I.4 MODIFICATIONS TO THE STANDARD (BARYON DOMINATED) MODEL.

We will now take a look at the currently popular scenarios in which there is an additional "dark" component of the matter, underlying the luminous, presumably baryonic matter we observe. The evidence for the existence of dark matter, the indications of its possible nature, and the effect it could have in solving the problems of structure formation will be evaluated. The possibility of discovering more about the nature of the dark matter is one of the principal motivations for undertaking streaming motion studies, and so the predictions of the models for different dark matter candidates are of particular importance for the present work.

The existence of a non-luminous matter component was first inferred from the application of the virial theorem to clusters, and studies of the rotation curves of the outer parts of spiral galaxies. For all reasonable values of the Hubble constant, which effectively sets the linear scales and the absolute magnitudes involved, the total masses required to bind these structures gravitationally exceed the masses derived from studies of individual galaxies, by a factor of about 30. This has been the subject of much discussion (reviewed by Faber and Gallagher, 1979), but the consensus is that galaxies are associated with matter in addition to that composing the stars, gas and dust which can be observed directly.

Extension of these dynamical studies to larger and smaller scales shows a general trend towards higher mass-to-light ratios with increasing scale (e.g. Faber & Gallagher 1979). This indicates an underlying mass distribution that is less clumped than the visible mass distribution, and thus dominates more on larger scales. It should be noted that studies which depend on the dynamics of objects moving in a gravitational potential can only put lower bounds on the total mass, since there could exist an arbitrarily dense component, smooth on the scales observed, superimposed on the measured mass distribution, which would not affect the dynamics in any way. Such a component would have to be constrained by other methods, such as detections of the particles comprising it.

The arguments for missing mass are strengthened by the attractiveness of inflationary models for the development of the early Universe (Guth 1981). An inflationary episode elegantly explains several features of the global properties of the Universe which would

otherwise have to be introduced as initial conditions. These include the isotropy of the CBR around the sky, the homogeneity of the large scale matter distribution, and the so called monopole problem. The isotropy of the CBR is hard to understand, since it appears that the radiation from different directions must be coming from regions of the last scattering surface which have never been in causal contact, and yet still appear to be at identical temperatures. For similar reasons, it is hard to understand how the large scale structure of the Universe appears so homogeneous, if the structure we now see has developed from a number of causally non-connected regions. Finally, the monopole problem concerns predictions that large numbers of magnetic monopoles, or point discontinuities, should be left behind from a phase transition in the early Universe. The present density of these as calculated from the expected number density and individual masses should be very much larger than the present estimates of the total density of all matter (Preskill 1979, Zeldovich & Khlopov 1979). The existence of a large-scale cosmic magnetic fields also limits the number of monopoles, which tend to discharge such fields (Parker 1970). Finally, laboratory experiments indicate that the number density of monopoles is well below theoretical predictions.

The inflationary scenario solves all of these problems by postulating that all of the matter we presently observe was originally in a small, causally connected region, which was then rapidly inflated to encompass a region larger than the present horizon size. Since the radiation field was in equilibrium prior to inflation, and the inflation is thought to expand all matter and radiation smoothly, it is no surprise that the radiation field coming into the horizon is isotropic. The large scale homogeneity arises naturally if the region before inflation was itself smooth and homogeneous. The monopole problem is also solved since the number density of all particle species would be decreased by an enormous factor during inflation. Whilst Guth's original formulation of inflation has since been shown to be flawed in that the universe never escapes from the inflationary phase, more recent refinements (reviewed by Barrow & Turner 1982) have overcome most of the problems and the scenario is still probably tenable.

The main discrepancy between the resulting universe and observation is that inflation predicts a critical density Universe. to a high degree of accuracy, if the inflation increases characteristic scales by a large factor. The estimates from even the largest scale dynamical studies (such as Virgo infall measurements, below) put the value at no more than a third of this. This is probably not a serious problem, however, and indeed the near coincidence, with a mere factor of $\approx$3-5 difference between the observed and theoretically expected values, is sometimes taken as further evidence for the correctness of the inflation hypothesis.

Reconciling theory and observation can be done in two ways: either we must accept that our mass estimates are too low, and there is an unobserved component of matter making the total up to critical density, or we must try to alter the inflation so as produce a sub-critical density universe. The latter course is possible, given just the right amount of inflation, but is regarded as being unsatisfactory in the high degree of fine tuning required, since any small deviation from critical density immediately after inflation would be increased enormously by the present epoch. A critical density universe can be explained by any amount of inflation larger than a certain amount, so no fine tuning is required in this case.

An important consequence of inflationary models in the present context is that they predict a specific form for the initial fluctuation spectrum. Density fluctuations are expected to arise from quantum fluctuations in the scalar field which drives the inflation, affecting both the matter and radiation. These are adiabatic perturbations, with a scale-invariant spectrum (Guth and Pi 1982). This requires a power-law fluctuation spectrum of the type discussed by Harrison (1970) and Zeldovich (1972):

$$\frac{\delta\rho}{\rho} \propto M^{-\alpha} \qquad 1.3$$

The value of the index α is constrained to be ≈ 0 by the requirement that the universe be more homogeneous on large than on small scales, and to prevent the formation of numerous black holes from small scale fluctuations.

If the Universe is dominated by non-luminous matter, it is obviously vital that we should discover what form this matter is in. It is very unlikely that a critical density could be composed solely of baryonic matter, due to limits imposed by the observed light element abundances, and especially that of deuterium. These elements are thought to have formed in the early Universe, and their abundances provide a good diagnostic of the prevailing conditions at that time. These "nucleosynthesis" constraints put limits on the present value of the quantity $\Omega_b h^2$, where Ω_b is the present density of baryonic matter in units of the critical density, and h is the present value of the Hubble constant, in units of 100 kms^{-1} Mpc^{-1}. The observed abundances of deuterium and ^4He, corrected for the amounts thought to have been produced and destroyed in stars and the interstellar medium, place strong constraints on $\Omega_b h^2$ for a given CBR temperature, via the following inequality (Primack 1984, following Yang et al. 1984):

$$\Omega_b h^2 < 0.035\ (T_\odot/2.7K)^3 \qquad 1.4$$

For h in the region 0.5 to 1, as is conventionally accepted, $\Omega_b=1$ is definitely ruled out. If we are to accept the arguments for a critical density universe as conclusive, it appears we must accept that on the order of 90% of matter in the universe is both non-baryonic and non-luminous.

Making this assumption immediately helps to solve the problem mentioned above concerning the time required for present structure to form, given the isotropy of the CBR. We can now relax the CBR constraints on decoupling-epoch density perturbations, if weakly interacting particle species, such as massive neutrinos, make up the dominant mass. Such a matter component would decouple from the remainder of the matter and radiation well before the baryon decoupling era, and could then form mass structures which would not necessarily be reflected in the radiation field. The baryonic matter would then be able to fall into the potential wells around these overdensities as soon as it decoupled from the radiation, hastening the otherwise slow initial stages of collapse.

Thus it is possible to say from these simple arguments that the dominant matter in a critical density universe is likely to be non-baryonic, and that there are some indications that it should be weakly interacting, at present affecting the visible matter only via gravitational interactions. This still leaves room for a wide range of candidates for the missing matter, with, as it turns out, important consequences for predictions of large scale streaming motions. We will now examine the two main candidates for this dark matter.

I.5 THE DARK MATTER

The main debate about the nature of the dark matter, and the question of most relevance to large scale streaming motions, is whether the particles concerned were relativistic or not at the time of baryonic decoupling. This is of great importance since it has a strong influence on the minimum scales on which the matter can clump, and hence on the development of structure.

The leading candidate for relativistic or "hot" dark matter is massive neutrinos, although some other possibilities have been suggested. While there have been claims to have detected the rest mass of the electron neutrino, it should be pointed out that the evidence is tenuous at best, with the only positive measurements, by one group (Lyubimov et al.

1980), remaining unconfirmed despite several attempts. However, since most of the other dark matter candidates are particles not even known to exist, it is clear that we have no choice but to proceed at this speculative level. Taking massive neutrinos as our preferred candidate, therefore, we will now look at the predictions of the hot dark matter (HDM) model for the development of structure.

The laboratory measurements of the neutrino rest mass indicate, however tentatively, a mass of about 20 eV, a figure in reasonable agreement with the requirements for critical density (Bond et al. 1980), given estimates of the total number of neutrinos "freezing out" in the early Universe. More recent attempts to measure or place upper limits on the masses of neutrinos from the arrival times of neutrinos detected from supernova 1987a in the LMC have proved contradictory. Under the assumption of simultaneous emission of neutrinos, the arrival time spread of a few seconds might suggest masses of the electron, muon and tau neutrinos in the right region for them to comprise the dark matter (e.g. Hillebrandt et al. 1987). This interpretation seems contrived, and the balance of opinion would appear to be that the supernova data support a zero rest mass for the neutrino, with an upper limit of ≈ 5-10eV (Arnett & Rosner 1987, Bahcall & Glashow 1987). The question remains very much open, however.

Neutrinos would decouple from the baryonic matter well before the baryonic decoupling era, and interact only via the gravitational force from that time onwards. They would remain relativistic until after baryonic decoupling, with important consequences for the characteristic sizes of structures formed. This arises since such particles stream relativistically out of any overdensity (Silk 1968) from the time they decouple until the temperature drops to a value at which they become non-relativistic. Thus this free-streaming has the effect of preventing the growth of small-scale fluctuations. The smallest mass which can avoid erasure by this streaming process is referred to as the free-streaming Jeans mass (Bond et al. 1980, Bond & Szalay 1983):

$$M_J = 3.2 \times 10^{15} (m_\nu/30\text{eV})\, M_\odot \qquad 1.5$$

This mass is of order 10^{15} $M_\odot$ for neutrinos of mass 20 eV.

Thus, in a neutrino dominated model, supercluster-sized objects must be the first to form, with baryonic matter falling into fluctuations of this size in the neutrino density, as soon as it decouples from the radiation. Fragmentation must then occur to produce smaller scale objects. The important aspect of this model for the purposes of this discussion is that these early large scale overdensities will tend to produce streaming

motions on similar scales, which could be on the order of several 100's of kms^{-1} on 100 Mpc scales by the present epoch (Schaeffer and Silk 1984).

The main problem with this model, apart from the doubts about the neutrino mass, is that the predicted epoch of formation of galaxy sized objects is at redshifts < 2 (Klypin & Shandarin 1983; White, Frenk & Davis 1983; Centrella & Melott 1983; Dekel & Aarseth 1984) in direct contradiction to the observations of galaxies at redshifts of 3 (Djorgovski et al. 1985; Lilly 1988) and quasars at redshifts greater than 4. There are additional problems from the observation that the amount of dark matter trapped by rich clusters compared with galaxies is not as large as would be expected from this model, and difficulties in producing the amount of small scale clustering actually observed (Schaeffer & Silk 1984). This also leaves unanswered the question of the nature of the dark matter in dwarf spheroidal galaxies (Tremaine and Gunn 1979), which cannot be comprised of neutrinos if these have a mass of <500 eV. This arises from limits on the neutrino phase-space density, which gives the following lower limit for the neutrino mass, if they comprise the dark matter halo in these galaxies, assuming an isothermal distribution (Primack 1984):

$$m_n > (120eV)(100kms^{-1}/\sigma)^{1/4}(1kpc/r_c)^{1/2}(g_\nu/2)^{-1/4} \qquad 1.6$$

where σ is the one-dimensional velocity dispersion, r_c is the core radius of the isothermal sphere, and g_ν is the total number of neutrino species (particles plus antiparticles). Whilst it is possible that the dark matter here is of a different form to that making up the majority of the Universe, it is clearly more elegant if we can explain all dark matter problems with a single hypothesis. On the other hand, it should be noted that doubt has recently been cast on the strength of the evidence for excess non-luminous matter in dwarf galaxies (Godwin & Lynden-Bell 1987).

Because of these problems, the hot dark matter model has generally been neglected recently in favour of those invoking non-relativistic, cold dark matter (CDM), which leads to a quite different picture of the evolution of structure. There is probably even more uncertainty about the nature of the particles which could make up such matter, and certainly no known particle species seems to have the required properties. The essential characteristics are that the matter should be made up of weakly interacting massive particles which would be non-relativistic by the time they decoupled, so that free-streaming would be negligible. All fluctuations in the dark matter density would be able to collapse, forming potential wells on a large range of scale sizes. After baryonic decoupling, baryons could fall into any of these overdensities with mass greater than the

Jeans mass. For baryonic matter at decoupling, this is about 10^5 M_o, and it is therefore expected that such masses will be the first to collapse. There are indications, however, that gas clouds of this size will not be able to cool efficiently (White and Rees 1978) and that masses in the range 10^9 to 10^{12} M_o may cool and complete their collapse most rapidly. This mass range conveniently brackets the observed masses of galaxies.

The basic evolutionary picture in a CDM dominated Universe is the almost simultaneous formation of small scale structures, probably globular cluster- or galaxy-sized, clusters and superclusters (Davis et al. 1985). An important question then is how the structures formed by the baryonic matter reflect the underlying distribution of the dark matter. They obviously cannot have the same distribution since the dark component would then be reflected in the masses indicated by the dynamical measurements. The realisation that there is not a one-to-one correspondence between the luminous and dark matter distributions leads to the concept of 'biased' galaxy formation.

The idea of biasing first arose when it was found that the first numerical simulations involving CDM did not fit the observed amplitude and scale of galaxy clustering (Davis et al. 1985). In particular, it was impossible to match both the slope and the amplitude of the galaxy correlation function at any stage of the simulations with the presently observed values. In order to give better agreement, it was assumed that galaxy formation probability is a very non-linear function of the background density. Galaxies are then conjectured to form only at peaks in the mass distribution, with all fluctuations which do not reach this critical level having no effect on the formation of luminous structures, even though they might be important in determining the overall mass distribution (Kaiser 1984). It should be noted that biasing in the opposite sense (i.e. mass *more* clustered than galaxies) has been postulated to explain some of the problems of HDM models (e.g. Braun et al. 1988).

The model of CDM with biasing has become widely accepted over the last couple of years, since it does seem to be able to give the best fit to the observed properties of the Universe. However, there are problems in accounting for some of the large scale features of the Universe, such as voids (Kirshner et al. 1981), and it may be that the good agreement in other respects is a result of the number of free parameters made available by the choice of dark matter and the type of biasing. The most interesting point about biased CDM models for the present work is, however, the predictions of streaming velocities. Due to the nature of the biasing described above, the distribution of mass is predicted to be much smoother than would be inferred by assuming that mass traces light (Dekel 1986). Moreover, the absence of damping by free-streaming means

there are relatively more fluctuations on small spatial scales. As a result, the induced large scale streaming motions are predicted to be very small indeed, < 100 kms^{-1} on 60 h^{-1} Mpc scales (e.g. Vittorio and Turner 1987). This is one of the first testable predictions of this model, and if large motions on these scales can be detected and confirmed, they would certainly weigh very heavily against biased CDM models.

One other possibility which is currently attracting attention is that "cosmic string" may be at least partially responsible for forming the initial density enhancements. Cosmic string, like magnetic monopoles, is thought to be produced in the phase transition driving inflation (Kibble 1976). Indeed, inflation is not a necessary consequence of this phase transition, whereas cosmic string and monopoles seem to arise inevitably. The string is essentially a one-dimensional discontinuity in space-time, with a mass per unit length thought to be $\sim 10^{21}$ kgm^{-1} (Turok 1986). It is initially formed in a connected, "random walk" distribution, but is thought to evolve into a series of daughter loops by a process of intersecting with itself. These massive loops could then interact with the cosmic fluid, producing structures on scales which would depend in part on the type of matter dominating the density. The full consequences of incorporating cosmic string into cosmological models have not yet been examined, although early results from N-body simulations seem promising (Turok 1985), and it does seem likely to ease the problems caused by the CBR constraints.

II OBSERVATIONAL TESTS OF COSMOLOGICAL MODELS

In this section I will review the observational methods presently under investigation which appear capable of discriminating between the different cosmological models discussed above.

II.1 GALAXY CATALOGUES AND REDSHIFT SURVEYS

Galaxy catalogues provided the opportunity for some of the earliest observational tests of cosmology (e.g. Shapley 1930 and subsequent papers), and continue to be useful as deeper, more complete and more homogeneous catalogues become available. The simplest use to which such catalogues can be put is the largely qualitative one of delineating the types of structure in the galaxy distribution. The discovery of superclusters, galaxy voids and the possible filamentary structure in the galaxy distribution all required the existence of databases of large numbers of galaxy positions

and redshifts, with some understanding of the selection systematics so that the reality of the structures thus revealed could be estimated.

However, this approach has remained basically qualitative, despite attempts to develop methods of analysis, such as percolation (Bhavsar & Barrow 1985), to determine the reality and significance of the large scale structure thus discovered. This makes it difficult to constrain models using such methods alone. The most widely used statistical technique applied to the galaxy distribution is the correlation function, which estimates the excess probability over random chance of finding galaxies around any particular galaxy, as a function of separation. The function usually calculated is $\xi(r)$ (Peebles 1980), defined such that

$$\langle n \rangle = n\delta V_1[1+\xi(r_1)] \qquad 1.7$$

where $\langle n \rangle$ is the mean number of galaxies found in a volume δV_1, of radius r_1, centred on a random galaxy.

For galaxy catalogues without redshifts, this test can be applied to the angular separations of galaxies on the sky, although projection effects tend to wash out much of the true correlation and the technique is thus less sensitive. The function calculated in this case is $\omega(\theta)$, such that

$$\langle n \rangle = n[1+\omega(\theta_1)]\delta\Omega_1 \qquad 1.8$$

where $\langle n \rangle$ is the mean number of galaxies in a solid angle $\delta\Omega$ centred on a random galaxy. This angular correlation function has the advantage that many more galaxies can normally be included than is the case if redshifts are required.

Over small separations, Groth and Peebles (1977) found the angular correlation function to be well approximated by:

$$\omega(\theta) = A\theta^{-\delta} \; ; \quad \delta = 0.77\pm0.04 \qquad 1.9$$

The spatial correlation function can be derived from this, and is given by:

$$\xi(r) = (r_o/r)^{\gamma} \; ; \gamma = 1.77\pm0.04 \qquad 1.10$$

This power-law form for the function was found to continue out to separations of ≈2.5°, at which scale a sharp break was observed and the correlation function began a rapid fall-off. This was interpreted as evidence for a preferred clustering scale of ≈9 h^{-1} Mpc. More recent studies tend to find a somewhat lower value for this scale. Shanks et al. (1980) and Stevenson et al. (1985) found a break at an angular scale corresponding to 3 h^{-1} Mpc from scans of UK Schmidt and AAT plates, whilst Shanks et al. (1983) found a break scale of 5-6 h^{-1} Mpc for a sample of 340 galaxies with redshifts.

Recently attempts have been made to calculate the correlation function for rich clusters of galaxies (Bahcall and Soneira 1983). The large amplitude discovered for the cluster-cluster correlation function, up to ≈30 h^{-1} Mpc, has proved very hard to reproduce in numerical models, and if confirmed should prove an important measurement, since it requires large amplitude fluctuations on 10-30 Mpc scales which do not arise naturally in most models. However, there are now indications that selection effects are at least partially responsible for the measured cluster-cluster correlations (Sutherland 1988, discussed in more detail in Chapter 4).

Correlation function methods have the strength that they are well-defined statistical tests which can readily be compared with analytical models or numerical simulations of galaxy formation. Thus, the galaxy-galaxy correlation function has been used as the principal method of normalising the CDM N-body simulations which have been the basis of the most influential theories of galaxy formation in recent years (see, e.g., White et al. 1987).

There are deficiencies in the correlation functions as defined above. Kaiser (1987) has demonstrated that spatial correlation functions may be biased by peculiar velocities, which may either enhance or smooth out real spatial structures. They are not sensitive to the morphology of the galaxy distribution, and are, for example, notoriously insensitive to filamentary structures (Oort 1983). As such, they can not be considered to give a full description of the nature of galaxy clustering. Another weakness is that, by definition, correlation functions only probe the luminous matter distribution which almost surely does not trace that of the dark matter. Since the theoretical models describe the evolution of the total matter distribution, this weakens the constraints that can be put on such models from correlation functions. An interesting future investigation would be the correlation between the Lyman α clouds and galaxies, which would give information on the evolution of clustering and the nature of any biasing mechanisms (Davis 1985).

Finally, galaxy catalogues are being increasingly used to determine dipole anisotropies in the galaxy distribution around the sky (Yahil et al. 1986, Meiksin and Davis 1986, Lahav 1987). This is clearly a very crude measure of the galaxy distribution, but it is useful to compare the bulk distribution of luminous matter with the galaxy peculiar velocity field. This question will be discussed in more detail later. For light dipoles derived in this way to be believable, it is necessary for the galaxies to be selected in a homogeneous fashion, which is why the result which has attracted most attention is the "IRAS dipole", a North-South anisotropy in the distribution of galaxies detected by the IRAS satellite at far-IR wavelengths (principally 60μm). This selection avoids many of the biases inherent in selecting galaxies from catalogues with ill-defined selection criteria, but may also introduce some others. Several interesting new results in this field are discussed in Chapter 4.

II.2 CBR ANISOTROPIES

The discovery of the Cosmic Background Radiation at microwave frequencies (Penzias and Wilson 1965) has provided the only direct probe of the nature of the Universe beyond a redshift of ≈4. In the simplest cosmological models, the radiation we see has remained essentially unchanged since the radiation field decoupled from matter at redshifts of ≈1400. Barring later reionisation of the matter, which could smooth out the radiation field, the radiation must bear the imprint of any fluctuations present at decoupling. This effectively defines the initial conditions from which the production of structure must occur, and consequently the amplitude of CBR fluctuations is a key observational parameter.

To date, however, the only convincing departure from isotropy that has been discovered is the pure dipole variation in the temperature of the radiation field, of amplitude ≈3mK. This is most easily explained as being of local origin, being simply a reflection of the motion of the Local Group of galaxies at 610 kms^{-1} through the CBR, toward galactic coordinate l=272°, b=30° (Lubin and Villela 1986). Repeated searches for anisotropy on angular scales from several degrees down to minutes of arc (Fomalont et al. 1984, Uson & Wilkinson 1984, Mandolesi et al. 1986, and others, reviewed by Kaiser & Silk 1986) have failed to find convincing evidence for any departure from isotropy.

The limits are already at the level where several models are excluded, particularly those in which the mass density is dominated by baryons. The most powerful constraints arise considering the CBR isotropy jointly with other measurements such as the cluster-cluster

correlation function or the galaxy peculiar velocity field (Juszkiewicz et al. 1987). These joint constraints will be discussed in detail in Chapter Four.

Future studies aimed at detecting lower level fluctuations in the CBR, or at least pushing the limits down further, are clearly amongst the most important observations to be made in cosmology.

II.3 STRUCTURE AT HIGH REDSHIFT--QUASARS AND PRIMEVAL GALAXIES

One parameter of great interest is the epoch at which galaxy formation occurs, since the predictions of when this occurs are strongly model-dependent. Whilst the discoveries of quasars at redshifts of ~4 is of great interest, the extreme nature of these objects means that they do not constrain the epoch of formation of 'normal' galaxies. What is required is the detection of a young galaxy or protogalaxy which can plausibly be considered an earlier evolutionary stage in the formation of galaxies like those seen at low redshift. The redshift of such an object, or preferably several such objects, would then place a strong lower limit on the epoch by which galaxy formation should have taken place.

To date, no such primeval galaxies have been found, despite several optical and infrared searches (Partridge & Peebles 1967a,b, Davis & Wilkinson 1974, Koo & Kron 1980, Boughn et al. 1986, Collins & Joseph 1988). One problem is that the predictions of the properties of primeval galaxies are uncertain, depending strongly on such factors as the time over which star formation occurs, and the amount of dust present in the protogalaxy during this time. This makes it hard to put strong constraints on the epoch of galaxy formation from these non-detections, and any really useful results from these searches will come only when the first candidates are detected. An interesting recent discovery is that of a radio galaxy at a redshift of 3.395 (Lilly 1988). This appears to have an evolved stellar population which would imply a formation epoch for this one object of ≈7-8.

II.4 DENSITY ENHANCEMENTS AND STREAMING MOTIONS

It has been stated several times in the foregoing discussion that overdensities on particular scales are likely to lead, via gravitational interactions, to streaming velocities on similar scales. The purpose of this section is to present a sample of the literature which investigates quantitatively the likely magnitude of such streaming velocities. These will be quoted for comparison with observational results, which will be presented

in the next section. The majority of studies investigating this question have been concerned with the velocity field of the Local Supercluster (henceforth LSC), and the interpretation of this field as infall caused by the Virgo cluster. The arguments used are generally applicable to any such system in which gravitational infall is the dominant process, however.

The basic method applied in these studies was outlined by Silk (1974), who investigated the relation between density fluctuations in a Friedmann Universe and the induced change in the velocity field. The method of solution that Silk adopts is to introduce a perturbation, the gravitational attraction of the overdensity, into the Newtonian hydrodynamical equations of a uniform, isotropically expanding pressure-free fluid. It is assumed that the situation is spherically symmetrical, a reasonable assumption since the gravitational potential around an overdensity tends to be more nearly spherically symmetrical than the overdensity which produces it (Davis & Peebles 1983). In addition, this means that vorticity in the velocity field is assumed negligible, which most studies suggest is probably reasonable, in the case of the LSC.

Silk concludes that deviations from the Hubble Flow decrease with decreasing q_0, for a given fluctuation strength. For a density contrast of 3, he finds that the induced deviation in the Hubble Flow is 60% for q_o=0.5, but only 20% for q_o=0.1. Thus, accurate measurements of streaming velocities, along with estimates of the density enhancements assumed to be causing them, can lead to an estimate of q_o if the global density Ω_o is known. In practice, the reverse has generally occurred, and the particular case of streaming velocities within the LSC has been used in the past to estimate the density parameter, with an implicit dependence on the value of q_o adopted.

This is the approach adopted by Peebles (1976), who attempts to model the local velocity field using essentially Newtonian mechanics within a Friedmann-Lemaitre cosmology, with zero cosmological constant. He derives an equation for the streaming velocity in terms of the fractional overdensity and Ω_o:

$$V \sim H_o R \Omega_o^{0.6} \frac{\delta\rho}{\rho} \qquad 1.11$$

This assumes that the density contrast can be treated as a linear perturbation, which is probably true over the majority of the volume of space in which the velocity field is dominated by a particular mass concentration, but may break down near the centre. Peebles then estimates the strength of the Virgo cluster overdensity by number counts,

and utilises LSC streaming velocity measurements to put constraints on Ω_o. However, the data are not of sufficient quality to derive really useful constraints, and values for Ω_o of 0.1 and 1 are both considered consistent with the observed mass distribution around the Virgo cluster and an infall velocity of 250 kms^{-1}.

Yahil et al. (1980) use the revised Shapley Ames galaxy catalogue (Sandage and Tammann 1981) to derive the number distribution, and by inference the mass distribution, of the LSC. A simple analysis then finds the velocity which the Virgo-centred overdensity would induce via gravitational acceleration over a Hubble Time. At the distance of the Local Group from the Virgo cluster, the expected streaming velocity is $3700q_o$ kms^{-1}. Given a best estimate of the velocity of about 250 kms^{-1}, this implies a very small value for q_o. However, the assumption that the overdensity has been in existence at its present strength for a Hubble Time makes the calculated value likely to be a considerable overestimate.

This type of analysis was extended by Davis and Huchra (1982), who undertook their own large scale redshift survey of some 2400 galaxies. These were selected out to sufficiently high redshifts (about 4000 kms^{-1}) to give some information about mass structures on scales larger than the LSC. They use this database to calculate the density enhancement represented by the Virgo cluster, giving a value in the range 2.0 to 2.2, which leads to a value for Ω_o of 0.2 or 0.4, for Virgo infall velocities of 250 kms^{-1} or 440 kms^{-1} respectively. They then extend the calculation in the same way as Yahil et al., to derive the gravitational field of all the matter in their survey volume. This treatment yields values of Ω_o between 0.3 and 0.7. Whilst the errors on these results are large, they do seem to require the existence of a dark matter component in addition to that which shows up in smaller scale dynamical studies, and which cannot be solely baryonic.

All of the above studies contained, either explicitly or implicitly, the assumption of spherical symmetry. However, it is quite probable that a large scale structure in the early stages of evolution, such as the LSC, should have completed collapse in only one direction, forming a "pancake". Szalay and Silk (1983) approximated this situation with a flat matter distribution of infinite extent in one plane. They discovered that the resulting velocity field that was induced in a sample volume around this overdensity was significantly different from that around a spherical perturbation. Interpreting a pancake-induced velocity field as being due to a spherical perturbation could lead to the global density being underestimated by as much as a factor of 1.5. In reality, the actual situation is likely to be somewhere between these two extremes.

All the above studies were obviously only able to consider the density field in the region they surveyed. If there are strong density perturbations over larger scales, these could lead to velocity gradients across the LSC which would affect the results of the above analysis.

The analysis carried out by Clutton-Brock and Peebles (1981) differs from all those mentioned above in that it was specifically intended to investigate the larger scale streaming velocities implicit in the results of Rubin et al. (1973), described below. The mechanism invoked to create the streaming velocities was again simply gravitational acceleration acting over a period on the order of the Hubble Time, with the aim of seeing whether those density fluctuations which are presently observed would be capable of inducing such streaming velocities. The result is that the sizes of the induced velocities are strongly density dependent, and they can be calculated using the following expression

$$[<v^2>]^{1/2} = 300 \exp(\pm 0.1)\Omega^{0.6} \text{ kms}^{-1} \qquad 1.12$$

for linear scales on the order of 65 h^{-1} Mpc, comparable with the Rubin et al. sample. Thus they concluded that peculiar velocities on these scales are significant, but unlikely to be as large as the apparent motion of the Rubin et al. sample relative to the CBR ($\approx$800 kms^{-1}). This is particularly true in low density ($\Omega \approx 0.1$) universes.

I shall conclude this section by discussing the results of some other theoretical studies, in which the expected streaming velocities on particular scales have been investigated for different cosmological scenarios. Kaiser (1983) investigated neutrino dominated cosmologies, which are expected to give rise to significant intermediate scale streaming velocities, as a result of the constraints of free streaming processes. He compares the theoretical streaming velocities with the observational results presented by Hart and Davies (1982, discussed in the next section), and is able to put constraints on the Hubble constant and the redshift at which non-linear structure develops in a neutrino cosmology. Low values of the streaming velocity, as found by Hart and Davies, seem to exclude the neutrino model under the reasonable assumptions $h < 1$, and a redshift for the onset of non-linear collapse > 3.

Schaeffer & Silk (1984) and Melott (1985) have tried to reconcile the problems associated with neutrino dominated universes and the apparent non-detection of streaming motions. By considering the non-linear development of pancake structures

prior to galaxy formation, Schaeffer & Silk find that the expected streaming velocities are diminished, particularly if the region of space in question lies within a single pancake. If intermediate scale streaming motions are ultimately shown to be small, such considerations may be important in deciding the viability of neutrino dominated models.

Finally, Vittorio and Silk (1985) discuss critical density CDM models in which no significant biasing occurs, looking at predictions of the peculiar velocity field, and comparing them with the findings of de Vaucouleurs and Peters (1984). They find that CDM only gives velocities in reasonable agreement with these observations if biasing is not important, since the smoother dark matter distribution implied by the biasing hypothesis leads to very low peculiar velocities. De Vaucouleurs and Peters only detected streaming motions at low significance, but if later detections of intermediate scale streaming velocities are confirmed, this argument could be very important.

II.5 OBSERVATIONAL SEARCHES FOR DEVIATIONS FROM ISOTROPIC HUBBLE FLOW

In this section, a review will be presented of those studies which have produced observational results concerned with the nature of the Hubble Flow. The majority of these are detections of dipole velocities, interpreted either as motion of the Local Group with respect to a background of galaxies, or, more recently, as streaming flows of the entire sample under study with respect to the rest frame defined by the CBR. Some other studies are also of interest, such as those observations which defined the CBR rest frame, or which look for apparent dipole inhomogeneities in the matter distribution.

The discussion will be split into two sections, the first concerning the Local scale, essentially concerned with studies of the Local Supercluster (LSC) velocity field; and the second the Large scale, for studies out to distances corresponding to recession velocities of about 10,000 kms^{-1}.

II.5a THE LOCAL VELOCITY FIELD

The majority of studies of bulk matter motions undertaken to date have been concerned with the velocity field on Local scales, i.e. within the Local Supercluster. In this section, I will briefly discuss those results which have relevance to cosmology, and in particular to the density parameter Ω_o and the Hubble constant.

Most of the work done on these small scales is concerned with observations of the local velocity field in terms of a Local Group velocity induced relative to the centre of mass of the LSC. The component of this velocity towards the Virgo cluster may then be interpreted as due to gravitational attraction by a density enhancement in that direction, and it can be used to estimate a value for the dark matter component in the mass of the Virgo cluster. This in turn leads to an estimate of the global density parameter, Ω_o, under the assumption of a uniform luminous to dark matter ratio on scales larger than the LSC. An alternative approach is to refer the observed velocities to the frame defined by the CBR, to calculate whether the LSC, or more accurately the Virgo cluster, is at rest in this frame.

Many studies have been undertaken to determine the velocity of the Local Group towards the Virgo cluster. Davis & Peebles (1983) reviewed the situation at that time very fully, so I shall just briefly mention some of the more important results, and particularly those that have been published since 1983. An early study by Peebles (1976) using ScI galaxies derived a large value for the Virgo infall of 500±150 kms^{-1}, in good agreement with the later studies of Tonry & Davis (1981a,b). They derived values of 470±75 kms^{-1} and 416±90 kms^{-1} for elliptical and S0 galaxies respectively. Hart and Davies (1982), in a study discussed in greater detail below, measured a velocity of 450±55 kms^{-1}, but this study involved galaxies at distances of up to 50 h^{-1} Mpcand may be affected by larger scale motions. These results also agree with value obtained by assuming the Virgo cluster to be at rest with respect to the CBR, which gives a velocity of ≈450 kms^{-1}, using the Lubin & Villela (1986) CBR dipole measurement.

However, most other studies have yielded significantly lower values. Visvanathan & Sandage (1977), de Vaucouleurs & Peters (1981), de Vaucouleurs et al. (1981), Yahil (1981) and Aaronson & Mould (1981) all derived velocities between 150 & 230 kms^{-1}. Dressler (1984) reanalysed the Tonry & Davis (1981a,b) elliptical galaxy data and found a value of 250 kms^{-1} when correcting their measured velocity dispersions for aperture effects. Yahil (1984) concludes that a consensus has been reached at 250±50 kms^{-1}, whilst Davies & Staveley-Smith (1984) conclude from a variety of studies that the true velocity probably lies between 100 and 200 kms^{-1}.

The tendency seems to be for later, more accurate studies to indicate smaller infall velocities of the Local Group toward the Virgo cluster, possibly on the order of 200 kms^{-1}. If so, this is an interesting result, since it means that the Local Group motion must be largely generated by interactions with matter outside the Local Supercluster, and the Local Supercluster must itself be in motion with respect to the CBR. Taking a best

estimate of the Virgo infall velocity as ≈200 kms^{-1}, and comparing with the Local Group motion relative to the CBR (≈450 kms^{-1} in this direction), indicates a peculiar velocity of the Virgo cluster of ≈250 kms^{-1} along the line of sight. This provides an indication of significant motions on Supercluster scales. The remainder of this thesis will be concerned with determining whether such velocities are present on yet larger scales.

II.5b THE LARGE SCALE VELOCITY FIELD

This is probably the most interesting scale for Hubble Flow work at present, with measurements of streaming velocities over scales on the order of 50 h^{-1} Mpc becoming feasible at ever increasing accuracy, as the observational techniques involved improve. Most of the currently popular cosmological models give definite predictions of what these velocities should be, so direct confrontation between models and observations is now possible.

I shall introduce a further categorisation of the papers to be considered in this section, according to whether or not their results support significant streaming motions. This is a fairly arbitrary division, and does leave borderline cases which do not fit easily into either category, but it is, to an extent, imposed by the early development of this field. As a consequence of the interest generated by the Rubin et al. study of 1973, all results tended to be interpreted either as broadly supporting this result, or as contradicting it. It should be borne in mind, however, that the early debates were about the possible magnitude of the Local Group motion relative to the background of surrounding galaxies, whereas we are now more interested in the larger scale motions of whole samples of galaxies relative to the CBR rest frame.

II.5b.i STUDIES WHICH SUPPORT SIGNIFICANT STREAMING MOTIONS

I will start by considering the studies which can be interpreted as providing support for the idea of streaming motions on large scales, beginning with the one which stimulated so much of the early interest.

Rubin et al. (1973) considered the velocity anisotropy of 74 galaxies, mainly of type ScI, with recession velocities between 4000 and 7500 kms^{-1}. The sample was restricted to galaxies with apparent magnitudes between 14.0 and 15.0. It was found that the galaxies fell into two well defined groups on the sky, one being almost entirely occupied by galaxies with recession velocities around 4950 kms^{-1}, whilst galaxies in the other half of the sky predominantly had recession velocities of about 6400 kms^{-1}. If it can be

assumed that all these galaxies have the same absolute magnitude, then these two regions must in fact be occupied by galaxies at the same distance from us, and the discrepancy in velocities must be due to a departure from the Hubble Law. This can most easily be interpreted in terms of a motion of the Local Group with respect to these galaxies, at a velocity of about 750 kms^{-1}. This was the only result claimed in the paper, and that at a fairly tentative level, but all subsequent work can be seen as an attempt to confirm or refute it, particularly since it was later seen to imply the bulk motion of all the galaxies surveyed relative to the CBR.

A full description and analysis of the Rubin et al. work was presented in 1976 (Rubin et al. 1976a,b), with the number of galaxies included being extended to a total of 200, although only 96 of these were used in deriving most of the results. The final conclusion was a confirmation of the "Rubin and Ford" effect reported in the 1973 paper, but a rather more sophisticated analysis was done, to try to counter criticisms of the earlier paper. One aspect of this was the attempt to produce a volume-limited sample, the Minimum Bias Subset (MBS), of 96 galaxies from the original, magnitude limited, sample, in an attempt to reduce Malmquist bias. This is a serious problem in any study of the Hubble Flow which uses magnitude-selected objects which have a distribution of luminosities, since the nearer objects tend to be only those from the fainter end of the distribution, and the most distant only those from the brighter end. The effects of this problem were addressed by Fall and Jones in the paper discussed below.

In practice, it is possible to correct in part for the spread of luminosities of the objects observed, by identification of correlations between luminosity and other observable parameters. The Rubin et al. work of 1976 included two such correlations, corrections being made for galaxy type and linear diameter. The diameter correction was a new idea, but one which was apparently justified by the effect it had in decreasing the scatter of the galaxies when plotted on the Hubble diagram.

Using these corrections, Rubin et al. found a Local Group motion of 454 ± 125 kms^{-1} towards galactic coordinates $l=163^{\circ}$, $b=-11^{\circ}$. A note was made at the end of this analysis, concerning the possible conflict between this result and the early results concerning the CBR isotropy. An intermediate result of the calculation of the Local Group motion was that the solar motion with respect to the frame defined by the sample of galaxies was on the order of 600 kms^{-1}, whilst the motion of the sun with respect to the CBR frame was already constrained to be less than 300 kms^{-1}. This was therefore the first tentative identification of the possibility of streaming velocities of groups of galaxies on scales this large, although the point was not explicitly made.

The solution obtained for the Sc I galaxies was checked using data from Sandage (1975), in which it was argued that there is no significant deviation from the Hubble law. Rubin et al. reanalysed the data, which is composed of photometry of an all-sky sample of elliptical galaxies, and found an anisotropy in agreement with the result for the spiral galaxies.

The conclusions of the Rubin et al. 1973 paper were challenged by the analysis presented in a paper by Fall and Jones (1976). They found that the earlier result was completely consistent with an isotropic Hubble expansion, if the galaxies in the two regions identified by Rubin et al. in their 1973 paper are members of two large clusters which are actually at the distances indicated by the galaxy redshifts. Then, if the spread in luminosity of the observed galaxies is greater than the range of apparent magnitudes used to define the sample, Malmquist bias will lead to a systematic difference in the absolute magnitude of galaxies sampled from the two regions. Only the galaxies in the brighter tail will be sampled in the further cluster, and only the galaxies in the fainter tail in the nearer cluster. Fall and Jones suggested that the entire effect could be accounted for in this way. Their analysis clearly shows the importance of identifying and correcting for systematic effects likely to lead to such biases.

Further criticism of the Rubin et al. work was presented in a paper by Schechter (1977), although this did broadly support their conclusions. Schechter's criticism was with their use of the correction to galaxy magnitudes on the basis of their inferred linear diameters. The main argument was that since isophotal magnitudes and galaxy diameters are very strongly correlated, a correction based on measurements of the diameters alone can bring in little extra information, and the improvement found by Rubin et al. in the quality of their solutions was probably spurious. Repeating their analysis without this correction, Schechter found an identical solution within the errors, but at reduced significance. He also repeated the calculation using galaxies selected from the Second Reference Catalogue of Bright Galaxies (de Vaucouleurs et al. 1976), and obtained a different solution with a smaller formal uncertainty. This result was in disagreement with both the Rubin et al. result and with the CBR anisotropy; it agreed best with the hypothesis that the effect was due to galactic rotation alone.

Visvanathan (1979) looked at the velocity field of 311 E and SO galaxies, deriving their absolute magnitudes from their (u-V) colours. The use of such a distance independent indicator provides a good way of overcoming the biases incurred in the selection of candidate objects. The Local Group dipole velocity deduced relative to these galaxies

was 397±70 kms^{-1} toward l=140°, b=20°, in very good agreement with the Rubin et al. result. This result can now be converted to a CBR frame streaming motion of ≈840 kms^{-1}, toward l=290°, b=10°, using the Lubin and Villela (1986) CBR dipole result. However, the galaxies used were at much lower redshifts (<2500 kms^{-1}) than the Rubin et al. sample.

Jackson (1982) reanalysed the Rubin et al. data, along with the data obtained by Sandage which Rubin et al. had used to support their conclusions, and found no significant biases. He thus confirmed their solution. This was a important result since he used maximum likelihood techniques which were quite different to the least squares technique of Rubin et al.

Dressler et al. (1987) have recently presented the results of a study involving 390 elliptical galaxies, 300 of which are actually used in deriving velocity solutions. These galaxies have redshifts of up to 8000 kms^{-1}, but the mean depth of the sample is rather less than that used by Rubin et al. The luminosity indicator was a novel combination of indicators which had individually been used previously, combining measurements of central velocity dispersion, effective radius and surface brightness. A good correlation was discovered between the velocity dispersion and the diameter at which the mean surface brightness of the galaxy becomes 20.75 B mag arcsec^{-1}. The intrinsic scatter in this relation is claimed to give an error of 23% in the distance to each galaxy. They detected a bulk streaming motion of all galaxies out to 60h^{-1} Mpc of 599±104 kms^{-1} toward l=312°, b=6° relative to the CBR rest frame. This is in excellent agreement with the Rubin et al. result.

However, in a later paper (Lynden-Bell et al. 1988), the same authors reinterpreted their result as showing galaxy peculiar velocities only on much smaller scales. The region showing the strongest evidence for peculiar velocities was the region around the Hydra cluster at l≈300°, b≈10° , at redshifts of less than 4000 kms^{-1}. They showed that galaxies in this region have peculiar velocities of ≈1000 kms^{-1}, which they interpreted as infall into an as yet unidentified overdensity-the "Great Attractor". If this region is excluded from their solutions, the amplitude and significance of the streaming of the whole sample is much reduced.

II.5.b.ii STUDIES WHICH FIND NO SIGNIFICANT STREAMING MOTIONS

In one of the first responses to the Rubin et al. 1973 paper, Sandage (1975) used a sample of E and S0 galaxies selected from the Revised Shapley-Ames catalogue

(Sandage and Tammann 1981, in preparation at that time) to test the isotropy of the Hubble Flow. He plotted the galaxies on a Hubble diagram, and searched for any significant deviations from the Hubble line which might indicate peculiar motions. In particular, he looked for any correlation between such deviations and position on the sky corresponding to to the two regions discussed by Rubin et al. No such correlation was evident, arguing against the existence of the velocity anisotropy claimed in the Rubin et al. work. It could be claimed at this point that non-detection of streaming velocities relative to the Local Group must correspond to a large scale streaming motion relative to the CBR frame, since the Local Group is now known to have its own peculiar velocity. However, in this particular case this would be to attach too much significance to what was in reality just a crude initial test which lacked the required sensitivity.

The type of argument put forward by Sandage was repeated by Weedman (1976), who found no evidence for significant non-Hubble velocities in a sample containing the 10 brightest galaxies in each of 9 rich clusters with recession velocities from 1000 kms^{-1} to 11,000 kms^{-1}. Visvanathan and Sandage (1977) reached a similar conclusion from an analysis of elliptical galaxies in 8 nearby clusters. The method used in both cases was a simple analysis of the scatter on the Hubble diagram, a very insensitive way of detecting streaming velocities, since what appears to be a relatively small amount of scatter may in fact be significant evidence for streaming if it is strongly correlated with position on the sky.

The first study to use a sensitive third variable method and find no significant streaming was that of Hart and Davies (1982). They observed galaxies in the 21 cm HI line, using the observed width of this line as a luminosity indicator. The width of this line is often used as an indicator of the size and luminosity of galaxies, and is the basis of the "Tully-Fisher" relation (Tully and Fisher 1977), a strong empirical correlation between luminosity and linewidth. However, the relation has only been fully investigated using optical or near-IR magnitudes, and its reliability using 21cm fluxes is therefore unknown.

The sample used by Hart and Davies was 84 Sbc galaxies in the distance range 1000 to 5500 kms^{-1}, a significantly smaller volume than that of the Rubin et al. sample, and most of the Hart and Davies galaxies were within the LSC. They did, however, carry out solutions for this sample supplemented with galaxies in the same distance range as the Rubin et al. sample. This both increased the proportion of galaxies in the outer regions of this range and improved the sky coverage, especially in the south. The Local Group motion relative to this sample of galaxies was found to be 546±70 kms^{-1} toward

l=261° (± 9°), b=39° (± 7°). This was taken to be identical to the velocity relative to the CBR, within the errors; the difference corresponds to a streaming velocity of 143 kms^{-1} toward l=308°, b=-16°, insignificant within the errors.

This work was continued to increase the galaxy sample size, the results being reported by Davies and Staveley-Smith (1985). Data were presented for 500 galaxies with recession velocities of up to 6000 kms^{-1}, again using 21 cm fluxes and linewidths to estimate the distance to the galaxies. Their solution is again in marked disagreement with that of Rubin et al., showing at most marginal evidence for streaming motions, with their quoted Local Group velocity implying a bulk motion of magnitude 143 kms^{-1} toward l=283°, b=9°. They point out that this velocity is aligned with the direction to the Hydra-Centaurus Supercluster, which is largely outside their survey volume and may dominate the velocity field within it. One lingering doubt concerning this project is that the galaxies were selected from inhomogeneous catalogues, a procedure likely to lead to strong biases around the sky.

De Vaucouleurs and Peters (1984) investigated how the measured streaming velocity changed with increasing size of the sampled volume. A variety of luminosity indicators was used, since the data were taken from many sources. The overall conclusion was that they found mass motions on small scales, which swung round in direction as the scale was increased, to agree with the CBR dipole on scales corresponding to recession velocities of about 3600 kms^{-1}. Their conclusion that galaxies are at rest on scales greater than this must be regarded as somewhat speculative, however. It is based purely on extrapolation from a volume that barely exceeds that of the LSC, and would have little weight in the face of hard evidence for motions on such scales. A final problem with interpreting their solutions is that no errors are quoted.

Finally, Aaronson et al. (1986) have attempted to measure the net velocity of 10 clusters of galaxies, with recession velocities in the range 4000 to 11,000 kms^{-1}. They made observations of typically 10-20 galaxies per cluster, using the infrared Tully-Fisher relation as the luminosity indicator. Thus the relative distances to each of these clusters should be very well known, since any non-systematic errors such as those due to the intrinsic scatter in the 21 cm linewidth/luminosity relation are significantly reduced due to the number of objects observed. The overall streaming velocity deduced for the 10 clusters was 290 kms^{-1} toward l=42°, b=13°, with quoted errors in the velocity of ≈200 kms^{-1}. This is therefore very much smaller than the Rubin et al. result, and is in any case in a totally different direction and of very low significance.

This is possibly the most thorough study of the large scale velocity field which has failed to find evidence for significant streaming. In its favour are the very small formal uncertainties in the distance estimates to the clusters, owing to the large number of galaxies in each one, although this argument is weakened by the possibility of systematic differences in the zero point of the Tully-Fisher relation from cluster to cluster (Bottinelli et al. 1987). However the sky coverage of the clusters is poor; due to the need to use the Arecibo radio telescope to measure the 21 cm linewidths of the fainter galaxies, the clusters are confined to the relatively narrow declination strip observable with this telescope. This effect, and the small number of independent samples of the velocity field, increase the uncertainty in the interpretation of the result.

II.5.b.iii CONCLUSIONS FROM PREVIOUS STREAMING MOTION STUDIES

The programmes outlined above clearly yield a contradictory picture of galaxy motions, at least on the large scale. Within the Local Supercluster, where these measurements are easier, reasonable agreement seems to have been reached. Virgo infall is clearly detected to radial distances of about 20 h^{-1} Mpc, although it is not sufficient to explain all the observed motions.

On the larger scale, there is sufficient evidence from several sources for bulk motions of galaxies with respect to the CBR for this idea to be taken seriously. The most convincing arguments against such effects come from two of the most recent reports, contemporaneous with the work described in this thesis-the Aaronson clusters, which appear to be at rest in the CBR frame, and the interpretation by Lynden-Bell et al. of their data on ellipticals as showing only a relatively small scale infall pattern. The work presented in chapters Two and Three comprises two independent tests of which of these alternatives is most likely to be correct.

CHAPTER TWO

MEASUREMENT OF GALAXY STREAMING USING FIRST RANKED CLUSTER ELLIPTICALS

This chapter contains an analysis of data taken from the literature on the brightest galaxies in clusters. This was used to determine whether the rest frame defined by galaxy clusters is the same as that defined by the CBR. This analysis was particularly aimed at answering the questions raised by the work of Aaronson et al. (1986), discussed in Chapter One, who found no evidence for peculiar velocity of a small number of rich clusters, in the CBR frame.

I THE CLUSTER GALAXY SAMPLE AND DATA

I.1 SUITABILITY OF FIRST RANKED CLUSTER GALAXIES FOR STREAMING STUDIES

The brightest elliptical galaxies in rich clusters have been used in many previous studies aimed at determining the cosmological parameters H_o and q_o (Sandage 1973 and following papers; Gunn & Oke 1975). These galaxies have been used for this purpose principally since they are excellent standard candles (Sandage & Hardy 1973), which is the prime requirement for redshift-independent distance determination. This same property makes them very suitable for use in determinations of departures from pure Hubble Flow. They have been extensively investigated by Sandage and coworkers, who determined correlations between the absolute magnitude of the first ranked galaxies and the properties of their surrounding clusters, which enable one to reduce the scatter still further. In addition to being good standard candles, they are intrinsically very luminous and of high surface brightness, which means they can be selected, and give easily measurable redshifts and photometry, to greater depth than other types of galaxy. Finally, they are a particularly suitable class of galaxy for this work since redshifts and optical photometry were already available from the cosmological tests undertaken previously.

I.2 THE DATA

The data used are the V-band photoelectric photometry and redshifts of first-ranked cluster ellipticals listed in Table 1 of Sandage & Hardy (1973). These galaxies were used by Sandage and coworkers in this and later papers (e.g. Sandage 1975) in an attempt to determine the value of the deceleration parameter q_o. The galaxies have redshifts out to ≈0.4, but we selected only those galaxies with CBR-frame recession velocities <15,000 kms^{-1}. This provides a sample of 60 galaxies with a mean redshift of 7600 kms^{-1}. Of these, 15 are in fact members of groups defined by Humason, Mayall and Sandage (1956) rather than rich clusters, but this should not be important since the photometric properties of these were not found to differ significantly from the rest of the sample in the initial analysis by Sandage and Hardy.

Selecting only the low redshift galaxies has several advantages when using them for a streaming motion analysis. The dominant errors in deriving luminosity distances are magnitude-dependent, and thus the error in peculiar velocity scales with redshift. Therefore, including galaxies at very high redshift just increases the noise in the solutions with very little gain in information. In addition, truncating the sample in this way significantly reduces the effect of distance dependent selection effects. The most obvious of these is the Malmquist bias (Malmquist 1920), which causes the highest redshift galaxies to be of high luminosity and *vice versa*. For streaming motion studies it is important that the sample should be as homogeneous as possible, so the minimisation of this effect is highly desirable. A related selection effect for cluster galaxies has been investigated by Scott (1957), who finds a correlation between cluster richness and distance which could cause a bias similar to Malmquist bias. However, she shows the effect to be negligible out to the depth of our subsample.

The V magnitudes quoted by Sandage & Hardy and reproduced here in column 2 of Table 2.1 are corrected for galactic extinction and K-dimming, and to a standard metric aperture. The absorption corrections used were internally derived from the latitude dependence of the BVR colours of the ellipticals in the sample. The corrections adopted by Sandage and Hardy were as follows:

$$A_v = 0.099(\mathrm{cosec}(b) - 1), \text{ for } b<50^\circ \qquad 2.1$$

$$A_v = 0 \text{ otherwise.}$$

These corrections were also used in the present work.

No attempt was made to derive longitude dependent corrections. K-corrections were taken from Table 5 of Sandage (1973), but are small for redshifts typical of our subsample ($\approx$0.04 magnitude at 8000 kms^{-1}).

Sandage and Hardy also derived correlations between the absolute magnitude of the first-ranked cluster galaxies and the properties of the clusters they lie in. The particular cluster properties they investigated were the Abell richness class (Abell 1958) and Bautz-Morgan class (Bautz and Morgan 1970). The Abell quantized richness class was replaced by a continuous variable by counting the galaxies less than 2.5 magnitudes fainter than the third brightest cluster galaxy, within a 2 Mpc radius of the cluster centre. Bautz-Morgan class is a measure of the amount by which the first-ranked galaxy is brighter than other members of the cluster. The richness correction was found to be barely significant, whilst the Bautz-Morgan correction was much larger, $\approx$0.6 magnitudes between classes I and III. The effect of the two corrections was to reduce the scatter in absolute magnitudes from 0.35 to 0.28 magnitudes. This small scatter has since been confirmed by independent studies (e.g. Schneider et al. 1983), but is still not well understood, despite attempts to explain the evolution of brightest cluster galaxies, e.g. by dynamical merging (Hoessel, 1980). Table 2.1 contains data for the 60 galaxies used here, with the columns ordered as follows:

1 Cluster name,
2 V magnitude, corrected for galactic extinction, K-dimming and aperture,
3 Redshift from Sandage and Hardy, 1973,
4 Cluster richness class,
5 Cluster Bautz-Morgan class,
6 Galactic latitude, l^{II},
7 Galactic longitude, b^{II}

Table 2.1. Photometric and redshift data for 60 First Ranked Cluster Galaxies.

1	2	3	4	5	6	7
Abell	V_c	z	Richness	B-M	l	b
	8.44	.00381	1	III	287	70
	8.90	.00509	1	II-III	240	-57
	11.25	.0128	0	II	88	-48
	11.77	.0170	1	II	131	-29
426	11.50	.0181	2	II-III	151	-13
1656	11.51	.0222	2	II	57	88
1213	13.72	.0287	1	III	201	69
2151	13.12	.0341	2	III	32	44
119	13.74	.0387	1	II-III	126	-64
	13.66	.0428	0	II-III	84	-48
2589	14.11	.0440	0	I	93	-43
	12.03	.0169	0	III	127	-30
	12.29	.0180	0	II	142	-63
	12.58	.0215	0	II-III	140	-17
	13.15	.0301	1	I-II	104	-33
	12.52	.0303	2	I	63	44
	13.40	.0351	0	II	9	50
	13.19	.0298	0	III	261	-77
	10.89	.0113	1	II	302	22
	10.77	.0114	0	I	313	28
	11.04	.0138	0	I	320	27
	13.16	.0226	0	III	114	-32
	12.38	.0209	0	III	114	-40
	11.67	.0155	0	III	112	-60
	12.21	.0177	0	III	117	-60
	11.99	.0188	0	II	151	-54
	11.46	.0160	0	I	200	-33
	12.10	.0159	0	III	203	29
	12.16	.0200	0	I-II	191	44
	12.23	.0234	0	I-II	183	55
	10.92	.0087	0	III	311	46
	10.93	.0084	0	III	314	50
	10.51	.0076	0	III	83	71

	10.12	.0060	0	III	0	49
	12.46	.0204	0	II-III	92	-16
	12.78	.0258	0	III	82	-41
76	13.33	.0377	0	I	117	-56
147	14.23	.0441	0	III	131	-60
262	11.94	.0168	0	III	137	-25
376	14.02	.0487	0	I-II	147	-21
539	13.04	.0267	1	III	196	-18
548	13.49	.0391	1	III	230	-24
569	12.08	.0193	0	II	169	23
576	13.74	.0404	1	III	161	26
634	13.05	.0266	0	III	159	34
671	13.63	.0496	0	II	193	33
1060	11.02	.0115	1	III	270	27
1139	13.70	.0376	0	II-III	251	53
1228	13.60	.0344	1	III	187	69
1257	14.03	.0339	0	III	183	70
1314	13.16	.0335	0	III	152	64
1318	12.28	.0189	1	III	144	59
1367	12.09	.0204	2	II-III	234	73
1736	13.74	.0431	0	III	313	35
2147	13.33	.0351	1	II	29	45
2152	13.85	.0440	1	III	30	44
2162	12.97	.0318	0	II-III	49	46
2197	12.67	.0322	1	II	65	44
2657	14.26	.0414	1	II-III	97	-50
2666	12.39	.0273	0	I-II	107	-34

II DATA ANALYSIS

The basis of the solutions for anisotropies in the Hubble Flow is to use the Hubble Modulus technique first employed by Rubin et al. (1976b). The problem overcome by this technique is that we do not know two parameters which are needed to compare directly the distances to galaxies obtained from redshifts and inferred from photometry. The first is the Hubble constant, which is uncertain by about a factor of 2 at present and implies an equal uncertainty in physical distances inferred from redshifts. The second is the actual luminosity of the galaxies used, which would be needed to derive accurate distances from photometry for individual galaxies. These problems can both be overcome by averaging the properties of the whole sample and deriving deviations from the mean expansion for individual galaxies, without ever defining explicitly the distance to, or luminosity of, any particular galaxy.

This is done by calculating the Hubble Modulus, HM, from the measured magnitudes m and redshifts V_{obs} for each galaxy, where

$$HM = \log V_{obs} - 0.2m \qquad 2.2$$

The mean Hubble Modulus for the whole sample should then equal

$$\langle HM \rangle = \log H_o - 0.2M - 5 \qquad 2.3$$

where M is the absolute magnitude of the standard candles comprising the sample. This assumes a perfect Hubble expansion and that all galaxies are of equal absolute magnitude, and follows from a simple application of the inverse square law and the Hubble law. Once <HM> is known, it has essentially set a mean Hubble Flow relative to which peculiar velocities can be measured, without the need to know either H_o or M explicitly. Recession velocities can be predicted for each galaxy from their measured apparent magnitudes using

$$V_H = 10^{(0.2m + \langle HM \rangle)} \qquad 2.4$$

The difference between the predicted recession velocity V_H and the measured velocity V_{obs} is then our estimate of the peculiar velocity of the galaxy, along the line of sight, in the frame in which the redshifts were measured or corrected to.

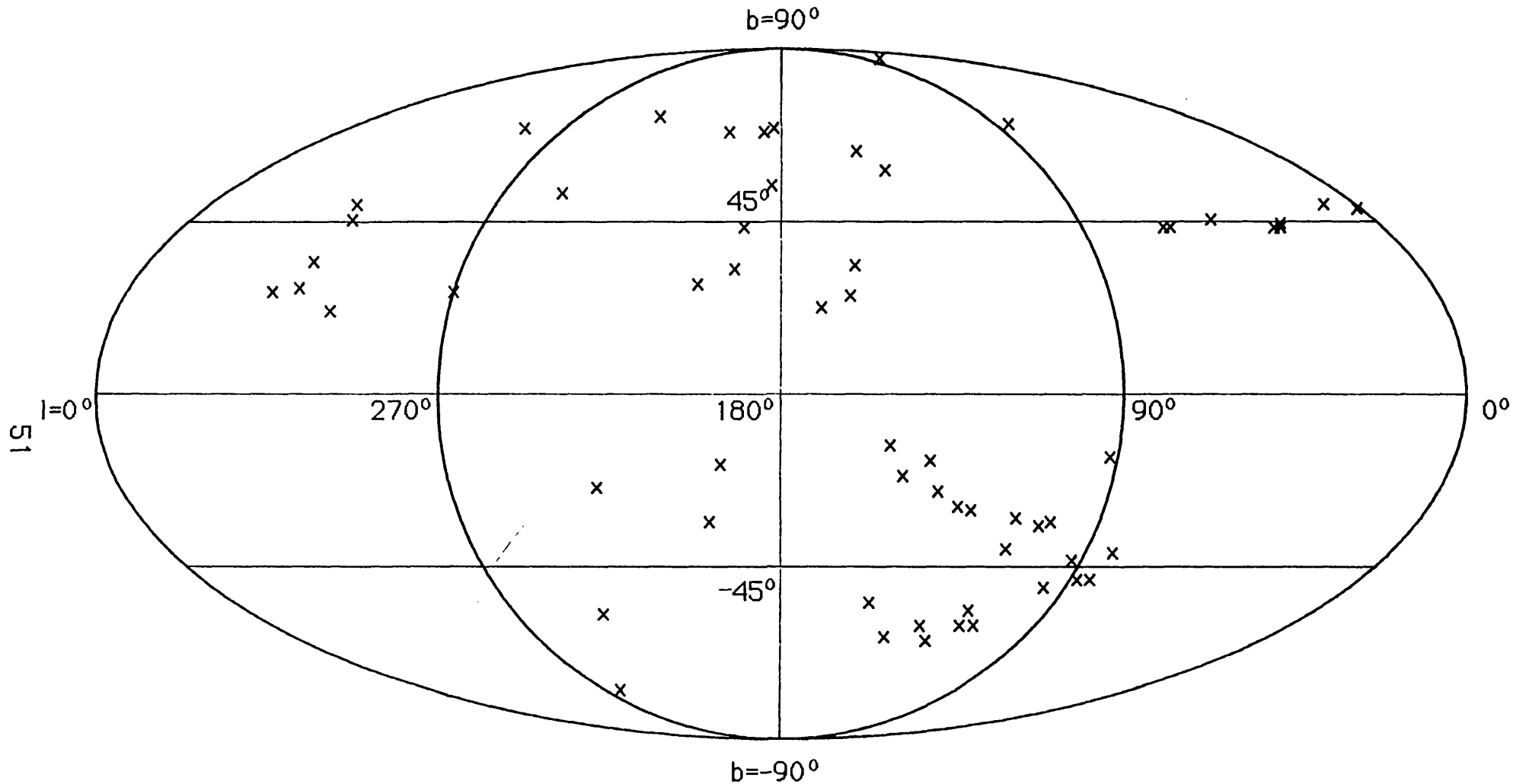


Figure 2.1 Sky distribution of 60 First Ranked Cluster Galaxies from Sandage and Hardy (galactic coordinates)

The method of analysis adopted for the bulk motion of the galaxy sample from the individual galaxy motions was dictated by the sky coverage of the 60 cluster ellipticals in our sample. As can be seen from Fig. 2.1, the distribution on the sky is patchy, and large areas are totally devoid of galaxies. This ruled out a general solution for a streaming vector, as was carried out by Rubin et al. for their spirals, since the components of the vector towards the blank regions would be completely undefined. Fortunately, the regions around the apex and antapex of the Local Group motion with respect to the CBR contain much of the sample, making it possible to test for the motion of the Local Group relative to the galaxies along this direction. Thus we were able to test the claim by Aaronson et al. (1986) that rich clusters of galaxies are at rest in the CBR-defined reference frame. If this were so, then the relative motion of the Local Group and the CBR should be reflected in an equal motion of the Local Group relative to the galaxies. We would see this as an apparent velocity anisotropy: galaxies in the apex direction would have low recession velocities, and those in the antapex direction high recession velocities, for a given apparent magnitude. This assumes that redshifts are measured in the Local Group frame.

Thus we undertook a restricted, one-dimensional type of solution, which was concerned only with the component of the relative velocities of the galaxies and the Local Group along the CBR dipole axis.

We solved for this motion of the Local Group relative to the galaxies by minimising the quantity

$$\chi^2 = \sum_i \left\{ \frac{[V_H(i) - V_{obs}(i)] - V_{LG} \cos\theta(i)}{\sigma(i)} \right\}^2 \qquad 2.5$$

where $V_H(i)$ is the recession velocity of the ith galaxy, calculated from equation 2.4; $V_{obs}(i)$ is the measured recession velocity of the ith galaxy; $\theta(i)$ is the angle between the line of sight to the ith galaxy and the CBR dipole apex direction, l=272°, b=30°; $\sigma(i)$, a weighting factor given to the ith galaxy, is the error in $V_H(i)$.

Minimisation of χ^2 solves for V_{LG}, the component of the motion of the Local Group relative to the sample of galaxies. This was done using a BASIC programme run on a BBC microcomputer using the following method. Differentiating equation 2.5 with respect to V_{LG} and setting to zero as the criterion for minimisation yields

$$\frac{\partial}{\partial V_{LG}} \frac{1}{\sigma(i)^2}\{\Sigma_i[V_H(i)-V_{obs}(i)]^2 + V_{LG}^2\Sigma_i \cos^2\theta(i) -$$

$$2V_{LG}\Sigma_i [V_H(i)-V_{obs}(i)] \cos\theta\} = 0 \qquad 2.6$$

Rearranging and noting that the first term in curly brackets goes to zero on differentiation, we get

$$V_{LG} = \frac{\Sigma_i \frac{1}{\sigma(i)^2} [V_H(i)-V_{obs}(i)] \cos\theta}{\Sigma_i \frac{1}{\sigma(i)^2} \cos^2\theta(i)} \qquad 2.7$$

For most of the solutions, each point in the summation is given a weighting inversely proportional to its measured recession velocity. This weighting is based on the assumption that the error is dominated by magnitude errors which are the same for all galaxies, giving a fractional error in V_H that is proportional to the distance to the galaxy. This procedure evidently gives more weight to the lower redshift galaxies, and reduces the effective depth of the sample. Calculating a mean redshift for the sample using the same weighting yields a depth of 5400 kms^{-1} which is probably the single figure which best characterises the scale we are investigating. This is not to say, however, that our results should be taken as being directly comparable with other samples which may have similar mean depth but a quite different redshift distribution and weighting scheme.

III SOLUTIONS FOR THE LOCAL GROUP MOTION

Table 2.2 shows solutions obtained for V_{LG}, the velocity of the Local Group relative to the sample of galaxies. Columns 2 and 3 of this table give the maximum and minimum redshift of the subsample used, column 4 gives the weightings used in calculating χ^2, and column 5 lists the mean effective redshift for this weighting and subsample. The number of galaxies in each subsample is given in column 6.

Table 2.2 Solutions for the Local Group motion relative to the sample of 60 cluster galaxies.

No.	cz(min) (kms^{-1})	cz(max) (kms^{-1})	Weighting	<cz>(eff)	N	V_{LG} (kms^{-1})
1	0	15000	Redshift	5400	60	-1±105
2	0	7500	Redshift	3800	31	-10±100
3	0	15000	Equal	7600	60	-295±220
4*	0	15000	Redshift	5800	59	90±125
5	2600	15000	Redshift	6800	55	-37±140
6†	0	15000	Redshift	5400	60	49±135

* Virgo cluster (NGC 4472) excluded from solution.
† Solution using magnitudes without cluster richness and Bautz-Morgan class correction.

The solution presented in the first line of Table 2.2 is that which I consider to be the "best", i.e. most representative solution for this sample of galaxies, with the most physically plausible weighting scheme. This solution clearly shows that we have failed to detect any relative motion of the Local Group and the sample of galaxies, with an error on this result of 105 kms^{-1}. This error is the formal statistical error in the minimisation procedure, under the assumption of normally distributed errors in the velocity residuals. Since this assumption may be false, I also did repeated solutions with a constant fraction (≈25%) of the galaxies omitted at random, such that every galaxy should have been excluded from the solutions many times. These solutions have an RMS scatter of approximately 100 kms^{-1}, consistent with the above estimate. Thus any non-Gaussian component of the errors must be small.

This error can be shown to be reasonable by comparing it with the size of the errors in predicting the recession velocities V_H from the corrected V magnitudes. The magnitude dispersion of 0.28 magnitudes quoted by Sandage and Hardy (1973) gives rise to a fractional error of ≈14% in distance determination, which is clearly the dominant error in determining the individual velocity residuals, as the measured redshifts are accurate to ≈2%. For a sample of 60 galaxies with a mean redshift of 5500 kms^{-1}, this again gives an expected error of ≈100 kms^{-1}. Finally, the value of the reduced χ^2 calculated above is 47/58, indicating that the solution is a reasonable fit to the data points under the assumed errors.

The other solutions in Table 2.2 were carried out to investigate the effect of taking different redshift cutoffs for the sample and applying different weightings to galaxies. The final solution shows the effect of the magnitude corrections for Richness and Bautz-Morgan class derived by Sandage and Hardy.

I found that reducing the outer redshift limit to 7500 kms^{-1} (line 2) had a negligible effect on the solution and reduced the error slightly, even though the number of galaxies in the sample was reduced. This is understandable since the errors on the velocity residuals are smaller for the nearer galaxies. The stability of the solutions to the outer redshift cutoff is encouraging, since systematics resulting from selection biases (e.g. Malmquist bias and the Scott effect) are more likely to affect the higher redshift galaxies.

Solution 3 shows the effect of the high redshift galaxies on the solution in a quite different way. Giving all galaxies equal weighting enhances the effect of the high redshift galaxies relative to solution 1, and thus probes whether the result we obtain is dominated by relatively local effects. In fact, the solution now becomes negative at marginal significance--i.e. it goes in the opposite sense to the relative motion predicted by the CBR dipole, if the galaxies were at rest in the CBR frame. Predictably the error on the solution has increased, by more than a factor of two. Thus solution 3 differs from solution 1 at only about the 1σ level.

The weightings adopted for solution 1 mean that the nearest few galaxies have a very high significance in determining the solutions. The effect of these innermost galaxies was investigated in solutions 4 and 5. Solution 4 was calculated as for solution 1 but with NGC 4472, the first-ranked galaxy in the Virgo cluster, omitted. This galaxy is particularly likely to have a large effect on the solutions since it has a sufficiently small redshift for local peculiar motions to be large relative to its recession velocity. Combined with the high weighting it received in solution 1, this makes it important to know what the solutions become when it is removed. This solution is again within 1σ of solution 1, which indicates that NGC 4472 does not have an unduly large effect on the solutions.

Solution 5 was done with all galaxies nearer than 2600 kms^{-1} (5 in all) removed. Again the solution is almost completely unaffected, showing that motions within the Local Supercluster are not having any significant effect on the solutions for the motion of the galaxy sample as a whole.

Finally, solution 6 shows the effect on the solutions when magnitudes were used which were not corrected for cluster Richness and Bautz-Morgan class. This was motivated by the realisation that these corrections were defined so as to minimise scatter in the Hubble diagram, and would thus have a slight tendency to force the solution we find, no relative motion of the galaxies and the Local Group. This effect could only be slight, however, since the corrections were defined globally, averaging over all directions on the sky, and could only slightly reduce any directionally dependent pattern of peculiar velocities, as is predicted from the CBR dipole. This is confirmed since solution 6 is again very similar to all previous solutions, with a slightly larger error as would be expected from the increased scatter in the absolute magnitudes without these corrections applied.

IV INTERPRETATION OF THE LOCAL GROUP VELOCITY RELATIVE TO FIRST RANKED CLUSTER GALAXIES

IV.1 COMPARISON WITH THE LOCAL GROUP MOTION RELATIVE TO THE CBR

All of the results discussed above are consistent, within the errors, with our main solution, for the whole sample with a redshift weighting, of -1 ± 105 kms^{-1}. Thus there is no significant motion of the Local Group relative to this sample of 60 galaxies. However, if the galaxy sample were at rest with respect to the CBR frame, this test should have detected a Local Group motion equal to that inferred from the amplitude of the dipole variation in the CBR temperature around the sky. I adopt a best value for the Local Group motion relative to the CBR of 610 ± 50 kms^{-1} (Lubin & Villela 1986), a well determined velocity that would be large enough to give an easily detectable Local Group motion in the test carried out here. Clearly this has not been found. This result is clear evidence for a net motion of the galaxies with respect to the CBR, with a velocity component of the cluster ellipticals along the CBR dipole axis of 610 ± 116 kms^{-1}.

Figure 2.2 shows the velocity residuals in the CBR frame for the 60 galaxies projected onto the plane of the galaxy, b=0°. In this diagram, the Local Group is positioned at the centre. The symbols (0) show the positions of the galaxies as inferred from the photometry, whilst the other ends of the lines show the distances derived from the redshifts, corrected to the CBR frame. Thus the length of each line represents the radial component of the peculiar velocity of each galaxy. It should be remembered that the

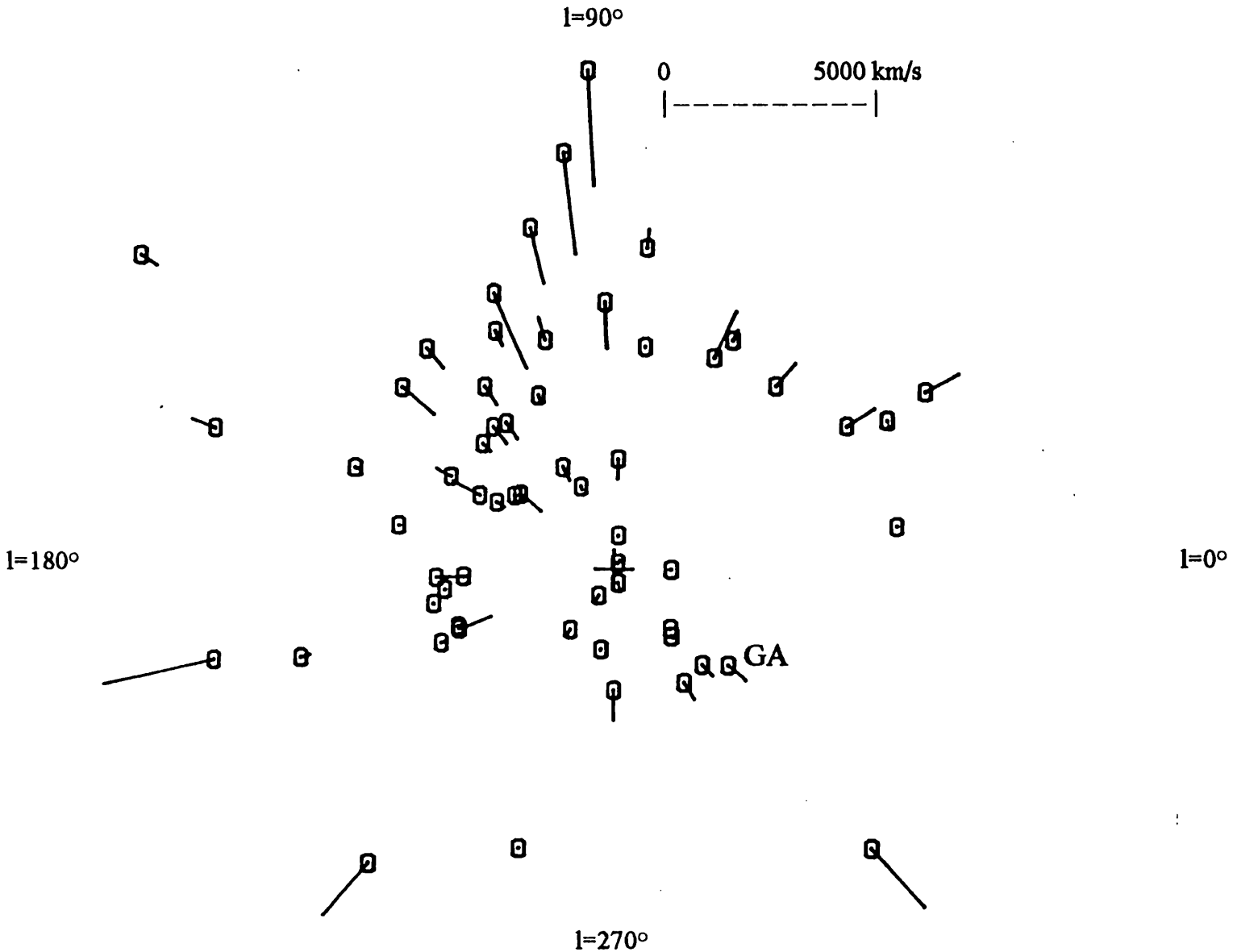


Figure 2.2 CBR-frame velocity residuals for the 60 cluster galaxies, projected onto the galactic plane. The position of the 'Great Attractor' is also shown (GA)

errors in the individual galaxies' luminosity distances are ≈15% of their actual distances, and that in projecting down the galaxy velocities from high latitudes, we are systematically underestimating the velocities in the plane of the diagram. This latter is unavoidable, given that only the radial component is measured, but it explains why galaxies close to the centre of the diagram appear to have small peculiar velocities.

Despite these problems, the streaming motion can be seen as a clear trend in the sense that the peculiar velocity vectors predominantly point towards the lower right in the diagram, corresponding to a direction on the sky of l≈300°. Possibly the most interesting feature of this plot is the scale over which the motion is apparent, with galaxies on opposite sides of the sky apparently sharing in the same overall flow.

This result is unlikely to be the result of Malmquist bias in the galaxy sample. This was tested by comparing the redshift distribution of galaxies in the apex and antapex directions along the axis of the CBR dipole. There is indeed an anisotropy in the distribution, which could lead to a systematic bias if the criteria used in selecting these clusters included an apparent magnitude cutoff, either explicitly or implicitly. However, the mean redshift in the apex direction, 6500 kms^{-1}, is *smaller* than that in the antapex direction, 8100 kms^{-1}, which should tend to produce an apparent motion in the CBR frame in the opposite sense to that which we measure. In any case, this sample should not contain significant Malmquist bias, since it is selected on the basis of cluster membership, rather than in terms of apparent magnitude. This is confirmed by the Hubble diagram presented by Sandage and Hardy (1973), which appears highly linear to a redshift of at least 20,000 kms^{-1}, a considerably greater depth than the subset of galaxies we use.

IV.2 COMPARISON WITH PREVIOUS STUDIES

The interpretation given above is that there is a net motion of the clusters in this sample relative to the CBR, with a component of 610±116 kms^{-1} along the direction toward l=272°, b=30°. The effective depth of this sample, with the weighting used for this solution, is 54 h^{-1} Mpc, which makes it one of the most distant galaxy samples used for measuring Hubble Flow anisotropies. A comparison will now be made with the most important large-scale studies previously discussed in Chapter One. These results are summarised in Table 2.3.

Table 2.3 Streaming motion components toward l=272°, b=30° derived from the work described in this Chapter, and in previous studies.

Authors	Galaxy type	Streaming component
James et al.	Brightest in clusters	611±115 kms^{-1}
Rubin et al.	Field spirals	779±135 kms^{-1}
Burstein et al.	Ellipticals	427±105 kms^{-1}
Aaronson et al.	Cluster spirals	-125±195 kms^{-1}
Hart & Davies	Sbc spirals	77± 70 kms^{-1}

The first is the original Rubin et al. study (1976a,b), later reanalysed by Schechter (1977) and Peterson and Baumgart (1986) with essentially unchanged results. The solution quoted by Rubin et al., a Local Group motion of 454±125 kms^{-1} toward l=163°, b=-11°, can now be converted into a CBR-frame streaming motion, using the accurate CBR anisotropy measurement of Lubin and Villela (1986). This gives a streaming motion of the galaxies with respect to the CBR of 885±135 kms^{-1} toward l=304°, b=26°. To compare this with our result for the first ranked cluster galaxies, it is necessary to take the component of this streaming along the CBR dipole axis. This component has a magnitude of 779±135 kms^{-1}, which is in fairly good agreement with the value of 610±116 kms^{-1} from cluster galaxy sample, the difference being just under 1σ.

The most directly comparable previous result is that for 10 galaxy clusters observed by Aaronson et al. (1986), using the IR Tully-Fisher relation on a large number of spiral galaxies within each cluster. The streaming velocity for this sample of clusters was 290±195 kms^{-1} toward l=42°, b=13°, corrected to the Lubin & Villela (1986) CBR dipole value, which is slightly different from that used by Aaronson et al. This gives a streaming component along the CBR axis of -125±195 kms^{-1} which is different from our result at the 3σ level. This discrepancy is hard to reconcile. Most of the Aaronson clusters are present in our sample, although there are still so few that a direct comparison of the two data sets is meaningless, given the errors on our individual cluster peculiar velocities. The range of redshifts covered by the two samples is very similar, as is the type of density environment sampled in the two cases. The two principal criticisms of the Aaronson study are the poor sky coverage and the assumption of a universal, unbiased Tully-Fisher relation from cluster to cluster (Bottinelli et al. 1988). The first is unlikely to explain the discrepancy found here since several of the Aaronson clusters lie in the CBR apex and antapex directions. The second remains a possibility, although

there is no reason to suppose that any bias in the TF relation would act so as to give the result actually found.

A final interesting comparison is with the 'Big Seven' study of elliptical galaxies (Dressler et al. 1987). Taking the component of their initially reported streaming vector (599 kms^{-1} toward l=312°, b=6°) along the CBR axis gives a value of 427 kms^{-1} ± 105 kms^{-1}. This differs from the cluster galaxy result by only 184 kms^{-1}, or by ≈1σ. Unfortunately, the agreement with their reinterpretation in terms of infall into a 'Great Attractor' is less good. Most of the significance for streaming in the clusters sample comes from the opposite direction to the Attractor, which is suggested to lie toward l=309°, b=9°, at a distance of ≈45 h^{-1} Mpc (see Fig. 2.2). These clusters are thus too far from the putative overdensity for it to explain more than a small fraction of the observed streaming. Thus the cluster galaxies do not provide support for the 'Great Attractor' model, and the initial agreement with the 'Big Seven' work must be seen as a coincidence.

IV.3 THE EFFECT OF CHOICE OF FRAME ON STREAMING SOLUTIONS

It has recently been suggested (Lucey & Carter 1988a) that the streaming motion we detect for the cluster ellipticals may be affected by the fact that the initial analysis (Sandage & Hardy 1973) was done using redshifts corrected to the Local Group frame of reference. This is important in this work since metric apertures were used, which require an accurate indicator of the distance to each galaxy in calculating the aperture corrections. The effect of using LG-frame redshifts can be seen by considering the case where the galaxy sample is truly at rest in the CBR frame. In this case, the galaxies towards the apex of the LG motion will have underestimated redshifts, which will lead to over-large metric apertures being defined. Thus these galaxies will seem to be systematically overluminous, and it would be concluded that they are streaming away from the LG. The reverse argument applies in the antapex direction. The derived CBR-frame streaming would then be in the sense that we actually find, so it is essential to determine whether this effect is likely to be important.

The size of this bias depends on the growth curve of the galaxies used. For example, if galaxies were to have a constant surface brightness, this effect would completely nullify the result presented here--the galaxies would appear to be at rest in <u>any</u> frame chosen for an analysis of the type carried out here. This is clearly sensible, since surface brightness is distance-independent, and aperture photometry on a galaxy of uniform surface brightness contains no distance information. However, the galaxies used here are

obviously not of uniform surface brightness, and the bias is thus considerably reduced. An approximate calculation was made by estimating the effect of a 10% change in aperture at the metric radius used by Sandage & Hardy, this being the approximate error in redshifts induced by the LG motion of ≈600kms^{-1} at the mean depth of our sample. The elliptical growth curves of Thuan & Romanishin (1981) were used. The size of the change was ≈6% in the total included flux, or ≈3% in distance. For galaxies at a mean redshift of 6000 kms^{-1}, this would give a spurious streaming of at most ≈180 kms^{-1}. This bias cannot explain the observed effect.

However, it should not be assumed that the streaming component we find is overestimated by 180 kms^{-1} due to the above effect. Our solution is completely self-consistent, in that the redshifts used to derive the metric apertures are (fortuitously) measured in that frame which is unaffected by the measured streaming. Thus the redshifts we use are good estimators of distance and in this case the Lucey and Carter critique is inappropriate. However, in general, corrections should be applied using CBR-frame redshifts if the ultimate aim is to derive streaming motions in that frame.

Lucey and Carter also made criticisms of the sample selection and photometry used in our analysis of the Sandage and Hardy data. In particular, they point out that the radio galaxies selected by Sandage and Hardy lie exclusively in the Northern Hemisphere and may affect the derived LG motion, if they have significantly different luminosities from the 'true' First Ranked galaxies. Thus they exclude all such galaxies from their analysis, along with the brightest galaxies in groups. Their analysis is independent of the Sandage and Hardy photometry, since they use photometry from the literature, which is available for 38 out of our sample of 60 galaxies out to a redshift cutoff at 10,000 kms^{-1}, and is generally of higher quality than that obtained by Sandage and Hardy.

Their results, using this higher quality but smaller data set, are somewhat discrepant from ours. Using the assumption that the galaxies are at rest in the CBR frame for fitting the metric apertures, the rest frame defined by the galaxies differs from that of the CBR by between 112 (±105) kms^{-1} and 299 (±250) kms^{-1}, depending on apertures and growth curves, compared with our result of ≈600 kms^{-1} . If the metric apertures are defined in the LG frame, the Lucey and Carter result becomes 250-300 kms^{-1}, in better agreement with ours but still not very significantly different from zero. Thus they conclude that there is no compelling evidence for galaxy streaming from their study of First Ranked cluster galaxies.

CHAPTER THREE

GALAXY STREAMING FROM AN ALL-SKY SAMPLE OF SCI SPIRALS

In this chapter I will present a description of a second attempt to measure the large-scale galaxy peculiar velocity field, and the results that were obtained. This study is complementary to the work with first-ranked cluster galaxies presented in Chapter Two, in several ways. Most importantly, it samples the velocity field with ScI spiral galaxies, which are generally found in the field and thus are environmentally independent from cluster galaxies. In addition, we used near-IR photometry to determine redshift-independent distances, avoiding many of the systematics inherent in the optical photometry used for the cluster galaxies.

I THE RUBIN ET AL. (1976a,b) STUDY

I.1 GALAXY SAMPLE SELECTION

The sample of galaxies we chose to examine in this work was that defined by Rubin et al. (1976a,b) in one of the first attempts to probe large-scale deviations from pure Hubble expansion. They initially selected 184 galaxies from the Zwicky et al. (1961-1968) catalogues, subject to the following selection criteria:

i) Their morphological classification, determined from examination of the Palomar Sky Survey (PSS) plates, should be ScI, ScII, or Sb?-Sc? I or II.

ii) They should have Zwicky (photographic) magnitudes between 14.0 and 15.0.

iii) Preference was given to nearly face-on galaxies because of the greater ease of classification of such galaxies.

Redshifts were obtained for all of these galaxies, and an attempt was made to reduce the Malmquist bias (Malmquist 1920) inherent in selecting by apparent magnitude by defining a 'Minimum Bias Subset'. This was done by excluding all galaxies with redshifts less than 3500 kms^{-1}, or with redshifts greater than 6500 kms^{-1} (with redshifts corrected to the Local Group frame of reference). This left a sample of 96 galaxies.

I.2 RUBIN ET AL. DATA AND ANALYSIS

Rubin et al. used the Zwicky photometry (Zwicky 1961-68) and their own redshifts to derive the motion of the Local Group relative to the sample of 96 galaxies. Redshift-independent distances were derived from the photometry by the Hubble Modulus technique described in chapter Two. The Local Group motion was then derived by fitting a dipole to the velocity residuals (V_H-V_{obs}), i.e. explaining the differences between the inferred distances and the measured redshifts in terms of the Local Group motion alone.

The best-fit dipole they calculated for the motion of the Galaxy and the Local Group of galaxies was 454±125 kms^{-1} toward galactic coordinates l=163°, b=-11°. This solution included a diameter correction later shown by Schechter (1977) to be spurious, and without which the solutions were found to be similar in amplitude and direction but reduced in formal significance to ≈3σ.

At the time, Rubin et al. commented that the corresponding solar velocity was anomalously large, at ≈600 kms^{-1}, compared to the limits on the anisotropy of the Cosmic Background Radiation. However, it was not until more accurate measurements of the CBR dipole were available that the implications of the derived velocity became apparent. Comparison of the Local Group motion with respect to the galaxies, and the most recent measurements of the CBR dipole (Lubin & Villela 1986), shows that if this measurement is correct it implies a net streaming of the galaxies at 885 kms^{-1} toward l=304°, b=26° (Clutton-Brock & Peebles 1981--note that they used the mean of earlier measurements of the CBR dipole).

II CRITICISMS OF THE RUBIN ET AL. RESULT

II.1 THE FALL AND JONES INTERPRETATION

The first, and one of the most serious criticisms of the Rubin et al. result was that of Fall and Jones (1976). They demonstrated that an earlier velocitv anisotropy result (Rubin et al. 1973) could be due to a combination of Malmquist bias and uneven sky coverage. The narrow apparent magnitude selection range of the sample galaxies unavoidably leads to a trend of apparent magnitude with redshift, via the Malmquist bias. Fall and Jones pointed out that if a galaxy sample is of unequal depth in different directions, there will then be a correlation between absolute magnitude and direction on the sky. This would then explain the anisotropy found by Rubin et al. They also showed that there was

indeed a variation in the depth of the initial galaxy sample around the sky, in the sense required to produce the observed effect, and that the bias was on the order of that required to explain the observations, at least for the initial sample of Rubin et al. (1973). Whilst these problems were at least partially answered by the selection of the Minimum Bias Subset as described above, they remained as a major question mark over the Rubin et al. result.

II.2 WEAKNESSES IN THE RUBIN ET AL. DATA AND ANALYSIS

A further criticism of the Rubin et al. analysis was that their sample selection criteria were not as strict as was claimed. They stated that the galaxy sample used for their work was composed purely of galaxies classified under the Sandage (1961) and van den Bergh (1960a,b) system as ScI, ScI-II or Sb?-Sc? I-II. However, independent classifications of the galaxies show that the range of morphological type of the galaxies in the Minimum Bias Subset is much broader than this. For example, the Uppsala Galaxy Catalogue (Nilson 1973) classifies some as early as Sa or SBa, and others as S...(spiral, otherwise unclassifiable). Many of the galaxies are barred, some strongly, and others appear to be in close groups or to have very close companions. To cite some of the more extreme examples amongst the 86 galaxies in our subsample, RF 5 is classified as SAB(s).../S... by Nilson on the de Vaucouleurs and van den Bergh systems respectively, with a note that it is distorted and in a group. RF 30 is classified SAB(s)ab/SBa, RF 151 SABab/Sb, RF 161 S... (disturbed) and RF170 SB... (singular). These factors are likely to have an effect on the star formation history of the galaxies, and certainly undermine their precision as standard candles.

Whilst such problems probably diminish the accuracy of the measurements made with this galaxy sample, they are not such a severe threat to the credibility of the results obtained as the Malmquist bias effects discussed above. This is because there is no reason to suspect a correlation with direction on the sky and thus morphological inhomogeneity is unlikely to cause an apparent, spurious detection of a streaming motion. The extra scatter in the absolute magnitudes of the galaxies will, however, cause a larger random error in the final value of the derived streaming motion.

A further problem with the Rubin et al. analysis, and all others relying on optical photometry for the derivation of redshift-independent galaxy distances is that of galactic extinction. This is important since, if wrongly corrected for, it will leave a systematic error in galaxy magnitudes which correlates with direction on the sky. This could then

manifest itself as a spurious streaming motion. Rubin et al. adopt a magnitude correction for Galactic extinction of the form

$$\Delta m_b = A_B(\mathrm{cosec}\,|b| - 1); \qquad A_B = 0.15 \qquad 3.1$$

where b is the galactic latitude of the galaxy concerned. They do not adopt Sandage's prescription (1973) of applying no correction for $|b| > 50°$. The coefficient A_B is also notoriously uncertain, estimates ranging from 0.11 (Peterson 1970) to 0.5 (Shane and Wirtanen 1954, 1967). The problem is a double-edged one; not only is an inaccurate correction likely to produce a spurious streaming motion, but there is also a danger of a true streaming signal being at least partially 'corrected away' by being confused with extinction effects.

A related but less worrying problem associated with optical measurements is that of internal extinction, which leads to highly inclined galaxies being faint compared with face-on ones. This is quite significant at B, since the corrections are approximately as large as those for Galactic extinction, but is effectively just another source of random scatter, which should not be correlated with direction, as far as streaming studies are concerned. Rubin et al. adopted a correction of the form

$$\Delta m_i = A_i(\sec(i) - 1); \quad A_i = 0.12 \qquad 3.2$$

Again the value of A_i is very uncertain, Holmberg (1958) quoting a value twice as large.

The final criticism that can be levelled at the Rubin et al. galaxy sample for deriving 3-dimensional streaming vectors is that the sky coverage is patchy and incomplete. This is to an extent unavoidable, given the clustered nature of the galaxy distribution, but it is particularly bad for this sample, with an almost complete lack of galaxies below declinations of about -40° (see Figure 3.1). The effect of this is that the component of the bulk velocity along the direction of the 'hole' is ill-determined and contributes disproportionately to the uncertainty in the final vector solution.

III A REANALYSIS OF THE RUBIN ET AL. SAMPLE USING NEAR-IR PHOTOMETRY

Given the importance of the Rubin et al. result for cosmology, it is not surprising that many attempts have been made to check their conclusions. As described in Chapter One, it has been shown that the use of different methods of analysis (e.g. Schechter

1977) or of independently obtained B-band photometry (Peterson and Baumgart 1986) confirm the "Rubin-Ford effect". However, although these results give added credibility to the Rubin et al. work, they cannot be considered truly independent measurements for two reasons: they use the same galaxy sample, and they all make use of optical photometry with all the resulting problems of extinction and extinction corrections outlined in the previous section. I will now discuss a reanalysis of the "Rubin-Ford effect" that makes use of near-infrared photometry to overcome the problems of extinction effects, and can potentially overcome some of the problems of Malmquist bias and selection systematics.

III.1 ADVANTAGES OF NEAR-IR PHOTOMETRY

Near-IR photometry of galaxies through the J (1.3 μm), H (1.6 μm) and K (2.2 μm) atmospheric windows is now a widely used technique, with the necessary instrumentation being available at most medium- and large-sized telescopes. The principal advantage for the work under discussion is the very much reduced effect of extinction compared with the optical. For example, the corrections needed at H are on the order of 6 times smaller than at B. This both reduces the scatter introduced in galaxy apparent magnitudes by internal and Galactic extinction, and more importantly reduces the systematic effects of differential Galactic extinction.

The other main advantage of near-IR photometry for redshift-independent distance determination is the ability to use two of the best galaxy luminosity indicators yet discovered. These are the H-band Tully-Fisher relation and the B-H colour-magnitude relation. Both make use of redshift-independent observables to correct the measured galaxy magnitudes so as to make them better standard candles.

In the case of the Tully-Fisher relation, the observable parameter used is the measured width of the 21cm neutral hydrogen line, corrected for inclination. This width is effectively a measure of the maximum rotational velocity reached in the disc of the galaxy, which correlates strongly with the amount of mass in the central regions of the galaxy. Thus it is found that brighter galaxies, having more stars, tend to have the greater line-widths, and it is therefore possible to remove much of the scatter in absolute magnitudes by using this correlation. It has been found empirically (Aaronson et al. 1979) that the correlation has about half the scatter for near-IR H magnitudes compared with optical B magnitudes, with which the relation was initially investigated (Tully and Fisher 1977). This is understandable since the basis of the relation is between the galaxy mass and luminosity, and H magnitudes measure the contribution from the older

red stellar population which dominates the total stellar mass. The blue luminosity is strongly affected by young hot stars, and therefore correlates more strongly with recent star formation history than with the total mass in stars. Using the H-band Tully-Fisher relation, it is possible to reduce the scatter in absolute magnitudes to about 0.45 magnitudes, making this possibly the most powerful galaxy luminosity indicator known. The main disadvantage of the H-band relation is that it has a steeper slope than the optical relation (≈10 compared with ≈5), and any uncertainty in the corrected linewidths will give a correspondingly larger magnitude error (Bottinelli et al. 1983). In particular, this makes it essential to determine accurate inclinations when using the H-band relation.

The physical basis of the relation has been the subject of much discussion, but no model has yet emerged which explains all the observed features. Aaronson et al. (1979, 1980) derived a simple model based on the assumptions that all spirals have the same mass profiles as a function of a dimensionless scale length, and all have the same central mass surface density and mass to light ratio. This predicts a luminosity proportional to the rotational velocity to the 4th power. This has been shown to be too simplistic by Burstein (1982), who finds that the assumption of a constant mass to light ratio is inconsistent with the other assumptions. The situation has been further complicated by the discovery by Bothun & Mould (1987) of large surface brightness variations at a given linewidth, and seems to preclude the possibility of a successful model based on simple dynamical grounds as proposed by Aaronson et al. (1979).

The second luminosity indicator using H-magnitudes is the B-Hcolour-magnitude relation (Visvanathan 1981, Tully et al. 1982, Wyse 1982). The distance-independent parameter used here is the B-H colour of the galaxy, which is again found empirically to correlate with the H absolute magnitude. This can be seen immediately as a consequence of the different slopes of the B- and H-band Tully Fisher relations, mentioned above. The basis of this relation is less well understood than the Tully-Fisher relation, but it must involve a link between the total mass of the galaxy and the recent star formation history, which determines the B-H colour. The scatter in this relation is not yet well determined, with the possibility that environment affects the slope and/or zero point of the relation. In any case, it is unlikely that the scatter will be smaller than that of the IR Tully-Fisher relation.

Bothun et al. (1985) have investigated the relation for galaxies in 7 clusters, and find that the slope is consistent within the errors. However, the intercepts were found to vary from cluster to cluster by as much as 1 magnitude. This increased the scatter in the

relation, for all data taken together, to 0.68 magnitudes, and cast serious doubts on the validity of the relation. Ellis et al. (1986) have examined this claim using a sample of 195 galaxies from the Durham-AAT redshift survey (Peterson et al. 1986) and do not support this claim. Indeed, they find that the residuals in the relation correlate with galaxy surface brightness at H, and by making use of this, e.g. from array photometry, it should be possible to get distance moduli accurate to 0.25 magnitudes.

There are two principal advantages associated with the ability to use these relations. The first is that they reduce the uncertainty in the absolute luminosity of the galaxies, and thus enable one to probe the peculiar velocity field with a greater degree of accuracy than would otherwise be possible with a given number of galaxies and a given amount of observing time. The second advantage is potentially even more important, since it involves the removal of selection biases such as those discussed by Fall and Jones. Malmquist-type biases all result in the selection of brighter galaxies at high redshifts. Thus it is possible to use a redshift-independent luminosity indicator to both identify and remove the effects of these biases, with an efficiency that depends on the scatter in the indicator.

III.2 NEW DATA: NEAR INFRARED GALAXY PHOTOMETRY

Given the advantages of near-IR photometry for studies of the galaxy peculiar velocity field, it was decided to base this reanalysis of the Rubin et al. work on J (1.3 μm), H (1.6 μm) and K (2.2 μm) photometry of the Rubin et al. Minimum Bias Subset. This photometry was obtained at the 1.5m Infrared Flux Collector (IRFC) on Tenerife, the 1.9m telescope at the South African Astronomical Observatory (SAAO) and at the United Kingdom Infrared Telescope (UKIRT). Almost all of the data used in the final analysis presented here were obtained at the IRFC and UKIRT. Good quality H-band photometry was obtained for 86 of the 96 galaxies in the MBS, 59 of them in one 4 night run at UKIRT. The distribution of the 86 galaxies is shown in Fig. 3.1. In addition the analysis will also make use of the high-quality B-band photoelectric photometry of Peterson and Baumgart (1986), supplemented from Graham (1976).

Typical photometric errors for our infrared data are ≈5% RMS for galaxies repeated on the same telescope, an ≈10% for galaxies repeated at different sites. Given the precision of the luminosity indicators (≈0.45 magnitudes) it is clear that the scatter resulting from photometry errors is negligible.

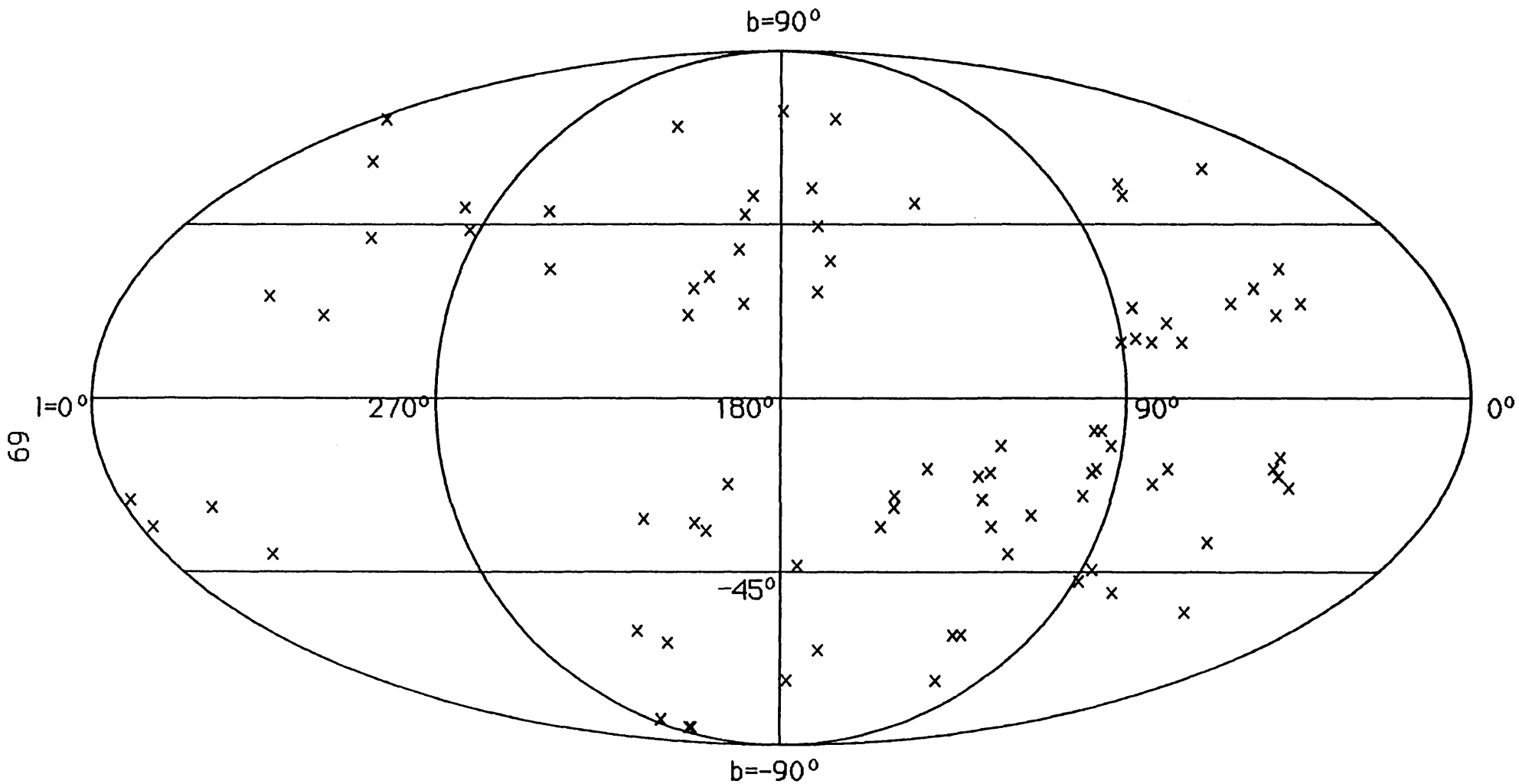


Figure 3.1 Sky distribution of 86 Sc galaxies from Rubin et al. 1976a,b (galactic coordinates)

Table 3.1 contains the following photometric and redshift data for these galaxies:

Column 1	Number in the Rubin et al. (1976a,b) list.
Column 2	Galactic longitude l^{II}.
Column 3	Galactic latitude b^{II}.
Column 4	H apparent magnitude, corrected for airmass and aperture effects, using optical diameters for the latter (see below).
Column 5	J apparent magnitude, corrected as H above.
Column 6	K apparent magnitude, corrected as H above.
Column 7	B apparent magnitude from Peterson & Baumgart (1986), corrected for airmass and aperture effects, using optical diameters.

Table 3.1 Photometric and redshift data for 86 Sc galaxies from the Rubin et al. Minimum Bias Subset.

RF	l^{II}	b^{II}	Redshift	$H_{-0.5}$	$J_{-0.5}$	$K_{-0.5}$	B_{-1}
1	111	-30	4613	11.70	12.35	11.37	14.25
5	114	-40	4807	11.10	11.78	10.80	14.67
7	111	-73	5555	11.84	12.59	11.52	14.05
8	116	-61	3996	10.43	11.08	10.15	12.90
9	121	-33	4521	11.04	11.71	10.73	13.91
10	119	-61	4198	12.47	13.04	12.23	14.34
11	122	-12	4927	11.58	12.35	11.29	15.10
12	124	-19	5122	13.07	13.69	12.80	15.24
14	125	-26	5823	12.44	13.07	12.14	14.70
15	250	-85	5396	10.75	11.44	10.46	13.25
16	252	-85	5714	11.05	11.70	10.75	13.56
17	127	-20	5626	12.17	12.86	11.87	14.82
18	260	-83	4984	12.29	12.88	11.96	14.25
20	260	-83	5761	12.47	13.17	12.22	14.55
24	177	-73	4930	13.21	13.78	12.93	14.96
27	166	-65	4506	12.52	13.13	12.24	14.41
30	141	-18	4342	10.89	11.61	10.59	14.20
34	152	-33	5363	12.54	13.18	12.21	14.65
35	149	-28	4811	12.32	12.98	12.01	14.68
38	149	-25	4286	12.08	12.77	11.76	14.83
40	221	-63	5060	10.86	11.53	10.58	13.38
41	230	-60	4726	11.61	12.27	11.31	14.07

42	175	-43	5668	10.67	11.41	10.36	14.05
50	201	-34	4204	10.95	11.64	10.68	13.47
53	204	-32	4433	11.16	11.90	10.86	14.18
54	194	-22	4614	11.52	12.21	11.25	14.16
55	218	-31	4441	11.49	12.20	11.18	14.34
67	170	28	6463	12.16	-	12.25	14.83
71	190	25	4457	11.21	11.85	10.92	13.75
72	205	22	5055	12.73	13.04	12.40	14.65
76	204	29	4729	11.39	12.04	11.12	14.23
77	166	36	5206	12.62	13.24	12.18	14.71
78	200	32	5696	11.77	12.53	11.75	14.17
79	192	39	4607	11.96	12.46	11.89	13.93
83	169	45	5048	11.70	12.51	11.22	13.45
86	191	48	4655	11.66	12.15	11.41	13.76
87	245	34	6913	12.15	12.68	12.00	14.40
88	189	53	5409	11.57	12.15	11.41	13.57
92	170	55	5278	11.97	12.26	11.37	14.10
96	252	49	4908	12.65	13.27	12.55	14.64
102	273	44	5764	11.70	12.37	11.40	14.29
103	138	51	3857	11.77	12.34	11.32	13.81
106	224	71	6837	12.44	13.08	12.33	14.83
109	179	75	6701	10.93	11.60	10.57	13.72
110	279	50	6111	11.54	11.88	11.08	13.66
112	156	73	6394	11.42	12.15	11.07	13.85
121	301	42	6680	10.96	11.70	10.74	13.73
124	303	22	4142	11.11	-	-	13.36
130	327	62	5562	11.17	11.83	10.85	13.80
133	356	73	6090	11.85	12.50	11.58	13.99
137	320	27	4890	12.03	12.43	-	13.48
145	33	60	5895	11.98	12.57	11.69	14.03
148	68	56	5707	11.48	12.08	11.20	13.82
151	70	53	5706	10.95	11.57	10.65	14.41
160	40	34	6112	12.12	12.76	11.81	14.50
161	50	29	4748	11.19	11.83	10.84	13.78
162	39	25	5978	11.93	12.57	11.59	14.44
164	47	22	6066	11.55	12.19	11.20	13.85
165	58	25	4716	11.64	12.27	11.30	13.85
168	85	24	5789	11.17	11.87	10.86	13.77

169	77	20	4557	11.45	12.14	11.11	14.15
170	74	15	4430	12.19	12.74	11.90	13.92
171	82	15	3843	12.57	13.20	12.23	14.18
172	86	16	3751	10.99	11.76	10.64	13.95
173	357	-26	5608	11.93	-	-	13.88
174	90	15	3420	11.39	12.09	11.08	13.55
176	48	-15	5000	11.97	12.73	11.69	14.44
177	356	-33	5715	11.53	-	-	13.44
179	49	-18	4598	11.75	12.54	11.45	14.41
181	47	-20	5039	11.28	11.93	10.95	14.28
182	43	-23	5697	11.06	11.73	10.73	14.17
187	58	-37	4388	11.62	12.27	11.30	14.19
188	80	-22	5367	12.22	12.87	11.98	14.52
189	93	-12	5044	11.49	12.31	11.06	14.50
191	96	-8	5202	11.87	12.75	11.34	14.65
192	98	-8	5203	11.60	12.33	11.53	14.60
193	47	-55	4708	12.04	12.70	11.80	14.78
195	96	-18	4382	11.94	12.59	11.64	14.27
196	97	-19	4472	12.04	12.69	11.71	14.69
197	76	-50	4463	11.96	12.60	11.64	14.32
199	98	-25	5629	12.37	13.04	12.12	14.93
200	87	-44	4520	11.58	12.23	11.25	13.74
201	89	-47	3172	11.69	12.30	11.40	13.40
204	336	-28	4453	10.81	-	-	13.45
207	328	-40	5074	11.91	-	-	14.02
209	77	-18	4519	10.40	11.12	10.04	13.55

III.3 PHOTOMETRIC CORRECTIONS

There are several corrections which have to be applied to aperture photometry if it is to give accurate and unbiased distance determinations. Most of these corrections are smaller at near-IR wavelengths than in the optical, but since IR astronomy is relatively young the values for the corrections in the literature are correspondingly less well determined. Thus wherever possible I have attempted to derive magnitude corrections internally from the dataset for comparison with the best previously determined values. Airmass corrections were determined on a night-by-night basis, using near-IR photometric standard stars which were observed at frequent intervals on all observing runs. A regression was done of

[(Catalogued magnitude)-(Measured magnitude)] against [Airmass], and the slope gives the airmass correction for that night in that band. On nights where observing was curtailed by weather and too few stars were observed for this approach, the airmass correction for each galaxy was obtained from the standard star closest to it in time and airmass. This approach is shown to be successful by the degree of agreement in the magnitudes of galaxies repeated on different nights at UKIRT, which typically differed by less than 5%. The derived corrections were in any case very small, ≈0.1 magnitudes/airmass in all three bands, and most of the galaxies were observed at airmasses of less than 1.5.

Aperture corrections are essential to avoid systematic offsets between photometry obtained at different telescopes, and biases as a function of redshift. Telescope-related differences come about since it was impossible to use the same sized apertures at the different telescopes used for this project. What was ideally required was a total magnitude for each galaxy, and therefore the largest available apertures were used. For the telescopes used to obtain the data presented here, these were nominally 27″, 35″ and 18″, at UKIRT, IRFC and SAAO respectively. Thus significant corrections are needed to derive magnitudes at the same effective apertures.

The second function of aperture corrections is to avoid a redshift-dependent effect that occurs as a result of using fixed apertures. A given aperture includes flux within a linear diameter that is proportional to redshift, and thus there is a systematic tendency for apparent luminosities to be overestimated for distant galaxies relative to nearer ones. This effect tends to exacerbate the effects of Malmquist bias.

To overcome both of these effects, reliable growth curves are needed. The H-band light profiles of spiral galaxies have been studied (Aaronson et al. 1979), and the growth curves approximated to a power law:

$$F(A) \propto A^{0.88} \qquad 3.3$$

This law was derived from a small sample of Sc galaxies, using aperture photometry with typically only 3 or 4 apertures per galaxy. Thus there is considerable doubt as to the accuracy of this particular functional form for the growth curve, especially over a wide range of inclinations. However, it will have to suffice until better data become available, and ideally area photometry of a large sample of Sc galaxies.

The second requirement is for a standard diameter to which the photometry can be corrected. Aaronson et al. (1979) in their initial work on the H-band TF relation used optical diameters, defined as the diameter at which the optical B-band surface brightness falls to the 25 magnitude (square arcsec)$^{-1}$ level. Theoretically, this is a convenient normalisation to take since surface brightness is a distance-independent observable and so should define a distance-independent photometry system. Unfortunately, for the MBS sample it can be shown to be a very ineffective at reducing the measured Malmquist bias in the sample, which is the aim of applying such a correction. The effectiveness was gauged by calculating absolute magnitudes for the galaxies on the assumption of pure Hubble Flow, i.e. that redshifts in the CBR frame are perfect indicators of distance. Regression of [Absolute magnitude] against [Log redshift] then gives a measure of the total bias in the sample.

In this way, I tested the standard aperture correction, using optical diameters from the Second Reference Catalogue of Bright Galaxies (de Vaucouleurs 1976). The diameters used were the D(0) values, which are measured to the 25 magnitude/sq arcsec isophote and corrected for inclination. This latter correction is very uncertain, but fortunately the galaxies in this sample are very face-on and so its effect is negligible. The H-magnitude aperture correction from Aaronson et al. (1979), to a standard value of log(A/D)=-0.5, is given by

$$\Delta H = -2.19 \log(A/D(0)) - 1.095 \qquad 3.4$$

which is subtracted from the raw magnitude. A is the telescope aperture in arcmin. As stated above, this correction serves the additional purpose here of accounting for the different apertures used to obtain the photometry. The effect of this alone can be separated out by applying a correction of 2.19(log A).

Regressing H_{abs}, corrected for the effects of different telescope apertures only, against log (Redshift) gives a slope of -5.1. Using magnitudes corrected to log(A/D(0))=-0.5, the same regression gives a slope of -4.2, i.e. the bias has been reduced, but by less than 20%.

An alternative approach to the removal of aperture effects is to use metric apertures. These are apertures defined to be a constant linear size at the distance of the galaxy, and are therefore based on the CBR-frame redshift of the galaxy. The small redshift range of the galaxy sample used here means that cosmological corrections to the derived apertures are small, and the metric apertures can be taken as being inversely proportional

to redshift. The size of the effective aperture used was defined as the size of the UKIRT aperture projected to the mean redshift of the sample, thus minimising the size of the corrections. Using these aperture corrections, the regression slope of absolute magnitudes against log (Redshift) is reduced to -2.88, a much more significant reduction than normalising to optical diameters.

From this I conclude that there is a significant aperture effect in the raw magnitudes, which is more efficiently removed by correcting to metric diameters than to diameters defined at a particular optical surface brightness. This is to be expected, given the large scatter in optical properties of galaxies and the difficulty of measuring consistently to a given surface brightness. However, even the metric correction does not remove all of the effect, and this residual is probably due to Malmquist selection bias. Thus the high redshift galaxies are genuinely more luminous and of higher surface brightness than the low redshift galaxies.

Since this effect is highly significant and unlikely to be removed completely using aperture corrections, I prepared datasets in which it had been removed explicitly. This was done by regressing H_{abs} and B_{abs} against log [CBR-frame redshift], and thus deriving a correction which removed the trend in absolute magnitude with redshift. These will be referred to as 'Malmquist corrected' datasets.

Figure 3.2 shows the systematic trend in absolute magnitude with redshift, in the sense that higher redshift galaxies are brighter. This is after applying aperture corrections based on catalogued optical diameters. The important feature of this diagram is that the bias is present at all magnitudes, a consequence of the narrow apparent magnitude selection window which excludes both faint and bright galaxies. If the bias were of the more usual type where there is only a cutoff at faint magnitudes, it might be possible to define a complete, unbiased subset of the sample to some limiting redshift, but that is clearly impossible here.

III.4 GALACTIC AND INTERNAL EXTINCTION CORRECTIONS

One of the principal advantages of using near-IR photometry is the small size of the corrections for internal and galactic extinction compared with optical photometry. Due to the potential importance of these corrections, however, it is not safe to assume that they are negligible, so an attempt was made to derive them internally from the dataset. For comparison purposes, the same process was undertaken for the Peterson & Baumgart (1986) B photometry for the same galaxies.

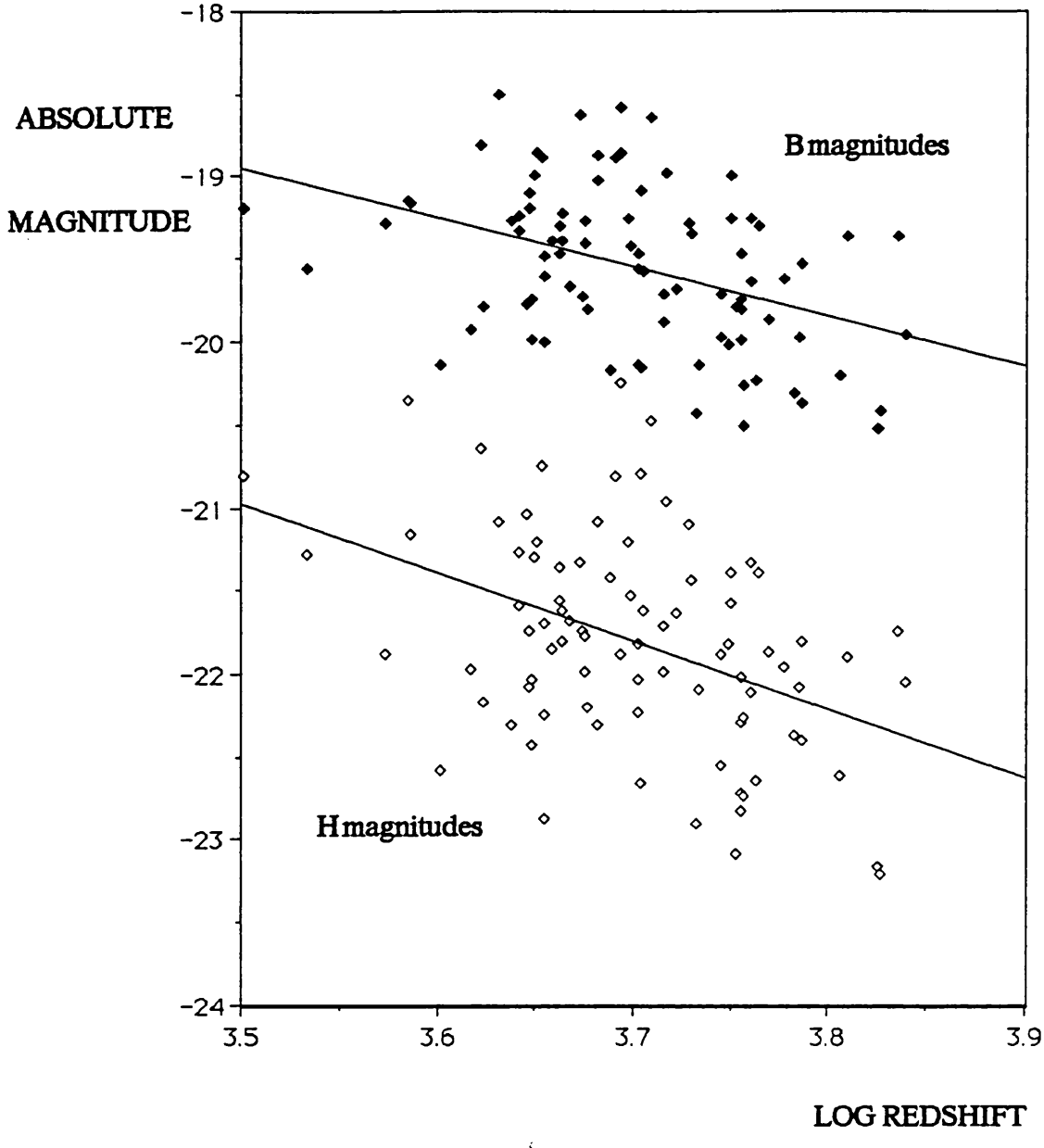


Figure 3.2 Malmquist bias shown as a trend in absolute B & H magnitude with redshift, for 86 Sc galaxies

Internal extinction is an inclination dependent effect. In the optical region it results in edge-on galaxies appearing fainter than face-on galaxies of the same intrinsic luminosity. In the near-IR the situation is more complex, since the effects of dust absorption are much less significant. Inclined galaxies may even appear brighter in a given circular aperture, since more stars will be projected along the line of sight.

From equation 3.2, the internal extinction coefficient A_i will be given by the slope of absolute magnitude (corrected for aperture only) plotted against (sec(i)-1). For the 86 galaxies in the present sample, the derived value of A_i is 0.22, 0.22 and 0.20 at J, H, and K respectively, and 0.36 at B, using aperture corrections based on optical diameters. This is a surprising result, since the difference between the optical and IR coefficients should be a factor of ≈5 to 10 on physical grounds. The simplest explanation is that there is a selection effect operating, in the sense that the more highly inclined galaxies are intrinsically faint. This is readily understood, since edge-on galaxies are more difficult to classify, and this subset of the sample is likely to contain galaxies of lower luminosity class which would have been excluded if face-on.

In light of this possibility, the most reasonable conclusion is that the true coefficient of the IR absorption is small, $\lesssim$0.03, and the B coefficient is given by the difference between the measured optical and infrared values. This gives a value of ≈(0.36-0.21) or 0.15, in good agreement with the generally accepted value. These values are used for the remainder of this analysis. The remainder of the inclination dependence is due to selection, an effect on the order of 0.2 magnitudes between face-on and 60° inclination. The effect of correcting for this bias will be discussed in section III.6, but the corrections are small due to the face-on nature of the galaxies in the sample.

The galactic extinction was derived in a similar way, regressing galaxy absolute magnitudes against (cosec|b|-1). The Peterson B magnitudes gave a slope of 0.17, close to the value of 0.15 adopted by Rubin et al. More interesting are the slopes obtained at J, H and K, of 0.09, 0.06 and 0.06 respectively. Thus there is tentative evidence that the effects of galactic extinction may not be completely overcome at near-IR wavelengths. A systematic may again be responsible, but, unlike the inclination bias, there is no obvious effect that could cause this. In any case, the bias at H and K is small enough to be negligible, and the B magnitude correction is close to the nominal correction adopted by Rubin et al., which will be used henceforth.

To conclude, I have investigated airmass, aperture, internal extinction and galactic extinction corrections for our new IR photometry of the MBS galaxies. Of these, only

airmass and aperture were found to have a definite effect at J, H and K, but biases have been identified in the dataset. The most significant of these is a redshift bias, resulting from Malmquist selection effect, which is slightly reduced by the use of aperture corrections based on optical diameters, and substantially reduced by the use of metric aperture corrections. The effect of correcting specifically for the residual Malmquist bias, and for the inclination bias, will be considered in section III.6.

III.5 LUMINOSITY INDICATORS

A possible way to remove the selection biases identified in the previous section is through the use of third variable luminosity indicators. These make it possible to identify explicitly those galaxies which are more or less luminous than the mean, and to correct them all to the mean luminosity. The methods to be investigated here use the B-H colour and the 21cm neutral hydrogen line width as the luminosity indicators.

III.5a THE B-H COLOUR-MAGNITUDE RELATION

The B-H colour-magnitude relation is an empirical relation between B-H colour of spiral galaxies and their H-band luminosity. It was discovered independently by Visvanathan (1981), Tully et al. (1982) and Wyse (1982). The physical basis of the relation is not well understood, but Tully et al. (1982) were able to model it by postulating an exponentially decreasing star formation rate, with a time constant that is inversely related to the galaxy mass. Thus smaller galaxies have a higher rate of star formation at present and are therefore bluer, but fainter at H, which traces the underlying stellar population and thus the mass.

Figure 3.3 shows the B-H colour vs. H absolute magnitude plot for the 86 MBS galaxies, using aperture B and H magnitudes. The B magnitudes used are from Peterson & Baumgart (1986) (68 galaxies), and Graham (1976) (18 galaxies). In both cases photoelectric photometry was used, and Peterson & Baumgart (1986) find no discrepancy between the two data sets, comparing photometry for galaxies included in both lists:

$$B_{PET} - B_{GR} = 0.03 \pm 0.03;$$

$$(B-V)_{PET} - (B-V)_{GR} = -0.01 \pm 0.02.$$

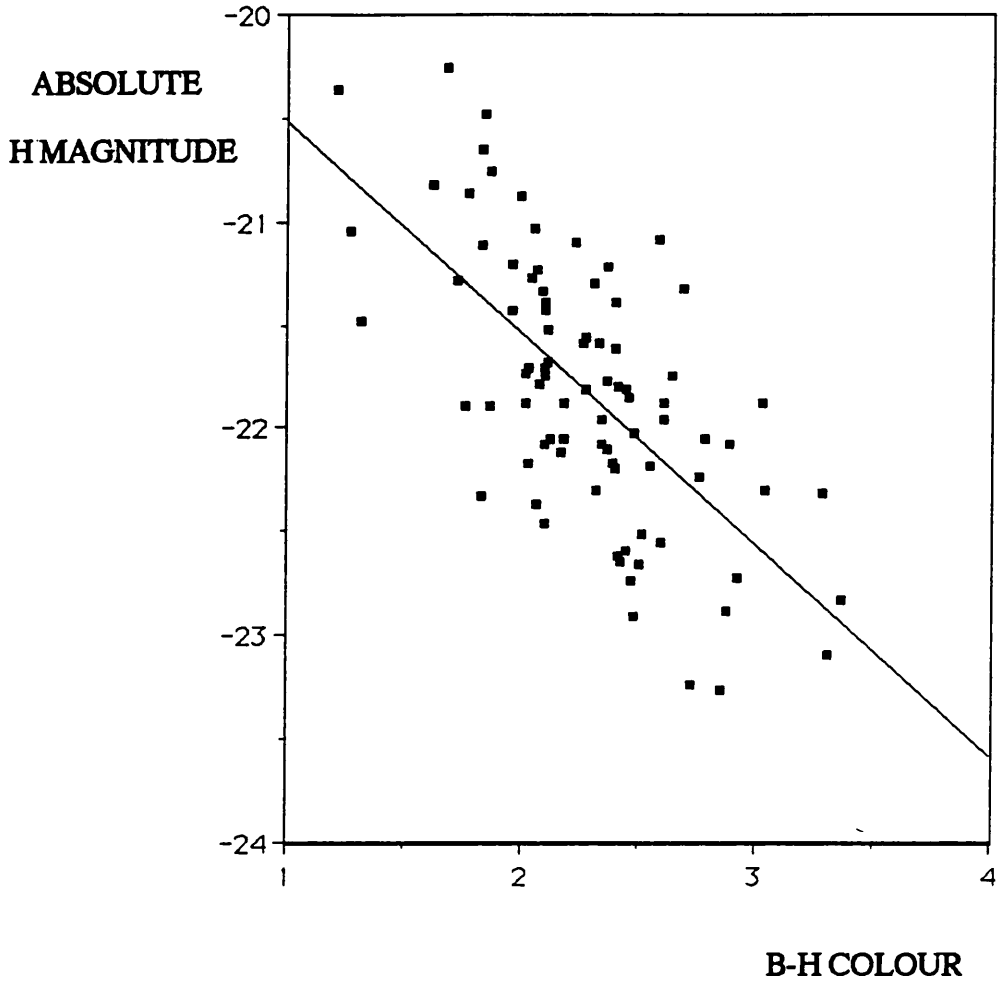


Figure 3.3 B-H colour-magnitude relation for 86 ScI galaxies

A strong correlation is evident in the colour-magnitude plot, which is confirmed by a correlation coefficient of 0.7. However, the slope obtained regressing H_{abs} on B-H is very small at -1.02, compared with slopes of ≈2 from the initial studies of the B-H C-M relation. Our data give a slope of -1.5 if the regression is done so as to minimise the perpendicular distances from the points to the line, but a correction based on this steeper slope is hard to justify physically. This is because the steeper slope gives corrected absolute magnitudes with a significant *positive* slope when plotted against B-H (an anti-Malmquist bias), implying that they have been over-corrected.

A possible reason for the low slope, compared to previously quoted values, can be found by considering the effect of applying a correction to the H magnitudes based on the slope of ≈-1, which is the correct one to use if the aim is to minimise the scatter in H_{abs}. Clearly, H - α(B-H), with α of -1, gives corrected H magnitudes that are identical to B magnitudes! Another way of expressing this is that the linear combination of B and H magnitudes which minimises the scatter in absolute magnitude is given by the B magnitudes alone. Including the H magnitudes merely increases the scatter.

This does not mean, however, that the B magnitudes provide a better standard candle than the H magnitudes. This is almost certainly another artefact of the selection procedure adopted by Rubin et al., which constrained the optical absolute magnitudes of these galaxies. Whilst their selection criteria specifically restricted the apparent magnitudes, the net result of this and the small redshift range is that the B absolute magnitudes lie within a range of ≈2 magnitudes. It is then only necessary to postulate a significant random scatter in B-H for there to be a spurious correlation between B-H and H_{abs}, with a slope of -1.

This is a fundamental problem in attempting to apply the C-M relation to this sample of galaxies. The selection bias makes it impossible to determine whether there is a true correlation between colour and absolute magnitude for these galaxies, and also makes it impossible to use colour information to remove biases and reduce scatter.

III.5b THE INFRARED TULLY-FISHER RELATION

The second luminosity indicator that we used to try to remove bias from the MBS sample was the infrared Tully-Fisher relation. This is a correlation between IR luminosity and the width of the 21cm neutral hydrogen line in spiral galaxies. The line is assumed to be broadened by rotation, and thus the width is a good indicator of the mass of the galaxy inside the radius of maximum rotational velocity.

The linewidth data used here were taken from Rubin et al. (1976a). They were corrected to edge-on inclination using axial ratios from the Second Reference Catalogue (de Vaucouleurs et al. 1976), according to the formula given by Rubin et al:

$$\cos^2 i = 1.042(b/a)^2 - 0.042 \qquad 3.5$$

The axial ratios measured by Rubin et al. (1976a) were also tried, but were found to give a much larger scatter in the Tully-Fisher relation than the values taken from the Second Reference catalogue.

Unfortunately, the galaxies in this sample are predominantly face-on (Fig. 5.1), which means that the corrections to edge-on linewidths are in many cases large and uncertain, and in several cases impossible to determine. As a result, the Tully-Fisher relation can only be applied to 60 of the 86 galaxies of our sample with $i > 25°$, and the errors in the edge-on linewidths of many of these are very large.

Figure 3.4 shows the Tully-Fisher relation obtained using metric-aperture corrected H magnitudes, and the regression slope of H_{abs} on $\log[\Delta V(0)]$, which is the appropriate one to use when using the relation to correct to a standard luminosity. Again, the use of a steeper slope, such as that found by minimising perpendicular distances in the regression, produces a negative correlation in absolute magnitude with [log (linewidth)]. In addition, the lower slope is the one that minimises the scatter in the corrected absolute magnitudes. The slope is very low, at ≈-1.1 (or -1.45 for optical diameter corrected magnitudes), compared to the normally quoted values of 8 to 12 (e.g. Aaronson et al. 1979). This is partly due to regressing onto the $\log[\Delta V(0)]$ axis, which has not always been the practice adopted elsewhere, but principally because of the number of face-on galaxies in this sample. Even with the most face-on galaxies excluded, the remainder are predominantly face-on, giving a large, non-Gaussian error in the $\log[\Delta V(0)]$ values. The scatter and derived slope of the relation are not significantly changed by the use of J or K magnitudes, or by the use of different aperture corrections. The Peterson B magnitudes barely give a significant relation at all. The regression slope in this case is -0.54, and the correlation coefficient is only 0.2, compared with 0.4 for the near-IR relations.

The procedure of regressing onto the log $[\Delta V(0)]$ axis has not been universally adopted elsewhere. In particular, Tully (1988) argues that the Malmquist bias is overcome by regressing onto the absolute magnitude axis, i.e. effectively assuming all the errors to be

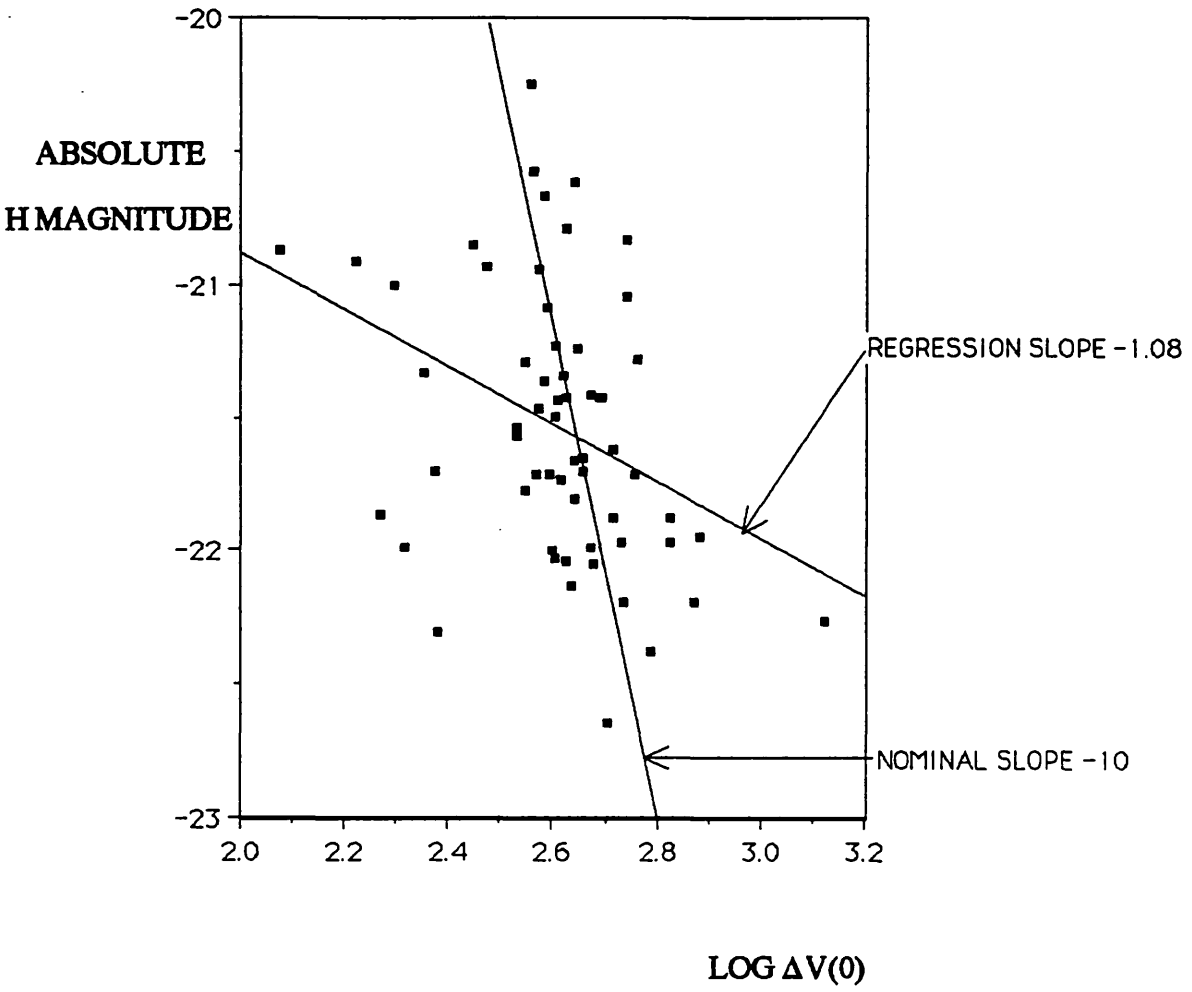


Figure 3.4 H-band Tully-Fisher relation for 68 Sc galaxies

in the log[ΔV(0)] values. This is because Malmquist bias causes a horizontal cutoff in the absolute magnitudes, parallel to the log[ΔV(0)] axis. Regressing in the way advocated by Tully then gives the line that bisects the line-width distribution at a given luminosity. This analysis is inappropriate for our sample, for two reasons. Firstly, the selection biases are more complex than the simple case considered by Tully, in which there is only a cutoff at the faint end. The Rubin et al. (1976a) selection criteria include both very narrow apparent magnitude limits which exclude both faint and bright galaxies, and narrow redshift limits. With such stringent selection criteria, the range of luminosities sampled is very small. In addition, Tully's analysis assumes that the errors in the observable parameters are small compared to the intrinsic scatter, which is certainly not the case here. In particular, there are large errors in determining edge-on linewidths due to the edge-on nature of the sample as mentioned above. In this case, regressing against absolute magnitude will result in too steep a slope. Thus I chose to use the regression which minimises the scatter in corrected absolute magnitudes, and also attempted to avoid the question of the 'correct' slope by solving for the velocity that minimises the scatter in the TF relation, with the slope left as a free parameter. In any case, the use of a steep slope, 8-12, results in similar streaming amplitudes, but with errors that are considerably increased due to amplification of the measurement errors.

The consequence of the large scatter in the TF relation for this sample is that it is very inefficient at removing selection biases from the sample. This was confirmed by repeating the "Malmquist Bias" regression, H_{abs} vs log[Redshift] for magnitudes corrected using the TF relation with the low slope derived above. The bias slope for magnitudes corrected using optical diameters decreased from -4.2 to -3.5; for metric aperture corrected magnitudes it decreased from -2.9 to -2.2. Thus the TF relation takes out less than 25% of the redshift bias in the galaxy sample, and is unfortunately of little use in countering the Fall and Jones argument described in section II.1.

III.6 SOLUTIONS FOR GALAXY STREAMING VELOCITIES

The method adopted to derive bulk streaming velocities from the corrected galaxy photometry was essentially that used by Rubin et al. in the initial study of this galaxy sample. In the simplest solutions, galaxy magnitudes were turned into distances using the "Hubble Modulus" approach described in Chapter Two. As for the cluster ellipticals, the difference between the predicted and measured redshifts was interpreted as the peculiar velocity of the individual galaxy. Redshifts were initially converted to the frame defined by the CBR, so that all velocities are relative to the cosmological rest frame.

The analysis of the Sc spirals differed from that of the cluster ellipticals in that the better sky coverage of the spirals makes possible a complete vector solution. This was done using FORTRAN programmes which called regression routines written by the National Algorithm Group (NAG), specifically routines GO2BDF and GO2CHF. The latter require as input the amplitude and directional unit vectors of the peculiar velocities for each of the 86 galaxy peculiar velocities. They then perform a linear regression by matrix inversion to find the best fit streaming vector to the data points. Standard errors are also calculated for the best fit velocity by the routine GO2CHF. The FORTRAN programmes written to carry out the streaming velocity solutions are listed in the appendix, with a further description of the NAG routines.

Table 3.2 shows the CBR-frame streaming dipoles calculated using magnitudes uncorrected by any luminosity indicators, using the Rubin et al. Hubble Modulus analysis. Line 1 gives the solution derived from the Peterson and Graham photoelectric B magnitudes, corrected for internal and galactic extinction as described above. Line 2 shows the effect of correcting for Malmquist bias in the B magnitudes. Lines 3 to 5 show solutions for J, H and K magnitudes, aperture corrected using optical diameters, and growth curves as derived by Aaronson et al. (1979) at H. Line 6 gives a solution with H magnitudes corrected for Malmquist bias, and line 7 a solution using H magnitudes, which are aperture corrected with metric diameters.

Table 3.2 CBR-frame streaming velocities for the 86 MBS galaxies, using the Rubin et al. 'Hubble Modulus' technique.

Dataused	Streaming velocity (kms^{-1})	l″(°)	b″(°)
B mags.	1037 ± 193	330	29
B mags.*	780 ± 196	340	24
J mags.	1001 ± 282	310	28
H mags.	971 ± 293	315	24
K mags.	1003 ± 316	321	25
H mags.*	583 ± 286	330	16
H mags.†	815 ± 253	326	15

* Malmquist bias correction applied

† Metric diameters used for aperture corrections-optical diameters used otherwise

All of these solutions imply a Local Group motion similar to that found by Rubin et al. (1976b), and they essentially confirm the conclusions drawn in an earlier stage of this reanalysis (Collins et al. 1986). The galaxies appear to be moving with respect to the frame defined by the CBR with a bulk velocity of ≈600-1000 kms^{-1}, toward l≈300°, b≈25°. It is interesting to note, however, that the Malmquist bias correction significantly reduces the amplitude of the effect, and that the near-IR magnitudes give a smaller amplitude than the B magnitudes. In all cases, the errors in the streaming directions are between 10° & 15°.

In all the solutions given in Table 3.2, galaxies were given a weighting inversely proportional to their redshifts, since the uncertainty in peculiar velocity scales with redshift, as explained in Chapter Two. Solutions were also done in which all galaxies received equal weighting. These were almost identical to the redshift-weighted solutions, with changes of < 2% in streaming amplitude, except for the Malmquist corrected solutions, where the changes were somewhat larger, ≈10-15%. However, this is within the errors and cannot be considered significant. Streaming directions were also unchanged within the errors.

Datasets were also prepared with magnitudes corrected for the inclination bias identified in section III.4. As expected, the effect of this bias was negligibly small for this face-on galaxy sample, the solutions changing in amplitude by at most ≈2%.

Solutions were also carried out using the Tully-Fisher relation with H magnitudes corrected for aperture using both metric and optical diameters. As discussed above, the procedure finally adopted here was to solve simultaneously for the best-fit slope to the relation, combined with a bulk streaming motion of the sample of galaxies, with the criterion for the adopted solution being that it should minimise the scatter about the TF regression slope. This is necessary because of the interdependence between streaming, and both the slope and vertical displacement of the adopted TF relation. Changing the former alters the latter and *vice versa*. In the event, however, this iterative process had very little effect, since the slope and intercept of the relation were virtually unchanged, i.e. the slope remained at -1.1 and -1.45 for metric and optical diameter corrections respectively.

Applying the corrections did affect the solutions somewhat, reducing both the amplitude and the errors on the amplitude of the streaming. With magnitudes corrected to metric diameters, the amplitude came down from 815±253 kms^{-1} to 503±203 kms^{-1}; for magnitudes corrected to optical diameters, the corresponding change was from 971±293 kms^{-1} to 590±251 kms^{-1}. The directions were unchanged within the errors.

III.7 THE IMPORTANCE OF CHOICE OF <HM>

All the solutions quoted above, with the exception of the iterated TF relation solutions, were carried out using the type of analysis used by Rubin et al. (1976b). As was explained in Chapter Two, this involves the use of a parameter called the "Hubble Modulus" to avoid the need for a specific choice of Hubble constant H_o. However, this method does implicitly involve setting a mean Hubble expansion internally, using the galaxies from within the sample. This process can be visualised as plotting a Hubble diagram of apparent magnitude vs. log[redshift], and calculating a best fit line. Vertical residuals between individual galaxy positions on this plot and the best fit line are assumed to be due completely to peculiar velocities. These latter can then be calculated directly from the residuals. The mean Hubble Modulus <HM> can be thought of as the slope of the best fit line in the Hubble Diagram.

However, this process is of doubtful validity for the galaxy sample we are using here. In the first place, the conclusion that the galaxies have a large bulk peculiar velocity is

likely to affect the value of <HM>, since the redshifts need to be corrected for streaming to give a direct indication of distance. This correction is easily applied, but there is the residual problem of smaller scale motions which do not affect the derived streaming velocity, but could still affect <HM>. More important is the Malmquist bias in the sample, which has a direct and significant effect on the slope of the Hubble diagram and thus on <HM>.

Given the possibility that the <HM> might be systematically miscalculated, the effect of varying it was investigated. Physically, the effect of changing it is to rescale the 'predicted' recession velocities calculated from apparent magnitudes, as can be seen from equation 2.4. In every case, it was found that values of <HM> could be found which significantly reduced both the amplitude of the streaming and the formal error in the solution. Table 3.3 shows how the streaming amplitude changes for the different datasets, first adopting the criterion of minimising errors in the solutions, and secondly minimising the streaming amplitude. The latter criterion is difficult to justify physically, but it is interesting as an absolute lower limit on the bulk motions predicted by a given dataset. Minimising the errors can be justified, however, since this gives effectively a maximum likelihood solution, with a normalisation to a Hubble expansion that gives a best fit to the hypothesis of a pure Hubble expansion plus a bulk streaming motion.

Dataused	Velocity-minimised solution V_{str} (kms^{-1})	Error minimised solution V_{str} (kms^{-1})
B mags.	552 ± 219	954 ± 193
B mags.*	487 ± 199	708 ± 195
H mags.	365 ± 273	367 ± 272
H mags.*	281 ± 245	331 ± 244
H mags.†	338 ± 249	420 ± 243

* Malmquist bias correction applied

† Metric diameters used for aperture corrections-optical diameters used otherwise

Table 3.3 CBR-frame streaming amplitudes for the 86 MBS galaxies, with <HM> varied to minimise streaming amplitude (Column 1) or errors (Column 2).

In summary, near-IR photometry of the MBS galaxies seems to support the hypothesis that they define a rest frame different to that of the CBR, and therefore that they are streaming with respect to the cosmological frame of rest. However, the amplitude of this streaming is substantially reduced by correcting for Malmquist bias, which is clearly significant in this galaxy sample. The streaming is still further reduced if a less rigid approach is adopted towards defining the mean Hubble Flow than the "Hubble Modulus" technique of Rubin et al.

The major significance of the agreement between the optical and infrared solutions is that differential galactic extinction can be ruled out as the cause of the apparent Hubble Flow anisotropy. If extinction were responsible (Hartwick 1975), a strong wavelength dependence in the effect should have been discovered, decreasing in amplitude with increasing wavelength. Since differential extinction was previously considered the most likely 'physical' explanation for the effect, this is a significant result. However, selection bias, which would affect the solutions regardless of waveband, remains a possibility. This will therefore be investigated in the next section.

IV ESTIMATING THE LIKELY IMPACT OF SELECTION EFFECTS

IV.1 A 'MONTE CARLO' SIMULATION OF SELECTION EFFECTS

In this section, the effects of selection biases will be simulated by numerical methods. That this is necessary can be judged from the strong Malmquist bias found in the galaxy sample, and the crudeness of the corrections available to remove it. The 'Malmquist correction' derived in section III.3 is unsatisfactory since it is derived from and applied to the whole sample, and may not adequately take out the directional bias that is important here. The TF relation for this sample is clearly too insensitive to do more than dilute the bias slightly. Therefore, a model was developed to simulate the selection process adopted by Rubin et al., and predict its quantitative consequences for derived streaming motions.

The bias I was particularly interested in simulating was that outlined by Fall and Jones (1976), which is explained in section II.1 of this chapter. This bias is a result of the narrow apparent magnitude range of the sample, and the three-dimensional 'clumpiness' of the sample. The consequence of the latter is to give a correlation between distance to galaxies and their direction on the sky. This gives the directional Malmquist bias described by Fall and Jones. This spatial component of the bias is impossible to simulate accurately, since it requires a knowledge of the 3-D clustering properties of Sc

galaxies (or more accurately of those galaxies that Rubin et al. would have allowed into their sample), which is not known to the required accuracy. Therefore, in the simulations, the positions of the galaxies were taken as those of the 86 MBS galaxies in our sample, both in redshift and position on the sky. The simulations then determined the likely luminosities of those galaxies, given the apparent magnitude criterion and the known distribution of galaxy luminosities.

The Rubin et al. galaxies were selected so as to have Zwicky magnitudes between 14 and 15; however, there are large systematic and random errors in the Zwicky magnitudes, and the effective selection range was less tightly constrained than this. The accurate photoelectric photometry of Peterson & Baumgart (1986) and Graham (1976), used in this thesis, gives a range of apparent magnitudes from 13.4 to 14.8, with a sharp cutoff at both limits and a fairly even distribution between them as shown in Fig. 3.5. The simulations therefore allocated each of the 86 galaxies an apparent magnitude that lies between these limits. However, there is not an equal probability of a galaxy at a given redshift having an apparent magnitude anywhere within the window, since the galaxy luminosity distribution function is not flat. To simulate the effects of the galaxy luminosity function on the selection process, the 'Field Galaxy' luminosity function of Schechter (1976) was used. The effect of the luminosity function can be seen by considering the lowest redshift galaxies. Those that lie within the selection window in apparent magnitude are of lower luminosity than average, and in fact lie on the ascending side of the Schechter luminosity function. Thus there is not an equal probability of finding galaxies anywhere within the apparent magnitude window, with rather more galaxies being on average towards the high luminosity end. This is taken into account by weighting the probabilities for galaxy selection by the appropriate section of the Schechter function for a given redshift.

The effect of this is to reduce the Malmquist bias effect for this sample, because the high redshift galaxies are selected from the 'descending' side of the peak in the luminosity function, and the probability weighting again tends to shift luminosities towards the mean. This is illustrated in Fig. 3.6. Thus, if the field galaxy luminosity function is flatter than that found by Schechter (for example if he underestimated the number of low luminosity galaxies), the bias will be rather stronger than found in these simulations.

A FORTRAN programme was written to simulate the selection process (see appendix). This calculates the position of the 1.4 magnitude selection window in absolute magnitude, given the CBR-frame redshift of each of the 86 galaxies. The form of the

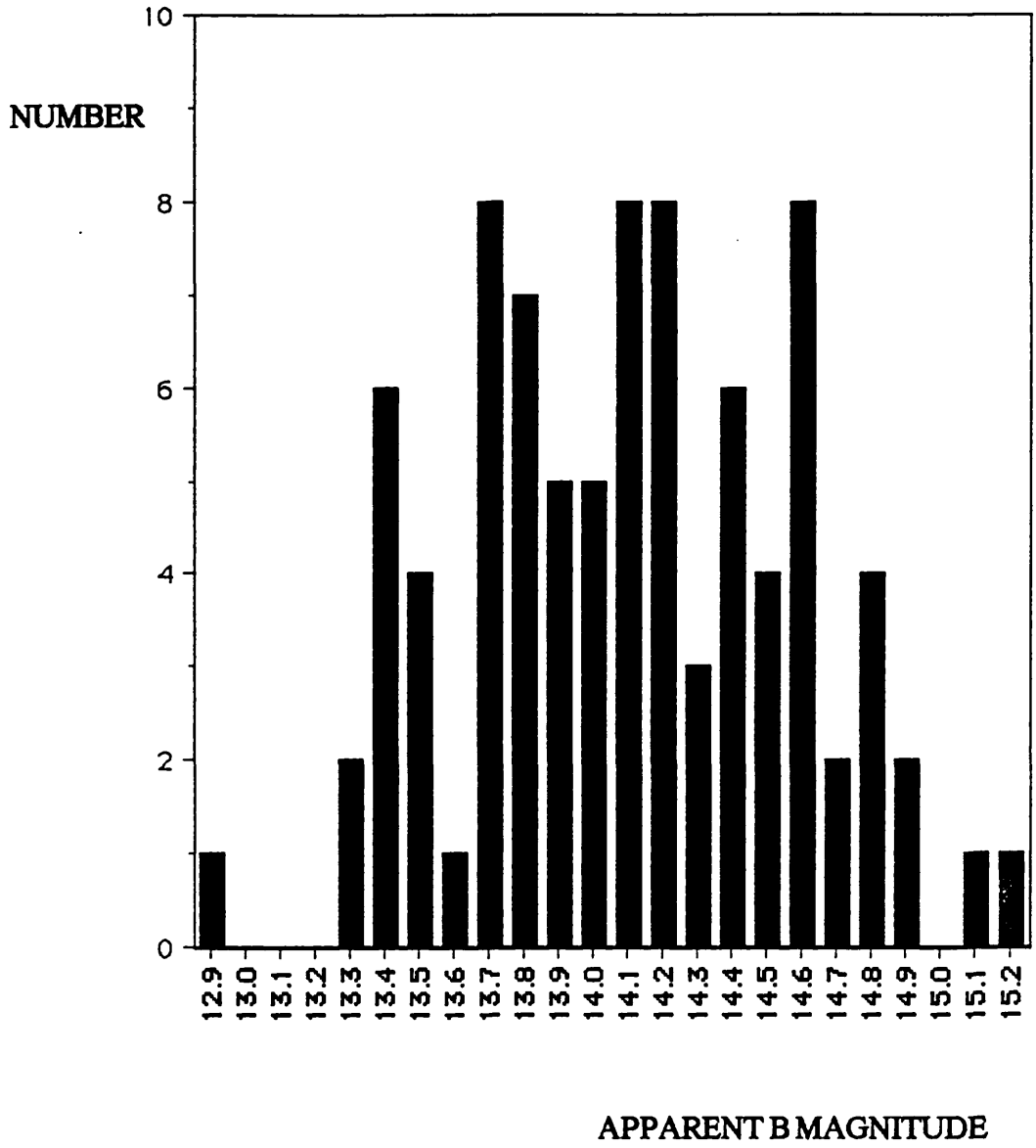


Figure 3.5 Distribution of apparent B magnitudes for 86 Rubin et al. galaxies

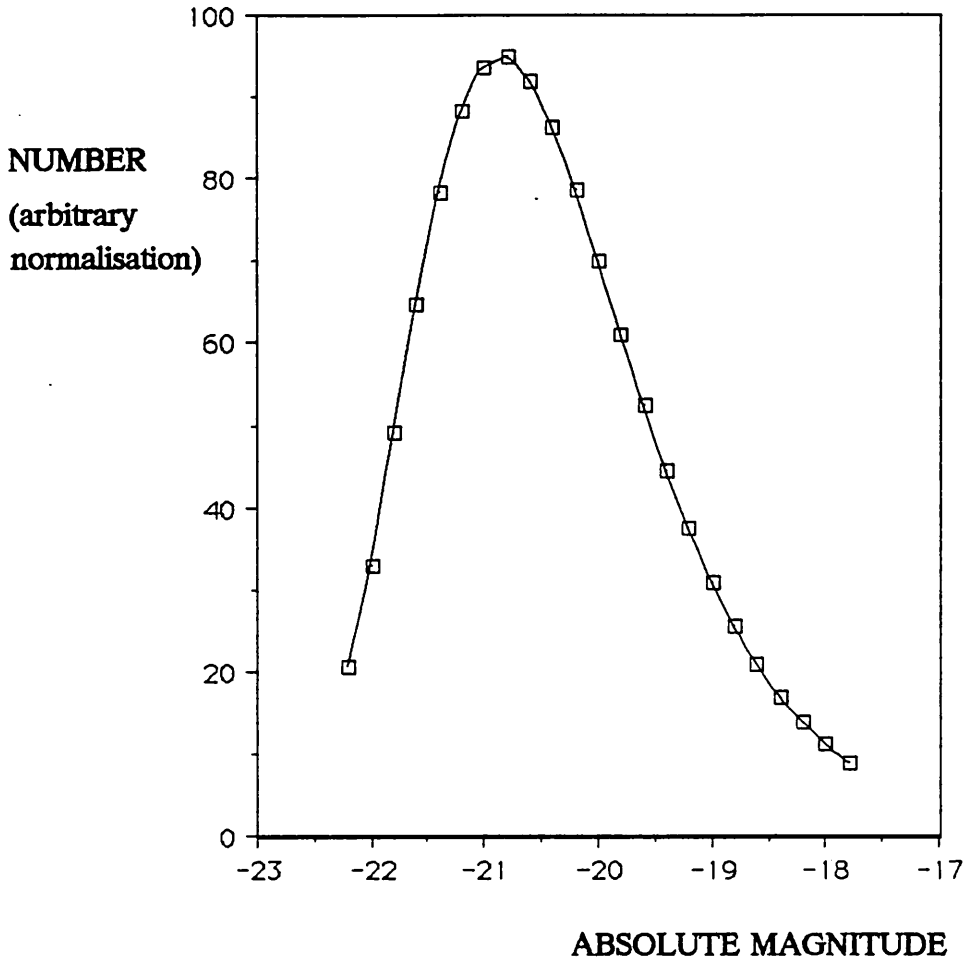


Figure 3.6 The Schechter luminosity function for field galaxies, used for weighting the selection in the Monte Carlo simulations

Schechter function within these limits is then calculated. This function, converted from luminosity to absolute magnitude, is given by

$$n(M)dM = K[10^{(0.4(M_*-M))}]^{0.26} \exp[-10^{(0.4(M_*-M))}]dM \qquad 3.6$$

where M* is -20.6, and K is a constant which normalises to the correct spatial density, which we are not concerned with here. For each galaxy's redshift, a random number is generated and allocated to an absolute magnitude inside the apparent magnitude window, with a probability weighted by the appropriate section of the luminosity function. This process is repeated for all the galaxies in the sample, and the absolute magnitudes are converted to apparent magnitudes. The data file with the simulated magnitudes is then saved, and streaming velocity solutions carried out using the programmes described in section III.6. This whole simulation was repeated about 100 times.

It should be noted that the implicit assumption in this simulation method is that there are no galaxy peculiar velocities, since redshifts are used to predict apparent magnitudes directly, using just the inverse-square law and a plausible luminosity function. Therefore any apparent streaming motion must be due to a selection bias with a directional dependence.

Figure 3.7 shows the distribution of streaming velocities found for the simulated samples, using the mean Hubble Modulus approach to determine the Hubble expansion. The distribution is broad, but there is clearly strong evidence for a bias in these samples which typically produces velocities between 400 and 850 kms^{-1}, with a peak in the 650 to 700 kms^{-1} range. This is clear evidence that the Rubin et al. selection procedure *does* introduce biases capable of causing spurious streaming motions. Figure 3.8 shows the directional distribution of the first 55 of the solutions with simulated data. This shows even more clearly that the apparent velocities found for these datasets are not randomly distributed on the sky. The direction of the streaming vector found for the Peterson and Graham B magnitudes is also shown, and it is evident that it is in close agreement with the predictions of the simulations. If there were no bias the solutions should be randomly distributed on the sky and very much smaller, on the order of the random errors of $\approx$250 kms^{-1}.

The process was repeated with the Schechter luminosity function replaced with a hypothetical flat luminosity function, to investigate how sensitive the solutions are to the precise form of the function. The corresponding results are shown in Figures 3.9 and 3.10. It can be seen that the bias is still present and is indeed slightly enhanced, as

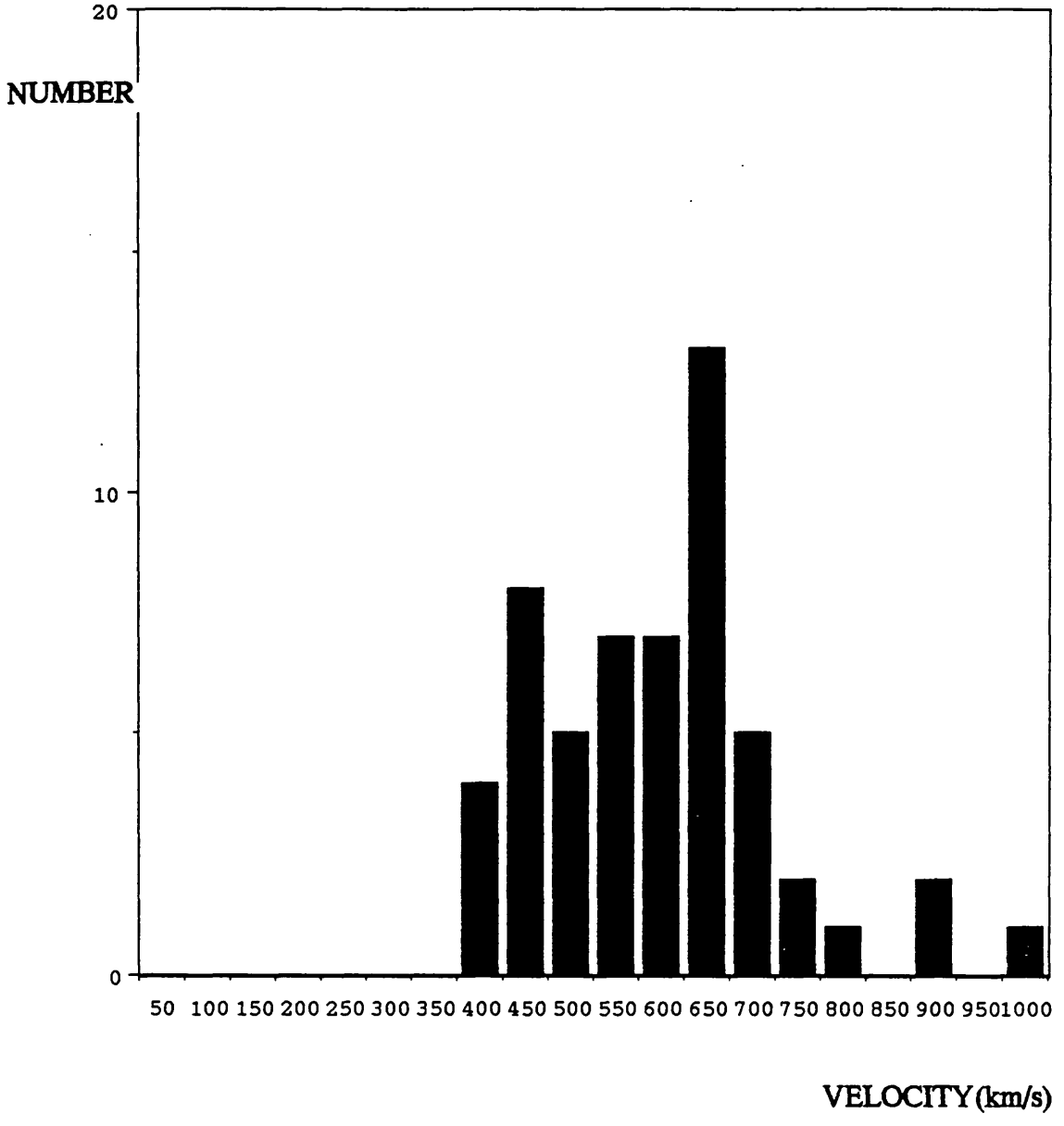


Figure 3.7 Distribution of streaming amplitudes for simulated data sets, using the Rubin et al. 'mean HM' type of solution and a Schechter luminosity function

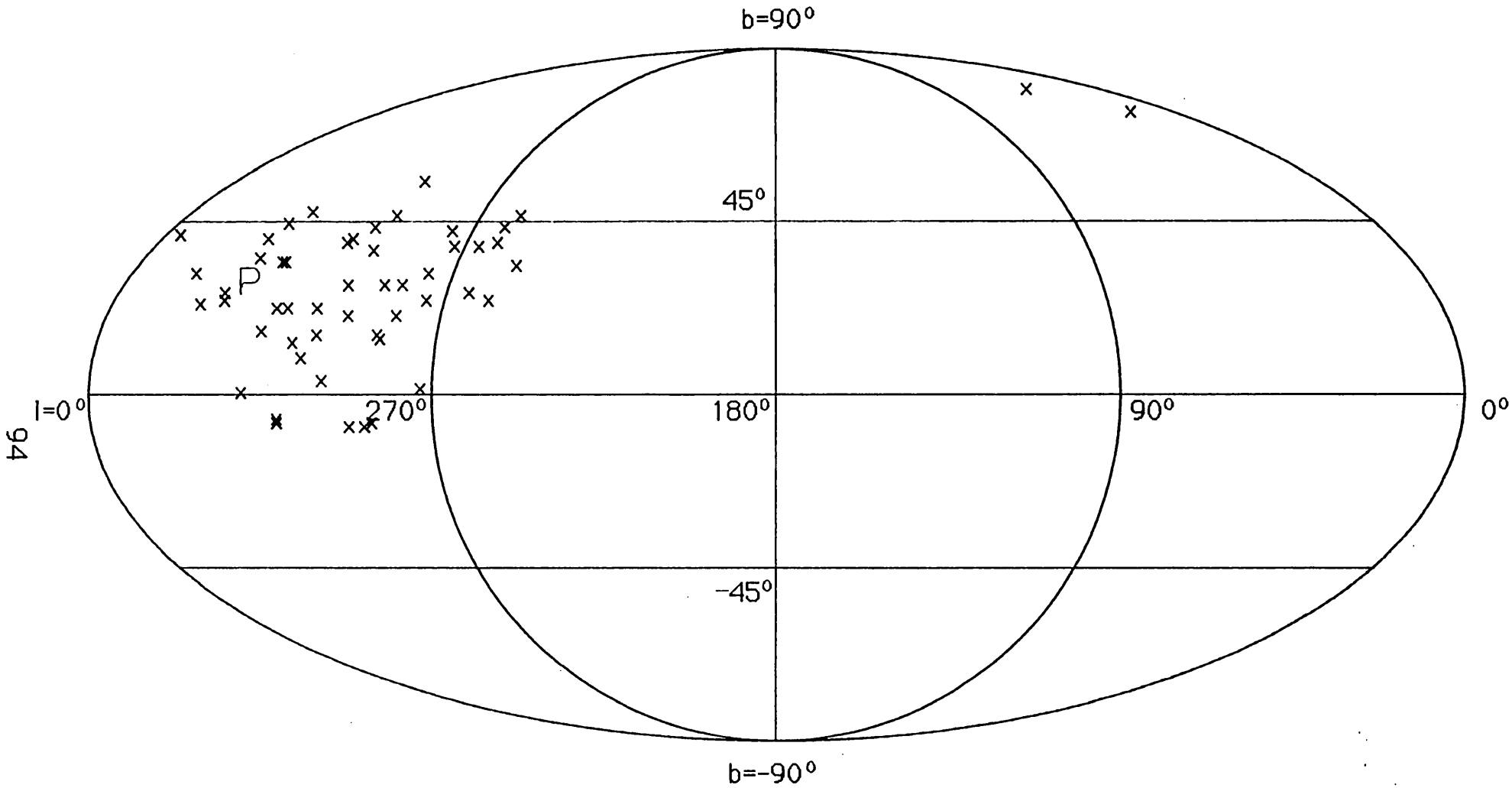


Figure 3.8 Directional distribution of streaming solutions for simulated data sets, using the Rubin et al.'mean HM' type of solution and a Schechter luminosity function

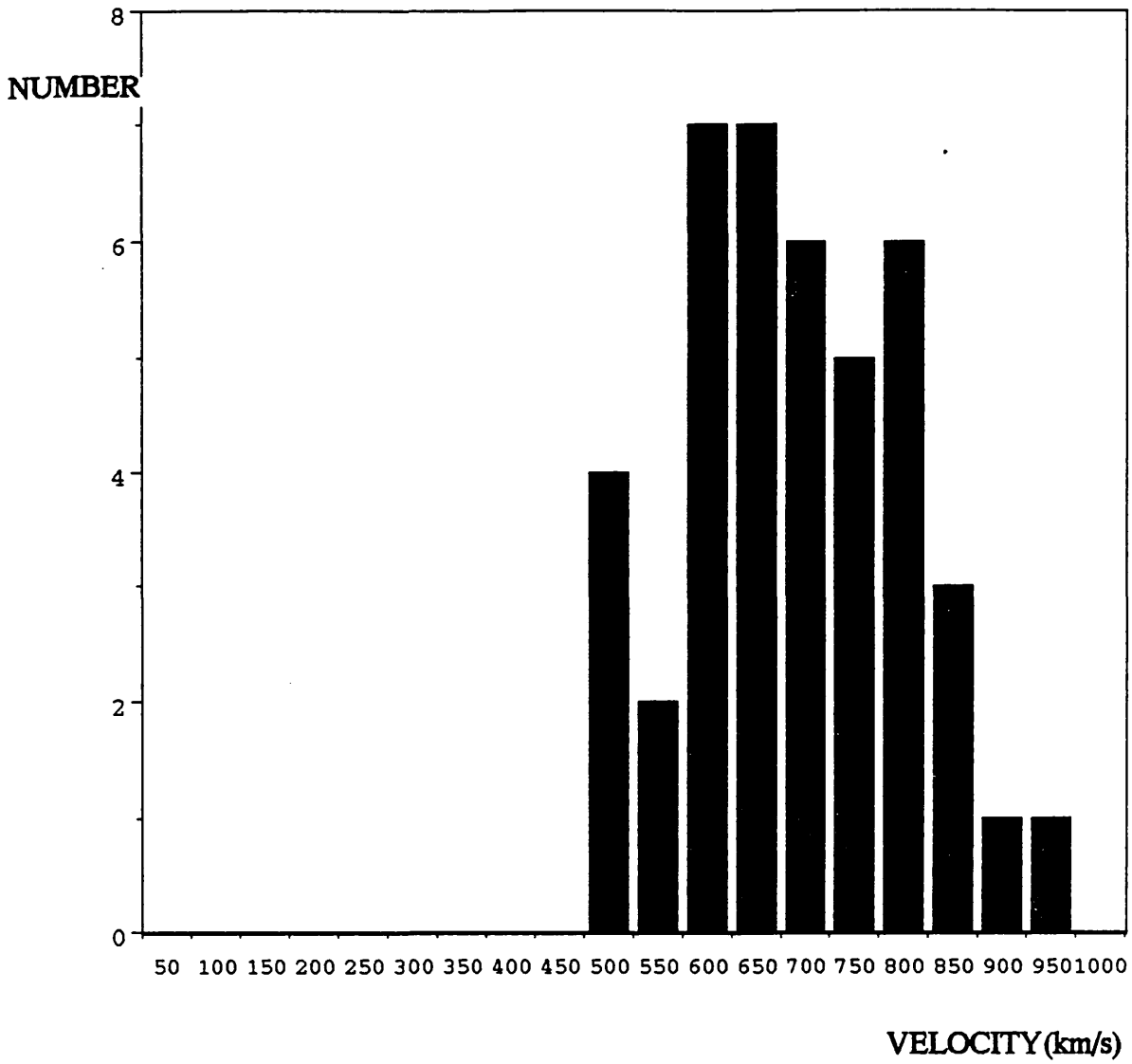


Figure 3.9 Distribution of streaming amplitudes for simulated data sets, using the Rubin et al. 'mean HM' type of solution and a flat luminosity function

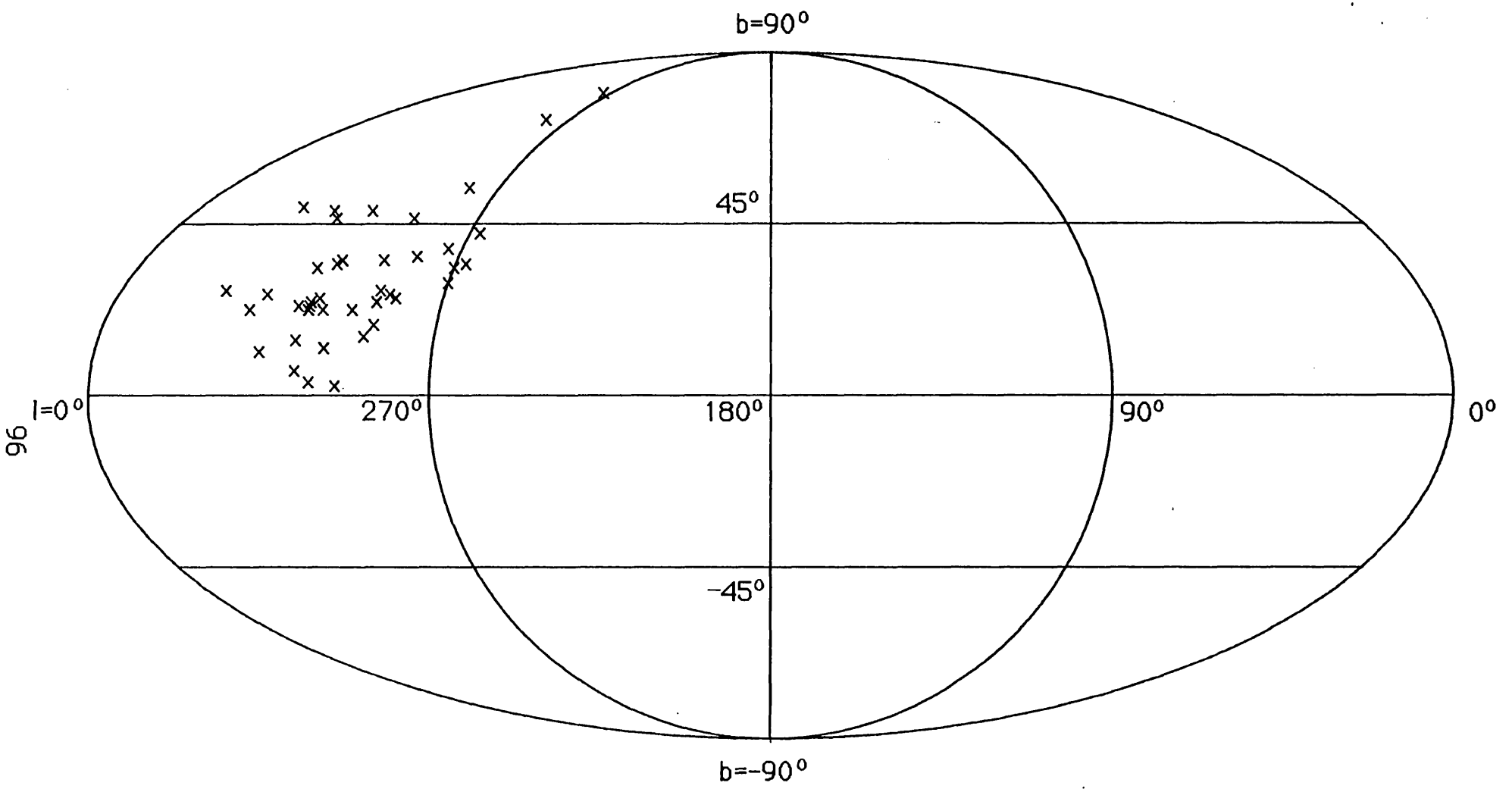


Figure 3.10 Directional distribution of streaming solutions for simulated datasets, using the Rubin et al. 'mean HM' type of solution and a flat luminosity function.

predicted. The spread of streaming directions on the sky is reduced and still concentrated around the direction found for the real data. The peak of the streaming velocity distribution is increased to ≈750 kms^{-1}. Whilst the true luminosity function is not likely to be well approximated by this totally flat function, it is worth noting that more recent estimates generally derive a function that is flatter at the faint end than Schechter's, certainly if dwarfs and irregulars are included (e.g. Binggeli 1986). Thus the true situation may lie between the two cases modelled here, but in any case the size of the bias is only weakly dependent on the form of the luminosity function.

The simulated data were also used to carry out solutions in which <HM> was adjusted to minimise either the errors or the streaming velocity. The two solutions were very similar in most cases; the distribution of minimum velocities shown in Fig. 3.11 is thus representative of both. Again the simulated data behave in a similar fashion to the real data, with the minimum velocities being approximately half those obtained using the Rubin et al. type of analysis.

Given that there is a strong bias in the selection process, it is clearly of interest to know whether a true streaming motion of, say, 600 kms^{-1} would have been detected. This is easily tested by taking the simulated datasets, which have no true streaming component, and vectorially adding the desired streaming velocity to galaxy redshifts. Figures 3.12 and 3.13 show the results of this process. In both cases, the amplitude of the streaming velocity was 600 kms^{-1}; in Figure 3.12 it is toward l=180°, b=0°, and in Figure 3.13 toward b=-90°. The effect on the solutions using a mean Hubble Modulus technique (x) is predictable, with the solutions lying between the locus of directions defined by the bias (≈l=300°, b=25°) and the direction of the superimposed streaming. Interestingly, the solutions for which the value of <HM> is iterated to minimise the streaming (o) lie further from the bias locus, and cluster more nearly around the direction of the 'true' streaming. This suggests that one effect of the Malmquist bias is that the mean Hubble Modulus is systematically miscalculated, and that the type of analysis used by Rubin et al. should not be employed.

IV.2 DIRECTIONALITY IN THE MALMQUIST BIAS

The near-alignment of the directional bias in this sample and the axis of the CBR dipole toward l=272°, b=30° is not coincidental. Some of the bias in using this sample for deriving streaming motions arises because the galaxies were selected within redshift limits, as well as apparent magnitude limits, in defining the Minimum Bias Subset. The former were applied using redshifts corrected to the Local Group frame of reference,

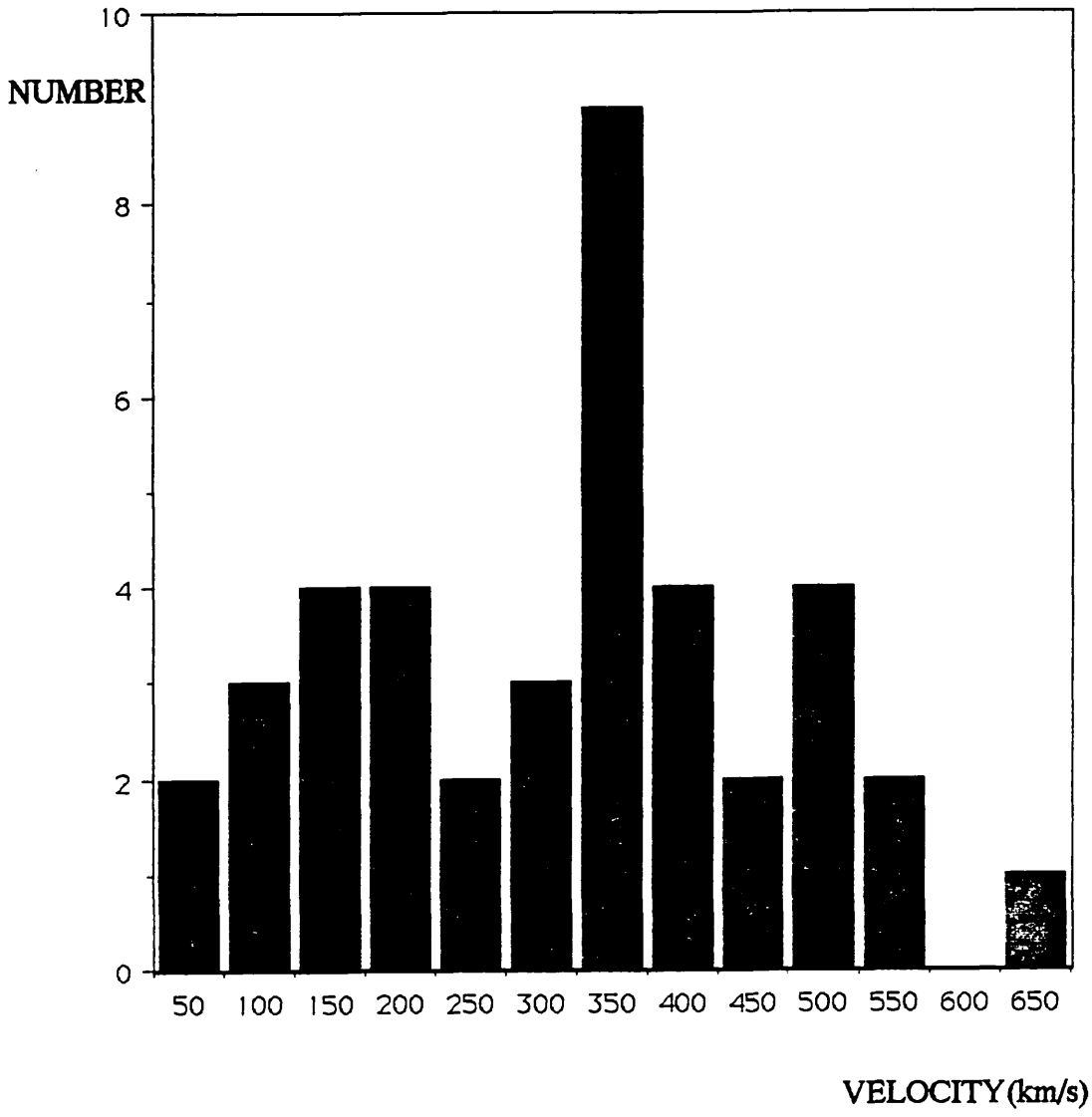


Figure 3.11 Distribution of minimised streaming amplitudes for simulated data sets, using a flat luminosity function

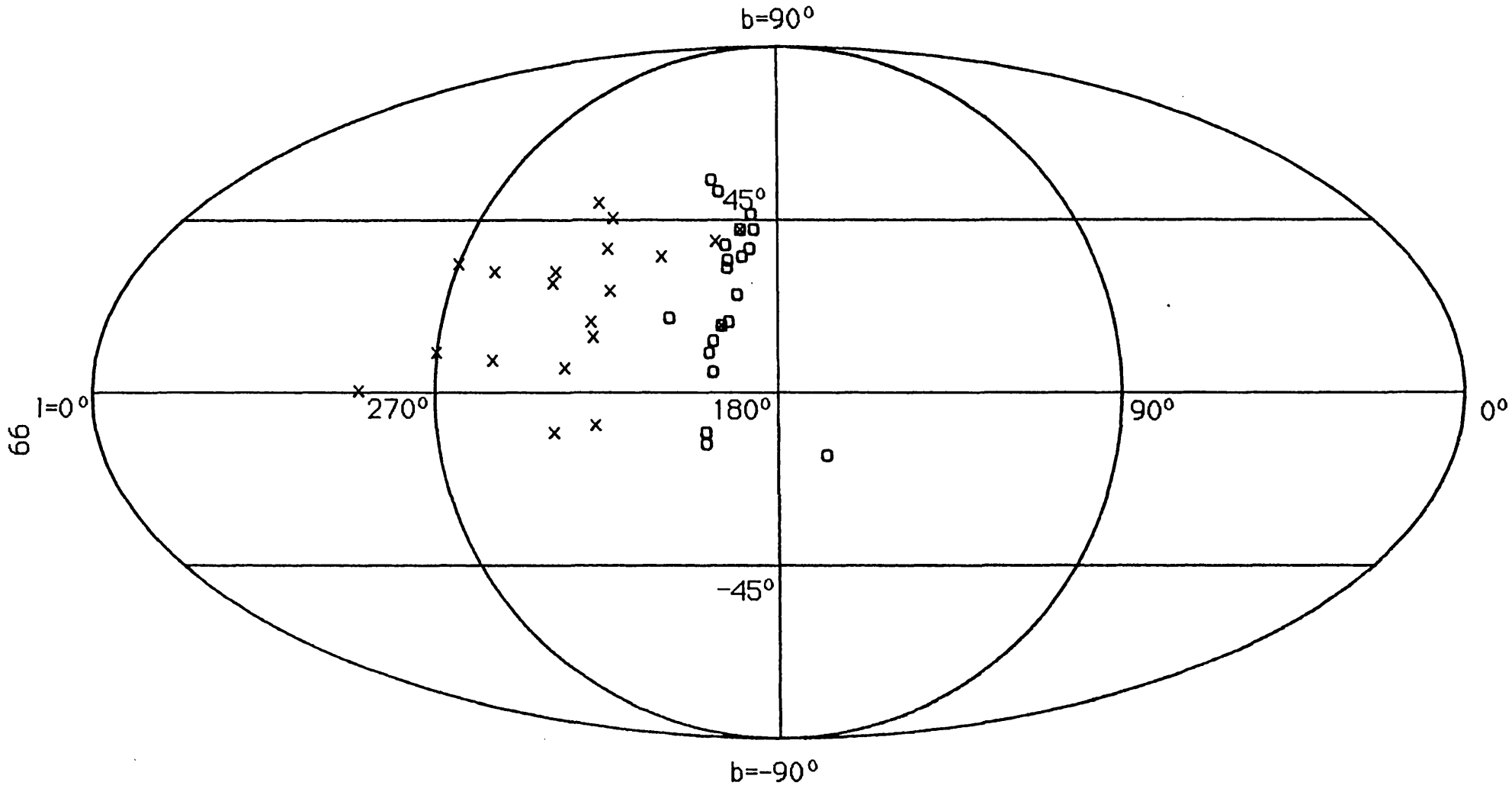


Figure 3.12 Directional distribution of streaming solutions for simulated data sets, with a superimposed streaming of 600 kms^{-1} toward l=180°, b=0°.
[x=mean HM solution, o=velocity minimised solution]

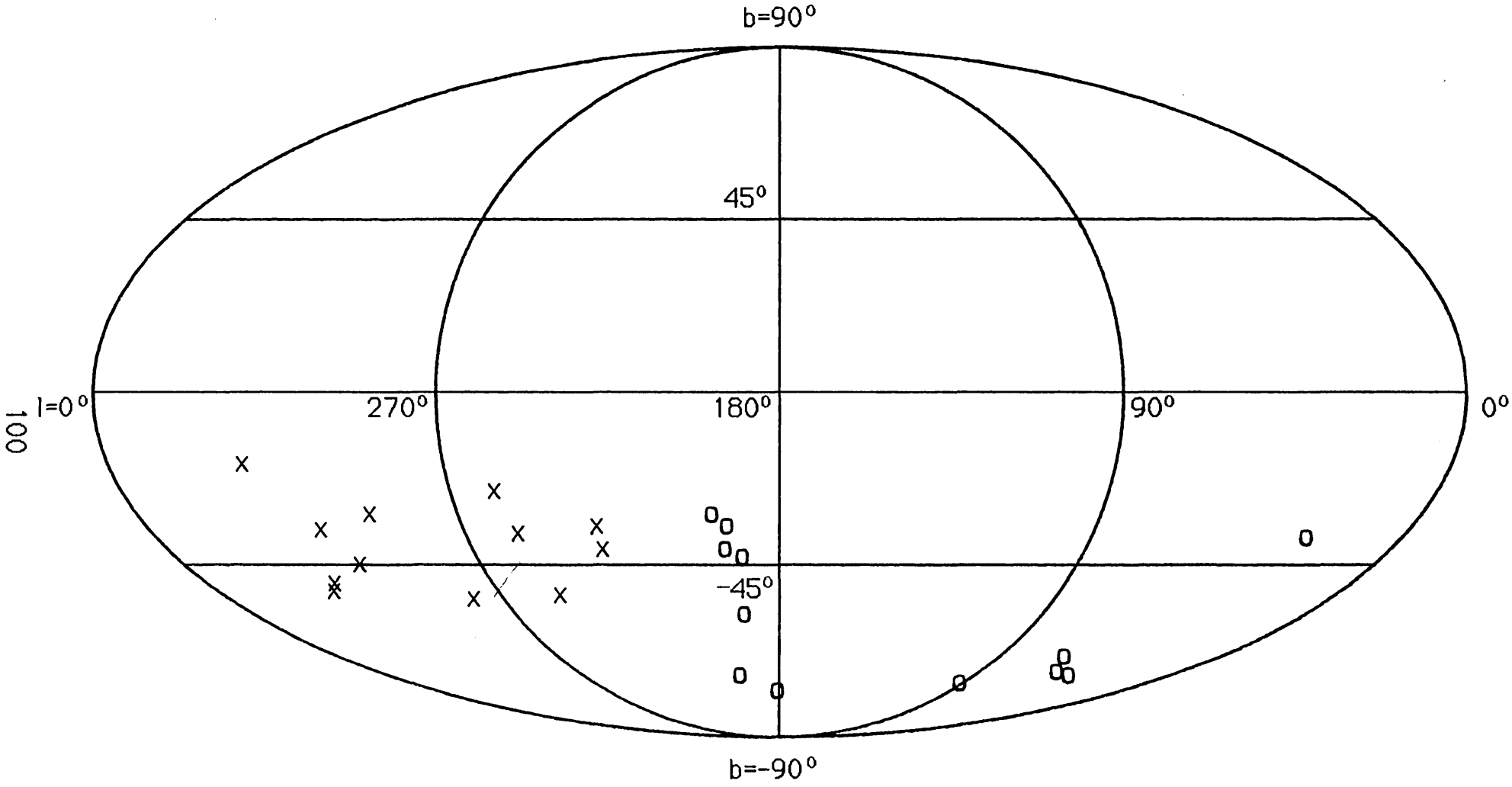


Figure 3.13 Directional distribution of streaming solutions for simulated data sets, with a superimposed streaming of 600 kms^{-1} toward b=-90°.
[x=mean HM solution, o=velocity minimised solution]

since the CBR dipole had not been accurately measured at that time. Thus, under the assumption of no streaming, galaxy redshifts in the LG motion apex direction are underestimated by ≈600 kms^{-1}, and those in the antapex direction are overestimated by the same amount. Since the applied redshift limits were 3500 to 6500 kms^{-1} in the LG frame, the *CBR frame* limits vary systematically around the sky, from 4100 to 7100 kms^{-1} in the apex direction to 2900 to 5900 kms^{-1} in the antapex direction. This uneven sampling depth is highly significant since we already know that there is a strong positive correlation between intrinsic luminosity and redshift. Therefore galaxies in the direction l=272°, b=30° will be intrinsically overluminous, and will have *underestimated* luminosity distances for their redshifts. They are thus concluded to have peculiar motions away from us. With the reverse being the case in the antapex direction, l=92°, b=-30°, there is a systematic tendency for the whole sample to appear to be moving toward the apex direction. This effect is clearly contributing significantly to the bias found here, since the apparent streaming motions for the simulated datasets tend to lie only ≈25° from the predicted direction.

This bias can be partially removed from the sample by excluding the 6 galaxies with CBR frame redshifts <3500 kms^{-1} or >6500 kms^{-1}. The effect is to reduce the amplitude of galaxy streaming slightly. For example, the solution using metric aperture corrected H magnitudes is reduced from 815 to 714 kms^{-1}, and using aperture corrected H magnitudes from 971 to 819 kms^{-1}. The effect on the simulated datasets is comparable, with streaming amplitudes reduced by ≈10 to 40%. However, this procedure only removes approximately half of this bias, since it is not possible to replace the galaxies which should have been included in the sample had the limits been applied in the CBR frame. A more rigorous attempt was made by including only galaxies with CBR-frame redshifts between 4100 and 5900 kms^{-1}, which removes the selection anisotropy completely but leaves only 69 galaxies in the sample. Using the Rubin et al. "Mean Hubble Modulus" technique, this reduced the streaming velocities to 766 kms^{-1} and 666 kms^{-1} for optical and metric diameter corrections respectively. Relaxing the "Mean HM" criterion, it was found possible to reduce these values to ≈350 kms^{-1}. Thus the redshift limits may be responsible for about half of the spurious streaming found with this sample.

IV.3 CONCLUSIONS FROM SIMULATIONS OF SELECTION BIAS

The strong conclusion from this is that the entire Rubin-Ford effect, and large-scale streaming derived from their galaxy sample, could well be due to their galaxy selection process. It is clear, at least, that this galaxy sample is not suitable for measuring the

galaxy peculiar velocity field since any true velocity would tend to be obscured by the strong inherent biases.

It is difficult even to put firm limits on the amplitude of streaming using the results presented here, although the simulations above do indicate that a bulk streaming with a component in excess of ≈400 kms^{-1} orthogonal to the 'bias' direction of l=320°, b=25° would have a noticeable effect on the measured streaming direction. Since the measured streaming coincides very accurately with the bias direction, the orthogonal component is probably smaller than this. If the real streaming were to lie along the bias direction, the accuracy with which it could be determined depends on how well the strength of the selection bias can be measured. Again, it is doubtful whether this can be determined to better than about 400 kms^{-1}, due to uncertainties in the width of the effective selection window used by Rubin et al., and in the shape of the luminosity function. The measured streaming does seem to be ≈200 kms^{-1} larger than the typical velocities predicted for the bias effect only, but this could easily be explained, for example if the effective apparent magnitude selection window were slightly narrower than the assumed 1.4 magnitudes. In any case, 200 kms^{-1} is well within the errors in the simulation procedure.

Thus I must conclude that there is no strong evidence from the Rubin et al. sample of galaxies for large-scale streaming motions of galaxies. However, the selection biases which force this conclusion also rule out the possibility of putting a strong upper limit on the streaming motions of field Sc galaxies using this sample.

CHAPTER FOUR

COMPARISON OF RESULTS WITH PREVIOUS STUDIES, AND CONSEQUENCES FOR COSMOLOGICAL MODELS

In this chapter an attempt will be made to summarise the present state of our understanding of the galaxy peculiar velocity field, taking into account the new results presented in Chapters Two & Three, and other recent results from the literature. This will be followed by a brief discussion of the consequences of these findings for the larger questions of the nature of the Dark Matter and the preferred models of galaxy formation.

I RELATED OBSERVATIONAL RESULTS

I.1 A COMPARISON OF RECENT STUDIES OF GALAXY PECULIAR VELOCITIES

The aim of this section is to determine how far we have advanced towards reaching a consensus view on the amplitude and scale of coherence of the galaxy peculiar velocity field since 1986, when my involvement with the work presented here began.

At the beginning of this period, the strongest evidence in favour of large scale (50-100 h^{-1} Mpc) coherent velocities was based on interpretation and reanalysis of the Rubin et al. (1976a,b) work, and in particular the studies of Peterson and Baumgart (1986) and Collins et al. (1986), both of which used independently obtained photometry. Of the earlier results, only that of Visvanathan (1979) derived a Local Group motion in good agreement with that found for the Rubin et al. spirals, which could thus be interpreted as evidence for the same bulk galaxy motion. The strength of this corroboration was weakened, however, by the smaller spatial volume occupied by the elliptical and S0 galaxies used by Visvanathan, since these galaxies had a maximum redshift of 2500 kms^{-1}.

For a time, it appeared that the idea of large-scale streaming had been considerably strengthened by the findings of the 'Big Seven' collaboration (Dressler et al. 1987). The spatial volume sampled in this study was intermediate between those of Visvanathan and Rubin et al., since the galaxies almost all had redshifts less than 6000 kms^{-1}. The derived streaming vector was in good agreement with the earlier studies, i.e. within the 1σ errors in both magnitude and direction.

The final evidence in favour of bulk motions of galaxies then came from the analysis of First Ranked Cluster Ellipticals discussed in Chapter Two (James et al. 1987). The one-dimensional nature of the solutions carried out precluded this from being taken as full confirmation of the earlier streaming vectors, but a comparison of the single velocity component that was measured yielded excellent agreement with the earlier results. Thus it appeared that there was good evidence, from at least 4 completely independent galaxy samples, that galaxies define a frame of rest that is significantly different from that derived from the CBR. Furthermore, the galaxy streaming vectors defined by these samples were all in good agreement, in spite of sampling very different environments (from field spirals to ellipticals in cores of clusters) and scales (mean redshifts $\approx$2000 kms^{-1} to $\approx$7500 kms^{-1}).

Thus, galaxy streaming motions gained credibility during 1986 and 1987. Whilst they were by no means universally accepted, and there were several contrary results, the Collins et al. and Dressler et al. papers motivated a very large number of theoretical studies aimed at determining which cosmological models could could give rise to such large scale coherent velocities (e.g. Vittorio et al. 1986, Vittorio and Turner 1987, Hoffman 1987, Peebles 1987b, van Dalen and Schramm 1988, Bertschinger 1988 and many others). Since then, the observational evidence has weakened considerably, with all four of the observational results discussed above being reinterpreted or challenged.

This re-evaluation began when the 'Big Seven' carried out a more detailed analysis of the peculiar velocity field of their elliptical galaxies, and found that most of the galaxies responsible for the apparent streaming motion were concentrated in a small region of the sky (Lynden-Bell et al. 1988). To accommodate this finding, they developed a model where the peculiar velocity field of their galaxies was dominated by localised infall into a 'Great Attractor' located just beyond those galaxies which exhibit significant peculiar velocities. Removing the galaxies in this region from the sample was found also to remove most of the evidence for large scale peculiar velocities. Specifically, with all galaxies within 60° of the 'Great Attractor' removed, the streaming amplitude falls from 600 kms^{-1} to $\approx$200 kms^{-1}, with a formal error of $\approx$100 kms^{-1}.

Whilst the existence of this 'Great Attractor' is potentially of interest in constraining cosmological models, it certainly poses less significant problems for existing models than the initial picture of coherent motion of the entire galaxy sample. In any case, this interpretation removes the agreement between this and the other three studies, none of which contains significant numbers of galaxies around the putative 'Great Attractor' at

l=307°, b=9°, redshift 4350 ± 350 kms^{-1}. Visvanathan excludes all galaxies beyond 2500 kms^{-1} to reduce selection bias in his sample, and very few of the Rubin et al. ScI spirals, or of our First Ranked Cluster Ellipticals, lie on the low redshift side of the Hydra-Centaurus complex where the infall pattern is most strongly detected by Lynden-Bell et al. Thus it would seem that the agreement of the earlier dipole streaming solution for the ellipticals sample with those from the other studies was coincidental.

Still more recently, Lucey and Carter (1988b) have attacked the evidence for even this smaller scale velocity flow towards the 'Great Attractor'. They have obtained CCD photometry, and the high resolution optical spectroscopy needed to derive redshifts and velocity dispersions, for 14 galaxies in the Centaurus region. These data are used to show that there are actually two line-of-sight components in the Centaurus cluster, with the dominant one at 3000 kms^{-1} and a smaller one at 4500 kms^{-1}. The distances derived for both components from the logD-logσ relation are found to be consistent with their measured redshifts, with distances normalised to the Coma cluster as was done by the 'Big Seven'. Thus they find no significant evidence for peculiar velocities in this region, using the same method as Lynden-Bell et al. (1988) but with higher quality data. The difference between the two results is not explained by Lucey and Carter, but the evidence for a 'Great Attractor' must now be considered tenuous.

The other widely-cited evidence for bulk motions of galaxies was the preliminary report (Collins et al. 1986) of our infrared reanalysis of the Rubin et al. galaxies. From the analysis presented in Chapter 3 it would now appear that this result, and all others obtained from this sample of galaxies, is strongly influenced by selection bias, and can not be used to support the idea of large scale galaxy motions.

Furthermore, a recent paper by Lucey and Carter (1988a) has challenged the conclusions of our paper on First Ranked Cluster Galaxies (James et al. 1987). They found independent photometry from the literature for 38 of the galaxies in our sample, and were thus able to carry out a partial check on our results. They first excluded all galaxies in groups rather than rich clusters, and those which had been selected from catalogues of radio galaxies. From this restricted dataset they found that the amplitude of the measured component of the galaxy bulk motion in the CBR frame was somewhat smaller than we determined for our full sample of 60 galaxies with Sandage and Hardy (1973) photometry. The value they derived was between 200 and 300 kms^{-1}, depending on whether metric apertures were calculated using CBR frame or LG frame redshifts. Given the larger errors, $\approx$200 kms^{-1}, resulting from the use of a smaller number of galaxies, Lucey and Carter argued that the evidence for streaming motions

from these galaxies was not significant. However, this cannot be considered a convincing rebuttal of our argument since the better agreement they find with zero streaming comes about largely as a result of the selective exclusion of galaxies from our sample and the corresponding increase in the errors. The question will not be definitively answered until the experiment is repeated with an independent, homogeneously selected, all-sky sample of clusters, preferably with CCD photometry to overcome the need for aperture corrections.

Finally, the LG motion result derived by Visvanathan (1979) must also be treated with some scepticism, especially as providing evidence for large scale galaxy motions. In the first place, the galaxy sample is not really comparable with the others discussed here, since Visvanathan excluded all galaxies beyond 2500 kms^{-1} from his solutions to minimise selection bias, and was thus mapping a much smaller volume. The real interest in this result came from the close agreement with that of Rubin et al. (1976b) which indicated coherence in the velocity field over a range of scales, since all of Visvanathan's galaxies lie at lower redshift than the MBS of Rubin et al. However, this agreement can now be seen as evidence that the Visvanathan study was affected by some of the selection problems discussed in Chapter Three as being responsible for the Rubin et al. result. In particular, Visvanathan applied his redshift cutoff of 2500 kms^{-1} *using LG frame redshifts*, as did Rubin et al., giving an anisotropic sampling depth under the reasonable assumption that CBR frame redshifts give the best unbiased distance determinations. Since Visvanathan himself states that his sample contains apparent magnitude selection bias even within the chosen redshift cutoff, the redshift anisotropy will inevitably cause an absolute magnitude bias in the same sense as for the Rubin et al. sample. This would be predicted to give a CBR frame streaming motion toward the LG CBR dipole. Indeed, the measured direction of $l=292°$, $b=12°$, which can be calculated from the LG motion quoted by Visvanathan, is very close to the predicted $l=272°$, $b=30°$.

Thus it must be concluded that at present the evidence for any departures from pure Hubble expansion is weak, at least on scales larger than the LSC. It is difficult to put a hard upper limit on the size of galaxy streaming motions from the studies done to date because of the uncertain size of the biases that have affected virtually all of them, but a true streaming of 400 kms^{-1} or larger is almost certainly excluded, on scales from ~30-70 h^{-1} Mpc.

I.2 OTHER RECENT RESULTS OF IMPORTANCE TO COSMOLOGY

In addition to the above, the constraints on cosmological scenarios from the cluster-cluster correlation function (Bahcall & Soneira 1983) have been greatly weakened by the recent discovery of significant projection effects in the cluster catalogues used (Sutherland 1988). The effect discovered by Sutherland is a result of the observed correlation between clusters and galaxies, which is observed to be positive out to at least 20 h^{-1} Mpc. Thus each individual cluster tends to be surrounded by a region of enhanced galaxy density, which will increase the apparent richness of any other cluster along a nearby line-of-sight. Clusters with too low an intrinsic richness to be included in the sample if they were along an isolated line-of-sight can then be included if they lie near another cluster. This both enhances the measured cluster-cluster correlation function over the true value, and gives rise to spurious structures elongated along the line-of-sight, which were indeed found by Bahcall & Soneira. Sutherland found that accounting for this effect reduced the amplitude of the correlation function by a factor of 2.8, and gave a correlation length r_o of $\approx$14 h^{-1} Mpc. This latter is still enhanced relative to that found for galaxies, but by a small amount which is consistent with the predictions of the CDM theory.

Another field of study which is complementary to streaming determinations and has yielded interesting recent results is the measurement of optical and infrared light dipoles. Recent interest in this subject was motivated primarily by the availability of the IRAS all-sky mid- to far-IR sky survey. The first two papers to exploit this resource in this way were Yahil et al. (1986) and Meiksin & Davis (1986). The strategies adopted in these two studies were very different, particularly with respect to the removal of contamination from cold galactic dust emission ('cirrus'), but the observed dipoles in the extragalactic IR light were very similar. The amplitude of the dipole is estimated in both studies to be between 5% & 10%, depending on IRAS band, flux limit and cirrus removal. Yahil et al. find the apex of the dipole to be toward $l=248° \pm 9°$, $b=40° \pm 8°$, whilst Meiksin & Davis calculate this direction to be $l=235° \pm 11°$, $b=45° \pm 11°$. Lahav (1987) used an optical catalogue of $\approx$15,000 catalogues to carry out a similar analysis, and again found a significant dipole, aligned toward $l=227° \pm 23°$, $b=42° \pm 8°$. All of these results are clearly in excellent agreement.

The major difficulty in interpreting these results was the uncertainty in the depth of the dipole anisotropy in the galaxy distribution. For the IRAS results, this was particularly difficult because of the wide range in IR luminosities which meant that IRAS detected significant numbers of galaxies out to a distance of at least 200 h^{-1} Mpc, but that the

sample was incomplete even within the LSC. Lahav estimated the mean depth of his optical sample to be 50 h^{-1} Mpc, but the galaxies comprising the dipole could well be preferentially at either low or high redshifts, with the former being more likely.

This problem was answered by Strauss & Davis (1987), who used a redshift survey of IRAS galaxies to find explicitly the depth at which the dipole was most prominent. They found that the dipole had converged to the direction quoted by Meiksin & Davis (1986) when galaxies were included to a redshift limit of 4000 kms^{-1}, thus implying that all the above dipoles are caused by galaxies within this radius. Villumsen & Strauss (1987) concluded that the dipole was due to galaxies at even smaller redshifts, $\approx$1750 kms^{-1}, and the most recent study (Lahav et al. 1988) arrives at a value between 1000 & 3000 kms^{-1}.

These results are clearly relevant to galaxy streaming measurements since the anisotropies reflected in these dipoles will undoubtedly be reflected in galaxy peculiar velocities. Most importantly, the measured dipoles are closely aligned with the direction of the motion of the Local Group relative to the CBR. This strongly suggests that we are seeing directly the mass concentration causing the LG motion. The good agreement between the mass dipole and the LG velocity then implies that there cannot be bulk velocities on scales larger than 40 h^{-1} Mpc. This supposition has recently been strengthened by the discovery of an even closer agreement, within $\approx 8^\circ$, between the LG motion and the dipole determined from a sample of colour-selected IRAS galaxies (Harmon et al. 1987). In addition, Lahav's optical dipole has been revised slightly (Lahav et al. 1988) to $l=261^\circ \pm 10^\circ$, $b=27^\circ \pm 8^\circ$, $\approx 10^\circ$ from the LG motion direction. These results are further independent evidence for the non-existence of large-scale streaming on 50-100 h^{-1} Mpc scales

Thus, two observational measurements which seemed to indicate the existence of extreme large scale power in the mass distribution have been shown to be flawed or overestimated due to systematics. In the next section I will discuss how this changes the relative attractions of the principal cosmological scenarios.

II CONSEQUENCES FOR COSMOLOGICAL MODELS

The result of the shift away from large scale galaxy motions is almost entirely to relax the constraints on cosmological models. The upper limit on the velocities over 30-70 h^{-1} Mpc scales, of $\approx$400 kms^{-1}, is not stringent, since the great majority of models do not unambiguously predict velocities larger than this. Thus, the principal effect is to

remove one of the main objections to theories which predict low peculiar velocities smoothed over these scales. In this section, I will briefly consider the current status of the more important competing models, in the light of this change in one of the most important observational constraints. As is common in this field, emphasis will be given to the neutrino and CDM models, which are unique at present in being completely specified under the simple assumptions of inflation ($\Omega = 1$) and current nucleosynthesis models ($\Omega_b \approx 0.2$). This leaves the amplitude of the power spectrum as the only parameter to be modelled, making comparisons with observations relatively straightforward.

II.1 NEUTRINO DOMINATED COSMOLOGIES

Neutrinos have been repeatedly considered as candidates for the dark matter, principally since they are the only plausible weakly interacting particles which are actually known to exist, even though they are not known to have the rest mass necessary for this model. Early calculations (e.g. White et al. 1983, White et al. 1984) showed that this scenario runs into problems in generating small scale structure, such as galaxies, sufficiently quickly. It also predicts a preferred scale for structure of $\approx$ 40 h^{-1} Mpc at the present epoch, with for example voids of this size occupying a significant fraction of the Universe. This structure is not observed, either subjectively in the the galaxy distribution found from redshift surveys, or quantitatively in the galaxy-galaxy or cluster-cluster correlation functions. These are important weaknesses, and when added to the uncertainties over whether the neutrinos do indeed have a non-zero rest mass, they resulted in a reduction of interest in neutrino-dominated models.

The strongest single prediction for the nature of structures formed in neutrino models is that there should be structure on large scales ($\geq$100 h^{-1} Mpc) with high density contrast. The apparent discovery of high amplitude velocity flows on these scales (Collins et al. 1986, Dressler et al. 1987) was therefore seen to turn this prediction from a weakness to a potential strength, particularly since there seemed to be no other models that naturally explained these observations. This factor was largely responsible for giving neutrino models a second lease of life, especially since the idea of biased galaxy formation has gained respectability and it is seen that structure that is present in the dark matter need not be reflected in the galaxy distribution.

With the weakening of the evidence for large scale velocity flows, presented here and elsewhere, the situation has come full circle. If there is no longer good evidence for bulk galaxy motions, as appears to be the case, the principal observational motivation in

favour of the neutrino scenario is removed. This is not to say that any of the streaming motion results discussed here weigh significantly *against* this model. Kaiser (1983) calculates that, for a Universe dominated by neutrinos, peculiar velocities smoothed over a scale of $\approx 25\ h^{-1}$ Mpc are likely to be $\geq 390 kms^{-1}$ for reasonable choices of the initial power spectrum and the epoch of formation of nonlinear structure. Extrapolating to a scale of $50\ h^{-1}$ Mpc, comparable to the ScI and FRCG sample sizes, this limit decreases to between 70 and 250 kms^{-1}, depending on the index of the initial fluctuation spectrum, using Kaiser's own scaling relation. Thus it is quite possible for a neutrino dominated universe to give rise to peculiar velocities as low as indicated by these recent measurements, but the previous strong motivation for this model has disappeared. Higher precision studies are still required to exclude this model using streaming velocity measurements or limits.

II.2 THE COLD DARK MATTER MODEL

Several calculations have been made of the predicted amplitude of the galaxy peculiar velocity field for the CDM model, over a range of different smoothing scales. Vittorio and Turner (1987) quote typical values for $25\ h^{-1}$ Mpc and $50\ h^{-1}$ Mpc smoothing scales, assuming that galaxies trace the dark matter distribution accurately:-

$$V_{25} = 156\ kms^{-1}\ (\Omega_{NR})^{-0.18}\ h^{-0.78}$$

$$V_{50} = 83\ kms^{-1}\ (\Omega_{NR})^{-0.33}\ h^{-0.92}$$

where Ω_{NR} is the present mass density in CDM. The corresponding upper limits at the 90% confidence level are given by

$$V_{25} = 250\ kms^{-1}\ (\Omega_{NR})^{-0.18}\ h^{-0.78}$$

$$V_{50} = 135\ kms^{-1}\ (\Omega_{NR})^{-0.33}\ h^{-0.92}$$

If any significant degree of biasing (see Chapter One) is required, the dark matter must be more smoothly distributed than galaxies, and these velocities would be reduced.

These predictions seemed strongly at variance with the published results of Collins et al. (1986), Dressler et al. (1987) and James et al. (1987). At present, however, the problems of reconciling measurements with predictions seem considerably diminished, following the latest developments discussed above. The results based on the Rubin et

al. sample can no longer be used as arguments against CDM, since the apparent streaming is largely due to selection bias. The 'Big 7' results may pose some problems if the 'Great Attractor' model survives closer scrutiny, but the reanalysis by Lucey and Carter (1988b) seems likely to remove even this constraint. Streaming of galaxy clusters remains an open question, with the apparent detection of streaming by James et al. (1987) opposing the results of Aaronson et al. (1986) and Lucey and Carter (1988a).

Thus, at the present time there is no observational result that clearly violates the degree of isotropy of the Hubble Flow that is predicted by the CDM model, and as explained above the cluster-cluster correlation function can also be reconciled with the predictions of this model.

II.3 OTHER MODELS--STRINGS AND ISOCURVATURE FLUCTUATIONS

Several other cosmological models have recently been discussed in the context of large scale peculiar velocities. Cosmic strings are considered likely to affect the velocity field if they exist (van Dalen & Schramm 1988), although there are substantial uncertainties in our understanding of the likely properties of strings. As a result, the predictions are more model dependent than for either neutrinos or CDM alone, and are generally complicated by more free parameters. This is particularly true since a significant dark matter component must be included as well as the strings in Ω=1 models. Van Dalen and Schramm conclude that a [String + CDM] model produces a smooth Hubble Flow, with bulk motions less than that claimed by Dressler et al. (1987) at a 93% confidence level, whereas [String + neutrinos(HDM)] enables them to reproduce this measurement. The significance of the string in the latter model is not principally in the production of the large scale power, but that it might seed the development of the small scale structures, particularly galaxies, that are lacking in conventional HDM simulations. Additional constraints were applied from the observed isotropy of the CBR, and the necessity to generate small scale velocities reflected in the CBR dipole. Van Dalen and Schramm conclude that streaming measurements exclude the [String + CDM] model and favour [String + HDM]; I would now argue that this preference was probably premature.

Finally, the peculiar velocity field predicted by isocurvature models has been investigated in some detail. In these models, the total mass in the Universe is smoothly distributed, but the baryons are clumped, and some other particle species makes up the deficiency in low baryon number regions. These conditions are thought likely to arise in models where axions dominate the total mass density (Bardeen et al. 1987). However,

one of the principal motivations for preferring these models is not theoretical, but that they predict a high degree of large scale clustering power at the present epoch (Peebles 1987b). If there is no strong evidence for large scale peculiar velocities, as I have suggested, this motivation is removed and it is doubtful whether isocurvature models are worthy of further investigation, at least without some new observational support.

III CONCLUSIONS

The main conclusion to be drawn from the foregoing is that the constraints on cosmological models from large scale velocity flows are not as stringent as has been thought. None of the models considered above--HDM, CDM, string models or models with isocurvature fluctuations--is seriously challenged, or supported, relative to the others, by the present observations. However, on a more positive note, it is clear that the potential for such discrimination between models exists and is attainable, principally by more careful control over selection systematics in galaxy samples. The Rubin et al. experiment of the 1970's failed in only this one area; in the final chapter I will describe a new attempt to rectify this failing, and look at other ways forward in this promising area of observational cosmology.

CHAPTER FIVE FURTHER STUDIES OF GALAXY STREAMING MOTIONS

I A NEW STUDY OF THE PECULIAR VELOCITIES OF FIELD SPIRALS

I.1 SCIENTIFIC JUSTIFICATION

In the first half of this chapter, I will describe a new study which is intended to repeat and improve on the analysis first carried out by Rubin et al. Below, I attempt to justify this study by arguing the scientific merits of another study of this type.

The principal argument is the great importance of streaming motion studies to cosmology, as has been indicated by the number of papers proposing cosmological models to accommodate the measurements of streaming that have already been made. The two most frequently cited of these are the preliminary report of our work on Sc spirals (Collins et al. 1986), described in detail in Chapter Three, and the 'Big Seven' study of ellipticals (Dressler et al. 1987). These two papers have probably stimulated more theoretical activity than any other observational results published in the last three years. However, they are both seriously flawed. The shortcomings of the former sample have been explained at length in Chapter Three, and clearly undermine the significance of this result. The work on ellipticals, whilst clearly important, is not the last word on galaxy streaming. The principal limitations are that the galaxy sample is relatively local in scale, predominantly at redshifts less than 6000 kms^{-1}, and that ellipticals preferentially sample the velocity field around clusters, which may give only partial information about the overall mass distribution. The selection of the galaxies used from catalogues is a potential source of bias in the sample, and may explain the discrepancy with the results of Lucey and Carter, (1988b). Despite these faults, these papers have clearly shown that streaming motion measurements have the potential to uncover information of great importance to cosmology.

A second argument is that, although many studies have been carried out to date, no consensus has emerged on even the most basic questions of galaxy peculiar velocities. There is considerah^{-1} debate on the size of velocities on all scales, from the pairwise relative velocity distribution up to the streaming of regions 200 h^{-1} Mpc in diameter. It is hoped that the study outlined in this chapter may hold the answer to many of these questions.

I.2 USE OF MODERN INSTRUMENTATION

An additional motivation for further study of the large scale peculiar velocity field is the availability of more sophisticated instrumentation, and the promise this holds for more accurate luminosity indicators. In particular, the widespread availability of sensitive CCD array detectors and IR arrays opens up many possibilities for more precise galaxy photometry. Coupled with advances in our understanding of the luminosity and dynamics of galaxies, twofold improvements in redshift-independent distance determinations should be possible within the next decade. Such improvements have already been tentatively demonstrated by Bothun and Mould (1987), and are discussed in detail later in this chapter.

I.3 SELECTION CRITERIA

The principal aim in selecting the sample of galaxies for this work was that it should be as free as possible from the biases that plague the Rubin et al. sample, whilst being at least comparably deep in redshift. We again decided to use ScI galaxies, which have several advantages for this work. Spiral galaxies were the obvious choice, principally because of the advantages of their being complementary to the 'Big Seven' work on ellipticals. ScI spirals were specifically chosen because they are intrinsically bright, and their characteristic morphology--a small nucleus and wide open arms with a clumpy, dusty appearance--is easily recognised even for relatively distant or highly inclined galaxies. The presence of large amounts of gas in Sc galaxies is also advantageous, since this enables us to obtain 21cm radio measurements with comparative ease. These measurements are important because they give us both accurate redshifts and the linewidths needed for the Tully-Fisher relation, which is central to this study.

Galaxies for the new sample were selected from the Palomar Observatory Sky Survey plates and the United Kingdom Schmidt Telescope sky survey, the latter making possible a complete sky coverage. This was not available to Rubin et al., whose sample was consequently deficient in southern galaxies. Such an uneven sky coverage is liable to give rise to large uncertainties when deriving streaming vectors, and our sample is much more satisfactory in this respect.

All plates with $|b| > 30°$ were scanned, and potential candidates selected down to a diameter on the plates of about 0.7 mm. These are the smallest galaxies it is possible to classify with any degree of certainty from the sky survey plates. This procedure

therefore minimises the Malmquist bias in the sample for a given depth, although selection bias is bound to be present beyond some redshift limit. It should be possible to remove the worst effects of this bias by identifying the largest redshift at which the sample is complete, and excluding galaxies at higher redshift. All candidate galaxies were independently classified by Dr C.A. Collins and myself. Galaxies were then included in the sample only if there was agreement on their classification as ScI, if they were not strongly barred or distorted, and if they were not in clusters and had no apparent nearby companions. Table 5.1 contains data on these galaxies in the following format:

Col. 1 Galaxy name (if NGC, UGC or IC)
Col. 2 Right Ascension (1950)
Col. 3 Declination(1950)
Col. 4 Redshift
Col. 5 Approximate inclination
Col. 6 Measured major axis

Table 5.1 Names, coordinates, approximate diameters and inclinations for the sample of 218 ScI galaxies.

NAME	RA (1950) HH MM.M	DEC DD MM	REDSHIFT kms^{-1}	INCL (°)	MAJ AXIS arcmin
	00 00.6	-02 11	7323	67	1.05
	00 08.1	33 05		72	1.25
	00 11.5	-30 59		32	0.7
	00 17.7	-54 48		55	1.0
NGC 99	00 21.4	15 30	5184	36	1.1
	00 38.1	-00 35		31	0.75
NGC 234	00 40.9	14 04	4448	39	1.15
	00 55.5	48 23	6812	47	1.0
	00 57.8	-31 05		22	0.75
IC 65	00 58	47 25	2614	90	4.0
	01 02.2	-62 48		28	0.9
	01 04.7	39 08	5869	53	1.6
IC 1637	01 08.6	-30 41	6002	39	1.4
NGC 461	01 15.0	-34 06		47	1.15
	01 15.3	-79 19		47	1.0
	01 19.3	15 31		55	1.0
	01 19.6	-44 19	7170	48	1.6
	01 22	-37 36		42	0.8
NGC 551	01 24.8	36 55		75	1.4
NGC 606	01 32.1	21 10	9956	42	1.0
NGC 628	01 34.0	15 32	656	28	9.0
NGC 673	01 45.7	11 17	5173	42	1.4
NGC 690	01 46.6	-16 50		48	1.1
	01 49.6	-24 34		62	0.8
IC 1763	01 56.9	-28 03		32	0.7
NGC 783	01 58.2	31 38	5195	54	1.3
	01 59.0	-33 27		34	0.9
	02 00.0	-28 54		65	1.5

IC 1776	02 02.6	05 52	3405	39	1.4
	02 07	-23 39		58	1.6
IC 211	02 08.5	03 38	3266	47	2.0
NGC 858	02 10.2	-22 41	12356	38	1.0
NGC 864	02 12.5	5 46	1559	57	4.0
NGC 895	02 19.1	-05 45	2287	47	3.3
NGC 908	02 20.8	-21 28	1470	65	4.85
	02 21.6	-21 15		40	0.9
	02 22	-19 22		48	0.95
NGC 918	02 23.1	18 16	1516	56	2.4
NGC 921	02 24	-16 05		66	1.0
NGC 954	02 26.9	-41 38	5353	65	1.5
	02 34.6	23 05		64	1.05
	02 41.5	-32 09		76	1.6
NGC 1114	02 47	-17 10		69	1.5
NGC 1187	03 00.4	-23 04	1394	47	4.3
NGC 1171	03 00.7	43 12	2742	62	1.8
NGC 1232	03 07.5	-20 46	1684	38	7.0
	03 15.5	-13 40		46	0.7
IC 1954	03 30.1	-52 04	1116	60	2.8
NGC 1406	03 37.4	-31 29	1068	90	3.5
	03 38.0	-72 33		68	1.2
IC 350	03 42	-11 55		44	0.95
	03 48.6	-25 26		23	1.3
	03 51.6	-17 44		74	0.9
	03 57.9	17 27		66	1.0
NGC 1526	04 04.8	-65 59		51	0.7
	04 10.2	-13 15		46	0.7
IC 2070	04 23.7	-58 05		64	1.35
	04 38.5	-63 08		25	1.1
NGC 1642	04 40.3	00 30	4640	20	1.7
NGC 1703	04 52.1	-59 49	1526	42	3.2
	04 53.3	02 51	4450	62	1.0
	04 54.1	-10 07		68	1.8
	04 59.5	-15 10		35	0.85
	05 00.5	-21 00		68	0.6
	05 03.0	70 26	4875	34	1.2
NGC 1796	05 07.9	-61 26	8895	25	1.1
	05 13.6	-22 46		66	1.0
	05 27.3	-44 13		40	0.9
	05 34.0	-79 55		28	0.9
	05 47.1	-39 04		69	1.0
IC 2150	05 49.6	-38 20		80	2.45
UGC 3581	06 50.0	80 04	4690	51	1.0
	07 20.0	41 31		45	1.1
IC 2202	07 27.8	-67 28		77	2.0
NGC 2466	07 45.7	-71 17	5161	33	1.6
	07 53.3	49 42	3539	36	1.1
	07 55.9	60 25	5992	62	1.4
	07 56.5	16 34	4878	36	1.1
	07 59.5	27 35		71	1.05
UGC 4301	08 13.0	28 47		69	1.0
	08 14.5	21 50	3631	39	1.65
IC 2282	08 16.3	24 56	4657	42	0.8
	08 27.3	61 10	6330	36	1.1
IC 509	08 29.0	24 10	5482	30	1.6
UGC 4512	08 35.5	61 08		62	0.9
NGC 2649	08 41.0	34 54	4075	24	1.2

UGC 4623	08 47.1	76 41		82	2.5
NGC 2742	09 03.6	60 40	1392	67	2.35
NGC 2755	09 04.7	41 55	7547	62	0.8
NGC 2776	09 08.9	45 10	2643	42	2.6
UGC 4919	09 14.5	45 52	8096	52	1.1
NGC 2889	09 24.8	-11 25	3377	21	1.6
UGC 5066	09 27.8	46.37		74	0.9
NGC 2906	09 29.5	08 40		62	1.0
NGC 2919	09 32.1	10 30	2469	73	1.3
	09 35.0	84 02		42	0.8
NGC 2942	09 36.1	34 14	4374	51	1.7
NGC 2969	09 39.3	-08 24		0	1.3
NGC 2998	09 45.5	44 18	4777	72	3.0
NGC 3029	09 47.5	-07 56		49	1.2
NGC 3052	09 52.1	-18 24	3582	42	1.6
NGC 3055	09 52.7	04 31	1913	62	1.0
	09 54.5	-07 40		46	0.7
NGC 3074	09 56.7	35 38	5115	39	1.9
	09 59.0	11 00		74	1.2
	10 01.0	-14 45		67	1.4
	10 01.5	14 30	8991	25	0.55
NGC 3153	10 10.2	12 55	2806	71	2.0
	10 13.9	-28 57		58	0.9
NGC 3184	10 15.3	41 40	599	25	5.5
	10 28.1	-30 08	4170	32	1.4
	10 37.5	-17 24		42	0.8
NGC 3344	10 40.7	25 10	698	23	6.5
NGC 3362	10 42.2	06 52	8360	36	1.1
NGC 3423	10 48.6	06 06	1013	39	3.5
UGC 6015	10 51.1	46 17		41	0.65
NGC 3523	10 59.2	75 24	7100	26	1.05
NGC 3506	11 00.6	11 21	6400	21	0.8
	11 14.8	36 20		36	1.1
NGC 3631	11 18.2	53 27	1161	42	4.0
NGC 3672	11 22.5	-09 31	1737	70	3.7
UGC 6440	11 23.5	02 15	9854	64	0.95
	11 29.0	-02 01	4745	38	2.0
NGC 3938	11 50.2	44 24	838	40	4.5
NGC 4456	12 25.2	-29 43		64	1.05
NGC 4480	12 27.9	04 31	2285	64	1.8
	12 37.7	-09 01	6360	56	0.85
NGC 4712	12 47.1	25 45	4452	73	2.0
NGC 4981	13 06.2	-06 31	1677	45	2.2
NGC 5012	13 09.1	23 12	2632	58	2.25
NGC 5042	13 12.8	-23 43	1390	70	4.7
NGC 5118	13 20.9	06 39	6976	42	0.8
NGC 5123	13 21.0	43 20	8265	35	1.15
UGC 8427	13 22.0	06 47		62	1.0
UGC 8448	13 24.3	20 13	7146	42	0.8
NGC 5172	13 26.9	17 19	4085	62	2.0
IC 4267	13 37.8	-26 00		75	1.1
	13 29.4	-22 42		62	1.2
UGC 8520	13 30	80 45		60	0.95
IC 900	13 32.2	09 36	7080	52	1.1
NGC 5230	13 33.1	13 56	6893	33	1.6
	13 36.8	-22 15		32	0.7
IC 4318	13 40.6	-28 43		48	1.1
NGC 5293	13 44.4	16 31	5781	49	1.4

NGC 5457	14 01.5	54 35	231	25	23.0
NGC 5494	14 09.5	-30 25	2638	36	2.2
NGC 5660	14 28.0	49 50	2336	32	2.1
NGC 5690	14 35.2	02 30	1778	87	2.9
	14 44.8	-17 52		42	1.6
	14 46.0	-04 30		42	1.2
	14 46.2	-20 38		62	1.2
NGC 5874	15 06.4	54 56	3128	53	1.7
	15 10.8	02 42		41	0.85
	15 22.6	58 14	2661		
	15 32.7	41.19		62	1.1
UGC 10151	16 00.9	27 09		53	0.8
UGC 10282	16 11.0	32 38		53	0.8
	16 14	56 00		57	0.7
NGC 6118	16 19.2	-02 10	1578	73	4.1
	16 27.9	08 44		19	0.95
NGC 6260	16 51	63 50		34	0.6
	17 23.0	45 00		40	0.9
NGC 6379	17 28.4	16 19	5963	33	1.0
NGC 6412	17 31.2	75 45	1328	29	1.7
	17 45	20 53			0.9
NGC 6479	17 47.3	54 10		38	0.75
NGC 6532	17 58.3	56 13		69	1.5
	18 18.9	68.19		38	1.0
NGC 6640	18 26.3	34 16		52	0.95
NGC 6719	18 57.6	-68 40		68	1.7
	20 08.2	-38 21		73	1.4
	20 25.6	-19 10		41	0.65
NGC 6922	20 27.3	-02 21	5665	38	1.0
NGC 6919	20 28.2	-44 23	6628	42	1.2
	20 29.3	-46 25		42	0.8
NGC 6925	20 31.2	-32 09	2775	84	4.0
NGC 6946	20 33.8	59 59	48	0	10.0
	20 36.5	-28 40		62	0.8
	20 48.9	-31 05		21	0.8
NGC 7003	20 58.4	17 36		52	0.95
NGC 7015	21 03.3	11 13	4876	31	1.5
NGC 7038	21 11.8	-47 26	4802	64	2.7
	21 19.9	-45 59	2650	88	3.2
NGC 7073	21 26.5	-11 45		0	0.6
NGC 7083	21 31.8	-64 08	3049	62	3.6
NGC 7124	21 44.8	-50 48	5027	72	2.2
NGC 7156	21 52.0	02 42	4177		
	22 05.3	-32 42		65	1.4
NGC 7218	22 07.5	-16 55	1782	77	2.3
NGC 7230	22 11.6	-17 18		0	0.65
	22 12.5	15 02		53	0.8
	22 20	02 3[illegible]		49	0.6
	22 24.9	-30 18		22	0.7
NGC 7298	22 28.2	-14 27	5039	46	1.4
	22 35.1	-32 45		49	0.9
	22 41.6	38 06	4767	60	1.6
	22 41.8	-49 33		76	1.3
	22 51.0	-17 45		51	0.85
	22 53.0	-24 13		38	0.75
	22 54.0	28 10		22	0.75
	22 54.0	-25 13			

NGC 7442	22 56.9	15 17	7268	28	0.9
	23 00.2	32 20	5965	28	0.9
	23 12.4	-49 40		34	1.5
	23 13.8	-22 26		28	0.9
NGC 7610	23 17.1	09 54	3546	47	2.0
NGC 7678	23 26.0	22 08	3489	38	1.5
NGC 7685	23 27.9	03 37	5642	53	1.6
	23 31.5	44 25		55	1.0
IC 5332	23 31.6	-36 23	707	28	9.0
NGC 7713A	23 34.5	-38 00	2980	31	1.5
	23 48.6	00 46	8214	77	1.7
	23 49.7	-25 41		74	1.2
	23 51.9	-02 13		20	0.9
	23 52.4	-34 53		46	0.7
	23 58.4	-40 59		74	1.2
	23 58.4	-33 53		38	1.0

An attempt was also made to select a significant fraction of the galaxies at high inclination, facilitating the use of the Tully-Fisher relation by minimising the inclination corrections. This is a matter of compromise, however, since it is inevitably more difficult to classify highly inclined galaxies accurately. The distribution of inclinations is shown in Figure 5.1, although the inclinations are very approximate, having been calculated from major and minor axis measurements made by eye. Whilst there are obviously many face-on galaxies in the sample, they are on average more inclined than the Rubin et al. galaxies, as can be seen from Figure 5.1. The use of CCD imaging, particularly in the I-band, described below, should also prove useful in determining accurate inclinations even for some of the more face-on galaxies. Pierce & Tully (1988) have found it possible to derive accurate determinations of inclinations as low as 30° by a process of ellipse fitting to CCD array images.

I.4 OBSERVATIONAL METHODS: PHOTOMETRY AND LUMINOSITY INDICATORS

The principal aim of this study is the same as our reanalysis of the Rubin et al. work; to derive accurate and unbiased redshift-independent distances to all galaxies in the sample. One way to improve on previous attempts to do this is to make use of the extra information from the widely-available CCD array detectors which permit accurate surface photometry to be made over entire galaxies, in one integration.

The main advantage of area photometry is that having full surface brightness information makes aperture corrections unnecessary. Photometry can be normalised to a particular surface brightness, measured directly from the image concerned. This is preferable to the use of externally derived optical diameters, which are derived from lower quality

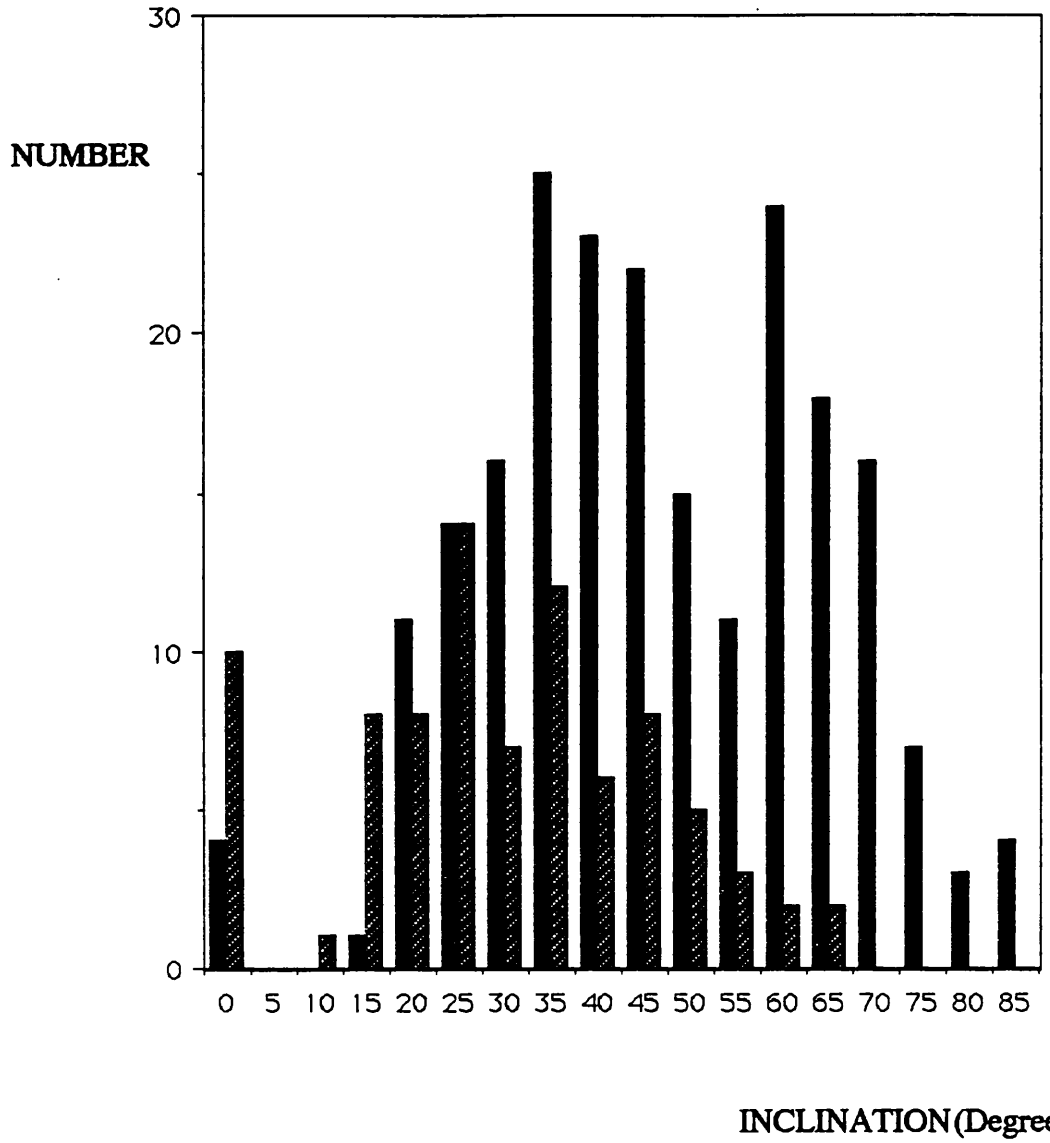


Figure 5.1 Distribution of inclinations for the ScI galaxies in our new sample (black) compared with that for the Rubin et al. sample (shaded)

photographic images and have been shown in Chapter Three to do little more than introduce scatter into the photometry. Contaminating foreground stars can also be removed easily from array images by excluding the affected pixels from the image. The other general advantage for this work is the possibility of deriving inclinations more accurately and systematically than from a single catalogued axial ratio. Ellipses can be fitted to contours at several surface brightness levels within each image, thus providing independent checks on the inclination of each galaxy.

The other advantages of surface photometry are in the application of luminosity indicators. Pierce (1986) and Bothun and Mould (1987) have investigated the use of the Tully-Fisher relation with I-band CCD images, and the latter show that it is possible to reduce the scatter in the relation to ≈0.3 magnitudes using these methods, compared with ≈0.45 magnitudes for the H-band relation, the best that has been found using aperture photometry. Some of the improvement is undoubtedly due to the removal of the need for aperture corrections, with a further contribution from the ability to apply the relation using photometry at different surface brightness levels or at different linear diameters on the galaxies.

The reasons for this latter improvement can be understood by considering the background to the Tully-Fisher relation. The relation is essentially due to a correlation between luminosity and mass, but it is not the total mass of the galaxy that determines the edge-on linewidth that is the observable used here. The reason is that the rotation velocity curve of most spiral galaxies increases only in the central part of the galaxy, and then remains flat over a large range of radius. Thus the measured linewidth is not dependent on the slit length or aperture used on the galaxy, as long as they are large enough to include all of the inner, corotating part of the galaxy. However, measured luminosity is clearly strongly dependent on aperture. Conventional aperture photometry methods applied to the TF relation would tend to include varying amounts of the luminosity contribution from the outer part of the galaxy, where the rotation curve is flat, and would thus almost certainly contribute to the scatter in the relation.

Thus, it is at least plausible that there is a characteristic diameter that minimises scatter in the TF relation by matching the diameter to the radius at which the rotation curve flattens out. This was attempted for the early studies using aperture photometry by correcting photometry to a diameter corresponding to a given optical isophote. However, it should be possible to identify and apply such a diameter much more effectively using array images of galaxies. A source of scatter found by Bothun et al. was a variation in disc surface brightness at fixed linewidth, which they were able to reduce empirically by

using total magnitudes for low linewidth galaxies, and magnitudes within a particular surface brightness contour for galaxies with larger linewidths. This is a good illustration of the flexibility made possibility with area photometry.

Madore & Woods (1987) have recently proposed a new form of the Tully-Fisher relation which may be able to exploit the extra dynamical information made available by modern observing techniques. They find a strong correlation between the local rotation velocity at a given radius and the total luminosity interior to that radius, for a sample of 46 Sb and Sc galaxies. The principal obstacle to implementing this method at present is the need for rotation curves with sufficient spatial resolution, which requires substantial observing time and restricts the method to galaxies at less than 5000 kms^{-1}. The method also requires further investigation to check that the zero point of the relation is stable from galaxy to galaxy, and particularly between different environments. Whatever the outcome of these checks, it is clear that this is the type of luminosity indicator which will be developed in the future, simply because of the extra information that is incorporated compared to the global dynamic and luminosity parameters used in the original Tully-Fisher relation.

B- and I-band photometry are being used for the present study. The principal advantages of I-band are those of lower extinction which were used to justify the use of H-band photometry in the reanalysis of the Rubin et al. spirals (Chapter Two). I-band is centred on approximately 0.9 μm, considerably shortward of the J, H and K bands, and photometry is therefore more susceptible to the effects of extinction. However, the widespread availability of CCD cameras with standard I-band filters makes this much more feasible than using the 'true' NIR bands. Ultimately, the best luminosity indicators may be derived from measurements with the new generation IR array cameras, but at present these are not widely available, and the absolute calibration and repeatability of photometry are too uncertain for them to be used at present.

B-band photometry is also being obtained, to investigate the use of the B-I colour as a luminosity indicator (Pierce 1986). Again, the use of area photometry enables the B-I colour-magnitude relation to be investigated over a range of radii and surface brightnesses. Although the reduced spectral range of B-I, compared with B-H colour, is a disadvantage since it reduces the discrimination between different stellar populations, which is the likely basis of the relation, this effect may be offset by the increased precision which area photometry makes possible.

I.5 OBSERVATIONS

The data required for the completion of this project are redshifts, B- and I-band CCD photometry and 21 cm linewidths for each of the galaxies in the sample. Catalogued redshifts are available for about half of the galaxies, but the remainder require redshifts to be measured. This is most quickly achieved via optical spectroscopy. For most of the sample, this requires only ≈2 m telescopes. The CCD photometry of these galaxies is also very straightforward, and can be done with ≈1 m telescopes. Radio measurements of 21cm linewidths pose more of a problem for galaxies at redshifts of ≈7000 kms^{-1}, since there are few radio telescopes large enough to give the required sensitivity. At present we are planning to apply to use Jodrell Bank for the northern galaxies and the Parkes radio telescope in Australia for the southern galaxies.

I.6 ANALYSIS OF THE NEW GALAXY SAMPLE

Figure 5.2 shows the sky coverage of the 218 ScI spirals we have selected for this new study. Whilst there is clearly significant clumping of the galaxies on the sky, there are no large areas devoid of galaxies, and thus all components of the streaming vector should be well determined, a significant advantage compared with the RF sample.

We tested the homogeneity of classification of our galaxies by comparison with the Uppsala Galaxy Catalogue (Nilson 1973). This catalogue was prepared by repeated scanning of the POSS plates, and selecting all galaxies with diameters on the plates greater than 1.0 mm. This procedure is almost identical to that used here, and Nilson's classifications provide a good test of the reliability of ours. We achieved a highly uniform galaxy sample, and of those of our galaxies in the UGC, ≈75% are classified as Sc, compared with only ≈45% of the RF sample. Luminosity classes are not given in the UGC. In addition only ≈20% of our sample are classified as barred, compared with ≈40% of the RF sample. This latter is not surprising, since RF did not select against barred galaxies, whereas it was decided prior to the selection of our sample that inclusion of both barred and non-barred galaxies would be likely to increase the dispersion in absolute magnitude, and affect the reliability of the luminosity indicators.

Whilst it is difficult to derive any firm parameters describing the galaxy sample prior to obtaining all the observational data, it is possible to get some indication of the characteristic depth of the sample and of the likely selection biases. Catalogued redshifts are available for about half of the sample, but these galaxies are not typical of the sample as a whole, and are likely to represent the brighter members of the sample preferentially.

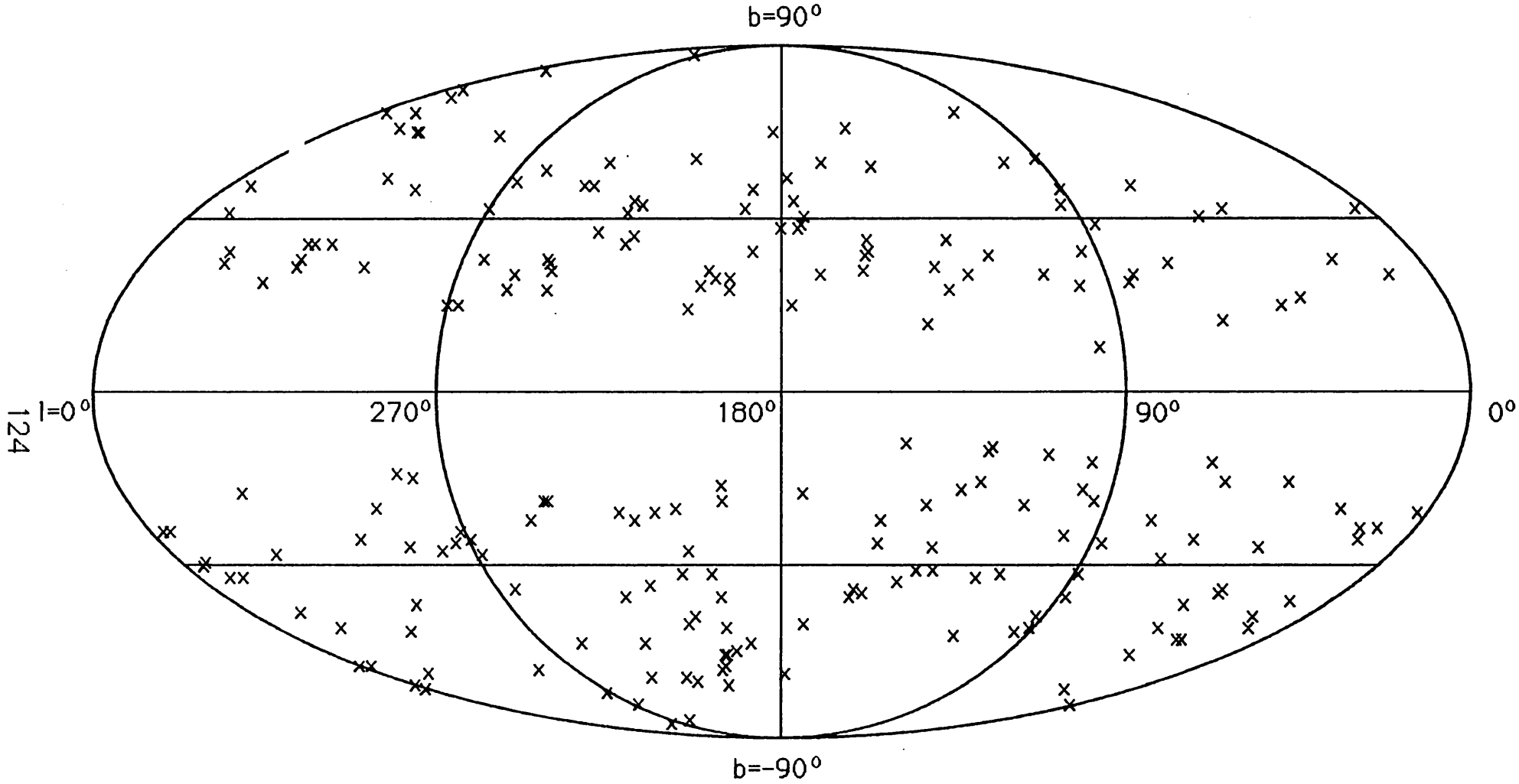


Figure 5.2 Sky coverage of 218 Sc spirals (galactic coordinates)

However, there are enough to calibrate a rough diameter-redshift relation, which can be used in a statistical sense to gauge the effective selection depth of the sample.

Figure 5.3 shows the estimated linear diameter of those galaxies that have measured redshifts, plotted against redshift. There are uncertainties on the order of 20% in the measured diameters, and a further error comes from the assumption of pure Hubble Flow in estimating the distances of galaxies directly from measured redshifts. Despite this, there is clearly a strong trend in the sense that the more distant galaxies in this subset of the sample are larger and, presumably, more luminous than those nearby. This is rather worrying, since it implies a strong selection bias in the sample. However, the bias is likely to be greatly over-estimated compared to that for the whole sample, due to the additional condition that the galaxies in Figure 5.3 should all have catalogued redshifts. There is an element of magnitude-limited selection in all galaxy catalogues, even if it is not explicitly stated, which would produce a correlation in the sense actually found, even if our full sample were completely bias-free. Expressed another way, many of the galaxies in the remainder of our sample will almost certainly lie toward the bottom right-hand corner of Figure 5.3, and will thus reduce the strength of the bias at a given redshift limit.

However, the bias is bound to remain to some extent. The shaded and cross-hatched areas on Figure 5.3 show the regions excluded by taking linear diameter cutoffs of 1.0 and 0.7 mm respectively on the Sky Survey plates. The real situation for our sample is likely to lie somewhere between the two, which includes galaxies smaller than 1.0 mm, but in diminishing numbers due the difficulty of classifying them. By comparing the linear diameters of the nearest galaxies with the areas excluded by diameter selection, it can be seen that significant bias is likely to set in between $\approx$4000 and 7000 kms^{-1}, i.e. galaxies which would have been selected if nearby will have too small an apparent diameter to be included if beyond the redshift limit.

It is possible to estimate the size of this residual effect for the full sample by using the measured diameters as a crude distance indicator. The diameter-redshift relation is calibrated in Figure 5.4. Diameters can then be used to predict redshifts, at least on a statistical basis. The completeness of the sample as a function of this estimated redshift is then calculated, by predicting the expected number of galaxies within redshift 'bins', under the assumption of a constant spatial density of galaxy, and comparing with the number actually in the sample in the same redshift range.

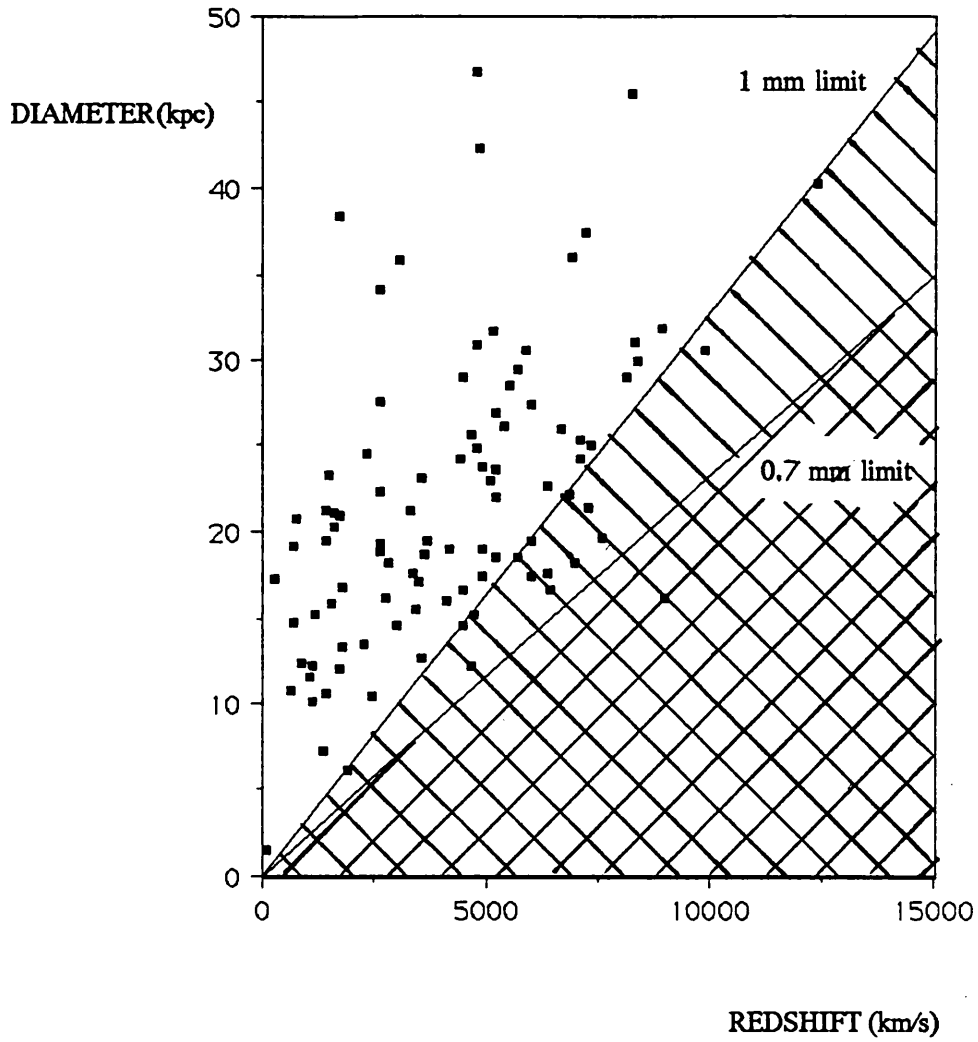


Figure 5.3 Linear diameter-redshift relation for galaxies in new sample with catalogued redshifts

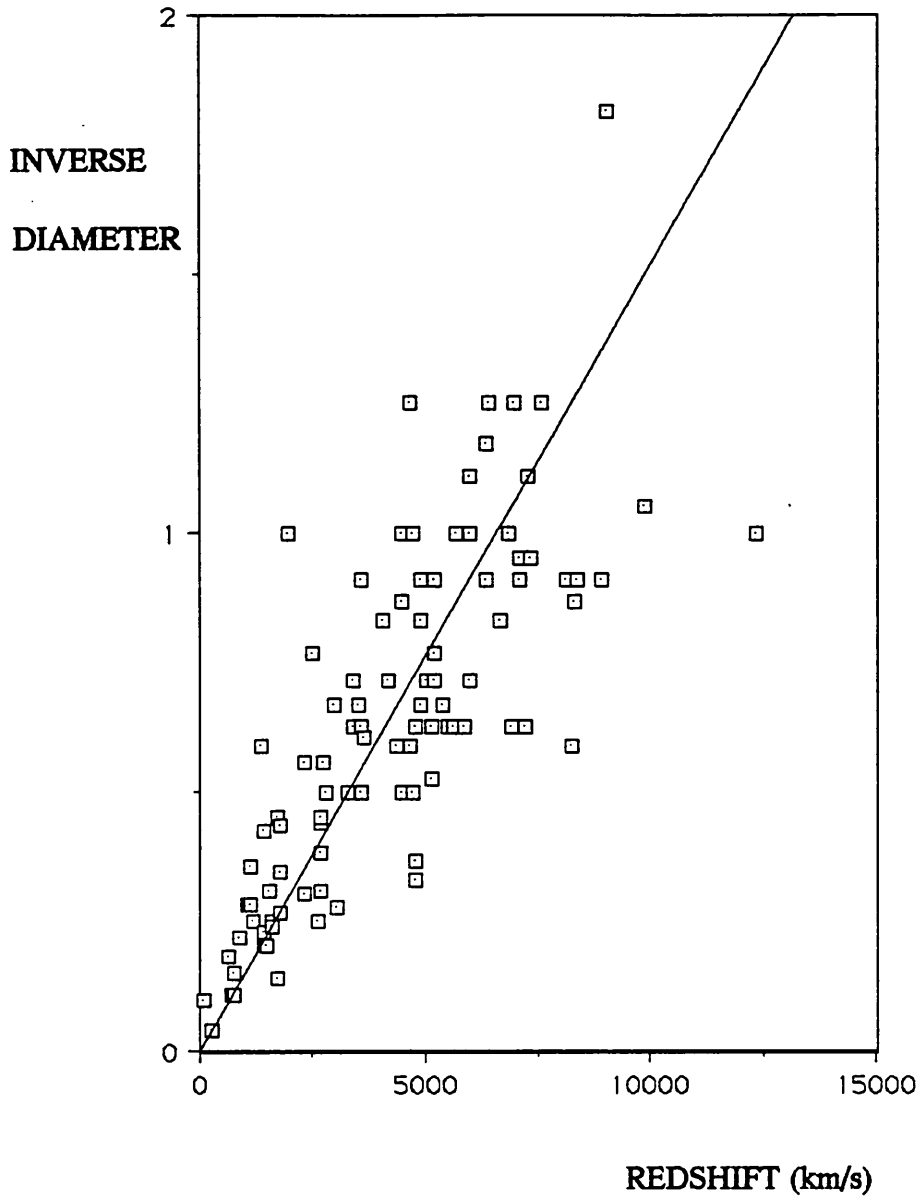


Figure 5.4 Calibration of the apparent diameter-redshift relation for the new sample of Sc galaxies

Figure 5.5 shows the completeness, i.e. number of galaxies in the sample compared to the predicted number, as a function of estimated redshift. There is evidence for a downward trend at all redshifts, which is relatively weak below 6000-7000 kms^{-1}, but very strong beyond 7000 kms^{-1}. Thus it may be possible to define a volume limited subset of the whole sample out to a maximum of $\approx$7000 kms^{-1}, even though this was impossible with the Rubin et al. galaxy sample, because of our much broader selection criteria.

However, the main conclusion of this analysis of the new galaxy sample must be that selection biases are going to be present in any galaxy sample, however carefully selected. The credibility given to results obtained using such samples must therefore rest on the efficiency with which biases can be removed. For streaming motions, this requires luminosity indicators with an intrinsic scatter much smaller than the amplitude of the bias in the galaxy sample.

II FURTHER ANALYSIS OF GALAXY STREAMING USING FIRST RANKED CLUSTER ELLIPTICALS

In spite of the great advances in developing extragalactic distance indicators such as the Tully-Fisher and Faber-Jackson relations (Tully and Fisher 1977, Faber and Jackson 1976), First Ranked Cluster Galaxies still seem to give the best redshift-independent distance determinations, with a scatter in absolute magnitude of only $\approx$0.3 magnitudes. This tight correlation was used in deriving the results described in Chapter Two, which demonstrated the feasibility of using these galaxies to map the velocity field to large scales. It is now possible, for a minimal expenditure of telescope time, to improve greatly on this preliminary study, and to investigate the doubts raised by Lucey and Carter (1988a).

Most importantly, the Southern extension to the original Abell catalogue (Abell 1958) has been prepared (Abell et al. 1988) and is shortly to be published. This has been carefully matched to the existing Northern catalogue, making possible the selection of a homogeneous all-sky sample of clusters. This removes any uncertainty about how Sandage and Hardy (1973) selected their clusters, and whether their methods were suitable for the use to which we put the sample. Complete sky coverage also allows a full solution for streaming motion amplitude and direction to be carried out, which is a significant improvement over the one-component solution we were obliged to adopt.

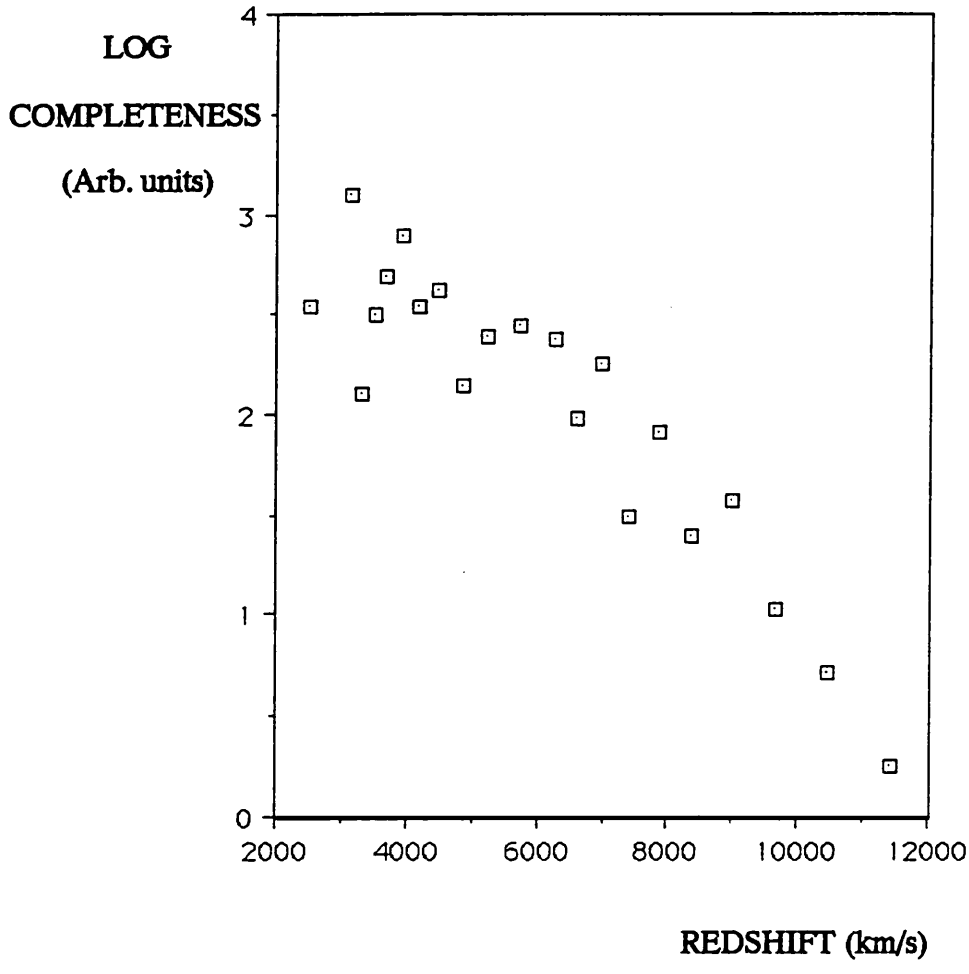


Figure 5.5 Completeness of the new galaxy sample as a function of redshift

In addition, array photometry can be obtained with a very short allocation of telescope time, using only ≈1 metre telescopes, because of the high surface brightness of these objects. Again, I-band imaging should be ideally suited to these cluster galaxies, which are intrinsically red, and this filter also gives the advantages of lower extinction compared to the BVR photometry used by Sandage and coworkers. As for the spirals, array photometry permits flexibility in defining effective apertures to be used when deriving magnitudes. This is very important in preventing redshift-dependent biases, and may reduce the scatter in the derived absolute magnitudes to even less than the 0.28 magnitudes found by Sandage and Hardy. The high surface brightness also eases the task of obtaining optical redshifts, which will be necessary for some of the Southern clusters.

Given the above, and the amount of work that has already been done on First Ranked Cluster Galaxies, for example on deriving richness and Bautz-Morgan classes and on measuring redshifts, it is clear that important further results can be obtained with a minimal amount of observational effort.

III FUTURE WORK

For fundamental advances to be made in future studies of the galaxy peculiar velocity field, a deeper understanding of the nature of galaxies is required. Galaxies will be used as standard candles with increasing confidence as we discover more about their star formation histories and evolution, and understand the role played by dark matter in determining their dynamics. Given a better description than is presently available of the galaxy dynamics and luminosity generation, it should be possible to explain and refine the Tully-Fisher and Faber-Jackson relations, and the correlation between First Ranked Cluster Galaxy magnitude and cluster morphology. This will yield both higher precision and greater confidence in the measurement of galaxy peculiar velocities.

Further improvements would result from the development of a statistic which provides more detailed information on the nature of the velocity field, and thus of the mass fluctuation spectrum, than the simple 'bulk flow' solutions presented here. These solutions can be considered closely analogous to the 'light dipoles' such as the IRAS dipole, which have been used as a coarse indicator of the local galaxy distribution; what we need ideally is an analogue of the 2- and 3-point correlation functions, that can be applied to the peculiar velocity field. The main problem here is that we have only line-of-sight peculiar velocities for the galaxies studied, which makes it difficult to develop a

statistic that gives information on the velocity field without including spurious features arising from the clumpiness of the galaxies on the sky. Another desirable feature of such a statistic is that it should also be possible to apply it to the results of N-body simulations for direct comparison with the observed properties of the real Universe.

A less ambitious method for deriving more information from samples of galaxies with line-of-sight peculiar velocities is to solve for spherical harmonics of higher order than simply the dipole term. This requires better data than the latter since more free parameters are derived, and a uniform distribution of galaxies around the sky. The advantages of this method are that it is well-suited to data where only the radial component of the galaxy velocities are known, and that it is trivial to apply the same statistic to the N-body simulations. The main drawback is that a knowledge of, say, the quadrupole and octopole components of the velocity field tells you little more than the dipole term about the characteristic scale of coherence in the velocity field. There is no depth information to be obtained from a particular spherical harmonic, and there is thus no way to determine any characteristic scale which would give direct physical information about the mass distribution.

It is clear that studies such as those presented in this thesis are going to play an important part in the development of observational cosmology over the coming years. The information they give can be obtained in no other way, and promises, when combined with other measurements presently being made, to yield insights into the way galaxies and clusters formed, and the nature and distribution of the elusive dark matter.

REFERENCES

Aaronson, M. & Mould, J., 1981. *Publ. Astron. Soc. Pac.*, **93**, 20.

Aaronson, M., Bothun, G., Mould, J., Huchra, J., Schommer, R.A. & Cornell, M.E., 1986. *Astrophys. J.*, **302**, 536.

Aaronson, M., Huchra, J.P. & Mould, J., 1979. *Astrophys. J.*, **229**, 1.

Aaronson, M., Mould, J. & Huchra, J.P., 1980. *Astrophys. J.*, **237**, 655.

Abell, G.O., 1958. *Astrophys. J. Suppl.*, **3**, 211.

Abell, G.O., Corwin, H.G. & Olowin, R., 1988. *Astrophys. J.*, submitted.

Arnett, W. & Rosner, J.L., 1987. *Phys. Rev. Lett.*, **58**, 1906.

Bahcall, J.N. & Glashow, S.L., 1987. *Nature*, **326**, 476.

Bahcall, N.A. & Soneira, R.M., 1983. *Astrophys. J.*, **270**, 20.

Bahcall, N.A. & Soneira, R.M., 1984. *Astrophys. J.*, **277**, 27.

Bahcall, N.A., Soneira, R.M. & Burgett, W.S., 1986. *Astrophys. J.*, **311**, 15.

Balzano, V.A. & Weedman, D.W., 1982. *Astrophys. J. Lett.*, **255**, L1.

Bardeen, J.M., Bond, J.R. & Efstathiou, G., 1987. *Astrophys. J.*, **321**, 28.

Barrow, J.D. & Turner, M.S., 1982. *Nature*, **298**, 801.

Bautz, L.P. & Morgan, W.W., 1970. *Astrophys. J. Lett.*, **162**, L149.

Bertschinger, E., 1988 in *The Post-Recombination Universe*, eds. N. Kaiser & A.N. Lasenby (Kluwer).

Bhavsar, S.P. & Barrow, J.D., 1985. *Clusters and Groups of Galaxies*, eds. F. Madirossian, G. Giuricin & M. Mezzetti (Dordrecht: Reidel).

Binggeli, B., 1986, in *Nearly Normal Galaxies: From the Planck Time to the Present*, ed. S.M. Faber (New York: Springer-Verlag).

Bond, J.R. & Szalay, A.S., 1983. *Astrophys. J.*, **274**, 443.

Bond, J.R., Efstathiou, G. & Silk, J., 1980. *Phys. Rev. Lett.*, **45**, 1980.

Bothun, G.D. & Mould, J.R., 1987. *Astrophys. J.*, **313**, 629.

Bothun, G.D., Beers, T.C., Mould, T.R. & Huchra, J.P., 1986. *Astrophys. J.*, **308**, 510.

Bothun, G.D., Mould, J., Schommer, R.A. & Aaronson, M., 1985. *Astrophys. J.*, **291**, 586.

Bottinelli, L., Fouqué, P., Gouguenheim, ' , Paturel, G. & Teerikorpi, P., 1987. *Astr. Astrophys.*, **181**, 1.

Bottinelli, L., Gouguenheim, L., Paturel, G. & de Vaucouleurs, G., 1983. *Astron. Astrophys.*, **118**, 4.

Bottinelli, L., Gouguenheim, L., Paturel, G. & Teerikorpi, P., 1988. *Astrophys. J.*, **328**, 4.

Boughn, S.P., Saulson, P.R. & Uson, J.M., 1986. *Astrophys. J.*, **301**, 17.

Braun, E., Dekel, A. & Shapiro, P.R., 1988. *Astrophys. J.*, **328**, 34.

Burstein, D., 1982. *Astrophys. J.*, **253**, 539.

Centrella, J. & Melott, A.L., 1983. *Nature*, **305**, 196.

Chincarini, G. & Rood, H.J., 1975. *Nature*, **257**, 294.

Clutton-Brock, M. & Peebles, P.J.E., 1981. *Astr. J.*, **86**, 1115.

Collins, C.A. & Joseph, R.D., 1988. *Mon. Not. R. astr. Soc.*, **235**, 209.

Collins, C.A., Joseph, R.D. & Robertson, N.A., 1986. *Nature*, **320**, 506.

Davies, R.D. & Staveley-Smith, L., 1984. *Proc. ESO Workshop on the Virgo Cluster*, eds. Richter, O.-G. & Binggeli, B., Garching, European Southern Observatory.

Davis, M. & Huchra, J.P., 1982. *Astrophys. J.*, **254**, 437.

Davis, M. & Peebles, P.J.E., 1983. *Ann. Rev. Astron. Astrophys.*, **21**, 109.

Davis, M. & Wilkinson, D.W., 1974. *Astrophys. J.*, **192**, 251.

Davis, M., 1985. *Inner Space/Outer Space: The interface between cosmology and Particle Physics*, eds. E.W. Kolb, M.S. Turner, D. Lindley, K. Olive & D. Seckel (University of Chicago Press).

Davis, M., Efstathiou, G., Frenk, C.S. & White, S.D.M., 1985. *Astrophys. J.*, **292**, 371.

de Lapparent, V., Geller, M.J. & Huchra, J.P., 1986. *Astrophys. J. Lett.*, **302**, L1.

de Vaucouleurs, G. & Peters, W.L., 1981. *Astrophys. J.*, **248**, 395.

de Vaucouleurs, G. & Peters, W.L., 1984. *Astrophys. J.*, **287**, 1.

de Vaucouleurs, G., de Vaucouleurs, A. & Corwin, H.G., 1976. *Second Reference Catalogue of Bright Galaxies*, Austin: University of Texas Press.

de Vaucouleurs, G., Peters, W.L., Bottinelli, W.L., Gouguenheim, L. & Paturel, G., 1981. *Astrophys. J.*, **248**, 408.

Dekel, A. & Aarseth, S.J., 1984. *Astrophys. J.*, **283**, 1.

Dekel, A., 1986. *Nearly Normal Galaxies: From the Planck Time to the Present*, ed. S.M. Faber (New York: Springer-Verlag).

Djorgovski, S., Spinrad, H., McCarthy, P. & Strauss, A., 1985. *Astrophys. J. Lett.*, **299**, L1.

Dressler, A., 1984. *Astrophys. J.*, **281**, 512.

Dressler, A., Faber, S.M., Burstein, D., Davies, R.L., Lynden-Bell, D., Terlevich, R.J. & Wegner, G., 1987. *Astrophys. J. Lett*, **313**, L37.

Ellis, R.S., Mobasher, B. & Sharples, R.M., 1986. *Galaxy Distances and Deviations from Universal Expansion*, eds. Madore, B.F. & Tully, R.B., Reidel, Dordrecht, Holland.

Faber, S.M. & Gallagher, J.C., 1979. *Ann. Rev. Astron. Astrophys.*, **17**, 135.

Faber, S.M. & Jackson, R.E., 1976. *Astrophys. J.*, **204**, 668.

Fabian, A.C., Nulsen, P.E.J., & Canizares, C.R., 1984. *Nature*, **310**, 733.

Fall, S.M. & Jones, B.J.T., 1976. *Nature*, **262**, 457.

Fomalont, E.B., Kellerman, K.I. & Wall, J.V., 1984. *Astrophys. J. Lett.*, **277**, L23.

Godwin, P.J. & Lynden-Bell, D., 1987. *Mon. Not. R. astr. Soc.*, **229**, 7P.

Graham, J.A., 1976. *Astr. J.*, **81**, 681.

Groth, E.J. & Peebles, P.J.E., 1977. *Astrophys. J.*, **217**, 385.

Gunn, J.E. & Oke, J.B., 1975. *Astrophys. J.*, **195**, 255.

Guth, A.H. & Pi, S.-Y., 1982. *Phys. Rev. Lett.*, **49**, 1110.

Guth, A.H., 1981. *Phys. Rev.*, **D23**, 347.

Harmon, R.T., Lahav, O. & Meurs, E.J.A., 1987. *Mon. Not. R. astr. Soc.*, **228**, 5P.

Harrison, E.R., 1970. *Phys. Rev.*, **D1**, 2726.

Hart, L. & Davies, R.D., 1982. *Nature*, **297**, 191.

Hartwick, F.D.A., 1975. *Astrophys. J. Lett.*, **195**, L7.

Haynes, M.P., 1986. *Nearly Normal Galaxies: From the Planck Time to the Present*, ed. S.M. Faber (New York: Springer-Verlag).

Hillebrandt, W., Höflich, P., Kafka, P., Müller, E., Schmidt, H.U., Truran, J.W. & Wampler, J., 1987. *Astron. Astrophys.*, **177**, L41.

Hoessel, J.G., 1980. *Astrophys. J.*, **241**, 493.

Hoffman, Y., 1987. *Astrophys. J.*, **318**, L7.

Holmberg, E., 1958. *Medd. Lund. Obs.*, Ser. 2, No. 136.

Humason, M.L., Mayall, N.U. & Sandage, A., 1956. *Astron. J.*, **61**, 97.

Jackson, R.E., 1982. Unpublished Ph.D. Thesis, University of California.

James, P.A., Joseph, R.D. & Collins, C.A., 1987. *Mon. Not. R. astr. Soc.*, **229**, 53.

Jeans, J., 1902. *Phil. Trans.*, **199A**, 49.

Jones, B.J.T., 1988. *The Post-Recombination Universe*, eds. N. Kaiser & A.N. Lasenby (Kluwer).

Juszkiewicz, R., Gorski, K. & Silk, J., 1987. *Astrophys. J.*, **323**, L1.

Kaiser, N. & Silk, J., 1986. *Nature*, **324**, 529.

Kaiser, N., 1983. *Astrophys. J. Lett.*, **273**, L17.

Kaiser, N., 1984. *Astrophys. J. Lett.*, **284**, L9.

Kaiser, N., 1987. *Mon. Not. R. astr. Soc.*, **227**, 1.

Kibble, T.W.B., 1976. *J. Phys.*, **A9**, 1387.

Kirshner, R.P., Oemler, Jr., A., Schechter, P.L., & Schechtman, S.A., 1981. *Astrophys. J. Lett.*, **248**, L57.

Klypin, A.A. & Shandarin, S.F., 1983. *Mon. Not. R. astr. Soc.*, **204**, 891.

Koo, D.C. & Kron, R.G., 1980. *Pub. Astr. Soc. Pacific.*, **92**, 537.

Lahav, O., 1987. *Mon. Not. R. astr. Soc.*, **225**, 213.

Lahav, O., Rowan-Robinson, M. & Lynden-Bell, D., 1988. *Mon. Not. R. astr. Soc.*, **234**, 677.

Larson, R.B., 1987. *Nearly Normal Galaxies: From the Planck Time to the Present*, ed. S.M. Faber (New York: Springer-Verlag).

Lilly, S.J., 1988. *Astrophys. J.*, **333**, 161.

Lubin, P. & Villela, T., 1986. *Galaxy Distances and Deviations from Universal Expansion*, eds. Madore, B.F. & Tully, R.B., Reidel, Dordrecht, Holland.

Lucey, J.R. & Carter, D., 1988a. *Mon. Not. R. astr. Soc.*, 231, 15p.

Lucey, J.R. & Carter, D., 1988b. Preprint.

Lynden-Bell, D. & Wood, R., 1968. *Mon. Not. R. astr. Soc.*, **138**, 495.

Lynden-Bell, D., Faber, S.M., Burstein, D., Davies, R.L., Dressler, A., Terlevich, R.J. & Wegner, G., 1988. *Astrophys. J.*, **326**, 19.

Lyubimov, V.A., Novikov, E.G., Novik, V.Z., Tretyakov, E.F. & Kosik, V.S., 1980. *Phys. Lett.*, **94B**, 266.

Madore, B.F. & Woods, D., 1987. *Astrophys. J. Lett.*, **323**, L25.

Malmquist, K.G., 1920. *Medd. Lunds. Obs.*, Ser. 11, No. 22.

Mandolesi, N. et al., 1986. *Nature*, **319**, 751.

Meiksin, A. & Davis, M., 1986. *Astr. J.*, **91**, 191.

Melott, A.L., 1985. *Astrophys. J.*, **289**, 2.

Nilson, P., 1973. *Uppsala General Catalogue of Galaxies*, Uppsala Astr. Obs. Ann., Vol. 6.

Oemler, A., 1987. *Nearly Normal Galaxies: From the Planck Time to the Present*, ed. S.M. Faber (New York: Springer-Verlag).

Oort, J.H., 1983. *Ann. Rev. Astr. Astrophys.*, **21**, 373.

Parker, E.N., 1970. *Astrophys. J.*, **160**, 383.

Partridge, R.B. & Peebles, P.J.E., 1967a. *Astrophys. J.*, **147**, 868.

Partridge, R.B. & Peebles, P.J.E., 1967b. *Astrophys. J.*, **148**, 377.

Peebles, P.J.E., 1965. *Astrophys. J.*, **142**, 1317.

Peebles, P.J.E., 1969. *Astrophys. J.*, **155**, 393.

Peebles, P.J.E., 1971. *Astrophys. Space Sci.*, **11**, 443.

Peebles, P.J.E., 1976. *Astrophys. J.*, **205**, 318.

Peebles, P.J.E., 1980. *The Large Scale Structure of the Universe*, Princeton University Press.

Peebles, P.J.E., 1982. *Astrophys. J.*, **257**, 438.

Peebles, P.J.E., 1987a. *Astrophys. J. Lett.*, **315**, L73.

Peebles, P.J.E., 1987b. *Nature*, **327**, 210.

Penzias, A. & Wilson, R., 1965. *Astrophys. J.*, **142**, 419.

Peterson, B.A., 1970. *Astron. J.*, **75**, 695.

Peterson, B.A., Ellis, R.S., Efstathiou, G., Shanks, T., Bean, A.J., Fong, R. & Zou, Z.L., 1986. *Mon. Not. R. astr. Soc.*, **221**, 233.

Peterson, C.J. & Baumgart, C.V., 1986. *Astr.J.*, **91**, 530.

Pierce, M.J. & Tully, R.B., 1988. *Astrophys. J.*, **330**, 579.

Pierce, M.J., 1986. *Galaxy Distances and Deviations from Universal Expansion*, eds. Madore, B.F. & Tully, R.B., Reidel, Dordrecht, Holland.

Preskill, J.P., 1979. *Phys. Rev. Lett.*, **43**, 1365.

Primack, J.R., 1984. *Dark Matter, Galaxies and Large Scale Structure in the Universe*, Lectures presented at the International School of Physics "Enrico Fermi", Varenna, Italy.

Rees, M.J., 1985. *Mon. Not. R. astr. Soc.*, **213**, 75P.

Rubin, V.C., Ford, W.K. & Rubin, J.S., 1973. *Astrophys. J. Lett.*, **183**, L111.

Rubin, V.C., Ford, W.K., Thonnard, N., Roberts, M.S. & Graham, J.A., 1976a. *Astr. J.*, **81**, 687.

Rubin, V.C., Thonnard, N., Ford, W.K., & Roberts, M.S., 1976b. *Astr. J.*, **81**, 719.

Sandage, A., 1961. *Hubble Atlas of Galaxies*, Carnegie Institution of Washington, Publication 618.

Sandage, A., 1973. *Astrophys. J.*, **183**, 711.

Sandage, A., 1975. *Astrophys. J.*, **202**, 563.

Sandage, A. & Hardy, E., 1973. *Astrophys. J.*, **183**, 743.

Sandage, A. & Tammann, G.A., 1981. *A Revised Shapley-Ames Catalog of Bright Galaxies*, Washington: Carnegie Institution of Washington.

Schaeffer, R. & Silk, J., 1984. *Astrophys. J. Lett.*, **281**, L13.

Schechter, P., 1976. *Astrophys. J.*, **203**, 297.

Schechter, P., 1977. *Astr. J.*, **82**, 569.

Schneider, D.P., Gunn, J.E. & Hoessel, J.G., 1983. *Astrophys. J.*, **264**, 337.

Scott, E.L., 1957. *Astr. J.*, **62**, 248.

Shane, C.D. & Wirtanen, C.A., 1954. *Astron. J.*, **59**, 285.

Shane, C.D. & Wirtanen, C.A., 1967. *Pub. Lick. Obs.*, **22**, Part1.

Shanks, T., Bean, A.J., Efstathiou, G., Ellis, R.S., Fong, R. & Peterson, B.A., 1983. *Astrophys. J.*, **274**, 529.

Shanks, T., Fong, R., Ellis, R.S. & MacGillivray, H.T., 1980. *Mon. Not. R. astr. Soc.*, **192**, 209.

Shapley, H., 1930. *Harvard Obs. Bull.*, **No.874**, 9.

Silk, J., 1967. *Nature*, **215**, 1155.

Silk, J., 1968. *Astrophys. J.*, **151**, 459.

Silk, J., 1974. *Astrophys. J.*, **193**, 525.

Stevenson, P.R.F., Shanks, T., Fong, R. & MacGillivray, H.T., 1985. *Mon. Not. R. astr. Soc.*, **213**, 953.

Strauss, M. & Davis, M., 1987 in *The Evolution of Large Scale Structure in the Universe, IAU Symp. No. 130*, eds. J. Audouze & A. Szalay (Reidel: Dordrecht).

Sunyaev, R.A. & Zeldovich, Ja. B., 1972. *Comm. Astr. Space Sci.*, **4**, 173.

Sutherland, W., 1988. *Mon. Not. R. astr. Soc.*, **234**, 159.

Szalay, A.S. & Silk, J., 1983. *Astrophys. J.*, **264**, L31.

Thompson, L.A., 1982. *Astrophys. J.*, **266**, 446.

Thuan, T.X. & Romanishin, W., 1981. *Astrophys. J.*, **248**, 539.

Tonry, J.L. & Davis, M., 1981a. *Astrophys. J.*, **246**, 666.

Tonry, J.L. & Davis, M., 1981b. *Astrophys. J.*, **246**, 680.

Tremaine, S.D. & Gunn, J.E., 1979. *Phys. Rev. Lett.*, **42**, 407.

Tully, R.B. & Fisher, J.R., 1977. *Astr. Astrophys.*, **54**, 661.

Tully, R.B., 1988. *Nature*, **334**, 209.

Tully, R.B., Mould, J.R., & Aaronson, M., 1982. *Astrophys. J.*, **257**, 527.

Turok, N., 1985. *Phys. Rev. Lett.*, **55**, 1801.

Turok, N., 1986. *Nearly Normal Galaxies: From the Planck Time to the Present*, ed. S.M. Faber (New York: Springer-Verlag), pp. 431-450.

Uson, J.M. & Wilkinson, D.T., 1984. *Nature*, **312**, 427.

Van Dalen, A. & Schramm, D.N., 1988. *Astrophys. J.*, **326**, 70.

van den Bergh, S., 1960a. *Astrophys. J.*, **131**, 215.

van den Bergh, S., 1960b. *Astrophys. J.*, **131**, 558.

Villumsen, J.V. & Strauss, M.A., 1987. *Astrophys. J.*, **322**, 37.

Visvanathan, N. & Sandage, A.R., 1977. *Astrophys. J.*, **216**, 214.

Visvanathan, N., 1979. *Astrophys. J.*, **228**, 81.

Visvanathan, N., 1981. *Astr. Astrophys.*, **100**, L20.

Vittorio, N. & Silk, J., 1985. *Astrophys. J. Lett.*, **293**, L1.

Vittorio, N. & Turner, M.S., 1987. *Astrophys. J.*, **316**, 475.

Vittorio, N., Juszkiewicz, R. & Davis, M., 1986. *Nature*, **323**, 132.

von Weizsäcker, L.F., 1951. *Astrophys. J.*, **114**, 165.

Wasserman, I., 1978. *Astrophys. J.*, **224**, 337.

Weedman, D.W., 1976. *Astrophys. J.*, **203**, 6.

White, S.D.M. & Rees, M.J., 1978. *Mon. Not. R. astr. Soc.*, **183**, 341.

White, S.D.M., Davis, M. & Frenk, C.S., 1984. *Mon. Not. R. astr. Soc.*, **209**, 27P.

White, S.D.M., Frenk, C.S. & Davis, M., 1983. *Astrophys. J. Lett*, **274**, L1.

White, S.D.M., Frenk, C.S., Davis, M. & Efstathiou, G., 1987. *Astrophys. J.*, **313**, 505.

Wyse, R.F.G., 1982. *Mon. Not. R. astr. Soc.*, **199**, 1P.

Yahil, A., 1981. *10th Texas Symposium for Relativistic Astrophysics*, ed. R. Ramaty & F.C. Jones (Ann. N Y Acad. Sci.).

Yahil, A., 1984. *Proc. ESO Workshop on the Virgo Cluster*, eds. Richter, O.-G. & Binggeli, B., Garching, European Southern Observatory.

Yahil, A., Sandage, A. & Tammann, G.A., 1980. *Astrophys. J.*, **242**, 448.

Yahil, A., Walker, D. & Rowan-Robinson, M., 1986. *Astrophys. J. Lett.*, **301**, L1.

Yang, J., Turner, M.S., Steigman, G., Schramm, D.N. & Olive, K.A., 1984. *Astrophys. J.*, **281**, 493.

Zeldovich, Ja.B. & Khlopov, M., 1979. *Phys. Lett.*, **79B**, 239.

Zeldovich, Ja.B., 1970. *Astr. Astrophys.*, **5**, 84.

Zeldovich, Ja.B., 1972. *Mon. Not. R. astr. Soc.*, **160**, 1P.

Zwicky, F., Herzog, E., Wild, P., Karpowicz, M. & Kowal, C.T., 1961-1968. *Catalogue of Galaxies and Clusters of Galaxies*, California Institute of Technology, Pasadena, Vols. 1-6.

APPENDIX

A.1 FORTRAN PROGRAMMES USED TO DERIVE STREAMING MOTION DIPOLE VELOCITIES QUOTED IN CHAPTER 3

Description

The following programme was used to derive a bulk streaming motion for the galaxy samples described in Chapter 3. Modified versions of this programme were used to carry out solutions using the Tully-Fisher and colour-magnitude luminosity indicators.

The main FORTRAN programme reads in all data from a file with the format described in the second comment statement. Line-of-sight peculiar velocity components are then calculated from the 'predicted' redshift $V_H = 10^{(0.2m + <HM>)}$, and the measured CBR-frame redshift. The Hubble Modulus <HM> can be calculated using the routine HMBAR. listed at the end of the main programme, which uses the method of Rubin et al. (1976a) to determine this parameter, or can be input as a free parameter as described in Chapter 3.

The galactic coordinates are converted into cartesian components, where the x axis is l=90°, b=0° the y axis is l=0°, b=0° and the z axis is b=90°. These components and the amplitudes of the peculiar velocities (x_i, y_i, z_i, d_i) are then stored in an array which is the input to the first of the NAG routines, GO2BDF. If different weightings are adopted for the different galaxies, the parameters stored in this array are

$\left(\frac{x_i}{\sigma_i} , \frac{y_i}{\sigma_i} , \frac{z_i}{\sigma_i} , \frac{d_i}{\sigma_i} \right)$, where σ_i is the weighting for the ith galaxy.

GO2BDF produces a 4x4 matrix of sums of squares and cross-products about zero of all the variables in the regression, i.e.

$$\begin{pmatrix} \Sigma x_i^2 & \Sigma x_i y_i & \Sigma x_i z_i & \Sigma x_i d_i \\ \Sigma x_i y_i & \Sigma y_i^2 & \Sigma y_i z_i & \Sigma y_i d_i \\ \Sigma x_i z_i & \Sigma y_i z_i & \Sigma z_i^2 & \Sigma z_i d_i \\ \Sigma x_i d_i & \Sigma y_i d_i & \Sigma z_i d_i & \Sigma d_i^2 \end{pmatrix} = \text{SSP}$$

and a 4x4 matrix, RZ, of correlation-like coefficients for all the variables in the regression, i.e.

$$\begin{pmatrix} 1 & \frac{\Sigma x_i y_i}{(\Sigma x_i^2 \Sigma y_i^2)} & \frac{\Sigma x_i z_i}{(\Sigma x_i^2 \Sigma z_i^2)} & \frac{\Sigma x_i d_i}{(\Sigma x_i^2 \Sigma d_i^2)} \\ \frac{\Sigma x_i y_i}{(\Sigma x_i^2 \Sigma y_i^2)} & 1 & \frac{\Sigma y_i z_i}{(\Sigma y_i^2 \Sigma z_i^2)} & \frac{\Sigma y_i d_i}{(\Sigma y_i^2 \Sigma d_i^2)} \\ \frac{\Sigma x_i z_i}{(\Sigma x_i^2 \Sigma z_i^2)} & \frac{\Sigma y_i z_i}{(\Sigma y_i^2 \Sigma z_i^2)} & 1 & \frac{\Sigma z_i d_i}{(\Sigma z_i^2 \Sigma d_i^2)} \\ \frac{\Sigma x_i d_i}{(\Sigma x_i^2 \Sigma d_i^2)} & \frac{\Sigma y_i d_i}{(\Sigma y_i^2 \Sigma d_i^2)} & \frac{\Sigma z_i d_i}{(\Sigma z_i^2 \Sigma d_i^2)} & 1 \end{pmatrix} = RZ$$

These matrices are then used by the second NAG routine, GO2CHF, which solves for the components l,m & n of the streaming velocity by performing a matrix inversion of RZ. This is mathematically equivalent to minimising the quantity

$$\sum_{i=1}^{n} (d_i - lx_i - my_i - nz_i)^2$$

or

$$\sum_{i=1}^{n} \frac{(d_i - lx_i - my_i - nz_i)^2}{\sigma_i^2}$$

the latter being the case if the galaxies receive different weightings σ_i.

GO2CHF produces a 3x3 array COEFF containing the 3 regression coefficients l, m & n, the standard errors on each of these coefficients and their t-values. The latter are not used.

The remainder of the programme calculates the amplitude of the calculated streaming, its direction in galactic coordinates and the error on the amplitude, from the values stored in the COEFF array.

DIPSOL.FOR

```
C     A PROGRAMME TO PRODUCE DIPOLE SOLUTIONS FROM A SPECIFIED
C     GALAXY DATA FILE, WEIGHTING THE SOLUTION BY RECESSION
C     VELOCITY,PHOTOMETRY ERROR OR GIVING EACH GALAXY EQUAL
C     WEIGHTING, AS SPECIFIED.


C     FORMAT OF GALAXY DATA FILE SHOULD BE:
C     COL(1)       RUBIN FORD NUMBER
```

```
C     COL(2)      B MAGNITUDE (WITH ALL APERTURE AND EXTINCTION
C                 CORRECTIONS)
C     COL(3)      GALACTIC LATITUDE b"
C     COL(4)      GALACTIC LNGITUDE l"
C     COL(5)      INCLINATION
C     COL(6)      NEAR IR MAGNITUDE (JHK), WITH ALL APERTURE AND
C                 EXTINCTION CORRECTIONS
C     COL(7)      ERROR IN NEAR IR PHOTOMETRY
C     COL(8)      CBR-FRAME REDSHIFT

C     DECLARE REAL (DOUBLE PRECISION) AND INTEGER VARIABLES

      REAL*8 RES(100,4),A(100,4),AMEAN(4),STD(4),SSP(4,4),CORR(4,4),
     *  R(13),COEFF(3,3),RZINV(3,3),CZ(3,3),WKZ(3,3),GAL(100,10)
      INTEGER M,N,IFAIL,I
      CHARACTER*50 NAME
      CHARACTER*50 NM

C     CHOOSE RELATIVE WEIGHTING OF GALAXIES IN SOLUTIONS-1 GIVES ALL
C     GALAXIES EQUAL WEIGHTING, 2 WEIGHTS INVERSELY BY REDSHIFT, 3
C     WEIGHTS BY IR PHOTOMETRY ERROR

      WRITE(*,*)('TYPE OF SOLUTION? TYPE 1 FOR UNWEIGHTED, 2 FOR
     *  VELOCITY WEIGHTED, 3 FOR PHOTOMETRY ERROR WEIGHTING')
      READ(*,*)(K)

C     ASSIGN VALUES TO THE INTEGER VARIABLES (IFAIL IS AN ERROR
C     CHECK USED BY THE NAG ROUTINE, WHICH IS SET TO 1,2 OR 3 IF AN
C     ERROR OCCURS)

      M=4
      WRITE(*,*)('NUMBER OF GALAXIES TO BE INCLUDED IN REGRESSION?')
      READ(*,*)(N)
      IFAIL=0

C     INPUT GALAXY DATA FROM A SPECIFIED FILE

      WRITE(*,*)('NAME OF GALAXY DATA FILE')
```

```
      READ(*,'(A50)')NAME
      OPEN(UNIT=1,STATUS='OLD',FILE=NAME)
      DO 20 I=1,N
            READ(1,*)(GAL(I,J),J=1,10)
20    CONTINUE

C     READ IN MEAN HUBBLE MODULUS TO BE USED

      WRITE(*,*)('MEAN HUBBLE MODULUS TO BE USED?')
      READ*,HMBAR

C     WORK OUT PREDICTED RECESSION VELOCITIES FROM MAGNITUDES, AND
C     SUBTRACT THE MEASURED RECESSION VELOCITIES TO GIVE VELOCITY
C     RESIDUALS

      DO 25 I=1,N
            GL=GAL(I,4)
            GB=GAL(I,3)
            H=GAL(I,6)
            VR=GAL(I,8)
            EP=(H*0.2)-HMBAR
            VM=(10**EP)
            RES(I,1)=GL
            RES(I,2)=GB
            RES(I,3)=VM-VR
            RES(I,4)=VR
25    CONTINUE

C     CONVERT GALACTIC COORDINATES TO X,Y & Z COMPONENTS, AND STORE
C     IN THE NEW ARRAY A, ALONG WITH THE VELOCITY RESIDUAL DATA.
C     ALLOCATE THE WEIGHTINGS W TO THE INDIVIDUAL GALAXIES

      DO 40 I=1,N
            W=RES(I,4)
            IF (K.EQ.2) W=RES(I,4)
            IF (K.EQ.3) W=GAL(I,7)
            A(I,1)=(SIND(RES(I,1))*COSD(RES(I,2)))/W
            A(I,2)=(COSD(RES(I,1))*COSD(RES(I,2)))/W
```

```
            A(I,3)=(SIND(RES(I,2)))/W
            A(I,4)=(RES(I,3))/W
40    CONTINUE

C     CALL THE NAG ROUTINES G02BDF & G02CHF

      CALL G02BDF(N,M,A,100,AMEAN,STD,SSP,4,CORR,4,IFAIL)
      CALL G02CHF(N,M,M-1,SSP,M,CORR,M,RESULT,COEFF,M-1,RZINV,M-1,
     *  CZ,M-1,WKZ,M-1,IFAIL)


C     TEST WHETHER ROUTINE HAS RUN SUCCESSFULLY-IF NOT PRINT OUT THE
C     ERROR CODE 'IFAIL'

      IF(IFAIL.NE.0) WRITE(*,1000),IFAIL

C     CALCULATE AMPLITUDE AND DIRECTION (l" & b") OF THE CBR-FRAME
C     STREAMING FROM THE XYZ COMPONENTS PRODUCED BY G02CHF

      VSTR=((COEFF(1,1)**2)+(COEFF(2,1)**2)+(COEFF(3,1)**2))**0.5
      GLDIR=ATAND(COEFF(1,1)/COEFF(2,1))
      IF (COEFF(2,1).GT.0) GLDIR=GLDIR+180
      IF (GLDIR.LT.0) GLDIR=GLDIR+360
      BDIR=-(ASIND(COEFF(3,1)/VSTR))
      ERR1=(COEFF(1,1)*COEFF(1,2)/VSTR)**2
      ERR2=(COEFF(2,1)*COEFF(2,2)/VSTR)**2
      ERR3=(COEFF(3,1)*COEFF(3,2)/VSTR)**2
      ERRTOT=(ERR1+ERR2+ERR3)**0.5

C     WRITE OUT CBR-FRAME STREAMING AMPLITUDE, ERROR AND DIRECTION

      WRITE(*,*) (VSTR,ERRTOT,GLDIR BDIR)

      STOP

1000  FORMAT(1X,'FAILURE-IFAIL VALUE ',I2)
      STOP
      END
```

HMBAR.FOR

```
      A ROUTINE TO CALCULATE THE MEAN HUBBLE MODULUS USING THE
      METHOD OF RUBIN ET AL. (1976)

      DIMENSION A(100,10)
      CHARACTER*50 NAME
      N=86
      WRITE(*,*)('NAME OF DATA FILE?')
      READ(*,'(A50)') NAME
      OPEN(UNIT=8,STATUS='OLD',FILE=NAME)
      DO 100 I=1,N
            READ(8,*)(A(I,J),J=1,10)
100   CONTINUE
      C=0
      HM=0
      DO 200 I=1,N
            GMAG=A(I,6)
            GVEL=A(I,8)
            HM=HM+(GMAG*0.2)-(LOG10(GVEL))
            C=C+1
200   CONTINUE
      WRITE(*,300)HM/C
300   FORMAT(1X,'MEAN HM IS ',F10.5)
      STOP
      END
```

A.2 THE FORTRAN PROGRAMME USED TO SIMULATE THE SELECTION BIAS IN THE RUBIN ET AL. SAMPLE OF GALAXIES, AND TO DERIVE STREAMING VELOCITIES FROM THE SIMULATED DATA

DESCRIPTION

The following programme illustrates the changes that were made to produce the solutions to simulate selection bias as described in Chapter 3. The only significant difference from the programme described above (DIPSOL.FOR) is the routine which replaces the measured H magnitudes from the input data file HMET.DAT with randomised magnitudes constrained only by the apparent magnitude 'window' and weighted by a luminosity function. This is done by first calculating a random number from 0 to 10,000 for each of the 86 galaxies. For each galaxy, the form of the Schechter luminosity function is then calculated for the 1.4 magnitudes which lie within the selection window appropriate for the redshift of the galaxy. The relative probability of a galaxy in each 0.05 magnitude slice of the window is then calculated from the amplitude of the Schechter function, with the total in the whole window normalised to 10,000. One of these absolute magnitude slices is then chosen for the galaxy, from the random number it was allocated earlier. This is repeated for all 86 galaxies. The absolute magnitudes are then converted to apparent magnitudes and saved in a galaxy data array, and streaming motion solutions carried out exactly as for the real observational data.

```
      PROGRAM  MALMSOL

C     PROGRAMME TO MAKE SIMULATED DATA FILES WITH RANDOMISED
C     MAGNITUDES, USING THE RUBIN-FORD SPATIAL DISTRIBUTION AND A
C     SCHECHTER LUMINOSITY FUNCTION, AND DOING A 'MEAN HM' TYPE
C     VELOCITY SOLUTION FOR EACH

      REAL*8 GAL(100,10),IRAN (10000),INUM(100),RES(100,4),A(100,4)
      REAL*8 AMEAN(4),STD(4),SSP(4,4),CORR(4,4),R(13),COEFF(3,3),
     *  RZINV(3,3)
      REAL*8 CZ(3,3),WKZ(3,3),VSOL(4)
      INTEGER M,N,NSOL,IFAIL,NSTART,IBIG,ISEED

      N=86
```

```
C     INPUT BASIC GALAXY DATA FROM HMET.DAT.  THE H PHOTOMETRY WILL
C     SUBSEQUENTLY BE REPLACED BY SIMULATED MAGNITUDES

      OPEN(UNIT=1,STATUS='OLD',FILE='HMET.DAT')
      DO 20 I=1,N
            READ(1,*)(GAL(I,J),J=1,10)
20    CONTINUE


C     REPLACE H MAGNITUDES IN THE GALAXY DATA FILE WITH RANDOM
C     MAGNITUDES.  FIRST CALCULATE 86 RANDOM NUMBERS BETWEEN 0 AND
C     10000

      WRITE(*,*)('STARTING NUMBER FOR RANDOM NUMBER SEQUENCE')
      READ(*,*)(NSTART)
      IBIG=16384
      ISEED=15625
      NEW=ISEED
      DO 25 I=1,N+NSTART
            NEW=NEW*ISEED
            NEW=MOD(NEW,16384)
            IF(NEW.LT.0)NEW=IBIG+NEW
            IF(I.GT.NSTART)IRAND(I-NSTART)=1+(NEW*10000/16383)
25    CONTINUE

C     USE SCHECHTER FUNCTION TO CALCULATE THE NUMBER OF GALAXIES IN
C     EACH 0.05 MAGNITUDE SLICE OF THE 1.4 MAG SELECTION WINDOW FOR
C     THE REDSHIFT OF EACH GALAXY- H0 = 50 THROUGHOUT


            DO 30 I=1,N
                  WINL=-3.105-(5*LOG10(GAL(I,8)))
                  GNTOT=0
                  DO 35 J=1,29
                        GMAG=WINL+((J-1)*0.05)
                        GNUMA=10000*((10**(-0.4*(GMAG+20.6)))**1.26)
                        GNUMB=EXP(-(10**(-0.4*(GMAG+20.6))))
                        INUM(J)=GNUMA*GNUMB
```

```
                    GNTOT=GNTOT+INUM(J)
35              CONTINUE

C     FIND WHICH SLICE OF THE 1.4 MAG WINDOW THE NTH RANDOM NUMBER
C     CORRESPONDS TO, AND ALLOCATE AN ABSOLUTE MAGNITUDE TO THE NTH
C     GALAXY ACCORDINGLY

                IRAND(I)=IRAND(I)*GNTOT/10000
                ISLICE=1
                IRUN=0
                DO 50 J=1,29
                      IRUN=IRUN+INUM(J)
                      IF(IRUN.LT.IRAND(I)) ISLICE=ISLICE+1
50              CONTINUE
                BABS=WINL+(0.05*ISLICE)
                GAL(I,6)=BABS+(5*LOG10(GAL(I,8)))+16.505
30          CONTINUE

C     CALCULATE THE MEAN HUBBLE MODULUS FOR THE 86 GALAXIES

            HM=0
            DO 200 I=1,N
                  GMAG=GAL(I,6)
                  GVEL=GAL(I,8)
                  HM=HM+(GMAG*0.2)-(LOG10(GVEL))
200         CONTINUE
            HMBAR=HM/N

C     PRODUCE DIPOLE SOLUTIONS FROM FILE JUST ALTERED,
C     WEIGHTING THE SOLUTION BY RECESSION VELOCITY
C
C     FIRST ASSIGN VALUES TO THE INTEGER VARIABLES

            M=4
            IFAIL=0
```

```
C     WORK OUT PREDICTED RECESSION VELOCITIES FROM MAGNITUDES, AND
C     SUBTRACT THE MEASURED RECESSION VELOCITIES TO GIVE VELOCITY
C     RESIDUALS

            DO 250 I=1,N
                  GL=GAL(I,4)
                  GB=GAL(I,3)
                  H=GAL(I,6)
                  VR=GAL(I,8)
                  EP=(H*0.2)-HMBAR
                  VM=(10**EP)
                  RES(I,1)=GL
                  RES(I,2)=GB
                  RES(I,3)=VM-VR
                  RES(I,4)=VR
250         CONTINUE


C     CONVERT GALACTIC COORDINATES TO X,Y & Z COMPONENTS, AND STORE
C     IN THE NEW ARRAY A, ALONG WITH THE UNCHANGED VELOCITY RESIDUAL
C     DATA.

            DO 400 I=1,N
                  W=RES(I,4)
                  A(I,1)=(SIND(RES(I,1))*COSD(RES(I,2)))/W
                  A(I,2)=(COSD(RES(I,1))*COSD(RES(I,2)))/W
                  A(I,3)=(SIND(RES(I,2)))/W
                  A(I,4)=(RES(I,3))/W
400         CONTINUE

C     CALL THE NAG ROUTINES

            CALL G02BDF(N,M,A,100,AMEAN,STD,SSP,4,CORR,4,IFAIL)
            CALL G02CHF(N,M,M-1,SSP,M,CORR,M,RESULT,COEFF,
     *      M-1,RZINV,M-1, CZ,M-1,WKZ,M-1,IFAIL)


C     TEST WHETHER ROUTINE HAS RUN SUCCESSFULLY. IF SO PRINT OUT
```

```
C     RESULTS, OTHERWISE PRINT OUT THE ERROR CODE 'IFAIL'

            IF(IFAIL.NE.0) GO TO 2000

C     CALCULATE STREAMING VELOCITY AND DIRECTION, AND ERRORS

      VSTR=((COEFF(1,1)**2)+(COEFF(2,1)**2)+(COEFF(3,1)**2))**0.5
            GLDIR=ATAND(COEFF(1,1)/COEFF(2,1))
            IF (COEFF(2,1).GT.0) GLDIR=GLDIR+180
            IF (GLDIR.LT.0) GLDIR=GLDIR+360
            BDIR=-(ASIND(COEFF(3,1)/VSTR))
            ERR1=(COEFF(1,1)*COEFF(1,2)/VSTR)**2
            ERR2=(COEFF(2,1)*COEFF(2,2)/VSTR)**2
            ERR3=(COEFF(3,1)*COEFF(3,2)/VSTR)**2
            ERRTOT=(ERR1+ERR2+ERR3)**0.5
            VSOL(1)=VSTR
            VSOL(2)=ERRTOT
            VSOL(3)=GLDIR
            VSOL(4)=BDIR

C     WRITE OUT SOLUTIONS: AMPLITUDE, ERROR ON AMPLITUDE AND
C     DIRECTION

      WRITE(*,*)(VSOL(I),I=1,4)
      STOP

2000  WRITE(*,2500),IFAIL
2500  FORMAT(1X,'FAILURE-IFAIL VALUE ',I2)
      STOP
      END
```

PUBLICATIONS

The following research papers, to which I have contributed, are enclosed:

James, P.A., Joseph, R.D. & Collins, C.A., 1987. "Large-Scale Streaming Motions from First-Ranked Cluster Ellipticals," in 13th Texas Symposium on Relativistic Astrophysics, ed. Ulmer, M.P., p. 256, Singapore, World Scientific.

Wright, G.S., Joseph, R.D., James, P.A. & Robertson, N.A., 1987. "Evidence for Extended IR Emission in NGC 2798 and NGC 6240,"in Star Formation in Galaxies, ed. C.J. Lonsdale Persson, p. 707, NASA Conference Publication 2466, Washington, D.C.

James, P.A., Joseph, R.D. & Collins, C.A., 1987. "Large-Scale Streaming of Cluster Elliptical Galaxies," Mon. Not. R. astr. Soc., 229, 53.

Wright, G.S., Joseph, R.D., Robertson, N.A., James, P.A. & Meikle, W.P.S., 1988. "Recent Star Formation in Interacting Galaxies--III. Evidence from Mid-Infrared Photometry," Mon. Not. R. astr. Soc., 233, 1.

Joseph, R.D., Wright, G.S., James, P.A. & McLean, I.S., 1988. "Do Markarian Double Nucleus Galaxies Really Have Two Nuclei?", Mon. Not. R. astr. Soc., 232, 7P.

LARGE-SCALE STREAMING MOTIONS FROM FIRST-RANKED CLUSTER ELLIPTICALS

P. A. James, R. D. Joseph,
Blackett Laboratory, Imperial College, London SW7, England
C. A. Collins,
Astronomy Dept, University of Edinburgh, Edinburgh EH9 3HJ, Scotland

One of the most important constraints on cosmological models, and the cold dark matter model in particular, is the amplitude of the streaming motions of galaxies over scales of order 50-100 h^{-1} Mpc.[1,2] We have derived a new result in this field by using the V magnitudes and redshifts of first-ranked cluster ellipticals presented by Sandage and Hardy.[3] These galaxies are excellent standard candles, having a dispersion of only 0.3 in absolute magnitude. This dispersion permits us to infer galaxy distances to an accuracy of 14%, independently of their measured recession velocities. Thus they are excellent tracers of possible deviations from pure Hubble flow.

We have used this dataset to solve for that relative motion between the galaxy sample and the Local Group (LG) which minimises, in a least squares sense, the differences between distances inferred from apparent magnitudes, and those inferred from the redshifts. We restrict the solutions to one dipole, in the direction of the LG motion relative to the 2.8 K cosmic background radiation (CBR), since the sky coverage is incomplete in other directions. This is the direction in which an anisotropy in the Hubble flow about the LG would be expected to be most evident, were the galaxies at rest in the CBR frame. We have used the 60 galaxies in the Sandage & Hardy sample with redshifts <15,000 km/sec giving a mean effective redshift for the sample of 5400 km/sec.

We obtain a value for the velocity of the LG relative to the sample of -1 km/sec ± 105 km/sec. The error is the formal statistical error on the solutions, and was checked by doing a large number of resampling solutions with 25% of the points omitted at random from the minimisation procedure. Since the LG is moving relative to the CBR at 610 km/sec ± 50 km/sec, our solution provides evidence for a motion of the galaxy sample relative to the CBR with a component of magnitude 610 km/sec ± 116 km/sec along the direction $\ell = 272°$, $b = 30°$.

This result disagrees with that of Aaronson et al.[4], the only study of the large-scale velocity field to date which has found a galaxy sample to be essentially at rest in the CBR frame. However, these solutions using first-ranked cluster ellipticals are in good agreement with the conclusions of Collins et al.[1] and Dressler et al.[2], thus confirming the reality of streaming over scales of 50-100 h^{-1} Mpc.

REFERENCES

1. Collins, C., Joseph, R., and Robertson, N., Nature 320, 506 (1986).
2. Dressler, A., Faber, S., Burstein, D., Davies, R., Lynden-Bell, D., Terlevich, R., and Wegner, G. Preprint (1987).
3. Sandage, A., and Hardy, E., Ap.J. 183, 743 (1973).
4. Aaronson, M., Bothun, G., Mould, J., Huchra, J., Schommer, R. and Cornell, M., Ap.J. 302, 536 (1986).

EVIDENCE FOR EXTENDED IR EMISSION IN NGC2798 AND NGC6240

G. S. Wright[1] R. D. Joseph P. A. James and N. A. Robertson[2]
Blackett Laboratory, Imperial College,
London SW7 2BZ

(1) now at Royal Observatory, Blackford Hill, Edinburgh EH9 3HJ
(2) now at Department of Natural Philosophy, University of Glasgow, Glasgow G12 8QQ

ABSTRACT

Extended emission at 10 and 20 μm can be used to distinguish starbursts from "monsters" as the underlying energy source driving the luminous infrared emission in the central regions of galaxies. We have investigated the spatial extent of the mid-infrared emission in the interacting galaxy NCG2798 and the merger NGC6240. The 10 and 20 μm profiles of the IR source in NGC2798 are significantly wider than beam profiles measured on a standard star, supporting a starburst interpretation of its IR luminosity. For NGC6240 there is marginal evidence for an extended 10 μm source, suggesting that a significant fraction of its IR luminosity could be produced by a burst of star formation.

I. INTRODUCTION

One of the outstanding questions in extra-galactic IR astronomy is the nature of the underlying energy source powering the large IR luminosities found for many interacting galaxies.

Evidence is emerging that bursts of star formation of exceptional intensity compared to normal spirals and canonical "starburst" galaxies are responsible for the IR activity in interacting galaxies (cf. Joseph et al. 1984, Lonsdale et al. 1984, Cutri and McAlary 1985). Moreover, the subset of interacting galaxies in which a merger of the two participating galaxies has occurred are among the most luminous IR galaxies known (Joseph and Wright 1985) and it appears that the merger has resulted in a "super-starburst". However, this interpretation is open to debate because the interaction may provide the material to feed an accretion disk around a collapsed object in the nucleus. This "starbursts and monsters" debate (cf. Heckman et al. 1983) is especially controversial for the ultra-luminous merging galaxies such as NGC6240 and Arp220, although it applies to all the IRAS galaxies to some degree.

Potentially one of strongest arguments in favour of a starburst interpretation is spatially extended mid-IR emission. For a single central source heating a dust cloud, the dust can be heated sufficiently to radiate at 10 μm only if it is within a few pc of the source. So, measuring the extent of the IR emission discriminates between a compact source heating a dust cloud and luminosity sources distributed over several hundred pc, the latter being expected if the underlying energy source is a burst of star formation.

II. OBSERVATIONS

Observations of the interacting galaxy NGC2798, for which $L_{IR} \sim 6 \times 10^{10}$ L$_\odot$, and the merger NGC6240 which has $L_{IR} \sim 10^{12}$ L$_\odot$, were made at UKIRT in February 1986. N-S and E-W profiles of the IR sources were made by obtaining photometry on the optical

nucleus of the galaxy and then moving off the central pixel 0.75 arcsec at a time, using the UKIRT TV crosshead to obtain as accurate an offset as possible. To minimise systematic effects, such as drifts, each step out from the central pixel was made first to one side and then to the other. Observations of a nearby standard star were obtained using exactly the same method, so any residual systematic effects should be the same for both the galaxy and the star observations. A chopper throw of ~ 30 arcsec perpendicular to the offset direction was used for all the observations.

III. RESULTS

Profiles of NGC2798 in a N-S direction were obtained at both 10 and 20 μm and in an E-W direction at 10 μm. NGC6240 was observed with offsetting in a N-S direction at 10 μm. Figure 1 shows the profiles of the galaxies compared to the profiles of a nearby standard star. The position marked (0,0) is the position of the optical nucleus. The horizontal error bars are an estimate of the pointing error relative to the (0,0) position, based on the degree of consistency of the standard star profiles and the ease of guiding on the TV. The profile of the standard star has been scaled to give the best fit to the peak flux, and centred to produce the best alignment of the profiles. It is evident from these figures that the data for the galaxies indicate a wider profile than the beam profiles measured on a standard star. To estimate the significance of the difference between the galaxy profile and that of the star, we have calculated the significance with which each point lies outside the beam profile by comparing the point to profile distance with the error ellipse. The overall significance of the evidence for spatial extent is obtained by summing in quadrature the significances of each point. The significance levels of the spatial extents indicated in the galaxy profiles are given in Table I.

Table I

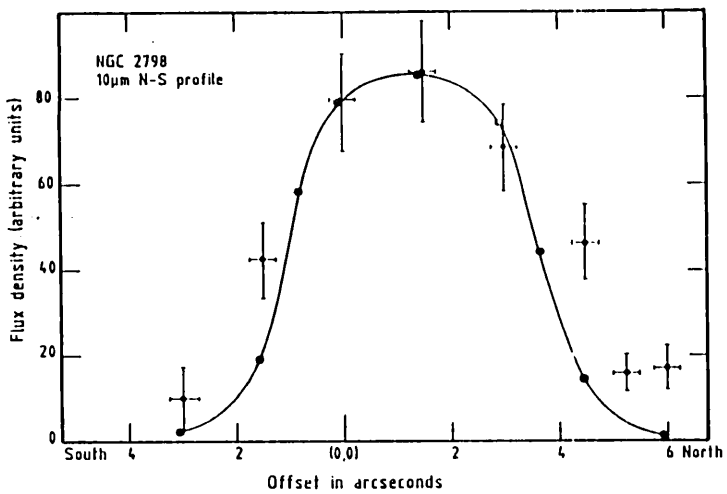
The significance of the difference between the galaxy and standard star profiles

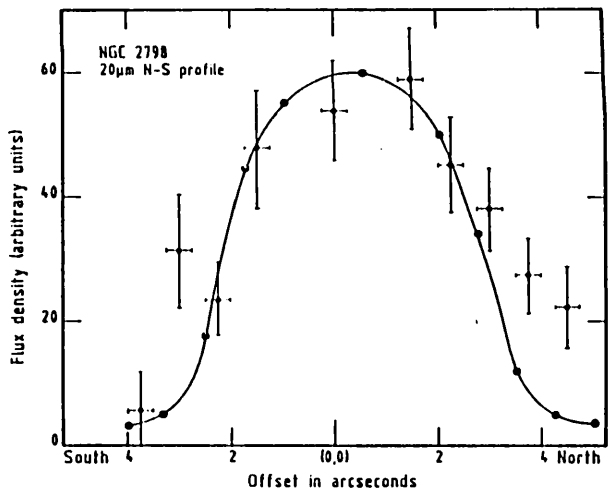
NGC2798 20 μm N-S	NGC2798 10 μm N-S	NGC2798 10 μm E-W	NGC6240 10 μm N-S
4.5 σ	4.5 σ	3 σ	3 σ

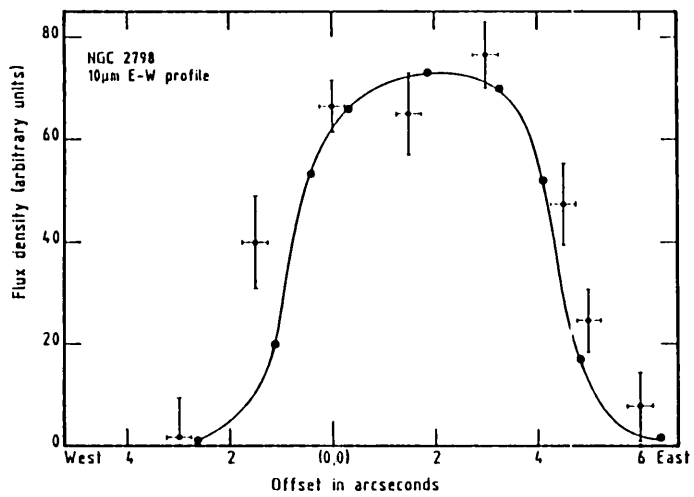
We have also explored the likely size of the sources, by convolving the beam profile with a top hat function of variable width and adjusting the width of the top hat, the scaling of the profile and its alignment to obtain the best fit to the data points. This gives a source size of approximately 4 arcsec for all the profiles.

IV. DISCUSSION

For NGC2798 there is good evidence for extent at both 10 and 20 μm, and this is consistent with our multi-aperture photometry at 10 μm. We find a flux of 190 ± 18 mJy in a 5 arcsec beam and 520 ± 105 mJy in an 8 arcsec beam. The IRAS data (770 and 3130 mJy at 12 and 25 μm respectively) when compared with our 10 and 20 μm data are also consistent with a spatially extended IR source. Non-equilibrium heating of small dust grains by a compact underlying energy surce is unlikely to be producing this extended emission because there is extent at 20 μm, where such grains would radiate less effectively, on a similar scale to the 10 μm emission. The spatial extent inferred for the source, ~ 4







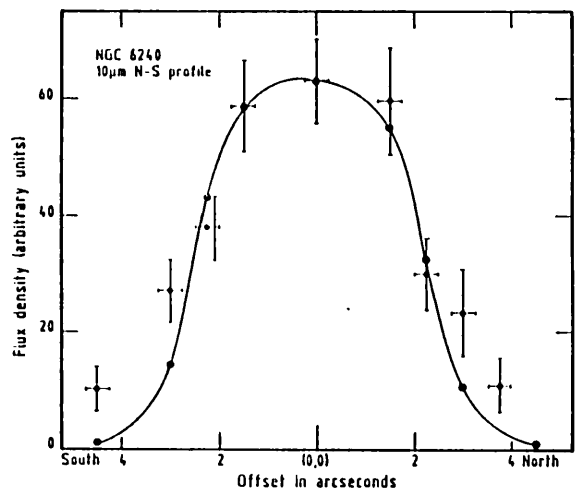


Figure 1. Profiles of the galaxies NGC2798 and NGC6240 compared with those obtained on a nearby standard star. The position marked (0,0) is the position of the optical nucleus.

arcsec, corresponds to 660 pc in NGC2798. This is much larger than the ~ 1 pc source size expected if the dust is heated by a single nuclear source. A burst of star formation is thus the most natural interpretation of the IRAS luminosity of NGC2798. The results for NGC6240 are more marginal than those for NGC2798. Nevertheless they indicate that for this ultra-luminous IR galaxy the nuclear source may be extended. This suggests that a massive burst of star formation could be the underlying energy source for a significant fraction of the enormous IR luminosity of this galaxy.

V. CONCLUSIONS

The data presented provide good evidence for spatially extended 10 and 20 μm emission in NGC2798 supporting a starburst interpretation for the 6 x 10^{10} $L_\odot$ IR luminosity of this interacting galaxy.

For NGC6240 there is marginal evidence (~ 3 σ) for an extended 10 μm source. This suggests that this ultra-luminous IR galaxy may indeed be the result of a super starburst, a conclusion which would be strengthened by the detection of extended 20 μm emission.

REFERENCES

Cutri, R.M. and McAlary, C.W. 1985, *Ap.J.*, 296, 90.
Heckman, T.M., van Breugel, W., Miley, G.K., and Butcher, H.R. 1985, *A.J.*, 88, 1077.
Joseph, R.D., Meikle, W.P.S., Robertson, N.A., and Wright, G.S. 1984, *M.N.R.A.S.*, 209, 111.
Joseph R.D. and Wright, G.S. 1985, *M.N.R.A.S*, 214, 87.
Lonsdale, C.J., Persson, S.E. and Matthews, K. 1984, *Ap.J*, 287, 95.

Mon. Not. R. astr. Soc. (1987) **229**, 53–59

Large-scale streaming of cluster elliptical galaxies

P. A. James and R. D. Joseph *Astrophysics Group, Blackett Laboratory, Imperial College, London SW7 2BZ*

C. A. Collins *Department of Astronomy, University of Edinburgh, Edinburgh EH9 3HJ, Scotland*

Accepted 1987 May 27. Received 1987 May 27; in original form 1987 February 13

Summary. We have investigated large-scale deviations from isotropic Hubble flow using first-ranked cluster elliptical galaxies. The sky coverage of the sample used precludes a general solution for a dipole anisotropy, but it is well suited to investigation of the component of any motion of these galaxies along a direction defined by the dipole anisotropy in the 2.7 K cosmic background radiation. We find the cluster ellipticals to have a velocity component along this direction of $\sim 600\,\mathrm{km\,s^{-1}}$. This result is consistent with the large-scale streaming found in our re-investigation of the Rubin *et al.* spiral galaxies in the infrared (Collins, Joseph & Robertson), and that found for a different sample of elliptical galaxies by Dressler *et al.* However, we do not confirm the recent result of Aaronson *et al.*, who found a Local Group motion consistent with their sample of 10 clusters being at rest with respect to the cosmic background radiation.

1 Introduction

Recent observations of two all-sky samples of galaxies have provided evidence for systematic large-scale deviations from isotropic Hubble flow. The first of these was the preliminary report of our re-investigation of the Rubin *et al.* (1976) sample of spiral galaxies using infrared techniques (Collins, Joseph & Robertson 1986). The application of infrared Tully–Fisher and optical–infrared colour–magnitude luminosity indicators confirms the 'Rubin–Ford effect', i.e. an apparent Local Group motion, relative to this all-sky galaxy sample, which is approximately orthogonal to the velocity inferred from the dipole anisotropy in the 2.7 K cosmic background radiation (CBR). We interpreted this result in terms of a systematic streaming velocity of these galaxies of $\sim 970\,\mathrm{km\,s^{-1}}$. Since the mean redshift of the sample is $5100\,\mathrm{km\,s^{-1}}$, this streaming is on a spatial scale of $\sim 100\,h^{-1}\,\mathrm{Mpc}$ (where the Hubble constant is $100\,h\,\mathrm{km\,s^{-1}\,Mpc^{-1}}$). A sample of elliptical galaxies of mean redshift $3000\,\mathrm{km\,s^{-1}}$ observed by Dressler *et al.* (1987) shows a similar streaming of $\sim 600\,\mathrm{km\,s^{-1}}$.

In contrast, a study by Aaronson *et al.* (1986) of the spirals in 10 clusters well outside the Local Supercluster, at redshifts of 4000 to 11 000 $\mathrm{km\,s^{-1}}$, directly contradicts these results. Aaronson *et*

al. find a Local Group motion with respect to these clusters in good agreement, in magnitude and direction, with the Local Group motion relative to the CBR. Thus the Aaronson *et al.* study indicates that these 10 clusters have no streaming component along this direction.

The confirmation of coherent streaming motions as large as ~700 km s^{-1} on scales of $>60h^{-1}$ Mpc would have profound implications for models of the origin of large-scale structure in the Universe. In particular, the cold dark matter models currently in vogue (*cf.* Blumenthal *et al.* 1984) do not produce streaming velocities this large (White *et al.* 1987). Thus it is of paramount importance to resolve the inconsistencies between these studies.

One sample of galaxies in the literature which is well suited to investigation of putative deviations from isotropic Hubble flow is the sample of first-ranked cluster ellipticals used by Sandage and coworkers in their efforts to determine the value of the deceleration parameter, q_0. The advantage of using first-ranked cluster ellipticals is that they belong to the high luminosity tip of the elliptical luminosity function, and therefore they should be excellent standard candles (with appropriate corrections for Bautz–Morgan and richness class). The sample we have used is selected from that given by Sandage & Hardy (1973). They find this sample to have an rms dispersion in absolute magnitude of 0.3, which implies an uncertainty in distance of only 14 per cent per galaxy. By comparison, the infrared distance indicators used by Collins *et al.* (1986) and Aaronson *et al.* (1986) have dispersions which give uncertainties in distance of ~20 per cent, and the distance indicator used by Dressler *et al.* (1987) has a precision of ~25 per cent per galaxy. Thus the first-ranked cluster ellipticals are indeed good standard candles.

2 Data analysis

The data used are the V-band photometry and redshifts of first-ranked cluster ellipticals listed in table 1 of Sandage & Hardy (1973). We have selected those galaxies with recession velocities $<15\,000$ km s^{-1}. This provides a sample of 60 galaxies, with mean redshift of 7600 km s^{-1}, of which 15 are members of Humason, Mayall, and Sandage groups. The velocities quoted by Sandage & Hardy are relative to the centre of the Local Group (based on a correction of 300 km s^{-1} toward $l=90°$, $b=0°$). Sandage & Hardy also corrected the V magnitudes for galactic extinction, aperture effects and K-dimming, as well as Bautz–Morgan and richness class. The apparent magnitudes are sufficiently bright, $m_V<15$, that we do not expect the Scott effect (Scott 1957) to be significant.

Unfortunately this sample of cluster ellipticals does not have good all-sky coverage, as shown in Fig. 1. This precludes carrying out a general solution to find the Local Group motion relative to this galaxy sample. However, the galaxies are well-distributed in both the apex and antapex directions of the CBR dipole vector. Thus they are an excellent sample with which to compare the Aaronson *et al.* (1986) solution, i.e. a Local Group motion approximately along the CBR dipole vector. Moreover, since these galaxies are by definition all members of clusters, they are a particularly appropriate sample with which to compare the Aaronson *et al.* (1986) cluster result.

We have used the type of analysis pioneered by Rubin *et al.* (1976). In this approach, one determines the motion of the Local Group relative to a mean Hubble flow defined by the sample of galaxies under study. This is done by calculating the Hubble Modulus, HM, from the measured magnitudes and redshifts for each galaxy, where

$$\mathrm{HM}=\log v_{\mathrm{obs}}-0.2m. \tag{1}$$

The mean Hubble Modulus for the whole sample should equal

$$\langle \mathrm{HM}\rangle=\log H_0-0.2M-5, \tag{2}$$

where M is the absolute magnitude of the standard candles comprising the sample. This essentially sets the Hubble flow for the sample, overcoming the need to know explicitly the Hubble constant and the absolute magnitude of the standard candles used. Recession velocities can be predicted for each galaxy, assuming isotropic Hubble flow, from:

$$v_{\mathrm{H}}=10^{(0.2m+\langle \mathrm{HM}\rangle)} \tag{3}$$

We then calculate velocity residuals, $v_{\mathrm{obs}}-v_{\mathrm{H}}$. As in previous work, an attempt is made to fit these velocity residuals (which are effectively peculiar motions of galaxies relative to the mean flow) with a dipole term, as would be found if there were motion of the Local Group relative to the galaxy sample.

The solution was found by performing a minimization of the quantity:

$$\chi^2=\sum_i \left\{\frac{[v_{\mathrm{H}}(i)-v_{\mathrm{obs}}(i)]-v_{\mathrm{LG}}\cos\theta(i)}{\sigma(i)}\right\}^2, \tag{4}$$

where $v_{\mathrm{H}}(i)$ is the recession velocity of the ith galaxy, calculated from equation (3); $v_{\mathrm{obs}}(i)$ is the measured recession velocity of the ith galaxy; $\theta(i)$ is the angle between the line-of-sight to the ith galaxy and the CBR apex direction, $l=272°$, $b=30°$; $\sigma(i)$, the weighting given to the ith galaxy, is the error in $v_{\mathrm{H}}(i)$.

Minimization of χ^2 solves for v_{LG}, the component of the motion of the Local Group relative to the sample of galaxies. Each point in the summation is given a weighting inversely proportional to its measured recession velocity. This weighting is based on the assumption that the error is dominated by magnitude errors which are the same for all galaxies, giving a fractional error in v_{H} that is proportional to the distance of the galaxy. This weighting reduces the effective redshift of the sample to 5400 km s^{-1}. Solutions were also obtained in which all points had equal weighting.

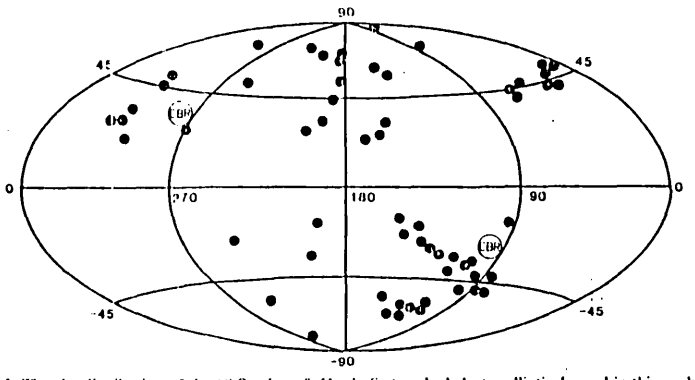


Figure 1. The sky distribution of the 60 Sandage & Hardy first ranked cluster ellipticals used in this analysis, in galactic coordinates. The apex and antapex directions of the CBR dipole are indicated.

3 Results

In Table 1 we present a variety of solutions for v_{LG}, the component of the Local Group motion relative to the galaxy sample. Columns 2 and 3 give the minimum and maximum redshift for the subsample used, column 4 gives the weighting used in the solution, and column 5 lists the effective redshift for this weighting. The number of galaxies in each subsample is given in column 6. The

component of Local Group motion along the CBR dipole, relative to the whole sample of 60 galaxies, is -1 ± 105 km s^{-1} (line 1 in Table 1). The error is the formal statistical error in the minimization procedure, under the assumption of normally distributed errors in the velocity residuals. Since this assumption may be false, we have done repeated solutions with a constant fraction of the galaxies omitted at random. These solutions have a scatter of approximately 100 km s^{-1}, consistent with the above estimate. Thus any non-Gaussian component in the errors must be small.

A lower limit to the expected error in the solution can be derived from the individual errors arising from the dispersion of the luminosity indicator. For a sample of 60 galaxies with a mean redshift of 5500 km s^{-1} and fractional error in velocity per galaxy of 14 per cent, the expected error is $\sim$100 km s^{-1}. Thus, the errors found above are indeed reasonable. This is confirmed by the reduced chi-square $\chi^2=47/58$, indicating that the solution we calculate is a reasonable fit to the data points under the assumed errors.

We have carried out several other solutions using the same data set. Table 1 lists the most important of these, and illustrates the essential robustness of the main result presented above.

Table 1. Solutions for v_{LG} discussed in the text.

Solution	cz (min) (km s^{-1})	cz (max) (km s^{-1})	Weighting	cz (eff) (km s^{-1})	N	v_{LG} (km s^{-1})
1	0	15000	Redshift	5400	60	-1 ± 105
2	0	7500	Redshift	3800	31	-10 ± 100
3	0	15000	Equal	7600	60	-295 ± 220
4*	0	15000	Redshift	5800	59	90 ± 125
5	2600	15000	Redshift	6800	55	-37 ± 140
6†	0	15000	Redshift	5400	60	49 ± 135

*Virgo cluster omitted from solution.
†Solutions using magnitudes not corrected for cluster richness and Bautz–Morgan class.

Reducing the outer redshift limit to 7500 km s^{-1} (line 2) does not change v_{LG} significantly, and unweighted solutions such as that in line 3, while noisier, are still consistent with our weighted solutions to within $\sim1\sigma$. We are not unduly affected by the presence of nearby clusters, as indicated by the effect of excluding Virgo (solution 4), which is the most influential cluster. Excluding all the clusters within $cz<2600$ km s^{-1}, to minimize the effects of the Local Supercluster, does not change the result significantly (solution 5).

Solution 6 given in Table 1 was carried out to check the effect of the Sandage & Hardy richness and Bautz–Morgan class corrections on our solutions. For this solution we used galaxy magnitudes which were not corrected for Bautz–Morgan and richness classes. Since the effect of these corrections is to reduce the scatter about the mean Hubble line for these galaxies, they will tend to reduce galaxy peculiar velocities and could therefore tend to force the result we actually find, zero streaming of galaxies relative to the Local Group. Such an effect will however be weakened by the fact that the corrections are defined on an all-sky basis and thus should not have a very marked effect on anisotropies correlated with position around the sky. We confirm that this is the case, since solution 6 is not significantly different from the other solutions.

4 Interpretation as evidence for streaming motions

If the galaxy sample were at rest with respect to the CBR, we should have detected a Local Group motion equal to that inferred from the amplitude of the dipole variation in the CBR temperature

around the sky. We adopt a best value for the Local Group motion relative to the CBR of 610 ± 50 km s^{-1} (Lubin & Villela 1986), a well determined value that would be large enough to give an easily detectable Local Group motion. Clearly we do not find this. We therefore interpret this result as evidence for a net motion of the galaxies with respect to the CBR, which gives the velocity component of the cluster ellipticals along the CBR dipole axis of 610 ± 116 km s^{-1}.

We have investigated whether Malmquist bias could be responsible for this apparent motion by comparing the redshift distribution of galaxies in the apex and antapex directions along our chosen axis. There is indeed an anisotropy, which could lead to a systematic bias if there were apparent magnitude selection criteria used in defining this sample. However, the mean redshift in the apex direction, 6500 km s^{-1}, is smaller than that in the antapex direction, 8100 km s^{-1}, which should tend to produce an apparent motion relative to the CBR frame in the *opposite* sense to that which we measure. In any case, we would not expect significant Malmquist bias for this sample, which is selected on the basis of cluster membership, rather than solely in terms of apparent magnitude. This is confirmed by the Hubble diagram presented by Sandage & Hardy (1973), which appears highly linear and extends to a considerably greater depth than the subset of galaxies we use.

5 Discussion

The interpretation given above is that there is a net motion of the clusters themselves of $\sim610\pm116$ km s^{-1} in the direction of the CBR dipole anisotropy. The effective depth of this sample, for the weighting described in Section 3, is $54\,h^{-1}$ Mpc, which makes it one of the most distant galaxy samples that has been used for anisotropy studies. As indicated in the Introduction, the two earlier studies of the Hubble flow on comparable scales are those of Collins *et al.* (1986) and Aaronson *et al.* (1986).

Aaronson *et al.* (1986) examined the velocity residuals of 10 clusters in the redshift range $4000<cz<11\,000$ km s^{-1}, giving an effective depth of $\sim60\,h^{-1}$ Mpc. They reduced the error in the distance modulus to each cluster to $\sim$6 per cent by obtaining photometry on 10–20 galaxies in each cluster, giving them very accurately measured velocity residuals. Fitting a velocity dipole to these velocity residuals, Aaronson *et al.* found a v_{LG} of 780 ± 188 km s^{-1} towards $l=255°$, $b=18°$, a result which is consistent with these clusters being at rest with respect to the CBR. The velocity difference between the Aaronson solution, projected along the CBR dipole axis, and our cluster result is 735 ± 215 km s^{-1}. This difference is statistically significant at 3.4σ.

The reason for the discrepancy between our result and that of Aaronson *et al.* (1986) is unclear. Both studies are sampling clusters in a similar redshift range. Since there are only eight clusters in common and the error on the distance modulus for any one cluster elliptical is typically ~1000 km s^{-1}, a statistical comparison between these eight clusters is not useful. Perhaps the most significant difference between the two studies is the number of clusters used in the analysis. If, for example, there are cluster peculiar velocities as large as the 1000–2000 km s^{-1} found by Bahcall, Soneira & Burgett (1986), averaging over a large number of clusters should reduce such peculiar velocities and provide a more reliable estimate of any underlying net streaming velocity.

Collins *et al.* (1986) argued that their infrared measurements, and use of a third variable as a luminosity indicator, confirmed the 'Rubin–Ford effect'. They then interpreted it in terms of large-scale streaming, relative to the CBR, of ~970 km s^{-1} towards $l=305°$, $b=45°$. The component of this velocity in the direction of the CBR dipole anisotropy is ~790 km s^{-1}. This is in good agreement, within the errors, with the component of the streaming motion found for the first-ranked elliptical sample. These two galaxy samples are completely independent and probe very different environmental regions of the Universe. This makes the consistency of the results even more striking and difficult to explain in terms of intrinsic variations in the properties of galaxies

158

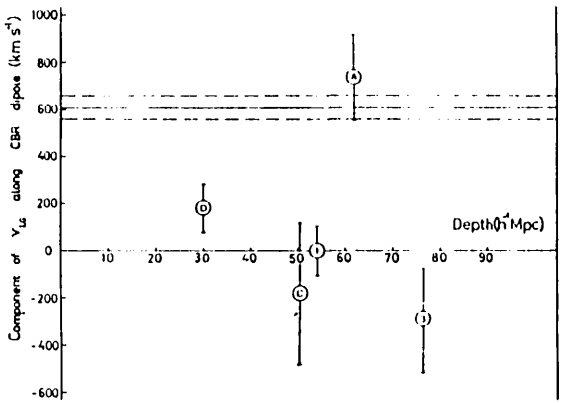


Figure 2. A comparison of the component of the Local Group motion relative to various galaxy samples, along the direction $l=272°$, $b=30°$. The characteristic depth of each galaxy sample used is plotted along the horizontal axis, and the velocity of the Local Group relative to the CBR, with the 1σ errors, is indicated by the line at the top of the diagram. Points are labelled to indicate the studies by (A) Aaronson *et al.* (1986); (C) Collins *et al.* (1986); (D) Dressler *et al.* (1987); and solutions 1 and 3 from this study, (1) and (3).

across the sky. The most plausible interpretation is that rich clusters of galaxies also participate in the bulk flow that has been reported for spiral galaxies on similar spatial scales.

Dressler *et al.* (1987) find a streaming motion of 600 ± 104 km s^{-1} towards $l=312°$, $b=6°$, for ~300 elliptical galaxies with a mean effective redshift of ~3000 km s^{-1}. This means that these ellipticals must have a velocity component along the direction of the CBR dipole of ~430 km s^{-1}. Thus this sample gives a streaming result in agreement within ~1σ with those for the two larger-scale galaxy samples.

Fig. 2 illustrates the component of LG motion determined in these studies and the present work, plotted against the scale of the galaxy sample used. The general agreement between the cluster ellipticals result and those of Collins *et al.* (1986) and Dressler *et al.* (1987) is clear; the Aaronson *et al.* (1986) result alone is discrepant.

The confirmation of streaming on scales of order $100h^{-1}$ Mpc has important consequences for present ideas on the formation of large-scale structure, and in particular for the nature of the dark matter component which seems to dominate the mass density. For example, it is difficult to produce such large coherent motions on these scales in the currently popular models in which the mass density is dominated by a cold dark matter component. This difficulty is one of two problems facing the 'standard' cold matter scenario for the formation of large-scale structure. The other is the large cluster–cluster correlation length compared to that observed for galaxies. In both cases the fundamental problem for cold dark matter is that the predicted coherence length for the matter at the present epoch gives rise to insufficient large-scale power (Dekel & Rees 1987). This suggests that investigation of alternative models, perhaps involving particles with larger damping scales (such as massive neutrinos), or models which give increased power on large scales, may be profitable.

Acknowledgments

It is a pleasure to thank Katy James for help with statistical analysis. PAJ is supported by a research studentship from the SERC, and CAC by a Research Fellowship from the University of Edinburgh.

References

Aaronson, M., Bothun, G., Mould, J., Huchra, J., Schommer, R. A. & Cornell, M. E., 1986. *Astrophys. J.*, **302**, 536.
Bahcall, N. A., Soneira, R. M. & Burgett, W. S., 1986. *Astrophys. J.*, **311**, 15.
Blumenthal, G. R., Faber, S. M., Primack, J. R. & Rees, M. J., 1984. *Nature*, **311**, 517.
Collins, C. A., Joseph, R. D. & Robertson, N. A., 1986. *Nature*, **320**, 506.
Dekel, A. & Rees, M. J., 1987. *Nature*, 326, 455.
Dressler, A., Faber, S. M., Burstein, D., Davies, R. L., Lynden-Bell, D., Terlevich, R. J. & Wegner, G., 1987. *Astrophys. J.*, **313**, L37.
Lubin, P. & Villela, T., 1986. *Galaxy Distances and Deviations from Universal Expansion*, p. 169, eds Madore, B. F. & Tully, R. B., Re del, Dordrecht, Holland.
Rubin, V. C., Ford, W. K., Thonnard, N., Roberts, M. S. & Graham, J. A., 1976. *Astr. J.*, **81**, 719.
Sandage, A. & Hardy, E., 1973. *Astrophys. J.*, **183**, 743.
Scott, E. L., 1957. *Astr. J.* **62**, 248.
White, S. D. M., Frenk, C. S., Davis, M. & Efstathiou, G., 1987. *Astrophys J.*, **313**, 505.

Mon. Not. R astr. Soc. (1988) **233**, 1–23

Recent star formation in interacting galaxies – III. Evidence from mid-infrared photometry

G. S. Wright,* R. D. Joseph, N. A. Robertson,†
P. A. James and W. P. S. Meikle *Blackett Laboratory, Imperial College, Prince Consort Road, London SW7 2BZ*

Accepted 1987 October 30. Received 1987 October 23; in original form 1987 June 5

Summary. In Paper I we used *JHKL* photometry of a sample of interacting galaxies to argue that interactions induce a burst of star formation in the nucleus of one member of the interacting pair with nearly 100 per cent efficiency. We have followed up this result by mid-infrared (10 and 20 μm) observations of a large fraction of this sample. We have added to these results existing mid-infrared data in the literature to obtain a comprehensive picture of the evidence for mid-infrared activity in the nuclear regions of interacting galaxies. We show that this information, combined with radio and optical data, provides a consistent picture of interaction-induced bursts of star formation in the central regions of these galaxies. Using a simple analytical starburst model we derive some of the quantitative features of these interaction-induced starbursts: they are unusually efficient in using available gas, and the initial mass function is heavily biased toward massive stars. The supernova rate and radio luminosity implied by this model are consistent with the observations. Finally we stress that, if the observed rate of interactions is representative, interaction-induced starbursts are likely to have occurred in the evolution of most galaxies. Such events may be related to other forms of activity in galactic nuclei.

1 Introduction

The discovery of highly energetic 'activity' in the nuclei of galaxies has been one of the highlights of modern astrophysics. The detailed elucidation of the properties and physics of this activity in its various forms continues to be a major endeavour. The spectrum of this activity runs from almost 'normal' spiral galaxies through Seyfert and radio galaxies to the quasars. Although there is as yet no consensus about the nature of this activity in galaxies, proposals for the underlying energy source have generally condensed around two mechanisms: thermonuclear energy generated in a

* Now at UK Infrared Telescope, 665 Komohana Street, Hilo, Hawaii 96720 USA.
† Now at Department of Physics & Astronomy, Glasgow University, Glasgow G12 8QQ.

recent burst of star formation ('starbursts'), or gravitational energy released as matter accretes on to a compact object ('monsters', *cf.* Gunn 1979).

Nuclear activity in galaxies frequently manifests itself by enhanced luminosity in the mid- and far-infrared (wavelengths 10–100μm). The quasi-thermal continuum spectra, peaking at $\sim$100μm, which characterize several classes of galaxies are generally attributed to emission from dust which has been heated by the radiation from OB type stars formed in a recent burst of star formation (*cf.* Rieke & Lebofsky 1979). However, the dust could equally well be thermalizing hard radiation from a central non-thermal source. Moreover, the continuum spectra of sources generally thought to be non-thermal, such as Seyfert 1 galaxies and quasars, often exhibit a steeply rising power-law spectrum between the visible and radio regions of the spectrum (Lawrence *et al.* 1985). Thus, mid-infrared photometry provides an important datum in investigation of the energetics and emission mechanisms associated with starbursts and 'monsters' in the nuclei of galaxies.

Interacting galaxies are a seminal class of galaxies to use as a laboratory in which to study the physics of both of these processes. The tidal effects of interactions result in substantial redistribution of material into deeply plunging orbits in and between the participating galaxies, and this material could fuel a burst of star formation, feed a 'monster', or both (*cf.* Toomre & Toomre 1972).

There have been several studies to investigate nuclear IR activity in interacting galaxies (*cf.* Joseph 1986). Joseph *et al.* (1984, hereafter Paper I) found from *JHKL* photometry of a sample of 44 interacting galaxies that, for $\sim$85 per cent of the sample, one member of every pair showed a K–L excess indicative of a steeply rising far-IR continuum spectrum. Lonsdale, Persson & Mathews (1984) presented mid-IR photometry for a group of 11 interacting and merging galaxies, showing that all of them have the rising continuum spectra typical of starburst galaxies. They also argued that at least a third of the galaxies detected in the *IRAS* 'Minisurvey' are interacting or merging galaxies. Cutri & McAlary (1985) detected 13 galaxies ($>3\sigma$) at 10μm in a complete sample of 39 interacting pairs. In all of these IR studies the authors argued that starbursts, fuelled and triggered by the interaction, were responsible for the large IR luminosities. Joseph & Wright (1985, hereafter Paper II) also investigated a particularly interesting subset of interactions: those in which two disc galaxies have lost their individual identities and have coalesced into a single object. They showed that the 10μm luminosities of these mergers were about an order of magnitude larger than those of Seyfert galaxies, and two orders of magnitude larger than classic starburst galaxies. The IR, optical, and radio evidence they adduced demonstrated that 'super-starbursts' of exceptional luminosity and spatial extent were present in these galaxies.

We have now carried out mid-infrared (10 and 20μm) observations of a number of the interacting galaxies identified in Paper I as likely to have a large 10μm excess from their K–L colours. In addition we have collected from the literature all the other mid-IR photometry of which we are aware on interacting galaxies. Thus, we aim to present a comprehensive review of the evidence for mid-IR activity in interacting galaxies. We emphasize that the data presented and discussed is for the central few arcsec in these galaxies, and it is therefore inappropriate to call on data obtained with the *Infrared Astronomical Satellite (IRAS)*. In fact, in many cases, the *IRAS* apertures, of several arcmin, include both members of an interacting pair of galaxies. We show in Sections 4 and 5 how the combined IR, radio, and optical data available for this sample of interacting galaxies provide a consistent picture of interaction-induced bursts of star formation in the central regions of these galaxies, and we will apply a simple starburst model to derive some of the quantitative features of this starburst activity. Finally, we will indicate the importance of these interaction-induced starbursts for the evolution of most galaxies, and the origin of 'monster'-type activity in particular.

By way of nomenclature, we use 'nuclear' to denote the central few arcsec in the galaxies under discussion. This encompasses regions up to a few kpc in some of these galaxies, much larger than the 'nucleus' often associated with non-thermal emission in Seyfert galaxies, radio galaxies, and quasars.

2 Observations and data reduction

These observations were made at the 3.8-m UK Infrared Telescope (UKIRT). Within the constraints imposed by sensitivity, observations were made of some of each of the morphological types of interactions discussed in Paper I. The 10 and 20μm measurements were made at the location of the peak of the emission at K. (However, due to instrumental complications it is likely that the IR beam was not fully centred on the source when the 10μm measurements of NGC 4088 and 2445 were made.) The aperture used for each observation is given in the table of results. Large chopper throws, typically 20–40 arcsec, were used to minimize the likelihood of chopping within the source.

Calibration stars were observed before and after each galaxy to monitor changes in extinction and sensitivity during the night. The standards used were BS 2990, 4069, 6406 and 5340, whose magnitudes at 10 and 20μm are listed in Gehrz, Hackwell & Jones (1974). The uncertainties due

Table 1. (a) Detections of interacting galaxies.

Galaxy		Aperture	10μm F.D.	20μm F.D.	K-L Colour
NGC	Arp		mJy	mJy	
1614	186	5	480 ± 35		1.1 ± 0.1
2623	243	4	80 ± 12	460 ± 70	0.8 ± 0.1
2798	283	8	520 ± 104	1911 ± 260	0.69 ± 0.04
		5	190 ± 18		
3227	94	8	313 ± 63	726 ± 123	0.81 ± 0.03
		5	330 ± 14		
3627	317	4	71 ± 12		
3786	294	8	47 ± 18		0.63 ± 0.06
4038	244[1]	5	45 ± 12	341 ± 103	
4088	18	8	60 ± 22		0.62 ± 0.06
5394	84	4	114 ± 20		0.5 ± 0.1
5930	90	8	147 ± 35	774 ± 154	0.63 ± 0.06
		5	112 ± 25		
6240		4	124 ± 15	1100 ± 120	0.83 ± 0.03

[1]Observations were made at 'Knot B' in Rubin, Ford & D'Odorico (1970).

(b) Upper limits for galaxies.

Galaxy		Aperture	3σ 10μm
NGC	Arp	(arcsec)	limit (mJy)
2445	143	8	90
3396	270	8	96
5258	240	8	96
5929	90	8	99
6052	209	5	180
A1718 +49B	102	5	60

161

to flux calibration are negligible compared to the statistical errors in the measurements. Corrections for atmospheric extinction were not made since these are small compared to the statistical errors. Some of the galaxies were observed more than once through the same aperture, either on different nights in the same observing run or on a subsequent run. No differences larger than the errors were found between the measurements.

Altogether 17 of the K–L excess galaxies in Paper I were observed at 10μm, and of these 11 were detected. The upper limits for the six non-detected galaxies are in no case strong enough to be inconsistent with the IR excess inferred from the K–L colours. The reduced data for the detected galaxies is presented in Table 1(a), while 3σ upper limits for those galaxies observed but not detected are listed in Table 1(b).

For those galaxies in the sample with additional 10μm observations now available in the literature, the independent measurements are compared in Table 2. With the exception of NGC 1614, all of the results agree within the errors quoted, and no systematic differences, except, perhaps, some aperture effects, are apparent. For NGC 1614 our 10μm photometry was obtained at the position of the K-peak measured from a guide star. Further observations at different positions suggest that the emission is extended and probably not coincident with the peak of the emission at K. The total flux in our map (*cf.* Section 4.2 below) is consistent with there being a centring difference between our measurements and the others in Table 2.

Table 2. Comparison of UKIRT photometry with other observations.

Galaxy NGC	Galaxy Arp	Aperture (arcsec)	10μm F.D. (mJy)	Reference
1614	186	5	480 ± 35	This work
		8	630 ± 20	Lebofsky & Rieke (1979)
		4.5	840 ± 50	Lonsdale et al. (1984)
2623	243	4	80 ± 12	This work
		4.5	93 ± 12	Lonsdale et al. (1984)
		5.5	105 ± 9	Lonsdale et al. (1984)
3627	317	4	71 ± 12	This work
		5.7	110 ± 22	Rieke & Lebofsky (1978)
3786	294	8	47 ± 18	This work
		6	52 ± 6	Cutri & McAlary (1985)
5394	84	4	114 ± 20	This work
		6	187 ± 62	Cutri & McAlary (1985)
5930	90	8	147 ± 35	This work
		6	155 ± 23	Cutri & McAlary (1985)

3 Data in the literature

In addition to the IR studies of interacting galaxies mentioned in the Introduction, a number of interacting galaxies have been observed as part of other observational programmes. Table 3 summarizes the 10μm photometry of other interacting galaxies which will be used in the following discussion to supplement our results in Table 1. Data from the literature presented in Table 2 are not repeated in Table 3. Galaxies are only included in this sample if they obviously fall into the types of interactions selected for Paper I. For example, those galaxies in the Arp (1966) *Atlas* which resemble dusty spirals with no obvious companions are not included even if 10μm observations are available. With these additional data we have a sample of 39 interacting or merging galaxies with 10μm detections in 5–8 arcsec apertures. In the following discussion we will use this sample, summarized in Table 5, to investigate IR activity in the nuclei of interacting galaxies.

Table 3. 10μm observations of interacting galaxies in the literature.

Galaxy NGC	Galaxy Pair[1]	Aperture (arcsec)	10μm F.D. (mJy)	Reference
520	A157	5	460	Condon et al. (1982)
2341	K125	6	65 ± 8	Cutri & McAlary (1985)
2342	K125	6	65 ± 8	Cutri & McAlary (1985)
2445	A143	4.5	68 ± 13	Lonsdale et al. (1984)
U3395	K140	6	97 ± 9	Cutri & McAlary (1985)
2964	K210	6	110 ± 11	Cutri & McAlary (1985)
2992	A245	4.5	255 ± 12	Lonsdale et al. (1984)
3256	VV65	15	1700 ±150	Graham et al. (1984)
3310	A217	map	1000	Telesco & Gatley (1984)
3395	A270	6	26 ± 9	Cutri & McAlary (1985)
3396	A270	6	55 ± 7	Cutri & McAlary (1985)
3656	A155	5.5	37 ± 6	Lonsdale et al. (1984)
3690	A296	5	1000	Gehrz et al. (1983)
3800	A83	6	28 ± 7	Cutri & McAlary (1985)
3808A	A87	4.5	50 ± 11	Lonsdale et al. (1984)
4038	A244[2]	4.5	36 ± 8	Lonsdale et al. (1984)
4194	A160	6	320 ± 45	Rieke & Low (1972)
4438	A120	4.5	33 ± 8	Lonsdale et al. (1984)
4568	K347	8	62 ± 19	Cutri & McAlary (1985)
5194	A85	9	50 ± 5	Telesco et al. (1986)
5929	A90	6	43 ± 14	Cutri & McAlary (1985)
IC883	A193	5.5	154 ± 9	Lonsdale et al. (1984)
5953	A91	6	64 ± 10	Cutri & McAlary (1985)
IC4553	A220	total	480	Soifer et al. (1984)
7469	A298	5.9	600 ± 40	Lebofsky & Rieke (1979)
7714	A284	6	250 ± 40	Rieke & Low (1972)
7752	86	12	116 ± 82	Cutri & McAlary (1985)
7761	K592	8	119 ± 20	Cutri & McAlary (1985)

[1] A is the number of the Arp pair and K denotes number in the Karachentsev (1972) catalogue.
[2] Position M in Rubin *et al.* (1970).

162

4 Results

4.1 ENERGY DISTRIBUTION

Examples of the continuum spectra of the interacting galaxies for which more than one point is available are plotted in Fig. 1. Despite the varying degrees of completeness of the spectra it is clear that they are all very alike, with a steep mid-IR rise similar to that of NGC253, which is also shown in the figure. These spectra, which must peak in the far-IR, are characteristic of the thermal radiation from dust grains which are at a range of temperatures. Such spectra are also commonly observed from galactic regions of star formation. Continuum spectra with these features for galactic nuclei are therefore generally assumed to be indicative of a recent burst of star formation, with the ultraviolet radiation from massive early-type stars thermalized by dust and re-radiated in the IR (*cf.* Rieke & Lebofsky 1979).

4.2 SPATIAL EXTENT OF THE IR EMISSION

The starburst interpretation proposed above can be distinguished from thermal IR emission due to dust heated by a compact central source (such as the nucleus of a Seyfert galaxy) by measuring the extent of the mid-IR emission. Simple considerations of energy balance show that if a dust

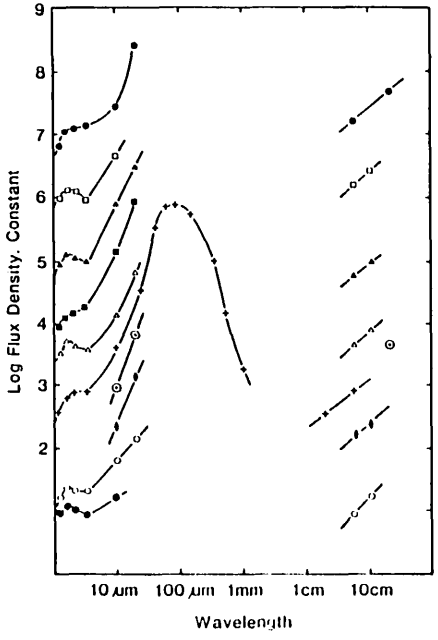


Figure 1. Continuum spectra of interacting and merging galaxies. The spectrum of the starburst galaxy NGC253 (+) is shown for comparison. Symbols denote NGC6240 (●), 5394 (□), 2798 (▲), 1614 (■), 5930 (△), 4038 (▽), 2623 (◆), 3227 (○), 3786 (◐). The mid-IR data is from Table 1 (a) with additional points at 20μm for NGC 1614 from Lebofsky & Rieke (1979) and for NGC3786 from Cutri & McAlary (1985). The radio data is taken from the references listed in Table 8.

grain of radius ~0.1 μm is in thermal equilibrium with a source of luminosity L which is a distance D away, then (*cf.* Graham *et al.* 1983)

$$D = 50[L(L_{\odot})/T^{5}(\mathrm{K})]^{1/2}\ \mathrm{pc}. \quad (1)$$

Thus, a dust grain exposed to a source of $10^{10}L_{\odot}$ is not hot enough to radiate significantly at 10 μm (i.e. ~300 K) if it is more distant than a few pc from the source. Detection of spatial extent at 10 μm on scales greater than a few pc therefore requires distributed luminosity sources. A starburst is the obvious astrophysical description of such a source distribution, and, indeed, the

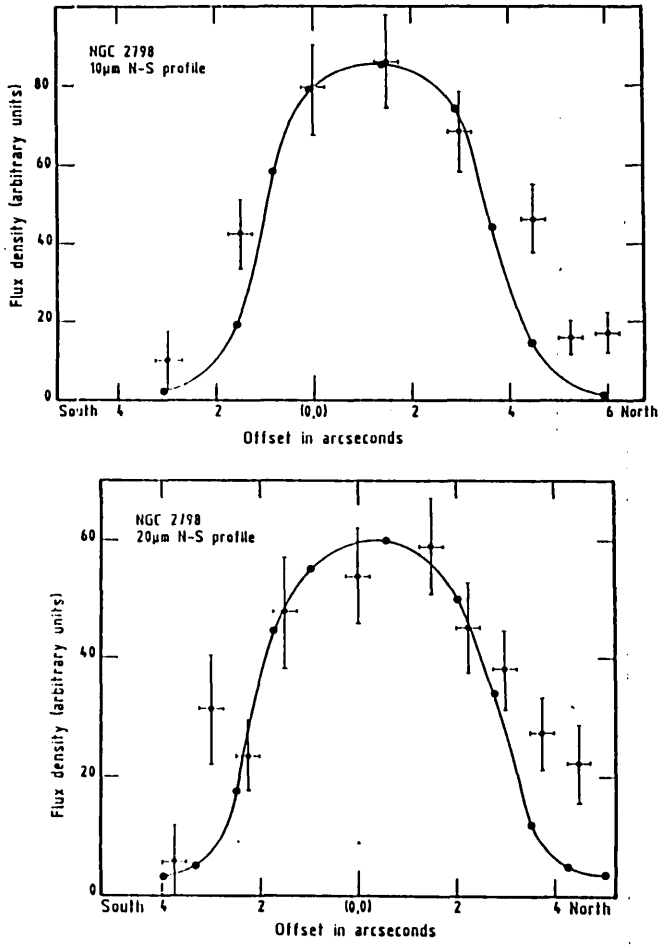


Figure 2. Scans of NGC2798 at 10 and 20 μm compared with identical scans of a star (continuous line). The north-south profiles were taken while chopping in an east-west direction. Observations were begun at the (0, 0) position, and successive points at increasing offset were obtained alternately on opposite sides of the (0, 0) position.

163

IR emission from starburst galaxies is characterized by spatial extent on scales of hundreds of pc (*cf.* Rieke 1976). To investigate this question we have looked for evidence of spatial extent at 10μm for three of the brightest interacting galaxies.

Evidence for spatial extent at 10μm in NGC2798 and 6240 was obtained as follows. Using a 5 arcsec beam, we first measured the optical nucleus of NGC2798 and on the peak at K for NGC6240. We then repeated the photometry, moving off the central position in steps of 0.75 arcsec. To minimize the systematic effects of any positional drift, successive measurements were made alternately on opposite sides of the nucleus. When obtaining these measurements along the east-west direction, we chopped in the north-south direction, and vice versa. Fig. 2 shows the measurements for NGC2798, compared to identical scans for a star (i.e. the beam profile for an unresolved source), and Fig. 3 shows similar scans for NGC6240.

NGC2798 is clearly extended both at 10 and 20μm. While the result for NGC6240 is more marginal, the galaxy points do show a tendency to lie above the beam profile. The significance of the evidence for spatial extent was estimated by comparing the sizes of the error ellipses on each point with the distance of the point from the beam profile. The significance of each point was then summed in quadrature to give the overall significance of extent for each scan. The north-south scans of NGC2798 at both 10 and 20μm are larger than the beam profile at the 4.5σ significance level, whereas the scan for NGC6240 is larger at the 3σ level.

We have also explored the likely size of the sources by convolving the beam profile with a top hat function, varying the height and width of the latter to derive the convolved profile which gives the best fit to the galaxy scans. This gives source sizes of ~4 arcsec.

Table 4 summarizes the results of less detailed mapping of NGC1614 and 3227 using a 5 arcsec beam. NGC1614 is extended to the south and east. Such a spatial distribution makes it possible to account for the differences in flux between the measurements presented here, those of Lonsdale *et al.* (1984), and those of Lebofsky & Rieke (1979) (*cf.* Table 2). There is, perhaps, less strong evidence for similar spatial extent in NGC3227. In order to investigate further the extent of the

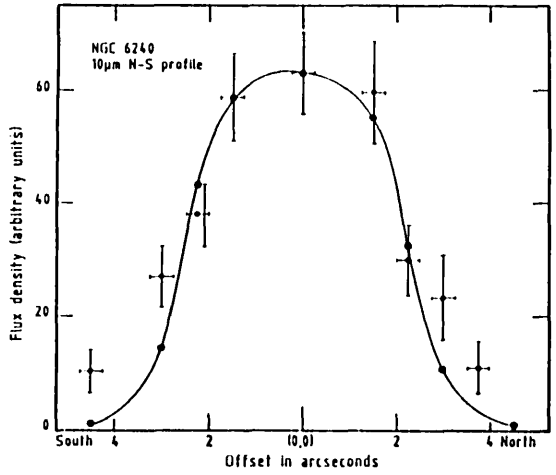


Figure 3. A scan of NGC 6240 at 10μm compared with an identical scan of a star (continuous line). Scans were obtained as described in Fig. 2.

Table 4. 5 arcsec aperture maps of galaxies.

Galaxy	Chopper throw (arcsec)	Offset from nucleus (arcsec)	10μm F.D. (mJy)
1614	30 E-W	0 , 0	480 ± 35
		3E , 0	174 ± 24
		3W , 0	64 ± 20
		0 , 3S	530 ± 24
		3E , 3S	260 ± 60
3227	30 N-S	0 , 0	330 ± 14
		3E , 0	23 ± 15
		3W , 0	82 ± 17
		0 , 3N	68 ± 19
		0 , 3S	71 ± 21

IR emission in NGC3227, measurements of the K–L colour in non-nuclear positions were made using an 8 arcsec beam. A K–L colour of 0.85±0.23 was measured at a position 8 arcsec west of the nucleus, which is virtually identical to the K–L=0.81 in an 8 arcsec aperture centred on the nucleus (Paper I). Since K–L colour excess (where K–L=0.3 is the normal galaxy colour) correlates well with 10μm excess (Joseph, Wright & Robertson, in preparation), these results further support the impression that the IR emission is extended in NGC3227.

In the case of NGC2798 the evidence for spatial extent from mapping was confirmed by multi-aperture 10μm measurements. Both beams were centred on the optical nucleus. Significantly less signal was detected with a 5 arcsec beam, 190±18 mJy, than with an 8 arcsec beam, 520±104 mJy.

The UKIRT measurements discussed here indicate that the IR sources in these galaxies are probably extended on scales ~4–5 arcsec, which correspond to linear dimensions of 2 and 3 kpc in NGC1614 and 6240, and 800 and 600 pc in NGC2798 and 3227. These scales are clearly inconsistent with heating by a single central source, and the results provide strong support for the starburst picture.

For some of the other galaxies in the sample measurements of spatial extent at 10μm have been presented in the literature. Maps by Gehrz, Sramek & Weedman (1983) of NGC3690–IC694 show that the 20μm emission is extended to >6 kpc in NGC3690. Lonsdale *et al.* (1984) have mapped IC883 and find the emission to be extended to the north-west. From the difference between their large and small aperture measurements the source must be greater than 4.5 arcsec or 3 kpc in extent. Telesco, Decher & Gatley (1986) have made a 10μm map of NGC5194 and they find low surface brightness emission extending more than 3 kpc. For NGC3310 the maps of Telesco & Gatley (1984) show that intense 10μm emission in this galaxy extends for more than 5 kpc. Maps at 10μm are used by Graham *et al.* (1984) to infer that the emission from NGC3256 is extended over at least 4 kpc.

In summary, for nine of the 39 interacting and merging galaxies detected at 10μm, there is a good indication of spatial extent on scales >1 kpc. If the dust is in thermal equilibrium, there must be sources distributed throughout the emitting region and so the observed spatial extent of the IR radiation indicates that the dust cannot be heated by a single central source. A starburst interpretation fits much more naturally with the data.

This interpretation of extended 10μm emission is, however, complicated by the recent realization that very small dust grains may be present (Sellgren 1984; Leger & Puget 1984). Such

grains can be heated to temperatures ~1000 K by absorption of a single ultraviolet (UV) photon, and thus they can emit at 10μm at distances considerably further from the energy source than considerations of thermal equilibrium would require. Such grains appear to be responsible for the mid-IR emission from reflection nebulae (Sellgren 1984) and for the diffuse 'IR cirrus' emission found in *IRAS* observations (Puget, Leger & Boulanger 1985).

However, 10μm emission from very small grains surrounding a Seyfert-like central energy source is unlikely to undercut the argument advanced above. Aitken & Roche (1985) show that the unidentified IR features at 7.7, 8.6 and 11.3μm, which appear to be carried by the very small grains (Sellgren 1984; Leger & Puget 1984), are strikingly absent in the mid-IR spectra of Seyfert galaxies and quasars, presumably because they cannot survive the hard UV radiation field in the central few arcsec of these galaxies. Thus extended 10μm emission from very small grains seems to be unlikely for the case of Seyfert-like active galactic nuclei.

Table 5. 10μm luminosities of interacting and merging galaxies.

Galaxy		Distance	L_{10}
NGC	Pair	(Mpc)	($L_\odot$)
520	A157	46	8×10^9
1614	A...6	90	4×10^{10}
2341	K125	103	6×10^9
2342	K125	103	6×10^9
2445	A143	80	4×10^9
2623	A243	110	8×10^9
2798	A283	35	5×10^9
U3395	K140	90	7×10^9
2964	K210	26	6×10^8
2992	A245	34	2×10^9
3227	A94	23	2×10^9
3256		50	4×10^{10}
3310	A217	20	4×10^9
3396	A270	32	5×10^8
3395	A270	32	2×10^8
3627	A317	12	8×10^7
3656	A155	53	9×10^9
3690	A299	63	4×10^{10}
3786	A294	51	1×10^9
3800	A83	69	1×10^9
3808A	A87	128	6×10^9
4038	A244	29	6×10^8
4088	A18	16	1×10^8
4194	A160	53	7×10^9
4438	A120	12	4×10^7
4568	K347	43	9×10^8
IC883	A193	140	2×10^{10}
5194		10	4×10^7
5394	A84	70	5×10^8
5929	A90	56	1×10^9
5930	A90	56	4×10^9
IC4553	A220	110	5×10^{10}
5953	A91	40	8×10^8
6240		150	2×10^{10}
7469	A298	102	5×10^{10}
7714	A284	59	7×10^9
7761	K592	86	7×10^9

On the other hand, Roche & Aitken (1985) also show that the spectral features associated with very small grains are common in starburst galaxies. Indeed, Aitken & Roche (1984) do find the 11.3μm feature to be strong in one of the merging galaxies in our sample, NGC 1614. In this case, the small grains are likely to be located in the neutral gas at the boundaries of H II regions (Ryter, Puget & Perault 1988), and therefore shielded from the hard UV radiation inside the ionized region.

In summary, small grains cannot account for extended 10μm emission from a Seyfert-like central luminosity source; they are apparently destroyed by the hard UV radiation field. If mid-IR emission from small grains is present in our sample of interacting galaxies, it is likely to arise in the neutral gas outside H II regions, and therefore their presence will be further evidence for starburst activity.

4.3 IR LUMINOSITIES

In Paper II we argued that mergers between disc galaxies produce the largest IR luminosities yet found in galaxies. Here we investigate non-merging interacting galaxy luminosities and compare them to the mergers. In Table 5 we list the 10μm luminosities, computed using $L_{10}=4\pi D^2 \nu S_\nu$, where L_{10} is the luminosity at 10μm, D is the distance, and S_ν is the 10μm flux density.

The significance of these luminosities is perhaps best appreciated by comparing them with the 10μm luminosities of other classes of galaxies, as in Table 6. Known interacting galaxies have been removed from the comparison sample of bright spirals (and are included in the interacting group). It is apparent that the 10μm luminosities of nuclear starbursts in interacting galaxies are about an order of magnitude larger than those in non-interacting galaxies. The comparison with merging galaxies is even more striking: mergers are more luminous by a further order of magnitude, and seem to constitute the luminous tail of a distribution of activity in interacting galaxies. Thus these data suggest that, on average, starbursts triggered by interactions are ~10–

Table 6. Nuclear 10μm luminosities.

Class of galaxy	N	Range ($L_\odot$)	Mean ($L_\odot$)	References
Interacting	24	4×10^7-7×10^9	2.5×10^9	This work
Merging	9	4×10^9-5×10^{10}	2×10^{10}	Joseph & Wright (1982)
Seyferts	50	4×10^8-10^{11}	4×10^{10}	Rieke (1978)
Starbursts: M82		10^9		Rieke & Lebofsky (1978)
NGC253		6×10^8		
NGC2903		1×10^8		
Bright spirals	17	10^8-7×10^8	2×10^8	Rieke & Lebofsky (1978)

100 times more intense than those in non-interacting spirals, and the luminosities of mergers are comparable to those of Seyferts.

The integrated IR luminosities, L_{IR}, *within these apertures*, may be estimated using the extrapolation $L_{IR}=15L_{10}$ (*cf.* Scoville *et al.* 1983; Telesco & Gatley 1984). These integrated luminosities will be used in discussion of starburst models in Section 6 below.

4.4 MASS–LUMINOSITY RATIOS

A useful way to parametrize the mass associated with star formation activity is in terms of the mass-to-luminosity ratio, M/L. (For the galaxies under discussion the bolometric luminosity is dominated by the IR luminosity.) The minimum mass-to-light ratio which can be maintained by thermonuclear energy generation for a Hubble time is $M/L\sim 1$ (in solar units, which are assumed hereafter). Thus a low value for M/L is evidence for significant recent star formation and implies that the star formation must be occurring in a short-lived burst.

Rotation curves from which masses can be estimated are available for seven interacting galaxies and three merging galaxies. For all of these, our apertures correspond to the linear region of the rotation curve. The mass within the volume covered by the 10 μm photometry has therefore been estimated from the rotational velocities by assuming a uniform density distribution

$$M(r)=rv^2(r)/G, \qquad (2)$$

where $M(r)$ is the mass within radius r, $v(r)$ is the rotational velocity at radius r, and G is the gravitational constant. A total mass has been estimated for NGC 2798 from the H I data of Peterson & Shostak (1977), which gives a total mass for the pair, by assuming that NGC 2798 and 2799 are of equal mass. Upper limits for the masses of NGC 6240 and 520 were estimated by assuming their measured line widths to be Doppler-broadened due to rotation.

Mass-to-light ratios for all these galaxies and references to the data from which the mass was derived are given in Table 7. These ratios are all $\lesssim 1$ and, in conjunction with the evidence from the continuum energy distributions and the spatial extent of the IR emission, they make a very strong case for recent episodes of star formation.

Table 7. The ratio of nuclear mass to total IR luminosity.

Galaxy		M/L	Reference
NGC	Arp	(solar units)	
520	157	<0.01*	Stockton & Bertola (1980)
1614	186	0.003	Ulrich (1972)
2798	283	<0.4*	Peterson & Shostak (1977)
2992	245	0.001	Heckman et al. (1981)
3227	94	0.02	Rubin & Ford (1968)
3256		0.01	Feast & Robertson (1978)
3396	270	0.002	D'Odorico (1970)
3395	270	0.007	D'Odorico (1970)
4088	18	0.02	Carozzi-Meyssonnier (1978)
4194	160	0.03	Demoulin (1969)
5194		0.3	Tully (1974)
6240		<0.08*	Fosbury and Wall (1979)
7714	284	0.01	Demoulin (1968)

*See note in text for method of estimating the mass.

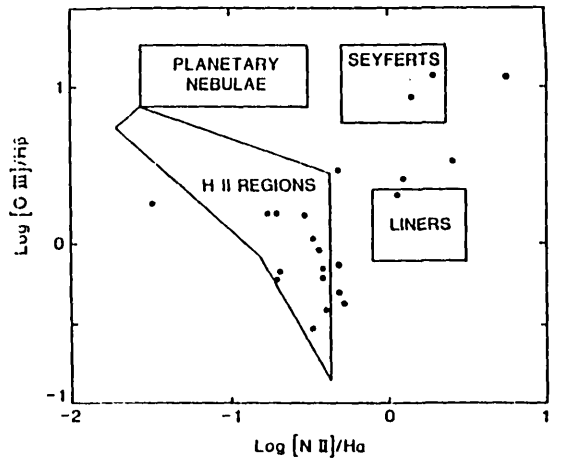


Figure 4. Optical emission line intensity ratios for all of the galaxies in the sample with the required data available. The contours denoting 'H II Regions', 'Seyferts', etc. are taken from Baldwin, Phillips & Terlevich (1979).

5 Optical and radio evidence for the starburst interpretation

If the starburst interpretation of the IR fluxes from interacting galaxies is correct, then these galaxies should have optical spectra indicative of recent star formation. There are optical spectra in the literature for 33 of the 39 interacting galaxies in the sample (Keel *et al.* 1985; Heckman 1983; Dahari 1985; Bushouse & Gallagher 1984; Balzano 1983; Rose & Searle 1982). The relative line intensities [O III]/Hβ versus [N II]/Hα for 22 of these are plotted in a Baldwin, Phillips & Terlevich (1979) diagram in Fig. 4. A further 11 galaxies have been classified in the literature using similar criteria. In total, 21 of the interacting galaxies have relative line intensities similar to those found in H II regions, four are classified as Liners, and six as Seyfert galaxies. The four galaxies with Liner-type spectra are NGC 6240, 2623, 3627 and 4438, and of these Keel *et al.* (1985) have classified the stellar continuum of NGC 4438 as having a significant component due to early-type stars.

The occurrence of six Seyfert galaxies in the sample, NGC 3227, 3786, 5929, 7469, 2992 and 5953, is probably not inconsistent with the number of Seyfert nuclei expected in a field sample of this magnitude range (*cf.* Keel *et al.* 1985). Seyfert-like optical spectra do not rule out the presence of a starburst since there is also intense star formation in the nuclear (i.e. the inner 1 kpc) region of some Seyferts. NGC 1068 is a classic example of such a galaxy, and in this case about half of the IR luminosity is provided by the Seyfert nucleus and about half by a surrounding 3 kpc disc of star formation (Telesco *et al.* 1984; Tresch-Fienberg *et al.* 1987). There is evidence that at least three of the galaxies in this sample which are classified optically as Seyferts are composites with star formation as well as Seyfert activity in their nuclear regions. Jenkins (1984) has studied NGC 5953 in detail and finds extremely luminous extended 'nuclear' emission lines indicative of H II regions as well as the compact non-thermal core. The radio data for NGC 2992 and 3227 all show a nuclear source extended on scales of 10–100 pc, consistent with a starburst.

Condon *et al.* (1982), Hummel, van der Hulst & Dickey (1984) and others have argued that steep-spectrum extended nuclear radio sources in spiral galaxies can be explained in terms of young supernovae and supernova remnants associated with recent bursts of star formation. The

Table 8. Radio data for interacting galaxies detected at 10 μm.

NGC	Pair	Radio spectral index	Radio size[1] (arcsec)	Reference
520	A157	-0.68	~ 10	Condon et al. (1982)
1614	A186		≥ 3	Condon et al. (1982)
2341/2	K125	-1.0	E	Stocke et al. (1978)
2445	A143		22	Burke and Miley (1973)
2623	A243	-0.8	0.5x0.4	Condon (1980a)
2798	A283	-0.6	2.5x2.5	Stocke et al. (1978)
2964	K210	-0.9	E	Stocke et al. (1978)
2992	A245		~ 8	Condon et al. (1982)
3227	A94	-0.7	3x3	Stocke et al. (1978)
3256	VV65	-1.3		Wright (1974)
3310	A217	-0.7	~ 10	Hummel (1981)
3395	A270	-0.7	E	Stocke et al. (1978)
3627	A317	-0.73	E	Hummel (1980), Israel & van der Hulst (1983)
3690	A299	-0.80	> 6	Gehrz et al. (1983)
4038	A244		E	Hummel (1980)
4088	A18	-0.77	E	Hummel (1980), Gioia et al. (1982)
4194	A160	-0.7	~ 6	Hummel et al (1984)
4438	A120	-0.85	3-12	Hummel (1980)
4568	K347	-0.95	E	Stocke et al. (1978)
IC883	A193	-0.7	E	Sulentic (1976), Heckman (1983)
5194		-0.81	E	Condon (1980b)
5394	A84	-0.6	5x6	Stocke et al. (1978)
5930	A90	-1.0	3x5	Stocke et al. (1978)
14553	A220	-0.6	1.3x0.5	Condon (1980)
5953	A91	-1.0	E	Stocke et al. (1978)
6240		-0.85	~ 5	Condon et al. (1982)
7469	A298	-0.6	4x2	Stocke et al. (1978)
7714	A284	-0.93	3.5x2	Condon et al. (1982)
7761	K592	-1.0	4x8	Stocke et al. (1978)

[1] E denotes galaxies whose radio emission has been classified as extended, although no size is given.

characteristics of the radio emission from the interacting galaxy sample are summarized in Table 8, to test whether they are consistent with this scenario. For 29 of the 39 interacting galaxies detected at 10 μm, the radio source has been resolved and has a non-thermal spectrum, typically of index $(\nu d\ln S_\nu/d\nu)\sim-0.7$. The two most compact sources are in NGC 2623 and IC 4553, with sizes ~0.5 arcsec (Condon 1980a, b), which corresponds to ~270 pc in these galaxies. By comparison, a typical Seyfert galaxy such as NGC 3031 has a compact radio source of size <1 pc and a spectral index of +0.1 (Kellerman *et al.* 1976). Thus, the interacting galaxies clearly do not have the characteristic radio properties of Seyfert galaxies. Their radio features are those expected for a starburst.

Taken together the IR, optical and radio measurements on this group of 39 interacting galaxies provide good evidence that the IR emission from the majority of the galaxies is powered by recent bursts of star formation. All but four of these galaxies (NGC 3786, 5929, 7469, 3656) have additional radio or optical evidence suggesting that star formation is occurring in their nuclei. Thus it is difficult to avoid the conclusion that starbursts are the dominant source of the IR activity in interacting galaxies.

6 Characteristics of starbursts in interacting and merging galaxies

We have shown in Sections 4 and 5 that the IR, radio, and optical properties of this sample of interacting and merging galaxies may be most plausibly understood in terms of a recent burst of star formation. We now wish to investigate the quantitative astrophysical implications of this interpretation using the simple analytical starburst models of Telesco & Gatley (1984), discussed in detail in Telesco (1985). In these models the initial mass function (IMF), the luminosity per star, and the main-sequence lifetime of the stars are all approximated by power-law functions of the stellar mass. A Miller–Scalo (1979) IMF is used, and we have adopted the numerical constants tabulated in Telesco & Gatley (1984).

6.1 STAR FORMATION RATES

We consider the formation of OBA stars in a starburst with a constant star formation rate that has proceeded for a sufficiently long time so that equilibrium has been established and the death and birth rates of massive stars are equal. The total luminosity of the starburst is related to the formation rate of OBA stars (1.6-60$M_\odot$) by

$$dM/dt\sim2\times10^{-10}L_{\rm IR} \quad (M_\odot\ {\rm yr}^{-1}). \tag{3}$$

For the values of $L_{\rm IR}$ typical of interacting and merging galaxies (*cf.* Table 5), the ISM is being converted into early-type stars at phenomenal rates, $\sim$1–100 $M_\odot\,{\rm yr}^{-1}$. By comparison, the star formation rate in the Galaxy, estimated from observations in the solar neighbourhood, corresponds to $\sim0.003M_\odot\ {\rm yr}^{-1}$ in a region ~1 kpc in diameter (*cf.* Miller & Scalo 1979). Our estimated star formation rates would increase by a factor of ~2 if a starburst age $\sim10^7$ yr had been assumed instead of OBA star formation in equilibrium. Extending the IMF to 0.1 $M_\odot$ would require a rate of conversion of gas into stars of all mass ranges a factor of ~3 times higher still.

6.2 DURATION OF THE STARBURSTS

The mass-to-light ratios provide a powerful constraint on the length of time during which the star formation rates derived above can be maintained, since the starburst will eventually consume all of the available gas. All of the M/L ratios in Table 7 are very small and imply short-lived starbursts. The *net* rate of consumption of interstellar material in the formation of OBA stars, M_c, can be estimated from equation (3) by assuming that massive stars ultimately return ~75 per cent of their mass to the ISM. Then

$$dM_c/dt\sim5\times10^{-11}L_{\rm IR} \quad (M_\odot\ {\rm yr}^{-1}). \tag{4}$$

If 10 per cent of the galaxy mass is gas, then the maximum duration T of the starburst is given by $TdM_c/dt=\epsilon M/10$, where M is the galaxy's mass and ϵ is the efficiency of conversion of gas into stars. Then

$$T\approx2\times10^9\epsilon M/L_{\rm IR} \quad ({\rm yr}). \tag{5}$$

167

The M/L ratios of the interacting and merging galaxies thus imply that their interstellar gas will be consumed in very short time-scales, $\sim 5\times10^{6}$–10^{8} yr. For most of the galaxies then, if the starburst is to be maintained for periods $>10^{7}$ yr, fresh material must be supplied to the nuclear region on this time-scale. The duration of a starburst nucleus must depend on the balance between interaction-driven infall of material and the outflow which will result from the large number of supernovae produced in the burst. Given the large fraction of interacting galaxies with starburst nuclei, it is evident that the interaction is continuing to supply fresh material for star formation on these timescales. In addition, the star formation efficiency must be much greater than the ~5 per cent observed in molecular clouds in the galaxy (Cohen & Kuhi 1979).

6.3 STARBURST INITIAL MASS FUNCTION

Since most of the mass of the starburst is in stars at the low-mass end of the IMF, the total burst mass is a sensitive function of the lower mass cut-off. Thus the M/L ratio can be used to constrain the lower mass cut-off to the IMF if the age of the starburst is known (*cf.* Rieke *et al.* 1980). We can use the following order of magnitude argument to set a lower limit to the starburst age. If the non-thermal nuclear radio emission is interpreted as arising from young supernovae and supernova remnants associated with the starburst, then the starburst must be sufficiently aged for a significant number of supernovae to have formed. Hence the starburst ages are $>10^{7}$ yr (*cf.* Kronberg, Biermann & Schwab 1985). This age may then be used to estimate the mass of stars formed in the starbursts in the interacting and merging galaxies.

In order to limit the lower mass cut-off to the IMF, an estimate of the mass of stars formed during the lifetime of the starburst for different lower mass cut-offs is needed. For a Miller–Scalo IMF extending from 0.1 to 60 $M_{\odot}$, 60 per cent of the mass is in stars less massive than 1.6 $M_{\odot}$ and 93 per cent in stars with mass is below 10 $M_{\odot}$ (Telesco 1985). Since these stars have lifetimes longer than or of the order of the starburst age of 10^{7} yr, a good estimate of the mass of stars formed in the burst can be obtained simply from the star formation rate and the duration of the burst. Telesco (1985) has calculated the quantity $L_{\rm IR}^{-1}dM/dt$ as a function of the starburst age and lower-mass cut-off to the IMF for the starburst models discussed above (i.e. a constant star formation rate). His results for a 10^{7}-year-old starburst are used with the starburst luminosity to

Table 9. Starburst masses compared to nuclear masses.

Galaxy NGC	Nuclear Mass ($M_{\odot}$)	Accumulated Starburst Mass, Lower Mass Cutoff ($M_{\odot}$)				
		0.1	0.8	1.6	3.2	6.5
520	1×10^{9}	1×10^{9}	7×10^{8}	5×10^{8}	3×10^{8}	$\underline{1\times10^{8}}$
1614	2×10^{9}	6×10^{8}	4×10^{8}	2×10^{8}	1×10^{8}	$\underline{7\times10^{7}}$
2798	3×10^{10}	7×10^{8}	4×10^{8}	3×10^{8}	2×10^{8}	9×10^{7}
2992	5×10^{7}	4×10^{8}	2×10^{8}	2×10^{8}	1×10^{8}	$\underline{4\times10^{7}}$
3227	4×10^{8}	2×10^{8}	1×10^{8}	8×10^{7}	$\underline{5\times10^{7}}$	2×10^{7}
3256	6×10^{8}	6×10^{8}	4×10^{8}	2×10^{8}	1×10^{8}	$\underline{7\times10^{7}}$
3396	2×10^{7}	7×10^{7}	4×10^{7}	3×10^{7}	2×10^{7}	$\underline{8\times10^{6}}$
4088	3×10^{7}	2×10^{7}	1×10^{7}	8×10^{6}	5×10^{6}	$\underline{2\times10^{6}}$
4194	3×10^{9}	1×10^{9}	6×10^{8}	4×10^{8}	$\underline{2\times10^{8}}$	1×10^{8}
5194	2×10^{8}	6×10^{8}	4×10^{8}	2×10^{8}	1×10^{8}	5×10^{7}
6240	5×10^{10}	3×10^{9}	2×10^{9}	1×10^{9}	7×10^{8}	4×10^{8}
7714	1×10^{9}	1×10^{9}	6×10^{8}	4×10^{8}	3×10^{8}	$\underline{1\times10^{8}}$

estimate the total mass of stars formed in the burst for the various lower mass cut-offs to the IMF. The results for lower mass cut-offs of 0.1, 0.8, 3.2 and 6.5 $M_{\odot}$ are compared to the masses of the galaxy nuclei in Table 9. For all except NGC 2798 and 6240 (for which only poor limits to the nuclear mass are available), the total burst masses are about the same as the total mass estimated for the starburst regions, if the IMF extends to 0.1 $M_{\odot}$. However, the starburst mass cannot account for *all* of the observed mass in the nuclear regions since the galaxies must also have the normal evolved stellar population. If the fraction of a disc galaxy's mass in gas is ~10 per cent, it is difficult to imagine that the starburst mass could be more than 10 per cent of the observed nuclear mass (and this would require ~100 per cent efficiency in converting gas into stars). In Table 9 the tabulated mass which is nearest to 10 per cent of the observed mass is underlined for each galaxy. It is evident that, for all except the two galaxies with poor mass estimates, the lower mass cut-off to the IMF must be ~3–6 $M_{\odot}$ if the starburst mass is ~10 per cent of the total mass.

This simple analysis suggests that, like the canonical starbursts in NGC 253 and M82 (Rieke *et al.* 1980; Kronberg *et al.* 1985), the extremely luminous starbursts found in interacting and merging galaxies have the remarkable feature that the star formation is restricted to massive stars. Apparently the star formation induced in the nuclei of interacting galaxies is both extremely efficient and biased towards massive stars.

6.4 SUPERNOVA RATES

The starburst model for these interacting galaxies can be further investigated by calculating a supernova rate from the IR observations. Type II supernovae, which evolve from stars more massive than ~10 $M_{\odot}$, are a direct consequence of a starburst. For a starburst with a constant star formation rate, such as those discussed above, and which is sufficiently evolved (~10^{7} yr) for supernovae to have occurred, the rates of formation and destruction of OB stars will be in equilibrium. The supernova rate should then be approximately equal to the star formation rate for these types of stars.

Using the model of Telesco & Gatley (1984) for a starburst $>10^{7}$ yr old and an IMF extending to 1.6 $M_{\odot}$, as before, we find the number of stars more massive than 10 $M_{\odot}$ formed per unit time is

$$dM(\mathrm{OB})/dt \sim 4\times10^{-12}L_{\rm IR} \quad (M_{\odot}\,\mathrm{yr}^{-1}). \tag{6}$$

The total IR luminosity may be extrapolated from the 10 μm flux density, S_{10}. Substituting these in the expression above gives the supernova rate R estimated from the rate of formation of massive stars:

$$R \sim 5\times10^{-7}D^{2}S_{10} \quad (\mathrm{yr}^{-1}). \tag{7}$$

In terms of the 10 μm luminosity of the galaxies, $R\sim6\times10^{-11}L_{10}$ yr^{-1}. For the 10 μm luminosities of interacting and merging galaxies in Table 5, which range from 4×10^{7}–$5\times10^{10}L_{\odot}$, the corresponding supernova rates will be ~0.003–3 yr^{-1}. Such rates are not unreasonable compared to estimates of supernova rates derived from the radio observations of supernovae in M82, ~0.2 yr^{-1} (Kronberg 1985), but they reflect the increased IR luminosities and hence star formation rates of the interacting galaxies compared to other starburst galaxies.

We noted above that for most of the interacting and merging galaxies detected at 10 μm, the radio emission has the spatial extent and spectral index expected if it arises from the supernovae and supernova remnants associated with the starburst. Since the 10 μm luminosity is a measure of the number of massive stars formed in a starburst, and the radio flux density is proportional to the supernova rate, which is also a function of the number of massive stars, the starburst interpretation of the radio emission implies that there should be a correlation between the 10 μm and radio flux densities. Fig. 5 is a plot of 10 μm luminosity against luminosity at 1413 MHz for all the

168

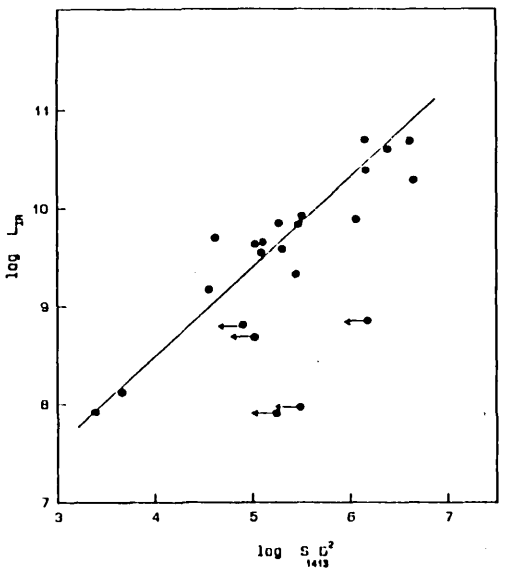


Figure 5. The correlation between IR (10 μm) and radio (1413 MHz) luminosities. The IR data is from Tables 1 and 3, and the radio data is from the references in Table 8.

interacting and merging galaxies for which radio data are available. For those galaxies without a radio measurement at 1413 MHz the flux density was estimated from that at other frequencies using the measured spectral index. Despite some scatter a clear correlation is apparent, implying an IR to radio flux density ratio of ~3. This is close to the ratio of 4 which Condon *et al.* (1982) found for their spirals. If we estimate the far-IR luminosities from the 10 μm flux density, as discussed in Section 4.3, this ratio between the 10 μm and radio flux densities also agrees to within a factor of 3 with the ratio found by Helou *et al.* (1985) for far-IR and radio flux densities from the discs of spiral galaxies. Thus the correlation in Fig. 5, which spans more than two orders of magnitude in the radio and IR luminosities, further supports the starburst interpretation of both the IR and radio data.

Several authors have derived a relation between radio flux density and supernova rate based on the evolutionary models of galactic remnants (e.g. Kronberg & Biermann 1981; Condon *et al.* 1982; Ulvestad 1982). Because their calculation refers specifically to the radio flux at 1413 MHz the relation of Condon *et al.* (1982) is used to infer the supernova rate from the radio emission. They derive a supernova rate

$$R \sim 4\times10^{-9} D^2 S_{1413} \quad (\mathrm{yr}^{-1}). \tag{8}$$

Equating the estimate of the supernova rate in equation (7), based on the starburst model, with equation (8) suggests that the IR to radio flux ratio for a starburst should be ~8. Given the large uncertainties in this estimate it is in reasonable agreement with the observed ratio of ~3.

Other authors (*cf.* Helou *et al.* 1985; Antonucci & Olszewski 1985) have calculated starburst models which make different assumptions about the fraction of the IR luminosity provided by high-mass stars and the radio energy output and lifetime of supernova remnants. These models give IR/radio flux density ratios differing by factors of 3–10 from each other and from the simple model adopted herein. The fact that all these estimates agree to within an order of magnitude, and that galactic nuclei and extended disc emission have about the same ratio, indicates that star formation and supernovae probably are sufficient to account for the radio luminosities.

7 Implications

The fact that interactions between galaxies trigger a luminous burst of star formation has profound implications for extragalactic astrophysics, since the frequency of galaxy–galaxy interactions should increase rather rapidly at epochs of increasing redshift. The frequency of interaction will be proportional to the galaxies' peculiar velocities with respect to the Hubble flow, divided by the interaction mean free path. The probability of interaction should therefore increase with redshift roughly as $(1+z)^4$. (The situation is slightly more complicated than this because the peculiar velocities are proportional to $1+z$, and at some point the increased probability of interaction due to the higher velocities will be compensated by the fact that interactions are less effective at high velocities.) About 7 per cent of galaxies are presently observed to have morphological disturbances such as bridges and tails which indicate an on-going interaction (Vorontsov-Velyaminov 1977). Since such features are generally short-lived, with lifetimes of $\sim 5\times10^8$ yr, if the current rate of interactions is representative, most galaxies are likely to have experienced interactions.

This fact underscores the importance of environmental considerations in attempting to understand many of the astrophysical properties of galaxies. The high probability of interactions over cosmic time-scales means that most 'normal' galaxies must have experienced interaction-induced starbursts. Star formation processes control the chemical evolution of galaxies, and since interaction-induced starbursts are apparently 1–2 orders of magnitude more luminous than starbursts triggered by other processes, with correspondingly higher star formation rates, interaction-induced starbursts are likely to have played a major role in the spectral and chemical evolution of most galaxies.

Interaction-induced starbursts also have implications for the morphological evolution of galaxies. Toomre (1977) and others have shown that the violent stellar dynamical relaxation which is a consequence of the merger of two disc galaxies produces a stellar velocity distribution and luminosity profile resembling an elliptical galaxy. A lacuna in this scenario is a mechanism for the merger remnant to divest itself of the gas associated with the two disc galaxies. In Paper II we argued that supernovae following a merger-induced superstarburst produce galactic winds over a sufficiently large spatial extent to sweep the merger remnant as free of gas as any elliptical galaxy.

Such processes may also play a role in the morphological evolution of spiral galaxies. Computations by Quinn & Goodman (1986) suggest that spiral galaxies acquire their bulges by accreting dwarf disc galaxies. In this model a similar process to that discussed above for ellipticals should follow, producing the low gas density characteristic of spiral galaxy bulges (Bosma 1978). This sequence of events – mergers, violent relaxation, starbursts, and galactic winds – appears to account qualitatively for the Hubble sequence: increasing M/L and decreasing bulge/disc ratio going from Sa to Sd.

Interaction-induced starbursts may also be the trigger for other types of activity in galactic nuclei. Balick & Heckman (1982) have recently reviewed the extranuclear clues to the origin of activity in galactic nuclei. Some of the clues they cite seem to be associated with interactions. For example, Seyfert galaxies commonly exhibit tidal distortions and have companions. But perhaps even more importantly, there is growing observational evidence of the effects of interactions and mergers in galaxies at higher redshifts. Lilly & Longair (1984) report evidence for the effects of

169

bursts of star formation from the optical–IR colours of 3CR radio galaxies at high redshifts ($z\sim1$). MacKenty & Stockton (1984) find strong emission lines in the extended luminous material surrounding the quasar Mrk 1014, which they plausibly attribute to an interaction-induced burst of star formation. Smith *et al.* (1986) have recently analysed deep CCD images of 31 low redshift QSOs ($z\leqq0.3$). They find that the host galaxies occupy the high luminosity tail of the general galaxy luminosity function, and about half the QSOs are hosted by morphologically peculiar galaxies (*cf.* also Stockton 1982). Heckman *et al.* (1986) have provided clear evidence that powerful radio galaxies are associated with morphologically disturbed galaxies.

One possible link between these morphological clues and the existence of interaction-induced starbursts has been proposed by Terlevich & Melnick (1985). They suggest that there must be a class of very hot and luminous extreme Wolf-Rayet stars, which they call 'Warmers', which appear in the post-main-sequence evolution of massive stars. They show that these Warmers will photoionize the interstellar gas to produce an emission line spectrum like that of a Seyfert 2 galaxy, and this spectrum will eventually evolve into a Liner-type spectrum. The existence of such a phase in the evolution of massive stars, in conjunction with the relatively higher frequency of interactions at earlier epochs, could account for some of the characteristic features of active galactic nuclei. Interaction-induced starbursts and super-starbursts, with the features elaborated above, will produce high-luminosity galaxies. These starbursts have exceptional efficiency in producing high-mass stars from the gas available. The post-main-sequence evolution of these stars results in objects which can provide the high-excitation and high-luminosity characteristics of some active galactic nuclei.

An alternative possibility is that interactions could be providing the fuel for a compact active nucleus (*cf.* Heckman *et al.* 1986). However, interaction-induced starbursts pose a problem for such a model. If high-luminosity starbursts are triggered in these interactions, the consequent supernova-driven winds would clear the nuclear regions of gas, thereby eliminating the proposed source of fuel for the compact source. Proposals that interaction-induced starbursts evolve into active nuclei face similar difficulties. In summary, although an association between nuclear activity and interactions is increasingly clear, the causal link between interactions and such activity, and the role of associated starbursts, remains obscure.

8 Summary and conclusions

We have followed up the *JHKL* survey of various morphological types of interacting galaxies with observations at 10μm. Adding these results to existing data we have formed a sample of 39 interacting and merging galaxies with 10μm detections ($>3\sigma$) in 5–8 arcsec apertures. These data confirm and quantify the results of Papers I and II. In particular we show

(i) From the shape of the continuum spectra, the spatial extent of the IR and radio emission, the mass-to-light ratios, and the optical emission line intensities, it is difficult to avoid the conclusion that the energy source powering the IR luminosity is a massive burst of star formation.

(ii) The IR luminosities of interacting galaxies are on average about an order of magnitude larger than those of typical starburst galaxies. The subset of interactions which have resulted in the merger of two disc galaxies are the most luminous galaxies in the sample, by a further order of magnitude. They are superstarbursts.

Using a simple analytical model of a starburst we find the following features to characterize interaction-induced starbursts.

(iii) Rates of formation of OBA stars of $\sim$1–100 $M_{\odot}\,yr^{-1}$ are required to maintain the high IR luminosities of interacting and merging galaxies.

(iv) In those galaxies for which mass estimates are available the starburst will consume the gas in $\sim10^7$ yr. The large fraction of observed interacting systems with evidence for starburst activity implies that the interaction must be refuelling the nuclear region on these time-scales.

(v) Interaction-induced star formation must be extremely efficient in converting gas to stars compared with processes in molecular clouds in the Galaxy.

(vi) The IMF of the starbursts in interacting and merging galaxies must be restricted to stars of mass >3–$6\,M_{\odot}$ (a feature which others have also found for other starburst galaxies).

(vii) The relative strength of the radio and IR emission from these galaxies is consistent with the starburst models, and supernova rates of $\sim1\,yr^{-1}$ are predicted on the basis of the IR luminosity.

These properties of interaction-induced starbursts, coupled with the higher frequency of interactions between galaxies at earlier epochs, indicate the central importance of interactions in the energetic, spectral, and chemical evolution of most galaxies. And while there is clearly an association between interactions and some other forms of nuclear activity in galaxies, the causal link(s) with interaction-induced starbursts are not clear. The existence of Warmers may provide one such link, but the pervasive galactic winds ensuing from a starburst would appear to eliminate the fuel needed for any model involving accretion on to a compact object.

Acknowledgments

It is a pleasure to thank Jack Abolins, Eric Becklin, Ian Gatley, James Graham, Tim Hawarden, Charles Telesco and Alar Toomre for stimulating discussions and critiques. Joel Aycock and Dolores Walther provided the excellent telescope support at UKIRT without which we could not have made some of these measurements. GSW was, and PAJ is supported by a research studentship from the SERC.

References

Aitken, D. K. & Roche, P. F., 1984. *Mon. Not. R. astr. Soc.*, **208**, 751.
Aitken, D. K. & Roche, P. F., 1985. *Mon. Not. R. astr. Soc.*, **213**, 777.
Antonucci, & Olszewski, 1985. *Astr. J.*, **90**, 2203.
Arp, H. C., 1966. *Atlas of Peculiar Galaxies*, California Institute of Technology, Pasadena.
Baldwin, J. A., Phillips, M. & Terlevich, R., 1981. *Publs astr. Soc. Pacif.*, **93**, 5.
Balick, B. & Heckman, T. M., 1982. *Ann. Rev. Astr. Astrophys.*, **20**, 431.
Balzano, V. A., 1983. *Astrophys. J.*, **268**, 602.
Bosma, A., 1978. *PhD thesis.*
Burke, B. F. & Miley, G. K., 1973. *Astr. Astrophys.*, **28**, 379.
Bushouse, H. A. & Gallagher, J. S., 1984. *Publs astr. Soc. Pacif.*, **96**, 273.
Carozzi-Meyssonnier, N., 1978. *Astr. Astrophys.*, **63**, 415.
Cohen, M. & Kuhi, L., 1979. *Astrophys. J. Suppl.*, **41**, 743.
Condon, J. J., 1980a. *Astrophys. J. Suppl.*, **53**, 459.
Condon, J. J., 1980b. *Astrophys. J.*, **242**, 894.
Condon, J. J., Condon, M. A., Gisler, G. & Puschell, J., 1982. *Astrophys. J.*, **252**, 102.
Cutri, R. M. & McAlary, C. W., 1985. *Astrophys. J.*, **296**, 90.
Demoulin, M.-H., 1968 *Astrophys. J.*, **153**, 31.
Demoulin, M.-H., 1969 *Astrophys. J.*, **156**, 325.
Dahari, O., 1985. *Astrophys. J. Suppl.*, **57**, 643.
D'Odorico, S., 1970. *Astrophys. J.*, **160**, 3.
Feast, M. W. & Robertson, B. S. C., 1978. *Mon. Not. R. astr. Soc.*, **185**, 31.
Fosbury, R. A. E. & Wall, J. V., 1979. *Mon. Not. R. astr. Soc.*, **189**, 79.
Gehrz, R. D., Hackwell, J. A. & Jones, T. W., 1974. *Astrophys. J.*, **191**, 675.
Gehrz, R. D., Stamek, R. A. & Weedman, D. W., 1983. *Astrophys. J.*, **267**, 551.
Gioia, I. M., Gregorini, L. & Klein, U., 1982. *Astr. Astrophys.*, **116**, 164.
Graham, J. R., Wright, G. S., Meikle, W. P. S., Joseph, R. D. & Bode, M. F., 1984. *Nature*, **310**, 213.

170

Graham, J. R., Meikle, W. P. S., Selby, M. J., Allen, D. A., Evans, A., Pearce, G., Bode, M. F., Longmore, A. J. & Williams, P. M., 1983. *Nature*, **304**, 709.
Gunn, J. E., 1979. *Active Galactic Nuclei*, p. 213, eds Hazard, C. & Mitton, S., Cambridge University Press.
Heckman, T. M., Smith, E. P., Baum, S. A., van Breugel, W. J. M., Miley, G. K., Illingworth, G. D., Bothun, G. D. & Balick, B., 1986. *Astrophys. J.*, **311**, 526.
Heckman, T. M., 1983. *Astrophys. J.*, **268**, 628.
Heckman, T. M., Miley, G. K., van Breugel, W. J. M. & Butcher, H. R., 1981. *Astrophys. J.*, **247**, 403.
Helou, G., Soifer, B. T. & Rowan-Robinson, M., 1985. *Astrophys. J.*, **298**, L7.
Hummel, E., 1980. *Astr. Astrophys. Suppl.*, **41**, 151.
Hummel, E., 1981. *Astr. Astrophys.*, **96**, 111.
Hummel, E., van der Hulst, J. M. & Dickey, J. M., 1984. *Astr. Astrophys.*, **134**, 207.
Israel, F. P. & van der Hulst, J. M., 1983. *Astr. J.*, **88**, 1736.
Jenkins, C. R., 1984. *Astrophys. J.*, **277**, 501.
Joseph, R. D., 1986. *Light on Dark Matter*, p. 447, ed. Israel, F. P., Reidel, Dordrecht, Holland.
Joseph, R. D. & Wright, G. S., 1985. *Mon. Not. R. astr. Soc.*, **214**, 87 (Paper II).
Joseph, R. D., Meikle, W. P. S., Robertson, N. A. & Wright, G. S., 1984. *Mon. Not. R. astr. Soc.*, **209**, 111 (Paper I).
Karachentsev, I. D., 1972. *Commun. Spec. Astrophys. Obs. USSR*, **7**, 1.
Keel, W. C., Kennicutt, R. C., Hummel, E. & van der Hulst, J. M., 1985. *Astr. J.*, **90**, 708.
Kellerman, K. I., Shaffer, D. B., Pauliny-Toth, I. I., Preuss, E. & Witzel, A., 1976. *Astrophys. J. Lett.*, **210**, L121.
Kronberg, P. P., 1985. *Supernovae as Distance Indicators*, p. 88, ed. Bartel, N., Springer-Verlag, Berlin.
Kronberg, P. P. & Biermann, P., 1981. *Astrophys. J.*, **243**, 89.
Kronberg, P. P., Biermann, P. & Schwab, F., 1985. *Astrophys. J.*, **291**, 693.
Lawrence, A., Ward, M., Elvis, M., Fabbiano, G., Willner, S. P., Carleton, N. P. & Longmore, A., 1985. *Astrophys. J.*, **291**, 117.
Lebofsky, M. J. & Rieke, G. H., 1979. *Astrophys. J.*, **229**, 111.
Leger, A. & Puget, J. L., 1984. *Astr. Astrophys.*, **137**, L5.
Lilly, S. J. & Longair, M. S., 1984. *Mon. Not. R. astr. Soc.*, **211**, 833.
Lonsdale, C. J., Persson, S. E. & Matthews, K., 1984. *Astrophys. J.*, **287**, 95.
MacKenty, J. W. & Stockton, A., 1984. *Astrophys. J.*, **283**, 64.
Miller, G. E. & Scalo, J. M., 1979. *Astrophys. J. Suppl.*, **41**, 513.
Peterson, S. D. & Shostak, G. S., 1977. *Astr. J.*, **79**, 767.
Phillips, M. M., Aitken, D. K. & Roche, P. F., 1984. *Mon. Not. R. astr. Soc.*, **207**, 25.
Puget, J. L., Leger, A. & Boulanger, F., 1985. *Astr. Astrophys.*, **142**, L19.
Quinn, P. J. & Goodman, J., 1986. *Astrophys. J.*, **309**, 472.
Rieke, G. H., 1976. *Astrophys. J.*, **206**, L15.
Rieke, G. H., 1978. *Astrophys. J.*, **226**, 550.
Rieke, G. H. & Lebofsky, M. J., 1978. *Astrophys. J.*, **220**, L37.
Rieke, G. H. & Lebofsky, M. J., 1979. *Ann. Rev. Astr. Astrophys.*, **17**, 477.
Rieke, G. H. & Low, F. J., 1972. *Astrophys. J.*, **176**, L95.
Rieke, G. H., Lebofsky, M. J., Thompson, R. I., Low, F. J. & Tokunaga, A. T., 1980. *Astrophys. J.*, **238**, 24.
Roche, P. F. & Aitken, D. K., 1985. *Mon. Not. R. astr. Soc.*, **213**, 789.
Rose, J. A. & Searle, L., 1982. *Astrophys. J.*, **253**, 556.
Rubin, V. C. & Ford, W. K., 1968. *Astrophys. J.*, **154**, 431.
Rubin, V. C., Ford, W. K. & D'Odorico, S., 1970. *Astrophys. J.*, **160**, 801.
Ryter, C., Puget, J. L. & Perault, M., 1987. Preprint, submitted to *Astr. Astrophys.*
Scoville, N. Z., Becklin, E. E., Young, J. S. & Capps, R. W., 1983. *Astrophys. J.*, **271**, 512.
Sellgren, K., 1984. *Astrophys. J.*, **277**, 623.
Smith, E. P., Heckman, T. M., Bothun, G. D., Romanishin, W. & Balick, B., 1986. *Astrophys. J.*, **306**, 64.
Soifer, B. T., Helou, G., Lonsdale, C. J., Neugebauer, G., Hacking, P., Houck, J. R., Low, F. J., Rice, W. & Rowan-Robinson, M., 1984. *Astrophys. J.*, **278**, L71.
Stocke, J. T., Tiffit, W. G. & Kaftan-Kassim, M. A., 1978. *Astr. J.*, **83**, 322.
Stockton, A., 1982. *Astrophys. J.*, **257**, 33.
Stockton, A. & Bertola, F., 1980. *Astrophys. J.*, **235**, 37.
Sulentic, J. W., 1976. *Astrophys. J. Suppl.*, **32**, 171.
Telesco, C. M., 1985. *Extragalactic Infrared Astronomy*, p. 87, ed. Gondhalekar, P. M., Rutherford Appleton Laboratory, Chilton.
Telesco, C. M. & Gatley, I., 1984. *Astrophys. J.*, **284**, 557.
Telesco, C. M., Decher, R. & Gatley, I. 1986. *Astrophys. J.*, **302**, 632.

Telesco, C. M., Becklin, E. E., Wynn-Williams, C. G. & Harper, D. A., 1984. *Astrophys. J.*, **282**, 427.
Terlevich, R. & Melnick, J., 1985. *Mon. Not. R. astr. Soc.*, **213**, 841.
Toomre, A., 1977. *Evolution of Galaxies and Stellar Populations*, p. 401, eds Tinsley, B. M. & Larson, R. B., Yale University Observatory, New Haven, Connecticut.
Toomre, A. & Toomre, J. 1972. *Astrophys. J.*, **178**, 623.
Tresch-Fienberg, R., Fazio, G. G., Gezari, D. Y., Hoffmann, W. F., Lamb, G. M., Shu, P. K. & McCreight, C. R., 1987. *Astrophys. J.*, **312**, 542.
Tully, R. B., 1974. *Astrophys. J. Suppl.*, **27**, 437.
Ulrich, M.-H., 1972. *Astrophys. J.*, **178**, 113.
Ulvestad, J. S., 1982. *Astrophys. J.*, **259**, 96.
Vorontosov-Velyaminov, B. A., 1977. *Astr. Astrophys. Suppl.*, **28**, 1.
Wright, A. E., 1974. *Mon. Not. R. astr. Soc.*, **167**, 251.

171

Do Markarian 'double nucleus' galaxies have two nuclei? The case of Mkn 788

R. D. Joseph[1], G. S. Wright[2], P. A. James[1] and I. S. McLean[2]

[1] *Astrophysics Group, Blackett Laboratory, Imperial College, London SW7 2BZ*

[2] *UK Infrared Telescope, 665 Komohana Street, Hilo, Hawaii 96720, USA*

Accepted 1987 December 16. Received 1987 December 11

Summary. Mkn 788 is a classic example of a 'double nucleus' Markarian galaxy. Previous studies have failed to distinguish between the two 'nuclei' in any physically significant way. We present an infrared image at 2.2μm taken with IRCAM on UKIRT, which shows source A to be the galaxy nucleus, whereas source B is probably an extra-nuclear H II region. This example suggests that it is premature to discuss 'double nucleus' Markarian galaxies as such until further studies can demonstrate the reality of the multiple nuclei.

1 Introduction

The sample of galaxies with strong ultraviolet continua identified by Markarian has been a rich source of material for investigation of nuclear activity in galaxies. One interesting aspect of this galaxy sample is the rather large fraction of them, about 10 per cent, which apparently exhibit double nuclei (Petrosyan, Saakyan & Khachikyan 1978). The origin of this nuclear structure, and its relation to the nuclear activity which many of these galaxies exhibit, is an intriguing problem. Two nuclei are, of course, suggestive of a recent merger between galaxies. Interest in these 'double nucleus' Markarian galaxies has therefore been highlighted recently by the discovery of the relation between ultraluminous infrared galaxies and interactions and mergers (Joseph & Wright 1985; Joseph 1986). Moreover there is growing appreciation of a connection between interactions and non-thermal nuclear activity in galactic nuclei (*cf.* Lilly & Longair 1984; Smith *et al.* 1986; Heckman *et al.* 1986). If it were established that Markarian 'double nucleus' galaxies really are the products of mergers, these two considerations would make them a particularly seminal class of galaxies with which to investigate the origin of nuclear activity in galaxies and its relation to interactions

One such 'double nucleus' Markarian galaxy which has received considerable attention is Mkn 788. Kollatschny, Netzer & Fricke (1986, hereafter KNF) obtained CCD images in Hα and [O III], optical spectroscopy, a 21-cm spectrum and a VLA map at 20 cm for this galaxy. They find that both sources have the characteristics of high-excitation star-formation regions, and they suggest that both are starburst nuclei. They found no way to decide from these data which of the two

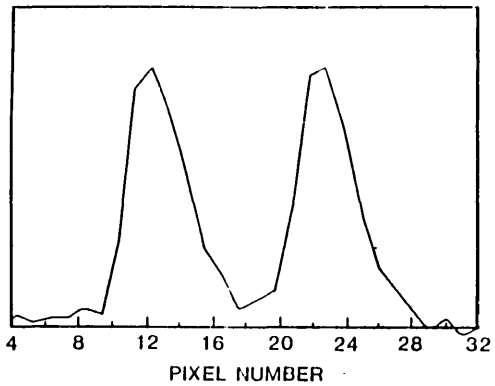


Figure 1. A slice through the optical continuum CCD image of Mkn 788, reproduced from Fig. 3 in KNF. The intensity scale is linear. One pixel = 1.91 arcsec.

sources is the dynamical centre of Mkn 788. An intensity cut through the optical continuum image showing the profiles for both nuclei was presented by KNF and is reproduced in Fig. 1. While source A is stronger in Hα, [N II], and [S II], source B is stronger in Hβ and [O II] and, as Fig. 1 shows, both sources seem identical in their optical continuum profiles.

Infrared imaging provides a powerful approach to the identification of galactic nuclei (*cf.* Telesco *et al.* 1985). Since the nuclear regions in many galaxies, and especially starburst galaxies, are often heavily enshrouded by dust, infrared observations can provide information on structure and physical conditions much deeper into a galaxy than can optical observations. In addition, the stars which constitute most of the mass of a normal galaxy have peaks in their continuum spectra in the near-infrared. For these reasons we obtained images in the *K*-band, 2.2 μm, of Mkn 788.

2 Observations

The observations were obtained at UKIRT on 1987 April 30 using the UKIRT infrared camera, IRCAM (McLean *et al.* 1986; McLean 1987). The detector array installed in the camera at this time was an engineering grade array of 62×58 InSb detectors, manufactured by Santa Barbara Research Centre. The camera was used in its high-resolution format, 0.62 arcsec pixel^{-1}, with a standard *K* (2.2 μm) filter. An exposure time of 120 s, in a staring mode (i.e. no chopping) was used for each image. Four images of the galaxy were interleaved with four images of a nearby blank sky field, and the blank sky frames were used to flat-field the galaxy images. Dark current frames were subtracted from object and flat-field images before division by the flat field. The mean sky level was then subtracted from each frame. The final *K*-band image was made by coadding the four galaxy images. Since each galaxy exposure was shifted a few arcsec from the previous one, the effects of bad pixels were eliminated in the coadded image.

3 Results

A contour plot of the infrared image of Mkn 788 is shown in Fig. 2. This figure shows that the western source (nucleus A in the notation of KNF) is much more sharply peaked than is source B. The integrated luminosity of Source A at 2.2 μm is about twice that of B, whereas the FWHM of A, 2 arcsec, is about one-third that of B. This is in sharp contrast to the optical CCD image of this

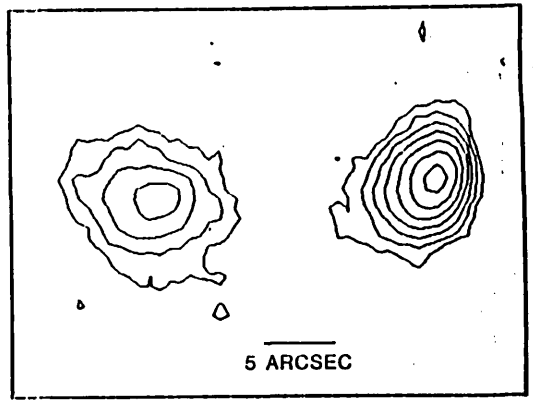


Figure 2. A contour plot of Mkn 788 at *K* (2.2 μm). The mean sky level has been subtracted after flat-fielding, and the image has been smoothed with a running block of 3×3 pixels (1.8×1.8 arcsec^2). The contour scale is linear in surface brightness.

galaxy – *cf.* fig. 1 in KNF, in which the two nuclei are virtually indistinguishable. This point is made more forcefully in Fig. 3(a), which shows a cut taken through the two infrared peaks. For comparison we have shown in Fig. 3(b) a similar cut taken through the nucleus in NGC 3690. This profile is taken from similar IRCAM *K*-band images of NGC 3690 obtained at UKIRT one night earlier. While source A has a profile characteristic of a galactic nucleus, source B does not. Thus

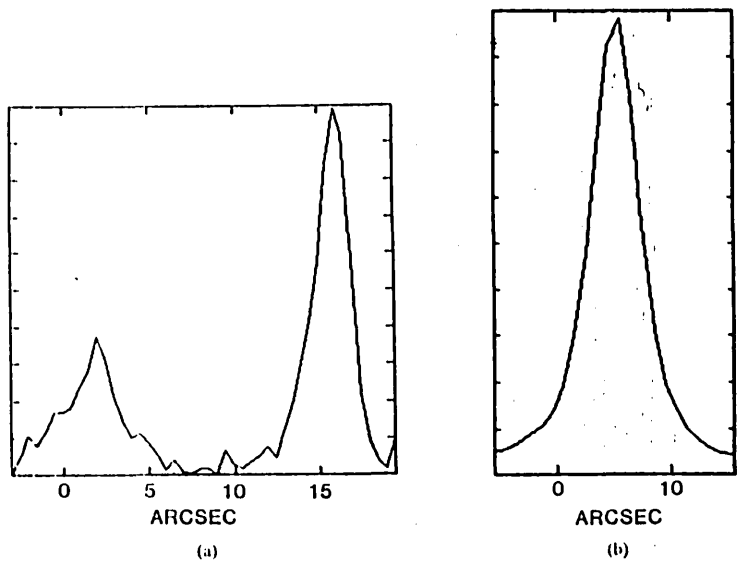


Figure 3 (a) A slice through the two peaks in the 2.2-μm image of Mkn 788. (b) A cut through a similar 2.2-μm image of the nucleus of NGC 3690A. The intensity scales are linear.

we suggest from the infrared images of Mkn 788 that source A is actually *the* nucleus of this galaxy.

The broader, lower-intensity profile of source B does not seem to be that of a galactic nucleus. A plausible interpretation is that source B is a giant extra-nuclear H II region, similar in character to such objects as 30 Doradus in the Large Magellanic Cloud (Werner *et al.* 1978), source C in NGC 3690 (Gerhz, Sramek & Weedman 1983), or the 'jumbo' H II region in NGC 3310 (Telesco & Gatley 1984).

From the relative star-formation activity estimated by KNF for sources A and B, about 3 to 1, we can estimate how the total infrared luminosity which KNF infer from *IRAS* data is apportioned between the two sources. This gives source B an infrared luminosity of $\sim 10^9 L_{\odot}$. This luminosity is about one-ninth that found for the 'jumbo' H II region NGC 3310 (Telesco & Gatley 1984) twice that found for the giant H II region NGC 5461 in M101 (Telesco & Gatley 1984) and 25 times that of 30 Dor (Werner *et al.* 1978). Thus the infrared luminosity of source B in Mkn 788 is consistent with our interpretation as a giant extra-nuclear H II region.

These interpretations are corroborated by the VLA map presented by KNF. The radio continuum of source A was detected at 20 cm, whereas source B was undetected to a limit about six times less than the flux density found for source A. This also suggests that source A is the true galactic nucleus.

4 Discussion

The optical features of both sources in Mkn 788 are so similar it is not surprising that they have been interpreted previously in terms of a double nucleus structure. It has taken infrared imaging to demonstrate which of the two sources has the light profile characteristic of a genuine galactic nucleus. It is tempting to speculate that many more of the 'double nuclei' in Markarian galaxies may also be shown by infrared imaging to be composed of a single nucleus and one or more giant extra-nuclear H II regions. In any case it is clear that caution is necessary in using these galaxies in discussions of interactions and mergers among galaxies.

This interpretation of the two sources in Mkn 788 is also consistent with the suggestion that 'double nuclei' turn up more frequently among Markarian galaxies than among the general galaxy population. Since the selection criterion, a strong ultraviolet excess, will tend to include galaxies with recent bursts of star formation, as well as galaxies with non-thermal nuclear activity, it would not be surprising if this selection criterion were to produce an unusually large number of galaxies with massive extra-nuclear star-formation regions, and hence apparent 'double nuclei'.

5 Conclusions

(i) An infrared image of Mkn 788 at 2 μm shows that it is not a double nucleus galaxy; one source is a typical starburst nucleus and the other is probably a giant extra-nuclear H II region.

(ii) There is a strong possibility that a similar conclusion would be reached for many other 'double nucleus' Markarian galaxies if infrared images were obtained for a larger sample. In any case it is clearly premature to pursue discussions of the Markarian multiple nucleus phenomenon, its relations to interactions between galaxies, and connections between these events and various forms of nuclear activity in galaxies, until further observations, perhaps of the type described here, have conclusively demonstrated the reality of the 'double nuclei' in Markarian galaxies.

Acknowledgments

It is a pleasure to thank Colin Aspin for his superb image processing software for IRCAM, and for much help in reducing the IRCAM data. Andrea Prestwich provided assistance with these observations. PAJ is a research student supported by the UK Science and Engineering Research Council and acknowledges with special thanks travel and subsistence provided by the SERC.

References

Gerhz, R. D., Sramek, R. A. & Weedman, D. A., 1983. *Astrophys. J.*, **267**, 551.
Heckman, T. M., Smith, E. P., Baum, S. A., van Breugel, W. J. M., Miley, G. K., Illingworth, G. D., Bothun, G. D. & Balick, B., 1986. *Astrophys. J.*, **311**, 526.
Joseph, R. D., 1986. *Light on Dark Matter*, p. 447, ed. Israel, F. P., Reidel, Dordrecht, Holland.
Joseph, R. D. & Wright, G. S., 1985. *Mon. Not. R. astr. Soc.*, **214**, 87.
Kollatschny, W., Netzer, H. & Fricke, K. J., 1980. *Astr. Astrophys.*, **163**, 31 (KNF).
Lilly, S. J. & Longair, M. S., 1984. *Mon. Not. R. astr. Soc.*, **211**, 833.
McLean, I. S., 1987. *Infrared Astronomy with Arrays*, eds Wynn-Williams, G. C. & Becklin, E. E., University of Hawaii.
McLean, I. S., Chuter, T. C., McCaughrean, M. J. & Rayner, J. T., 1986. *Instrumentation in Astronomy VI*, ed. Crawford, D. L., *SPIE*, **627**, 430.
Petrosyan, A. R., Saakyan, K. A. & Khachikyan, E. E., 1978. *Astrofiz.*, **14**, 69.
Smith, E. P., Heckman, T. M., Bothun, G. D., Romanishin, W. & Balick, B., 1986. *Astrophys. J.*, **306**, 64.
Telesco, C. M. & Gatley, I., 1984. *Astrophys. J.*, **284**, 557.
Telesco, C. M., Decher, R. & Gatley, I., 1985. *Astrophys. J.*, **299**, 896.
Werner, M. W., Becklin, E. E., Gatley, I., Ellis, M. J., Hyland, A. R., Robinson, G. & Thomas, J. A., 1978. *Mon. Not. R. astr. Soc.*, **184**, 365.